

University of Alberta

**Bone Targeting Salmon Calcitonin Analogues as Drug Delivery
Systems for Bone Disease**

by

Krishna Hari Bhandari

A thesis submitted to the Faculty of Graduate Studies and Research
in partial fulfillment of the requirements for the degree of

Doctor of Philosophy

in

Pharmaceutical Sciences

Faculty of Pharmacy and Pharmaceutical Sciences

©Krishna Hari Bhandari

Fall 2012

Edmonton, Alberta

Permission is hereby granted to the University of Alberta Libraries to reproduce single copies of this thesis and to lend or sell such copies for private, scholarly or scientific research purposes only.

Where the thesis is converted to, or otherwise made available in digital form, the University of Alberta will advise potential users of the thesis of these terms.

The author reserves all other publication and other rights in association with the copyright in the thesis and, except as herein before provided, neither the thesis nor any substantial portion thereof may be printed or otherwise reproduced in any material form whatsoever without the author's prior written permission.

ABSTRACT

The objective of this thesis was to design bone targeting salmon calcitonin (sCT) analogues as drug delivery systems for bone diseases. Non-PEGylated salmon calcitonin-bisphosphonate (sCT-BP) and PEGylated salmon calcitonin-bisphosphonate (sCT-PEG-BP) were investigated.

sCT-BP conjugates were synthesized by initially reacting sCT with sulfosuccinimidyl-4-[*N*-maleimidomethyl]cyclohexane-1-carboxylate (sulfo-SMCC) in dimethylformamide (DMF) in presence of triethylamine (TEA) at room temperature. Thiolated bisphosphonate (thiol-BP) was then reacted with sCT-SMCC intermediate to generate sCT-BP conjugates. To synthesize sCT-PEG-BP, sCT was reacted with maleimide-PEG-*N*-hydroxy succinimidyl carboxy methyl ester (NHS-PEG-MAL) to generate sCT-PEG-MAL which was then reacted with thiol-BP to generate sCT-PEG-BP. Conjugates were characterized by tris-tricine SDS-PAGE. The number of BP per sCT molecule was determined by phosphate and sCT assays and the effect of PEG-BP or BP on sCT secondary structure was examined by Circular Dichroism (CD). sCT analogues were evaluated for *in vitro* bone mineral affinity and specificity using a binding assay for bone hydroxyapatite and several other calcium salts. Successful conjugation of sCT with BP and the effect of such conjugation on antibody binding ability of sCT was indirectly determined using ELISA. Conjugates were incubated

with bone mineral in bone mineral coated osteologic plates. Presence of BP resulted into the binding of these conjugates on the bone mineral surface of these plates. sCT on such bound conjugates was then reacted with anti-sCT antibody. Finally, the intensity of the developed colour was measured. *In vitro* cell viability was evaluated in osteoclast (OC) precursor RAW 264.7 cells and sCT bioactivity and CTR binding potential was evaluated by *in vitro* intracellular cAMP stimulation assay in human T47D breast cancer cells. Similarly, *in vivo* activity was evaluated by determining the plasma levels of calcium after s. c. administration in normal, osteoporotic (OP) and osteoarthritic (OA) rats. Finally, efficacy in bone diseases like OP and adjuvant arthritis (AA) was studied using *in- vivo* micro-CT and a dose escalation study was performed in OP rats.

Our results showed that the chemical coupling of BP or PEG-BP to sCT has a tendency to alter its secondary structure from a less stable and readily aggregation prone random coil orientation into a more stable and desirable alpha helical form without altering its receptor and antibody binding specificity. Bone targeting sCT analogues exhibited significantly greater affinity and specificity for bone mineral over unmodified sCT, retained strong sCT bioactivity and CTR binding affinity. They were non-toxic to bone marrow cells and exhibited comparable hypocalcaemic effect to that of sCT in normal rats. They decreased plasma calcium in OP and OA rats. Compared to marketed unmodified sCT, these analogues showed significantly improved efficacy in terms of preserving bone

volume, BMD and trabecular micro-architecture in OP and AA rats. Bisphosphonate-mediated bone targeting of PEGylated or non-PEGylated sCT represents a new class of targeted antiresorptive compounds that have not previously been attempted. These bone targeting sCT analogues hold the promise of facilitating the delivery of sCT preferentially to skeletal bony tissues, thereby increasing its local concentration to bone surfaces, whilst maintaining sCT bioactivity and increasing efficacy.

ACKNOWLEDGEMENTS

This project was financially supported by a proof of principal grant from Canadian Institutes of Health Research (CIHR) and Osteoarthritis Alberta Team (Team OA) grant. I was personally funded by TEAM OA studentship, Ivy A Thomson and William A Thomson Graduate Scholarship, Queen Elizabeth II Graduate Scholarship, Dr Ronald Micetich Memorial Graduate Scholarship and various other scholarships from University of Alberta.

First and foremost, I would like to express my greatest gratitude to my supervisor, Dr. Michael R Doschak, for his efficient and endless guidance throughout this research work, for his encouragement from the beginning and generous support to the end of my study. His guidance has been important for my success in this degree.

I also thank my supervisory committee members, Drs. Carlos A. Velázquez, Raimar Löbenberg and John Mercer, for their guidance and advice. I am thankful to my lab mates Jillian Chapman and Imran Khan for their help with *in vivo* micro-CT, Arash Panahiphar for helping me in drug dosing and Madhuri Newa for helping me with cell culture. I also thank my colleagues Rohit Kalpavalle, Michael Lam, Biwen and Uchin Z, for their support throughout this degree.

TABLE OF CONTENTS

CHAPTER 1: INTRODUCTION

1. 1. Bone	1
Structure and composition	1
Remodeling	3
Osteoclast and osteoclastogenesis	4
Bone resorption	6
1. 2. Osteoporosis	8
Etiology and types	10
Therapeutic options and concerns	13
1. 3. Rheumatoid arthritis and pre- adjuvant arthritis rat model	17
1. 4. Bisphosphonates	20
1. 5. Calcitonin	22
Mechanism of action	23
Role of osteoclasts and calcitonin in rheumatoid arthritis (RA) and osteoarthritis (OA)	24
Advantages and disadvantages of calcitonin	25

1. 6. Polyethylene glycol	28
PEGylation	29
1. 7. Bone targeting	30
Bone targeting of salmon calcitonin	30
1. 8. Thesis proposal	34
Objective	34
Hypothesis	35
Significance	35

CHAPTER 2: EXPERIMENTAL PROCEDURES

2. 1. Materials	36
2. 2. Synthesis of thiol reactive sCT	36
sCT-SMCC	36
sCT-PEG-MAL	36
2. 3. Process optimization	37
2. 3. 1. sCT-SMCC	37
The effect of reaction time	37

The effect of sulfo-SMCC concentrations	37
The effect of triethyl amine concentrations	37
2. 3. 2. sCT-PEG-MAL	37
The effect of NHS-PEG-MAL concentrations	37
The effect of reaction time	37
2. 4. Thiol-BP characterization	40
LC-MS	40
Reactive thiol content	41
Phosphate content	41
2. 5. Coupling of functionalized sCT with thiol-BP	42
Synthesis of sCT-BP	42
Synthesis of sCT-cysteine	42
Synthesis of sCT-PEG-BP	42
2. 6. Process optimization for sCT-PEG-BP	43
The effect of buffer	43
The effect of buffer concentrations	43
The effect of thiol-BP concentrations	43

2. 7. Conjugate characterization	44
MALDI-TOF	44
Tris-tricine SDS-PAGE	44
Purification	45
Assay of sCT and phosphates: Extent of BP coupling per sCT	46
2. 8. In-vitro evaluation	47
Bone mineral affinity	47
Bone mineral specificity	48
sCT secondary structure	48
In-vitro cell viability assay	49
Anti-sCT antibody binding ability	50
sCT receptor binding ability and in-vitro bioactivity	51
2. 9. In-vivo bioactivity	52
Normal rats	52
Osteoporotic rats	53
Osteoarthritic rats	54

2. 10. In-vivo efficacy in bone diseases	56
Osteoporotic rats	56
Adjuvant arthritic rats	57
2. 11. sCT dose escalation in osteoporotic rats	59
2. 12. Statistical analysis	61
CHAPTER 3: RESULTS	
3.1. Synthesis of thiol reactive sCT	62
sCT-SMCC	62
sCT-PEG-MAL	64
3. 2. Process optimization	65
3. 2. 1. sCT-SMCC	65
The effect of reaction time	65
The effect of sulfo-SMCC concentrations	68
The effect of triethyl amine concentrations	79
3. 2. 2. sCT-PEG-MAL	85
The effect of NHS-PEG-MAL concentrations	85

The effect of reaction time	91
3. 3. Thiol-BP characterization	96
LC-MS	96
Reactive thiol content	98
Phosphate content	99
3. 4. Coupling of functionalized sCT with thiol-BP	100
Synthesis of sCT-BP	100
Synthesis of sCT-cysteine	103
Synthesis of sCT-PEG-BP	105
3. 5. Process optimization for sCT-PEG-BP	105
The effect of buffer	105
The effect of buffer concentrations	111
The effect of thiol-BP concentrations	111
3. 6. Conjugate characterization	118
Tris-tricine SDS-PAGE	118
Extent of BP coupling per sCT	122

3. 7. In-vitro evaluation	122
Bone mineral affinity	122
Bone mineral specificity	126
sCT secondary structure	127
In-vitro cell viability assay	130
Anti-sCT antibody binding ability	131
sCT receptor binding ability and in-vitro Bioactivity	133
3. 8. In-vivo activity	135
Normal rats	135
Osteoporotic rats	136
Osteoarthritic rats	137
3. 9. In- vivo efficacy in bone diseases	141
Osteoporotic rats	141
Adjuvant arthritic rats	144
3. 10. sCT dose escalation in osteoporotic rats	156

CHAPTER 4: DISCUSSION AND CONCLUSION	168
Problems, limitations and future study considerations	176
Conclusion	185
REFERENCES	186

LIST OF FIGURES

Figure 1: Conversion of RAW cells into osteoclasts.	4
Figure 2: Strategies for anti-resorptive therapy.	14
Figure 3: Generic structure of bisphosphonate.	20
Figure 4: Structure of salmon calcitonin.	22
Figure 5: Probable products when sulfo-SMCC is reacted with sCT followed by Thiol-BP.	38
Figure 6: Probable products when NHS-PEG-MAL is reacted with sCT followed by Thiol-BP.	39
Figure 7: MALDI-TOF spectra of sCT dissolved in DMSO at a concentration of 13.72 mg/mL.	62
Figure 8: MALDI-TOF spectra of the products of sCT and sulfo-SMCC reaction.	63
Figure 9: MALDI-TOF spectra of NHS-PEG-MAL in DMSO.	66
Figure 10: MALDI-TOF spectra of sCT-PEG-MAL.	67

Figure 11: Optimization of reaction time when reacting sCT with sulfo-SMCC: The effect of reaction after 10 minutes.	69
Figure 12: Optimization of reaction time when reacting sCT with sulfo-SMCC: The effect of reaction after 20 minutes.	70
Figure 13: Optimization of reaction time when reacting sCT with sulfo-SMCC: The effect of reaction after 30 minutes.	71
Figure 14: Optimization of reaction time when reacting sCT with sulfo-SMCC: The effect of reaction after 40 minutes.	72
Figure 15: Optimization of reaction time when reacting sCT with sulfo-SMCC: The effect of reaction after 50 minutes.	73
Figure 16: Optimization of reaction time when reacting sCT with sulfo-SMCC: The effect of reaction after 60 minutes.	74
Figure 17: The effects of sulfo-SMCC concentration when reacting sulfo-SMCC with sCT: 1: 3 mol/ mol ratio of sCT to sulfo-SMCC respectively.	75
Figure 18: The effects of sulfo-SMCC concentration when reacting sulfo-SMCC with sCT: 1: 5 mol/ mol ratio of sCT to sulfo-SMCC respectively.	76
Figure 19: The effects of sulfo-SMCC concentration when reacting sulfo-SMCC with sCT: 1: 7 mol/ mol ratio of sCT to sulfo-SMCC respectively.	77

Figure 20: The effects of sulfo-SMCC concentration when reacting sulfo-SMCC with sCT: 1: 10 mol/ mol ratio of sCT to sulfo-SMCC respectively.	78
Figure 21: The effect of a TEA concentration when reacting sCT with sulfo-SMCC: 0.05% v/v TEA.	80
Figure 22: The effect of a TEA concentration when reacting sCT with sulfo-SMCC: 0.1% v/v TEA.	81
Figure 23: The effect of a TEA concentration when reacting sCT with sulfo-SMCC: 0.2% v/v TEA.	82
Figure 24: The effect of a TEA concentration when reacting sCT with sulfo-SMCC: 0.3% v/v TEA.	83
Figure 25: The effect of a TEA concentration when reacting sCT with sulfo-SMCC: 0.4% v/v TEA.	84
Figure 26: The effect of NHS-PEG-MAL concentration in its reaction with sCT: 1:1 mol/ mol ratio of sCT to NHS-PEG-MAL.	86
Figure 27: The effect of NHS-PEG-MAL concentration in its reaction with sCT: 1:2 mol/ mol ratio of sCT to NHS-PEG-MAL.	87
Figure 28: The effect of NHS-PEG-MAL concentration in its reaction with sCT: 1:3 mol/ mol ratio of sCT to NHS-PEG-MAL.	88

Figure 29: The effect of NHS-PEG-MAL concentration in its reaction with sCT: 1:5 mol/ mol ratio of sCT to NHS-PEG-MAL.	89
Figure 30: The effect of NHS-PEG-MAL concentration in its reaction with sCT: 1:7 mol/ mol ratio of sCT to NHS-PEG-MAL.	90
Figure 31: The effect of reaction time in the reaction of sCT with NHS-PEG-MAL: Reaction products after 15 minutes.	92
Figure 32: The effect of reaction time in the reaction of sCT with NHS-PEG-MAL: Reaction products after 30 minutes.	93
Figure 33: The effect of reaction time in the reaction of sCT with NHS-PEG-MAL: Reaction products after 45 minutes.	94
Figure 34: The effect of reaction time in the reaction of sCT with NHS-PEG-MAL: Reaction products after 60 minutes.	95
Figure 35: Structure of thiol BP.	96
Figure 36: LC-MS spectra of thiol BP.	97
Figure 37: Reactive reactive thiol content of thiol-BP.	99
Figure 38: Phosphate content of thiol-BP.	101

Figure 39: MALDI-TOF spectra of the products of sCT-SMCC intermediate and thiol-BP reaction.	102
Figure 40: MALDI-TOF spectra of the products of sCT-SMCC intermediate and cysteine reaction.	104
Figure 41: MALDI-TOF spectra of the products of sCT-PEG-MAL intermediate and thiol-BP reaction.	106
Figure 42: The effect of buffers in the reaction between sCT-PEG-MAL and thiol-BP: Effect of 100 mM sodium acetate buffer pH 6.8.	107
Figure 43: The effect of buffers in the reaction between sCT-PEG-MAL and thiol-BP: Effect of 100 mM ammonium acetate buffer pH 6.8.	108
Figure 44: The effect of buffers in the reaction between sCT-PEG-MAL and thiol-BP: Effect of 100 mM sodium phosphate buffer pH 6.8.	109
Figure 45: The effect of pH 6.8 phosphate buffers concentrations in the reaction between sCT-PEG-MAL and thiol-BP: 50 mM sodium phosphate buffer.	112
Figure 46: The effect of pH 6.8 phosphate buffers concentrations in the reaction between sCT-PEG-MAL and thiol-BP: 10 mM sodium phosphate buffer.	113
Figure 47: The effect of thiol-BP concentrations in its reaction with sCT-PEG-MAL: 1: 5 mol/ mol ratio of sCT-PEG-MAL to thiol-BP.	114

Figure 48: The effect of thiol-BP concentrations in its reaction with sCT-PEG-MAL: 1: 10 mol/ mol ratio of sCT-PEG-MAL to thiol-BP.	115
Figure 49: Effect of thiol-BP concentrations in its reaction with sCT-PEG-MAL: 1: 20 mol/ ratio of sCT-PEG-MAL to thiol-BP.	116
Figure 50: The effect of thiol-BP concentrations in its reaction with sCT-PEG-MAL: 1: 40 mol/ mol ratio of sCT-PEG-MAL to thiol-BP.	117
Figure 51: Tris-tricine SDS-PAGE of sCT, sCT-SMCC and sCT-SMCC-BP.	118
Figure 52: Tris-tricine-SDS-PAGE of sCT, sCT-PEG-MAL and sCT-PEG-BP.	119
Figure 53: Determination of bone targeting potential (hydroxyapatite, HA, binding ability) of sCT-BP.	123
Figure 54: Determination of bone targeting potential: bone mineral affinity and specificity of sCT-PEG-BP.	125
Figure 55: Determination of bone targeting potential: bone mineral specificity of sCT-BP.	126
Figure 56: Circular dichroism (CD) spectra of sCT, sCT-SMCC, sCT-PEG, sCT-BP and sCT-PEG-BP.	129
Figure 57: <i>In vitro</i> cell viability assay.	130

Figure 58: Determination of anti-calcitonin antibody binding ability of sCT analogue by ELISA.	132
Figure 59: <i>In vitro</i> bioactivity of sCT analogue determined using intracellular cAMP stimulation in human T47D cells.	134
Figure 60: <i>In vivo</i> activity: effect of sCT analogues on plasma calcium level in normal rats.	136
Figure 61: <i>In vivo</i> activity: effect of sCT analogues on plasma calcium level in osteoporotic (OP) rats.	139
Figure 62: <i>In vivo</i> activity: effect of sCT analogues on plasma calcium level in osteoarthritic (OA) rats.	140
Figure 63: <i>In vivo</i> efficacy: effect of sCT analogues on bone mineral density (BMD) in osteoporotic (OVX) rats.	143
Figure 64: <i>In vivo</i> efficacy: effect of sCT analogues on bone volume in osteoporotic (OVX) rats.	144
Figure 65: Three-dimensional micro-CT renders of trabecular bone volume at baseline and at 12 weeks.	145
Figure 66: <i>In vivo</i> efficacy in adjuvant arthritis: % change in body weight.	146
Figure 67: <i>In vivo</i> efficacy in adjuvant arthritis: % change in paw diameter.	148

Figure 68: <i>In vivo</i> efficacy in adjuvant arthritis: % change in ankle joint diameter.	149
Figure 69: <i>In vivo</i> efficacy in adjuvant arthritis: % change in paw volume.	151
Figure 70: <i>In vivo</i> efficacy: effect of sCT analogues on bone mineral density (BMD) in adjuvant arthritic (AA) rats.	153
Figure 71: <i>In vivo</i> efficacy: effect of sCT analogues on bone volume in adjuvant arthritic (AA) rats.	154
Figure 72: Three-dimensional micro-CT renders of trabecular bone volume at baseline and at 21 days.	155
Figure 73: Dose escalation: effect of different doses of calcimar on bone mineral density (BMD) in osteoporotic (OVX) rats.	157
Figure 74: Dose escalation: effect of different doses of sCT-BP on bone mineral density (BMD) in osteoporotic (OVX) rats.	158
Figure 75: Dose escalation: effect of different doses of sCT-PEG-BP on bone mineral density (BMD) in osteoporotic (OVX) rats.	159
Figure 76: Dose escalation: effect of buffer and thiol-BP on bone mineral density (BMD) in osteoporotic (OVX) rats.	160
Figure 77: Dose escalation: effect of different doses of calcimar on bone volume (BV/TV%) in osteoporotic (OVX) rats.	161

- Figure 78: Dose escalation: effect of different doses of sCT-BP on bone volume in osteoporotic (OVX) rats. 162
- Figure 79: Dose escalation: effect of different doses of sCT-PEG-BP on bone volume in osteoporotic (OVX) rats. 163
- Figure 80: Dose escalation: effect of buffer and thiol-BP on bone volume in osteoporotic (OVX) rats. 164
- Figure 81: Dose escalation: three-dimensional micro-CT renders of trabecular bone volume at baseline, 4, 8 and 12 weeks at 5 IU/kg daily s. c. dose of calcimar or equivalent sCT-BP or sCT-PEG-BP. 165
- Figure 82: Dose escalation: three-dimensional micro-CT renders of trabecular bone volume at baseline, 4, 8 and 12 weeks at 10 IU/kg daily s. c. dose of calcimar or equivalent sCT-BP or sCT-PEG-BP. 166
- Figure 83: Dose escalation: three-dimensional micro-CT renders of trabecular bone volume at baseline, 4, 8 and 12 weeks at 20 IU/kg daily s. c. dose of calcimar or equivalent sCT-BP or sCT-PEG-BP. 167
- Figure 84: HPLC spectra of sCT. Gradient elution from 0 minute (A-100, B-0%) to 35 minutes (A-0%, B-100%). A-0.1 %v/v Trifluoroacetic acid in water, B: 0.1% v/v Trifluoroacetic acid in 95% v/v acetonitrile in water. 183

LIST OF ABBREVIATIONS

AA	Adjuvant arthritis
ATCC	American type cell culture
ATPase	Adenosine triphosphatase
BMD	Bone mineral density
BP	Bisphosphonates
BMPs	Bone morphogenic proteins
BRON	BP related osteonecrosis
BV/TV%	Bone volume
cAMP	Cyclic adenosine monophosphate
CD	Circular dichroism
CT	Calcitonin
CTR	Calcitonin receptor
Cys	Cysteine
DEXA	Dual energy X-ray absorptiometry
Disodium-EDTA	Disodium ethylenediaminetetraacetic acid
DMEM	Dulbecco's modified eagle medium

DMF	Dimethyl formamide
DMSO	Dimethyl sulfoxide
EIA	Enzyme immune assay
ELISA	Enzyme linked immuno sorbent assay
HRT	Estrogen hormonal replacement therapy
FBS	Fetal bovine serum
FDA	Food and drug administration
FGF	Fibroblast growth factor
GAM-HRPO	Goat anti-mouse IgG conjugated with horseradish peroxidase
HA	Hydroxyapatite
HBSS	Hank's balanced salt solution
HC	Hypercalcaemia of bone cancers
HPLC	High performance liquid chromatography
IBMX	3-isobutyl-1-methyl-xanthine
ICH	International conference on harmonisation
IGF	Insulin-like growth factor
IGF-II	Insulin like growth factor II

IL-1	Interleukin-1
IM	Intramuscular
IU	International unit
LC/MS	Liquid chromatography/mass spectrometry
Lys	Lysine
MALDI-TOF	Matrix-assisted laser desorption/ionization-time of flight
MCSF	Macrophage-colony-stimulating factor
μ CT	Microcomputed tomography
MMPs	Matrix metalloproteinases
MRI	Magnetic resonance imaging
MTT	3-[4, 5-dimethylthiazol-2-yl]-2, 5-diphenyl tetrazolium bromide
MWCO	Molecular weight cut off
NHS-PEG-MAL	Maleimide-PEG-N-hydroxy succinimidyl carboxy methyl ester
OA	Osteoarthritis
OD	Optical density
OP	Osteoporosis
OVX	Ovariectomized

PBS	Phosphate buffer solution
PBST	Phosphate buffer containing tween 80
PD	Paget's disease
PEGs	Polyethylene glycols
PMOP	Postmenopausal osteoporosis
PPi	Inorganic pyrophosphate
PTH	Parathyroid hormone
PTOA	Post-traumatic osteoarthritis
qCT	Quantitative computed tomography
RANK	Receptor activator of nuclear factor Kappa B
RANKL	Receptor activator of nuclear factor Kappa B-ligand
ROS	Reactive oxygen species
RPMI-1640	Roswell park memorial institute-1640
s. c.	Subcutaneous
sCT	Salmon calcitonin
SDS-PAGE	Sodium dodecyl sulfate polyacrylamide gel electrophoresis
SERMs	Selective estrogen receptor modulators

SMCC	N- Succinimidyl 4-(maleimidomethyl) cyclohexanecarboxylate
TEA	Triethylamine
TGF- β	Transforming growth factor- β
TMB substrate	3, 3', 5, 5'- Tetramethylbenzidine
TNFR	Tumor necrosis factor receptor
TRAP	Tartrate resistant acid phosphatase

CHAPTER 1: INTRODUCTION

1. 1. BONE

Structure and composition

The human skeletal system provides mechanical and structural support and protects the internal organs. It primarily consists of bone, a metabolically active connective tissue system. Bone helps in movement, production of blood cells and storage of minerals such as calcium, magnesium, and phosphate (Rho, Zioupos et al. 2002; Russell, Espina et al. 2006; Viguet-Carrin, Garnero et al. 2006).

There are two types of calcium in bone. One is in crystalline form as calcium phosphate and the other is in amorphous form which is easily exchangeable in those situations when speedy plasma calcium level tuning are required.

Bone is composed of 30% organic matrix and 70% inorganic minerals. Hydroxyapatite ($\text{Ca}_{10} [\text{PO}_4]_6 [\text{OH}]_2$) which is mainly responsible for bone strength (Niyibizi and Kim 2000) is a major constituent of inorganic mineral. The organic matrix contains 2% cells and 98% extracellular matrix. The extracellular matrix is composed of 95% collagen and 5% non-collagenous constituents, such as proteoglycans, osteocalcin (15 %), osteonectin (15 %), serum-derived proteins and growth factors such as insulin-like growth factor (IGF), bone morphogenic proteins (BMPs), fibroblast growth factor (FGF) and transforming growth factor- β

(TGF- β). Type I collagen comprises about 95% of all collagen in bone, and about 80% of the total proteins in bone (Niyibizi, Chan et al. 1994; Niyibizi and Eyre 1994)

Collagen proteins, more specifically Type I, II, III, V, and XI collagens are responsible for bone structural integrity and their composition and extent of cross-linking determines the ability of bone to resist structural stresses (Viguet-Carrin, Garnero et al. 2006; Valcourt, Merle et al. 2007)

Osteoblast, osteoclast and osteocytes are major cells in bone. Osteoblasts are known for their osteogenic properties. They form a tight layer of cells on bone surface and are responsible for the production of the extracellular matrix and its mineralization (Cheng, Lecanda et al. 1998; Lecanda, Towler et al. 1998; Ziambaras, Lecanda et al. 1998; Ferrari, Traianedes et al. 2000). Osteoclasts are bone resorptive cells. They make a tight junction in bone matrix. This is known as resorption pit which contain various resorptive enzymes. Osteocytes are fully differentiated osteoblasts. They respond to stress by signalling to osteoblast to initiate bone resorption or bone formation (Donahue, Guilak et al. 1995; Donahue, McLeod et al. 1995; Mosley 2000). Once entrapped in the bone matrix (osteoid), osteoblasts undergo a morphological change to become osteocytes (Han, Cowin et al. 2004).

Long bones have three regions. A rounded outer end containing the growth plate called the epiphysis. Underneath the epiphysis is the region

of metaphysis. The hollow cortical region in the central modullary cavity is called the diaphysis. The rigid outer bone is known as cortical bone or compact bone which is mostly found in long bones. It consists of tightly packed layers of collagen known as osteons, which are the basic structures of cortical bone (Parfitt 1994 a; Parfitt 1994 b). It is surrounded by an outer layer known as the periosteum. Trabecular bone also known as spongy bone or cancellous bone is found in the metaphysic (ends of long bone) and vertebral bones. Unlike compact bone, trabecular bone is undergoing bone remodelling at a faster rate (Aubin, Dansereau et al. 1998; Guise and Mundy 1998).

Remodelling

Bones are continuously being remodelled. Resorption phases are shorter in duration and last 2-3 weeks, while the formation phase require a longer time lasting 2-3 months. However, the amount of bone formation by osteoblasts balances the amount of bone resorption by osteoclasts in mature healthy bone.

During bone remodelling in healthy adult bone, bone formation and resorption can occur independent of one another and bone remodelling does not result in a net gain or loss of bone as the volume of bone that is resorbed is replaced by an equal volume of new bone (Karsdal, Qvist et al. 2006; Tanko, Karsdal et al. 2006; Henriksen, Tanko et al. 2007).

The local release of factors like Interleukin-1 (IL-1) activate osteoclasts to initiate the bone resorption, where as factors like TGF- β and insulin like growth factor II (IGF-II) increase bone formation via increased proliferation and differentiation of osteoblasts (Guise and Mundy 1998; Lipton 2004; Price, Lipton et al. 2004).

Osteoclast and osteoclastogenesis



Figure 1: Multinucleated tartrate resistant acid phosphatase (TRAP)-positive osteoclast was observed by TRAP staining. RAW 264.7 cells, a murine macrophage-like osteoclast precursor line, were stimulated with 50 ng/mL RANKL and 25 ng/mL MCSF for osteoclast generation (Newa, Bhandari et al. 2011)

Osteoclast cells are multinucleated and migratory in nature. They are responsible for resorbing organic and inorganic components of bone during development and are part of the bone remodeling cycle throughout life. These cells originate from hematopoietic precursors of the

monocyte/macrophage lineage that are present both in the bone marrow and peripheral circulation, and their numbers and/or activity are frequently increased in a wide range of clinical disorders that are associated with excessive bone loss (Holtrop and King 1977; Roodman 1996; Roodman 1996).

Osteoclast cells express the RANK receptor (receptor activator of nuclear factor Kappa β), which belongs to the tumor necrosis factor receptor (TNFR) super family. RANK is expressed on osteoclast precursors as well as in the mature osteoclasts (*Horowitz, Bothwell et al. 2005*).

RANK is the essential signaling receptor for osteoclast differentiation during the process of osteoclastogenesis. It is triggered by the osteoclast differentiation factor known as RANK-ligand (RANKL), a member of the TNF family, and is the ligand for RANK (Nakagawa, Kinoshita et al. 1998; Yasuda, Shima et al. 1998; Yasuda, Shima et al. 1998; Boyle, Simonet et al. 2003; Eghbali-Fatourehchi, Khosla et al. 2003). RANK signalling, with additional signalling through c-Fms, the receptor for macrophage colony stimulating factor (M-CSF), triggers the proliferation and fusion of mononuclear cells and the formation of multinucleated, mature osteoclasts (Boyle, Simonet et al. 2003; Eghbali-Fatourehchi, Khosla et al. 2003; Faccio, Novack et al. 2003; Faccio, Takeshita et al. 2003; Faccio, Zou et al. 2003).

Activation by M-CSF promotes the proliferation and survival of cells of the monocytic lineage, including osteoclasts and osteoclast precursors. M-CSF also induces the expression of RANK receptor in osteoclast precursors priming these cells to differentiate into osteoclasts in the presence of RANKL.

The deletion of one of M-CSF, RANK, or RANKL results in the inhibition of osteoclastogenesis thus leading to osteopetrosis (dense and brittle bone) in mice (Hermine, Mayeux et al. 1992; Suda, Takahashi et al. 1992; Tanaka, Takahashi et al. 1992; Arai, Miyamoto et al. 1999; Lam, Takeshita et al. 2000; Teitelbaum 2000 a; Teitelbaum 2000 b). In addition, M-CSF prevents osteoclast apoptosis by triggering anti-apoptotic Akt-kinase which is necessary for survival of osteoclasts (Bonni, Brunet et al. 1999; Datta, Brunet et al. 1999; Kelley, Graham et al. 1999; Marsh, Pomerantz et al. 1999).

Bone resorption

Osteoclasts become attached to the bone surface and initiate osteoclast-matrix interactions initiate bone resorption (Weir, Horowitz et al. 1993). Matrix metalloproteinases (MMPs) are required for the access of osteoclasts to the resorption sites and MMP inhibitors prevent bone resorption by preventing osteoclast recruitment to the resorption sites (Blavier and Delaisse 1995). In a resorption site, a tight sealing zone is formed under the osteoclast via tight attachment of the osteoclast plasma

membrane to the bone matrix (Hentunen, Lakkakorpi et al. 1995; Vaananen and Horton 1995; Gu, Hentunen et al. 2005; Obrant, Ivaska et al. 2005; Parikka, Peng et al. 2005). Podosomes that are formed in osteoclasts mediate their attachment to the extracellular bone matrix (Marchisio, Bergui et al. 1988; Hentunen, Lakkakorpi et al. 1991; Lakkakorpi and Vaananen 1991). Then, a large number of intracellular acidic vesicles are fused to the bone-facing plasma membrane (Mattsson, Skyman et al. 1997; Palokangas, Mulari et al. 1997), releasing acid into the resorption space to dissolve the hydroxyapatite crystals (Zhao, Laitala-Leinonen et al. 2001). In addition to this, ATPase proton pumps are expressed into the ruffled border membrane of osteoclast so that they can continually pump protons from the cytoplasm into the resorption lacuna (Tuukkanen and Vaananen 1986; Blair, Teitelbaum et al. 1989; Teti, Blair et al. 1989; Hentunen, Tuukkanen et al. 1990; Vaananen, Karhukorpi et al. 1990). This kind of increased acidity within the resorptive space is responsible for dissolution of bone mineral phase, exposing the collagen-rich organic matrix of the bone for the proteolytic enzymes such as matrix metalloproteinases (MMPs) and lysosomal cathepsin-K (Everts, Delaisse et al. 2002; Troen 2006; Troen 2006) which cleaves the native triple helix of type I collagen at multiple sites, resulting in the unwinding of the triple helix and thus making it readily available for degradation by proteinases (Boissy, Lenhard et al. 2003; Delaisse, Andersen et al. 2003; Garnero, Ferreras et al. 2003). Cathepsin K also activates tartrate resistant acid

phosphatase (TRAP), a phosphatase enzyme that can also generate reactive oxygen species (ROS) (Vaaraniemi, Halleen et al. 2004; Ljusberg, Wang et al. 2005; Leibbrandt and Penninger 2008; Vaananen and Laitala-Leinonen 2008), which has been indicated in the degradation of collagen(Halleen, Raisanen et al. 2003; Halleen, Tiitinen et al. 2006; Korpela, Tiitinen et al. 2006).

1. 2. OSTEOPOROSIS

Osteoporosis is a disease of low bone density and the micro-architectural deterioration of bone structure, which in combination, predispose the patient to enhanced bone fragility and fracture risk (Raisz 2005; Raisz 2005). This is, as a result of relative decline in the bone formation activity. In OP, the bone volume is gradually decreased, cortical bone is thinned, or the porosity of cancellous bone is increased remarkably. These changes thus greatly impair the mechanical properties of the bone (Rice, Cowin et al. 1988).

Osteoporosis is prevalent in approximately 44 million people aged 50 and older, which corresponds to 55% of the population in that age group in the United States (US Department of Health and Human Services. 2004. Bone health and Osteoporosis: There are 200 millions osteoporotic people worldwide. 1 in 3 women and 1 in 5 men over 50 years of age are osteoporotic. 30%–50% of women and 15%–30% of men are at risk of developing osteoporosis in their lifetime. In Canada, one in

four women and at least one in eight men over the age of 50 have osteoporosis. 1. 4 million Canadians are osteoporotic and it leads to 30,000 hip fractures a year. Total of 80% of fractures can be attributed to osteoporosis (http://www.osteoporosis.ca/index.php/ci_id/8867/la_id/1.htm. Accessed on May 7, 2012). The increased bone resorption in osteoporosis is due both to increased osteoclastogenesis and to decreased osteoclast apoptosis (Hanley and Josse 1996; Jones, Hogan et al. 1996; Sturtridge, Lentle et al. 1996).

Osteoporosis results in healthcare costs in the region of CAD 1.9 billion per year in Canada (http://www.osteoporosis.ca/index.php/ci_id/8867/la_id/1.htm, accessed on May 7, 2012) and USD 17 billion/ year in the US (Burge, Dawson-Hughes et al. 2007). In addition, indirect costs due to absence from work, job loss, and poor quality of life are huge.

Osteoporosis is commonly diagnosed by measuring bone density using Dual Energy X-ray Absorptiometry (DEXA) scan of the total hip, femoral neck, or lumbar spine. It can present itself with low impact fractures, or fragility fractures (Mauck and Clarke 2006). Other techniques that are sometimes used to diagnose osteoporosis include quantitative computed tomography (qCT), magnetic resonance imaging (MRI) and microcomputed tomography (μ CT) (Inzerillo and Zaidi 2002; Inzerillo, Zaidi et al. 2002; Zaidi, Inzerillo et al. 2002). It is not surprising to note that bone

density testing for all women over the age of 65 years, and for high risk women between 60 and 64 is recommended (Morita, Ebihara et al. 1994).

The peak bone density in both men and women is achieved usually in the early 20s. Men have 10-12% greater peak bone mass and greater bone size (Campion and Maricic 2003). Bone loss starts in both sexes at 50 years of age due to increased osteoclast mediated bone resorption, increased cortical porosity, and endocortical thinning. This is not compensated by increased bone formation as in younger age leading to permanent bone loss.

Etiology and types

Three etiologies for osteoporosis have been established, based on predisposing factors and clinical presentation, namely: postmenopausal (type I), senile (type II) and secondary (type III) osteoporosis (Burckhardt 1989; Gallagher 1992). In all types, the declining ability of the bone remodeling machinery results in bone fragility (Seeman and Delmas 2006).

Type I postmenopausal osteoporosis (PMOP) occurs in women between 51-75 years of age, in which estrogen deficiency shifts bone remodeling to favour resorption over formation resulting in a net bone loss. Type II senile osteoporosis affects women at about twice the rate of men, and occurs from ages 75 to 90 years. Type III or secondary osteoporosis is caused by medications (e.g. Prednisone), cancers, endocrine disorders,

chronic liver or kidney diseases. Secondary osteoporosis can affect young and middle-aged people as well. The net result for all of these conditions is the insidious loss of bone mass and the predisposition to traumatic bone fracture.

Factors that may increase the risk of osteoporosis include:

Drop in estrogen after menopause: The rate of bone loss increases significantly after menopause because the ovaries stop producing estrogen, a hormone that plays a major role in the bone repair process. Female athletes and women who suffer from anorexia nervosa may also be at increased risk for osteoporosis. In both cases, the menstrual cycle is disrupted or lost and levels of estrogen in the body drop dramatically. Women who experience early menopause (before the age of 45 years) are more likely to have osteoporosis.

Family history and body type: Osteoporosis tends to run in families, and the risk of this condition is greater for individuals with elderly relatives who have had a bone fracture, especially if it is a parent who has had a hip fracture. People of European and Asian descent are most at risk. People who are thin or "small-boned" also have a higher risk of osteoporosis. People who have had a fracture in the vertebrae are also at increased risk.

Lifestyle factors and health conditions: Lifestyle factors such as smoking and excessive drinking, taking specific medications (such as corticosteroids), and having certain medical conditions (such as those that

affect nutrition absorption [e.g., Crohn's disease, celiac disease], primary hyperparathyroidism, rheumatoid arthritis, and hypogonadism) may also contribute to bone loss. People with type 2 diabetes are more likely to suffer a hip or shoulder fracture than those without diabetes.

Lack of exercise: Bones need to be used daily in order for them to stay healthy. People who are physically active are less at risk of developing osteoporosis, as their bones are stronger and less likely to lose strength with age. By contrast, a person who is bedridden or inactive for a lengthy period of time loses bone mass very quickly and is at high risk of osteoporosis.

Lack of calcium: Children, adolescents, and adults need to eat the recommended amounts of vitamins and minerals. Calcium and vitamin D are very important in the maintenance of healthy and strong bones throughout life and in the prevention of osteoporosis. Osteoporosis Canada recommends 1,000 mg of elemental calcium daily for men and women between the ages of 19 and 50 years, and 1,200 mg for men and women over the age of 50 years. They recommend vitamin D in daily doses of 400 IU to 1,000 IU for adults without osteoporosis under 50 years of age, and 800 IU to 2,000 IU for both adults over the age of 50 and people with osteoporosis to help increase calcium absorption in the bones. Higher doses over 2,000 IU require medical supervision. Osteoporosis Canada also recommends regular weight-bearing exercises (such as

walking, weight training, or climbing stairs) and a healthy lifestyle with no smoking or excessive intake of alcohol.

Therapeutic options and concerns

Two strategies are applied in treating osteoporosis. The first is treatments using anabolic therapies to increase bone mass. The second approach utilizes antiresorptive therapies aiming to reduce the rate of bone resorption.

Parathyroid hormone (PTH) is the mainstay of anabolic therapy. Endogenous parathyroid hormone is the primary regulator of calcium and phosphate metabolism in the bone and kidney. The ability of intermittent PTH to increase strength and mass of trabecular bone has been well known (Lindsay, Nieves et al. 1997; Whitfield, Morley et al. 1999; Neer, Arnaud et al. 2001). It reduces vertebral and non-vertebral fractures (Girotra, Rubin et al. 2006). **Teriparatide, a parathyroid hormone analogues** builds new bone faster than it breaks it down. It is a recombinant amino terminal fragment of parathyroid hormone comprised of the first 34 amino acids of parathyroid hormone. Teriparatide's anabolic effects are manifested as an increase in skeletal mass, an increase in the number of osteoblasts and osteoclasts (allowing for an increase in bone remodeling), and an increase in bone strength. Depending on the level of exposure, PTH and teriparatide may also decrease bone mass.

Strontium ranelate shows an anabolic as well as antiresorptive effect in osteoporosis (O'Donnell, Cranney et al. 2006).

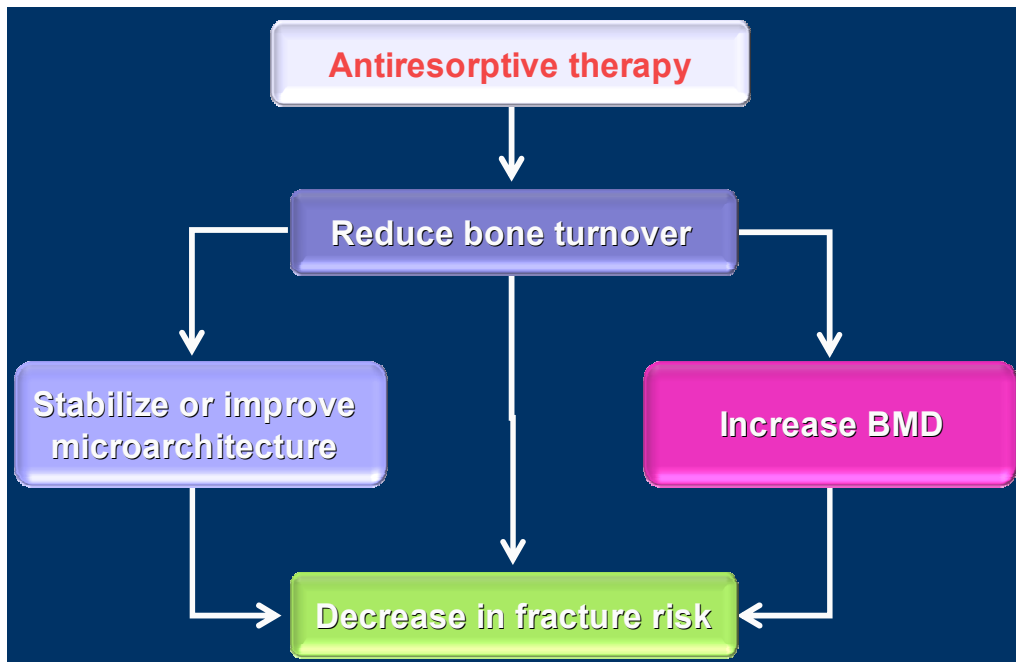


Figure 2: Strategies for anti-resorptive therapy.

Bisphosphonates such as alendronate, etidronate, risedronate, zoledronic acid, selective estrogen receptor modulators (SERMs; e.g., raloxifene), calcitonin (calcimar), denosumab, and estrogen hormonal replacement therapy (HRT) are used as antiresorptive strategies.

Bisphosphonates are used to prevent and treat osteoporosis. They decrease the rate of bone resorption and help repair bone, reducing the chance of fracture. The development of once per month oral dose

(Ibandronate) (Epstein 2006) or once a year infusion (Zoledronic acid) (Black, Delmas et al. 2007; Devogelaer, Brown et al. 2007; Lyles, Colon-Emeric et al. 2007; Lyles, Colon-Emeric et al. 2007) is patient friendly. Bisphosphonates are popular and reasonably effective alternatives to HRT and SERMs, but do have some limiting side-effects that include diarrhea, nausea, constipation, mild intestinal upset, severely suppressed bone turnover (Odvina, Zerwekh et al. 2005; Richer, Lewis et al. 2005) and possibility of development of osteomalacia and progressive osteolytic lesions resulting in lower patient compliance (Malden and Pai 2007).

Selective estrogen receptor modulators are used to prevent and treat osteoporosis in women. They have estrogen agonist activity in bone and antagonist properties elsewhere (Katzenellenbogen and Katzenellenbogen 2002; Rickard, Waters et al. 2002; Zhou, Nie et al. 2002). SERMs produce tissue specific, estrogen-like effects on bone and lipid metabolism without stimulating the uterus and breast. Raloxifene (Eli Lilly) is the first FDA approved SERM for the treatment of osteoporosis. It can increase bone mineral density and improve serum lipid profiles (Brantus and Delmas 1997; Delmas, Bjarnason et al. 1997; Delmas and Woolf 1997; Garnero and Delmas 1997). However, they are less potent than estrogen (Reid, Davidson et al. 2004; Reid, Eastell et al. 2004). They are thought to decrease incidence of vertebral fractures, with no effect on non-vertebral fractures (Ettinger, Black et al. 1999).

Calcitonin is produced by the thyroid gland. It strengthens bone.

Denosumab is a RANK ligand inhibitor that stops the breakdown of bone by acting as a decoy receptor. It helps to strengthen bones and lowers the chances of fracture. HRTs help to preserve bone.

All current therapeutic options for osteoporosis have exhibited a wide range of patient side-effects, some are quite severe. Hormone replacement therapy (HRT) using estrogen is capable of stimulating uterine and breast tissue, potentially resulting in cancer, and is also associated with increased coronary heart disease (Rossouw, Anderson et al. 2002; Espie and Cottu 2003; Espie, Daures et al. 2007). Selective estrogen-receptor modulators (SERMs), such as Raloxifene, are associated with an increased incidence of vascular thromboembolism (Osteoporosis Methodology Group, 2002). Parathyroid hormone has the potential to induce osteosarcoma (Palmer, Adami et al. 1988; Wermers, Khosla et al. 1998). The bisphosphonate (BP) drugs, in therapeutic concentrations, have the potential to cause BP related osteonecrosis (BRON) in the alveolar bone of the jaw. As BP drugs are sequestered in bone tissue, they exhibit long bone half-lives and may severely suppress bone turnover (Odvina, Zerwekh et al. 2005; Richer, Lewis et al. 2005), or result in the development of osteomalacia (Malden 2007; Malden and Pai 2007; Malden, Beltes et al. 2009). PTH has limitation of daily intermittent injections, and concerns about osteosarcoma induction in animal studies

(Palmer, Adami et al. 1988; Wermers, Khosla et al. 1998). However, it does not form new trabeculae (Nolan, Morley et al. 2003).

1. 3. RHEUMATOID ARTHRITIS AND PRE-ADJUVANT ARTHRITIS RAT MODEL

Rheumatoid arthritis is a chronic inflammatory disorder of joints typically involving the smaller joints of hands and feet. As the disease progresses, larger joints like knees, ankle and elbows may get involved. It is manifested by pain, swelling and limited movement. Unlike osteoarthritis, rheumatoid arthritis typically affects the lining of the bone leading to painful bone erosion and swelling. It is an inflammatory disorder and also involves autoimmunity. Rheumatoid arthritis is more prevalent in women. Post menopausal women aged 40-60 years are more susceptible to it. Symptoms of arthritis follow a rhythmic pattern of flare, relapse and remission. Swelling and pain fade alternatively with remission, but the bone deformation is the conclusive endpoint of this disease. Rheumatoid arthritis treatment follows two strategies. One is to reduce inflammation using non-steroidal anti-inflammatory drugs (NSAIDs) and the other is to prevent the bone damage and erosion using calcitonin and its analogues. .

Many animal models of rheumatoid arthritis have been cited in literature and have been used for reliable prediction of the pathogenesis, disease progression and testing of anti arthritis drugs efficacy. Selection of

the model depends upon the ability to predict the efficacy of agents tested, ease of testing and similarity of animal pathogenic conditions to human symptoms.

Adjuvant arthritis rat model:

Rat models of rheumatoid arthritis have consistently been reported in the literature for use in testing of anti-rheumatic drugs and disease research. This model is very similar to human rheumatoid arthritis in terms of signs and symptoms. The disease progression in this model can be evaluated by using visible physical signs and symptoms. In addition, bone resorption and periosteal proliferation can also be measured in this animal model (Pearson 1956; Carlson, Datko et al. 1985; Benslay and Bendele 1991).

The adjuvant rat model is distinguished from the classical rheumatoid arthritis model due to the reduced period of disease and the severity of disease progression. Experiments in these animals are performed for a shorter period of time to minimize their suffering due to the appearance of severe signs and symptoms of the disease. The pathogenesis of adjuvant arthritis rat model involves intra dermal injection of an arthrogenic suspension of heat killed *Mycobacterium butyricum*, finely ground and suspended in an immune stimulant adjuvant. This provokes an immune reaction in the rat involving release of inflammatory mediators and heat shock proteins that interact with the peptidoglycan

synthesis and stimulate metalloprotease enzymes, all resulting into bone resorption, swelling and inflammation (Van Vollenhoven, Soriano et al. 1988; Feige, Schulmeister et al. 1994; van de Langerijt, van Lent et al. 1994).

Most of the time, male (Lewis or Sprague Dawley) rats are used in this model, because this disease is much more variable in female rats in terms of onset and severity. Induction of adjuvant disease can be done with either Freund's complete adjuvant (FCA) supplemented with mycobacterium or by injecting synthetic adjuvant N, N-dioctyl decyl-N', N-bis(2-hydroxy-ethyl) propanediamine (Chang, Pearson et al. 1980).

Adjuvant can be injected at the base of the tail or in one of the foot pads. If injection is into the footpad, it allows study of the acute inflammatory reaction in that local area as well as the immunological reaction that develops approximately nine days later in the contra lateral paw and various organs.

To assess disease progression, caliper measurements of paw diameter or ankle joint width or paw volume or joint volume using a water displacement device are done prior to the onset of arthritis, and then every other day or at predetermined time points until the study is terminated.

Clinical evidence of arthritis occurs on day 9-10 post injection of adjuvant. Treatments are initiated on day 0 (prophylactic model dosing) or day 8 (therapeutic model). Various stress-related factors including manipulations during the test period (pharmacokinetic sampling),

frequency of dosing (QD vs BID) or type of vehicle used can influence the disease progression.

1.4. BISPHOSPHONATES

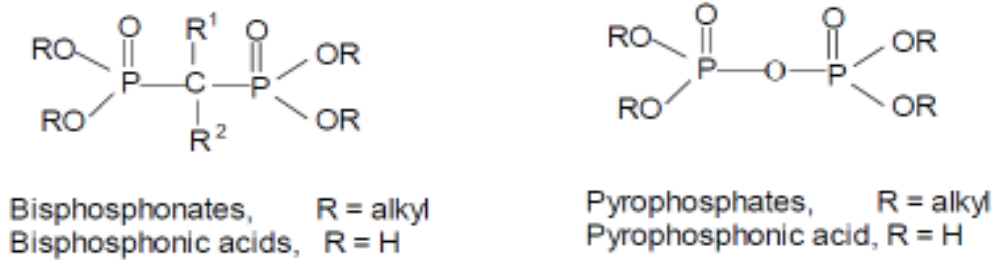


Figure 3: Generic structure of bisphosphonate.

Bisphosphonates are a group of stable synthetic analogues of the natural inorganic pyrophosphate (PPi) (Harris, Watts et al. 1999). But they differ in the central atom where BPs have a methylene carbon, a P-C-P backbone structure rather than an oxygen atom (P-O-P) as PPi. This structural feature renders bisphosphonate resistant to hydrolysis under acidic conditions or by pyrophosphatases (Francis and Meckel 1963; Francis and Briner 1973; Francis and Valent 2007).

Bisphosphonates are divided into two groups, non-nitrogen-containing (etidronate, clodronate and tiludronate) and the nitrogen-containing (pamidronate, neridronate, olpadronate, alendronate, ibandronate, risedronate and zoledronate) or amino- bisphosphonates,

which are more potent than non-nitrogen containing counterparts (Licata 2005) (Russell, Croucher et al. 1999).

Bisphosphonates bind avidly to the bone mineral surface and are subsequently internalized selectively by osteoclasts, where they inhibit the osteoclastic activity and induce apoptosis. The binding of the hydroxyl groups of bisphosphonates to hydroxyapatite of bone is responsible for the accumulation of bisphosphonates in bone (Meyer and Nancollas 1973). All bisphosphonates carry a negative charge associated with the phosphate groups at neutral pH, and as a result, they adhere themselves to the positively charge surface of hydroxyapatite crystals of bone (Francis and Valent 2007).

BPs inhibit the mevalonate pathway eventually inhibiting the enzyme farnesyl diphosphate synthetase. The absence of farnesyl diphosphate synthetase leads to induction of apoptosis of osteoclast (Luckman, Hughes et al. 1998; Rogers, Gordon et al. 2000; Rogers 2003). About half of an intravenously injected bisphosphonate dose is bound in bone within a few hours post administration and the remainder is eliminated by kidneys over a similar time-period.

Hydroxyapatite is a major component of the inorganic bone matrix and a target for bisphosphonate (Hirabayashi and Fujisaki 2003). Consequently a number of groups have explored the coupling of therapeutic agents with BPs in order to achieve bone selective targeting. This includes drug molecules (Niemi, Vepsalainen et al. 1999; Ezra,

Hoffman et al. 2000), proteins (Wright, Gittens et al. 2006), and radiopharmaceuticals (El-Mabhough, Angelov et al. 2006; Ogawa, Mukai et al. 2006). BPs are also used to deliver rhenium radionuclides and an anti-cancer agent as a therapeutic modality to bone metastases (El-Mabhough and Mercer 2005; El-Mabhough and Mercer 2008).

1.5. CALCITONIN

Calcitonin (CT) is an antiresorptive agent with specific inhibitory effects on osteoclast cells that leads to slowing down or inhibition of osteoclast-mediated resorptive bone loss (Chambers 1982; Chambers and Magnus 1982; Chambers and Ali 1983; Chambers and Dunn 1983; Chambers and Moore 1983; Chambers and Darby 1985; Chambers and Fuller 1985; Horton, Lewis et al. 1985).

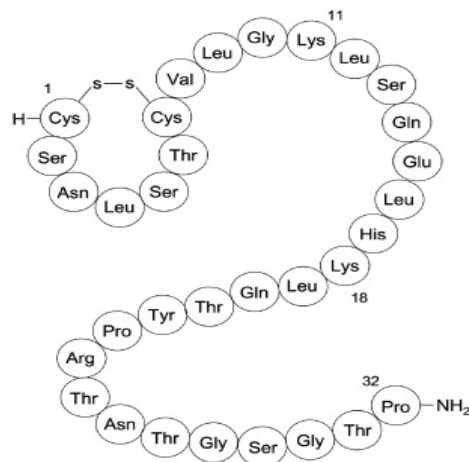


Figure 4: Structure of Salmon calcitonin showing 1-7 disulfide linkage between cysteine 1 and 7.

Calcitonin also positively influences osteogenesis and bone formation (Farley, Dimai et al. 2000; Okubo, Bessho et al. 2000). It also reduces blood calcium, thereby opposing the effects of parathyroid hormone (Boron 2004; Bouyer, Bradley et al. 2004). Calcitonin lowers blood calcium levels by increasing urinary calcium excretion and inhibiting bone resorption. CT may also act directly on chondrocytes, thus attenuating cartilage degradation and stimulating cartilage formation (Boron 2004; Bouyer, Bradley et al. 2004).

Mechanism of action

Mature osteoclasts express the calcitonin receptor on their surface (Zaidi, Inzerillo et al. 2002). Calcitonin receptors are of the G protein-coupled receptor family (comprising seven transmembrane-spanning receptor domains) whose signalling will inhibit osteoclast activity both *in vitro* and *in vivo* (Breimer, MacIntyre et al. 1988; Kartner, Yao et al. 2010; Ang, Pavlos et al. 2011; Ghayor, Correro et al. 2011; Itzstein, Coxon et al. 2011; Wang and Grainger 2011; Yan, Li et al. 2011).

Osteoclast resident calcitonin receptor (CTR) activation, by its ligand calcitonin, rapidly induces the loss of ruffled border and immobility followed by osteoclast cell retraction and arrest of bone resorption. Calcitonin receptor signalling also alters ion transporter distribution,

impairs enzyme activity (Moonga, Moss et al. 1990) and inhibits the osteoclastogenic effects of RANKL (Mancini, Moradi-Bidhendi et al. 2000).

Exposure of osteoclasts to CT rapidly results in the retraction of podosomes and the “ruffled border” membrane (Chambers 1982; Chambers and Magnus 1982), activation of adenylyl cyclase (Care, Bates et al. 1970; Murad, Brewer et al. 1970), and a decrease in bone resorption (Chambers and Darby 1985).

Role of osteoclasts and calcitonin in rheumatoid arthritis (RA) and osteoarthritis (OA)

Osteoclasts may play a role in the etiology of post-traumatic osteoarthritis (PTOA) (Andersson, Lundberg et al. 2007), the most common form of arthritis. At an early stage of disease pathogenesis, there is increased number of osteoclasts and hence a phase of increased bone resorption and turnover in periarticular subchondral bone volume (Bettica, Cline et al. 2002; Pelletier, Boileau et al. 2004; Shibakawa, Yudoh et al. 2005; Logar, Komadina et al. 2007; Berry, Maciewicz et al. 2010).

Increased osteoclast functional activity is directly responsible for the generalized bone loss that occurs in rheumatoid arthritis (Hirayama, Danks et al. 2002). In activated T-cells, RANKL is induced upon antigen-receptor engagement. In fact, activated CD4+ T-cells were indeed capable of inducing osteoclastogenesis (Kong, Boyle et al. 1999; Kong, Feige et al.

1999; Kong, Yoshida et al. 1999). Activated T-cells play a role in the resorption of bone via the up-regulation of RANKL (Yamaguchi, Aihara et al. 2006).

As the T cells are activated in autoimmune diseases like rheumatoid arthritis (Waalens, Forre et al. 1987; Maurer, Felzmann et al. 1992; Kotake, Udagawa et al. 2001; Brennan, Hayes et al. 2002; Ogawa, Ohtsuki et al. 2003; Harigai, Hara et al. 2004; Aerts, Dombrecht et al. 2008; Nakou, Katsikas et al. 2009; Kuca-Warnawin, Burakowski et al. 2011) and osteoarthritis, an antiresorptive strategy that selectively carries an active drug cargo to bone would be a highly desirable therapeutic approach to treat bone disease involving upregulated osteoclast activity and calcitonin has been reported to be advantageous in rheumatoid arthritis (Aida, Okawa-Takatsuji et al. 1994; Pappalardo, Rizzo et al. 1994; Kotaniemi, Piirainen et al. 1996; Ide and Suzuki 2001).

Advantages and disadvantages of calcitonin

sCT is a peptide hormone drug composed of 32 amino acids. sCT acts upon the calcitonin receptor (which is a G-protein receptor), found primarily on osteoclasts, to inhibit osteoclast activity in bones. Salmon CT (sCT) is preferred over human CT (hCT), due to its stability and potency (Silverman 2003);(Arvinte, Cudd et al. 1993).

When hCT was solubilized in water and hCT water solutions were mixed with phosphate buffer to give a final solution of 5 mM in phosphate buffer, pH 7.4, 145 mM NaCl (PBS), it precipitated into needle shaped fibrils. This fibrillation process was increased as the concentration of calcitonin in solution increased (Arvinte, Cudd et al. 1993).

SCT is currently marketed as injectable and nasal spray dosage forms to treat bone diseases such as osteoporosis, Paget's disease and hypercalcemia (Torres-Lugo and Peppas 2000; Yoo, Jun et al. 2000). However, conventional CT therapy is associated with several patient side-effects. In some patients, CT may result in deleterious gastric and/or vascular side effects (Gruber and Brautbar 1984; Gruber, Gutteridge et al. 1984; Gruber, Ivey et al. 1984). The nasal route of administration may result in local nasal irritation or ulceration (Carstens and Feinblatt 1991).

In addition, Salmon calcitonin may also result in an allergic and/or immunogenic response, including anaphylactic shock and/or death. Moreover, the systemic bioavailability of a nasally administered dose of CT ranges from 0.3%-30.6%, which compares poorly to the same dose administered by intramuscular (IM) injection (71% bioavailability) or by subcutaneous (SC) injection (66% bioavailability) (Overgaard, Agnusdei et al. 1991; Beglinger, Born et al. 1992; Lee, Ennis et al. 1994; Krasnoperov 1997; Chen, Lai et al. 2000; Buclin, Cosma Rochat et al. 2002; Miyazaki, Nakade et al. 2003; Miyazaki, Nakade et al. 2003).

Similarly, as the dry, defatted skeleton of humans comprise only 4 to 5% of total body mass, (Heymsfield, Pietrobelli et al. 2005), only a small proportion of the systemically bioavailable CT drug will be distributed to bone to elicit its therapeutic effect. Effective CT drug concentrations are also hampered by the rapid half-life of elimination. The terminal half-life is approximately 58 minutes for i.m. administration and 59 to 64 minutes for s.c.administration

(www.pharma.us.novartis.com/product/pi/pdf/miacalcin_injection.pdf,

accessed on May 12, 2012).

Due to these unfavourable pharmacokinetic profiles, high CT doses with increased dosing frequency and long term drug usage, patient are at risk of immune and other side-effects. In addition, it also renders CT therapy expensive, as osteoporosis and Paget's disease require administration of the drug on a long-term basis. However, despite those limitations, CT maintains efficacy in the treatment of osteopenic disease.

Although CT is a simple peptide in terms of amino acid sequence, it is highly unstable in general reaction conditions (Arvinte and Drake 1993).

The therapeutic use of calcitonin is known to be hampered by its physical instability (Cholewinski, Luckel et al. 1996; Stevenson and Tan 2000). In aqueous solutions, CT has a pronounced tendency to aggregate into long, thin fibrillar aggregates, yielding a viscous and turbid dispersion (Cudd, Arvinte et al. 1995). Also sCT was found to be most stable in

Aceate buffer, which is not commonly used in protein/peptide conjugation (Capelle, Gurny et al. 2009).

1. 6. POLYETHYLENE GLYCOL

Polyethylene glycols (PEGs) are widely used as thickeners, solvents, softeners, and moisture-carriers. They are also used as laxatives. PEG is a chemical compound composed of repeating ethylene glycol units. PEG compounds are also known as PEO (polyethylene oxide) and POE (polyoxyethylene).

Purified PEG is most commonly available commercially as mixtures of different oligomer sizes in broadly or narrowly defined molecular weight (MW) ranges. For example, "PEG 600" typically denotes a preparation that includes a mixture of oligomers having an average MW of 600. Likewise, "PEG 10000" denotes a mixture of PEG molecules ($n = 195-265$) having an average MW of 10,000 g/mol.

Polyethylene glycols have several chemical properties that make them especially useful in various biological, chemical and pharmaceutical settings. They are non-toxic, non-immunogenic and can be added to media and attached to surfaces and conjugated to molecules without interfering with cellular functions or target immunogenicities. PEGs are hydrophilic (aqueous-soluble) so the attachment to proteins and other

biomolecules decreases aggregation and increases solubility. Similarly, they are highly flexible providing bioconjugation without steric hindrance.

PEGylation

PEGylation is the process of covalent attachment of polyethylene glycol polymer chains to another molecule such as a drug or therapeutic protein. It is well established that, PEGylation enhances enzymatic stability of peptide drugs including calcitonin from proteolysis by forming an effective shield against degrading enzymes (Veronese and Pasut 2005). PEGylation of sCT increased drug efficacy in terms of plasma calcium lowering effect *in vivo* by virtue of increased molecular size contributing to reduced renal filtration, eventually allowing less frequent dosing (Hamidi, Azadi et al. 2006; Fee 2007; Ryan, Frias et al. 2011). PEGylation also confers an additional advantage of reducing immunogenicity through reduced recognition by reticuloendothelial system and thereby decreasing toxicity (Veronese and Pasut 2005). However, in those reports, therapeutic outcomes of improved pharmacokinetic profiles (Harris, Martin et al. 2001; Chen, Park et al. 2004; Hersel, Kreuzer et al. 2009; Alvarez, So et al. 2011) due to reduced proteolysis and increased circulation time (Kim, Cha et al. 2008) of PEGylated sCT were not evaluated in osteoporotic rats for one current therapeutic indication of sCT. Instead, the bioactivity was determined in terms of plasma calcium lowering effect alone.

1. 7. BONE TARGETING

Out of many available therapeutic agents used in bone diseases, only a few drugs are specific to receptors in the skeleton (Yoshida, Oida et al. 2002; Paralkar, Borovecki et al. 2003). A lack of bone-specificity can lead to serious complications, as demonstrated in the recent reports on the long-term adverse effects of hormone replacement therapy (HRT) (Wang, Miller et al. 2005; Lacey, Mink et al. 2002; Rossouw, Anderson et al. 2002). These and other authors report that by the incorporation of bone mineral affinity and specificity to a bone therapeutic agent, however, the pharmacokinetic profile can be dramatically altered to favour skeletal deposition and such bone targeting would be of benefit for many bone therapeutic agents.

Bone targeting of salmon calcitonin

Improvements in sCT efficacy, after conjugation to polyethylene glycol (PEGylation) have been reported (Lee, Moon et al. 1999; Lee, Tak et al. 1999; Yoo, Jun et al. 2000; Na, Youn et al. 2004; Youn, Jung et al. 2006). However, those improvements were mainly due to the improved solubility, stability and pharmacokinetic profiles of CT as a result of the PEGylation process. Due to the increased plasma circulation time of PEGylated CT, there would be a proportional increase in competition for CT uptake between all available CT receptors on other organs and tissues. Thus, the improvement in therapeutic efficacy may also translate

into an increase in unwanted side-effects, particularly if the therapy is systemic and not specifically targeted to bone.

A bone-targeting drug-delivery system for CT would be preferable over extending the drug bioavailability alone for several reasons, including transport efficiency and drug-payload delivery (Cenni, Granchi et al. 2008). However, some key issues should be considered prior to generalizing the advantage of administering PEGylated sCT to treat conditions of low bone volume.

One of the clinical indications of sCT is to inhibit bone resorption by regulating both the number and activity of osteoclasts (OC) (Suzuki and Takahashi 2001; Yamamoto, Noguchi et al. 2005; Yamamoto, Yamamoto et al. 2006; Granholm, Lundberg et al. 2007; Granholm, Lundberg et al. 2008; Karsdal, Henriksen et al. 2008), and by inducing profound rearrangement of the osteoclast cytoskeleton which results in the inhibition of osteoclast motility (Warshafsky, Aubin et al. 1985). These antiresorptive effects are mediated by sCT interaction with calcitonin receptors (CTRs) found primarily upon bone-resorbing OC (Sexton, Findlay et al. 1999) via activation of adenylyl cyclase enzyme activity (Jansen-Olesen, Mortensen et al. 1996), leading to greater calcium retention in bone and increase in bone density (Chabre, Conklin et al. 1992; Erlacher, Kettenbach et al. 1997; Hizmetli, Elden et al. 1998; Ballica, Valentijn et al. 1999; Casez, Tschopp et al. 2003; Matuszkiewicz-Rowinska, Niemczyk et al. 2004;

Hejdova, Palicka et al. 2005; Lee, Kim et al. 2010; Pappa, Saslowsky et al. 2011).

Although the major site of action of calcitonin is the calcitonin receptor (Sixt, Messlinger et al. 2009) (CTR, a G-protein coupled receptor), found primarily on osteoclasts (Inoue, Shih et al. 1999; Samura, Wada et al. 2000; Kukita, Kukita et al. 2001; Wada, Yasuda et al. 2001; Granholm, Lundberg et al. 2007; Granholm, Lundberg et al. 2008; Silvestris, Cafforio et al. 2008), CTRs are also widely distributed in non-skeletal tissues. CTRs in other tissues have been identified and high affinity calcitonin binding has been demonstrated in the intestine and kidney (Warshawsky, Goltzman et al. 1980), brain (Goltzman and Mitchell 1985), lung (Fouchereau-Peron, Moukhtar et al. 1981), placenta (Nicholson, D'Santos et al. 1988), ovaries (Chausmer, Stuart et al. 1980; Gorn, Lin et al. 1992), testes (Chausmer, Stuart et al. 1980), and spermatozoa (Silvestroni, Menditto et al. 1987).

Competition for the uptake of available free plasma calcitonin among such receptors and the high vascularity of kidney and intestine further leads to the low bioavailability of free calcitonin available for osteoclast inhibition. Thus, a drug-delivery strategy which increases the targeting and localization of CT to bone, and increases the retention time of CT in bone, would clearly increase the local concentration of CT available to the local bone microenvironment, with the potential to positively impact the effective drug dosage and monetary costs of therapy,

whilst reducing unwanted side-effects (Pierce and Waite 1987; Fujisaki, Tokunaga et al. 1997; Kasugai, Fujisawa et al. 2000; Yokogawa, Miya et al. 2001).

Also, in his studies measuring tissue distribution of PEGylated sCT, Yoo et al (2000) reported the highest amounts of sCT in kidney followed by in the liver, then lungs, spleen, heart and thyroid (Yoo, Jun et al. 2000).

Hence, the improved pharmacokinetic profile of PEGylated sCT relative to native sCT would still not necessarily translate into optimal bone-based therapeutic effects because of the disproportionate accumulation of PEGylated sCT in non-bone tissues, with the competitive uptake of sCT by such non-bone tissue resident CTRs, and degradation of sCT accumulated in these tissues. These factors collectively results in a small amount of active sCT available to reach bone and act upon its OC-resident CTRs, despite PEGylation.

Thus, in order to develop better bone based sCT therapeutics, it is imperative to improve sCT pharmacokinetics whilst also imparting bone mineral affinity. This offers the potential to positively impact sCT therapy *in vivo*, whilst reducing its concentration in non-bone loci containing the CTR.

Breakage of the cys 1 and 7 disulfide bond of sCT in order to effect the conjugation of lipid to sCT at cys 1 and 7 via thio-ether bonds, or PEGylation at Lys 11, 18 or the N-terminal amine did not affect sCT bioactivity (Na, Youn et al. 2004; Cheng, Satyanarayanajois et al. 2007).

Similarly, replacement of all Lys residues by Arg rendered a fully active CT analog, [Arg11, 18] sCT (D'Santos, Nicholson et al. 1988). Furthermore, elimination of the α -amino function from the N-terminus of CT, or its acetylation, resulted in the enhancement of hypocalcemic potency relative to the parent peptide (Rittel, Maier et al. 1976). Thus a bone targeting conjugates of CT utilizing these sites would likely retain CT bioactivity.

sCT is unstable in aqueous reaction conditions previously used to conjugate BP with model proteins. It has a tendency to aggregate into long, thin fibrillar aggregates, yielding a viscous and turbid dispersion in high concentration buffer. Although CT is soluble and stable in organic solvents, the insolubility of bisphosphonate in these solvents is a major obstacle to synthesize sCT-BP conjugates.

1. 8. THESIS PROPOSAL

Objective

The objective of this thesis was to synthesize and characterize various PEGylated and non-PEGylated sCT-BP conjugates and evaluate their efficacy in bone diseases like osteoporosis, osteoarthritis and adjuvant arthritis.

Hypothesis

Conjugation of BP or PEG to sCT would generate bioactive bone targeting sCT analogues. Such, BP conjugated PEGylated or non-PEGylated sCT would bind and concentrate in bone mineral hydroxyapatite (HA). This could improve sCT antiresorptive efficacy.

Significance

The broadest significance of this proposal is its potential to achieve improvements in the treatment efficiency of bone diseases. This work addresses one of the important problems of bone disease treatment – delivery of drugs to bone. Potential advantages of the proposed sCT delivery system are: selective adsorption and localization in bone, reduction of side-effects resulting from systemic administration of free sCT, improvement in physicochemical and pharmacokinetic properties of sCT and applicability of design principles to the delivery of other drugs and diagnostic agents. This project will generate an improved bone targeted sCT delivery system that could find clinical utility in osteopenic bone disease and related indications including osteoporosis (OP), osteoarthritis (OA), Paget's disease (PD) and hypercalcaemia of bone cancers (HC), osteolytic tumors, rheumatoid arthritis, psoriatic arthritis, ankylosing spondylitis, osteopenia, and hypercalcemia.

CHAPTER 2: EXPERIMENTAL PROCEDURES

2. 1. MATERIALS

Salmon calcitonin was purchased from Calbiochem (USA). NHS-PEG-MAL was from Creative Biochem (USA), sulfo-SMCC from Molecular Biosciences inc. (USA) and thiol-Bisphosphonate used here was synthesized by Surfactis Technologies Inc, France. High performance liquid chromatography (HPLC) grade water, dimethyl formamide (DMF), dimethyl sulfoxide (DMSO) and other reagents were from Sigma-Aldrich (USA).

2. 2. SYNTHESIS OF THIOL REACTIVE sCT

sCT-SMCC

30 μ L sCT in DMF (6.66 mg/mL) was mixed with 5 μ L sulfo-SMCC in DMF (26.182 mg/mL) and 5 μ L 0.8% TEA in DMF (final concentration of TEA 0.1% v/v) was then added. Reaction between the primary $-NH_2$ in sCT and NHS group of sulfo-SMCC was allowed to proceed at room temperature with constant stirring for 30 minutes.

sCT-PEG-MAL

sCT in DMSO (13.72 mg/mL) was mixed with NHS-PEG-MAL in DMSO (51 mg/mL) in 1:5 molar ratio and the reaction between the primary

-NH₂ in sCT and NHS group of NHS-PEG-MAL was allowed to proceed at room temperature with constant stirring for 60 minutes.

2. 3. PROCESS OPTIMIZATION

2. 3. 1. sCT-SMCC

Effect of reaction time: was studied by carrying the above reactions separately for 10, 20, 30, 40, 50, and 60 minutes.

Effect of sulfo-SMCC concentration: was also studied using sCT: sulfo-SMCC at 1:3, 1:5, 1:7 and 1:10 mol/mol ratios in the above manner for 30 min.

Effect of TEA concentration: was evaluated using 0.05, 0.1, 0.2, 0.3 and 0.4% v/v final concentration of TEA and carrying the reaction for 30 minutes using sCT: sulfo-SMCC at 1:5 mol/mol ratios.

2. 3. 2. sCT-PEG-MAL

Effect of NHS-PEG-MAL concentration: was studied using sCT: NHS-PEG-MAL at 1:1, 1:2, 1:3, 1:5 and 1:7 mol/mol ratios in the above manner for 60 minutes.

Effect of reaction time: was also studied by carrying the above reaction for 15, 30, 45 and 60 minutes using 1:3 molar ratio of sCT: NHS-PEG-MAL.

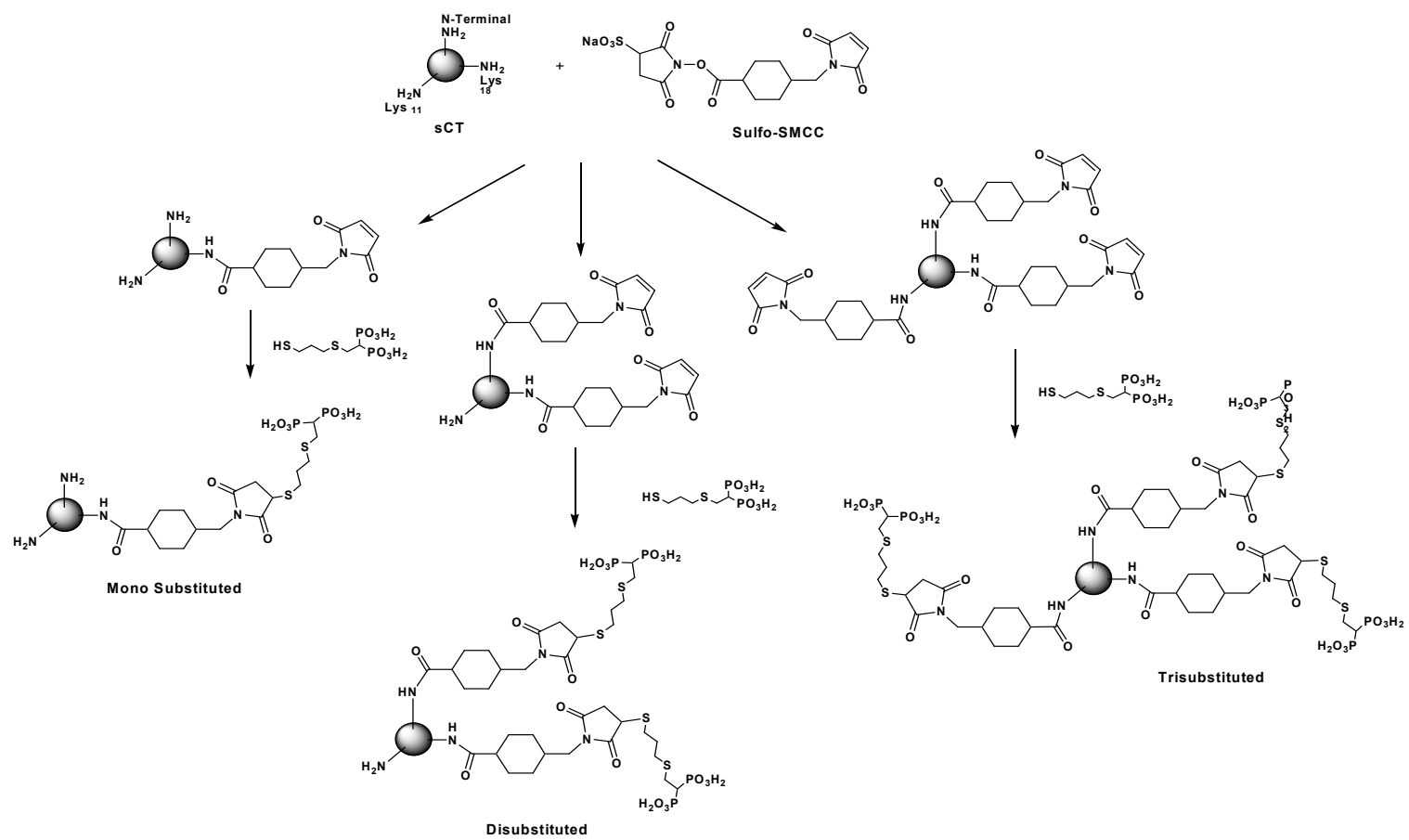


Figure 5: Probable products when sulfo-SMCC is reacted with sCT followed by Thiol-BP

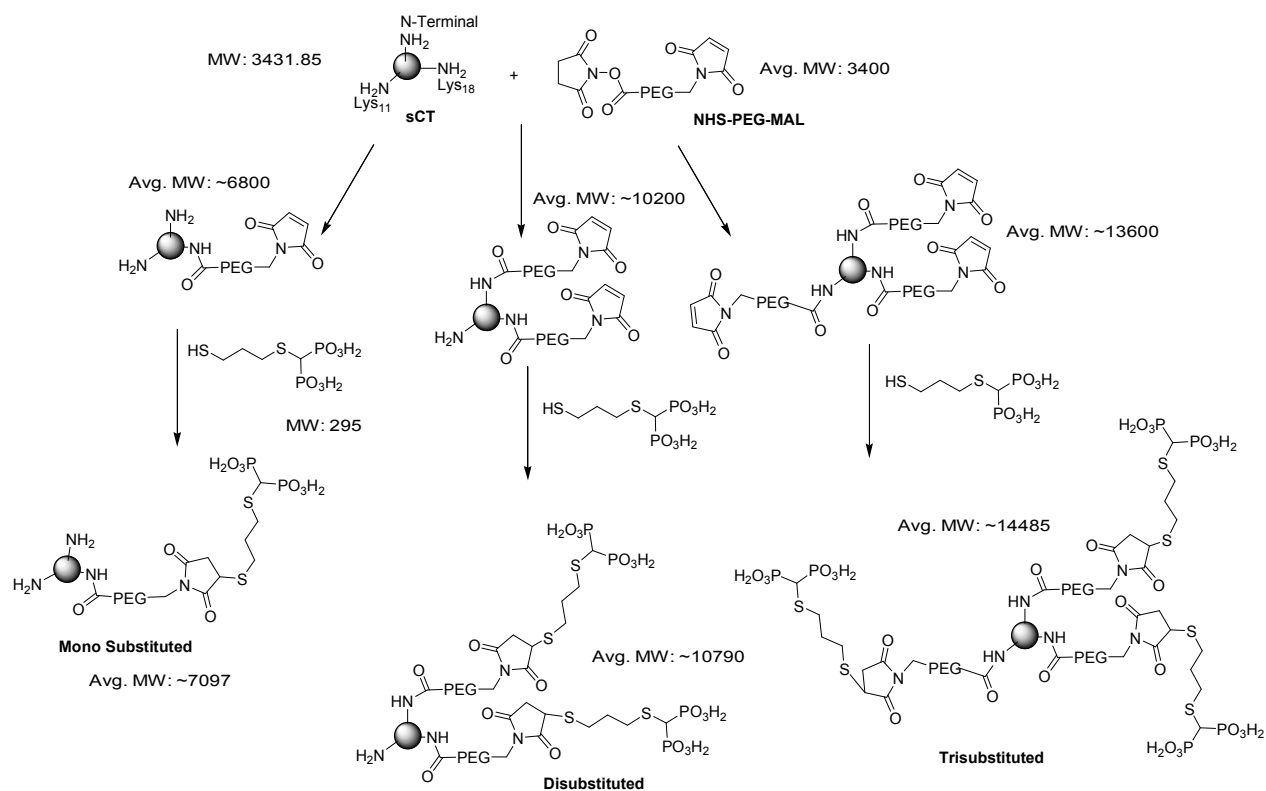


Figure 6: Probable products when NHS-PEG-MAL is reacted with sCT followed by Thiol-BP

DMSO was selected as a sCT and NHS stabilizing solvent because *US Pharmacopeia (USP)* provides acceptance limits based on historical toxicological data for residual solvents found in pharmaceuticals. Such solvents are divided into three classes—Class 1, Class 2 (eg DMF, acetonitrile), and Class 3 (DMSO). The use of Class 1 materials should be avoided whenever possible, and the use of Class 2 materials should be limited to the extent possible. Because of their low toxic potential, Class 3 materials may be used more freely.

2. 4. THIOL-BP CHARACTERIZATION

LC-MS

Thiol-BP was analysed using LC-ESI-MS (Waters Micromass ZQ 4000 spectrometer) coupled to a Waters 2795 separations module with an auto sampler (Milford, MA, USA). The mass spectrometer was operated in negative ionization mode. The nebulizer gas was obtained from an in house high purity nitrogen source. The temperature of source was set at 150°C, and the voltages of the capillary and cone were 3.11 KV and 24 V, respectively. Chromatographic separation was achieved using a Waters (Milford, MA, USA) X TerraMSC18 3.5 µm (2.1×50 mm) as the stationary phase. The mobile phase consisting of a mixture of acetonitrile: water containing 1% formic acid with initial ratio of 20:80, employing a linear gradient to a final ratio of 40:60 v/v over 13 minutes, was delivered at a constant flow rate of 0.2 mL/min.

Reactive thiol content

Amount of available reactive thiol groups present in Thiol-BP was calculated by Ellman's thiol assay. Briefly, 50 μL of 4 mg/mL Ellman's Reagent Solution in 0.1 M sodium phosphate, pH 8.0, and containing 1 mM disodium-EDTA was added to 250 μL of thiol-BP solution mixed and incubated at room temperature for 15 minutes. The yellow color developed was then measured at 412 nm. The amount of reactive thiol group was obtained using a calibration curve obtained with L-cysteine as a control. Accordingly, the amount of thiol BP used was calculated based on these assays.

Phosphate content

The amount of total phosphate was determined using Alendronate sodium (Sigma-Aldrich, USA) as a control using organic phosphate assay. Briefly, 50 μL of thiol BP sample of different concentration was mixed with 30 μL of 10% magnesium nitrate [$\text{Mg}(\text{NO}_3)_2$] in 95% ethanol in glass tubes and ashed over a flame. After boiling in 0.3 mL of 0.5 N HCl for 15 min, 0.1 mL of ascorbic acid (10% w/v) and 0.6 mL of ammonium molybdate [$(\text{NH}_4)_6\text{Mo}_7\text{O}_{24}\cdot 4\text{H}_2\text{O}$] (0.42% w/v in 1 N sulphuric acid [H_2SO_4]) were added to the tubes and the samples were incubated at 37°C for 1 h. The absorbance of the blue color developed was then determined at 820 nm. Amount of phosphate in thiol-BP was calculated using the calibration curve obtained with Alendronate sodium. Similarly,

the amount of phosphate groups in thiol-BP was also compared for the same concentration of Alendronate sodium.

2. 5. COUPLING OF FUNCTIONALIZED sCT WITH THIOL-BP.

Synthesis of sCT-BP

Thiol-BP was dissolved in 10mM phosphate buffer solution (PBS) pH 6.55 at a concentration of 4.225 mg/mL. 960 μ L of this solution (6 μ Mol reactive-SH, 4.056 mg BP) was reacted with functionalized sCT (SMCC) in 20:1 mol/mol (BP/sCT) ratio for 2 h at room temperature in dark. The reaction mixture was then incubated at 4°C overnight.

Synthesis of sCT-cysteine

Control conjugates were synthesized using L-cysteine. Functionalized sCT (sCT-SMCC) synthesized as above was reacted with L-cysteine dissolved in 10mM PBS pH 6.55 in 1: 20 mol/mol (sCT/cys) ratio for 2 h at room temperature in dark and the reaction mixture was then incubated at 4°C overnight.

Synthesis of sCT-PEG-BP

Functionalized thiol reactive sCT analogue (sCT-PEG-MAL) was added intermittently with constant stirring to thiol-BP solution in 100 mM sodium acetate buffer pH 6.8 at 1:20 molar ratio and the reaction between

the thiol reactive MAL groups in functionalized sCT and SH group of thiol-BP was allowed to proceed at room temperature in dark with constant stirring for 2 hours.

2. 6. PROCESS OPTIMIZATION FOR sCT-PEG-BP

The effect of buffer:

The effect of buffer on the coupling of MAL and SH was studied using 100 mM ammonium acetate pH 6.8 and 100 mM sodium phosphate pH 6.8 buffers as above.

The effect of buffer concentration:

The effect of buffer concentration on this reaction was studied using 10, 50 and 100 mM sodium phosphate buffer pH 6.8 in the above manner.

The effect of thiol-BP concentration:

The effect of thiol-BP concentration was determined by carrying the above reaction in 100 mM sodium phosphate buffer pH 6.8 using functionalized sCT: thiol-BP at 1:5, 1:10, 1:20 and 1:40 molar ratios.

2. 7. CONJUGATE CHARACTERIZATION

MALDI-TOF

In all cases, the reaction products were monitored by MALDI-TOF and the peak properties of reaction products were considered as the parameter for process optimization. Samples were diluted twenty fold in 50% acetonitrile/water. One μL of each sample was mixed with 1 μL of sinapic acid (10 mg/mL in 50% acetonitrile/water + 0.1% trifluoroacetic acid). One μL of the sample/matrix solution was then spotted onto a steel target plate and allowed to air dry. All MALDI-MS experiments were carried out using a Bruker Ultraflex MALDI-ToF/ToF (Bruker Daltonic GmbH) in positive mode. Data analysis was carried out using the flexAnalysis software (Bruker Daltonic GmbH).

Tris-tricine SDS-PAGE

Briefly, 10 μL of sample solution was mixed with 20 μL of loading buffer (premixed protein sample buffer for peptides and small proteins-Bio-Rad, USA, Cat#161-0739) and loaded in wells of the 16.5% tris-tricine/peptide precast gel (Bio-Rad, USA, Cat# 161-1107). Reference Polypeptide SDS-PAGE Standards (Bio-Rad, USA, Cat#161-0326) was diluted with sample buffer at 1:20 v/v ratio, heated at 95°C for 5 minutes, cooled and loaded at 5 μL /well. After electrophoresis at 100 V using tris/tricine/SDS buffer (Biorad, Cat#161-0744) , the gel was fixed with a solution of 40% methanol, 50% water and 10% acetic acid for 30 minutes.

Fixing solution was then removed and the gel was stained for 1 hr with Coomassie brilliant blue R-250 (0.008% in 10% acetic acid) at 95°C for 20 seconds, followed by staining at room temperature for 15 minutes. Gels were destained in water overnight and scanned.

Purification

Conjugates were purified by dialysis. MWCO 1000 D, Spectrum Laboratory, USA was used for sCT-BP to remove unconjugated BPs and MWCO 3500 D was used for sCT-PEG-BP. In both cases, the dialysis media was 20 mM acetate buffer pH 5. Buffer change was done at the time intervals of 1, 2, 3, 4, 5, 6, 12, 24, 48, 72, and 96 hours. Dialysis was performed at 4°C.

Alternatively, sCT-PEG-BP conjugates were purified using Zebra spin size exclusion chromatographic columns. 20 mM acetate buffer pH 5 was exchanged for storage buffer by placing the column in a 1.5 mL microcentrifuge collection tube and centrifuging at 1,000 × *g* for 1 minute to remove storage solution. Then, 50µL of buffer was added on top of the resin bed and centrifuged at 1,000 × *g* for 1 minute to remove buffer. This was repeated for two to three additional times. Finally, columns were placed in a new collection tube and the sample was placed at the top of the compact resin bed and centrifuged at 1,000 × *g* for 2 minutes to collect the sample.

Assay of sCT and phosphates: Extent of BP coupling per sCT

Amount of sCT in sCT-BP conjugates was determined by Micro BCA protein assay. Briefly, an aliquot of 100 μL suitably diluted sample was mixed with 100 μL of working reagent (micro BCA reagent A, B and C in a volume ratio of 50: 48: 2). The mixture was incubated at 37°C for 2 h and then cooled down to room temperature. Absorbance at 562 nm was measured using 96-well microplate reader. The amount of sCT was calculated by converting the absorbance into mass using the standard curve.

Similarly, the amount of total phosphate was determined using Alendronate sodium (Sigma-Aldrich, USA) as a control using an organic phosphate assay. Briefly, 50 μL of thiol BP sample of different concentration was mixed with 30 μL of 10% $\text{Mg}(\text{NO}_3)_2$ in 95% ethanol in glass tubes and ashed over a flame. After boiling in 0.3 mL of 0.5 N HCl for 15 min, 0.1 mL of ascorbic acid (10% w/v) and 0.6 mL of $(\text{NH}_4)_6\text{Mo}_7\text{O}_{24}\cdot 4\text{H}_2\text{O}$ (0.42% w/v in 1 N H_2SO_4) were added to the tubes and the samples were incubated at 37°C for 1 h. The absorbance of the blue color developed was then determined at 820 nm. The amount of phosphate in thiol BP was calculated using the calibration curve obtained with Alendronate sodium. The BP concentration (μM) of a sample was divided by its sCT concentration (μM) to yield an average number of BP coupling per sCT.

2. 8. IN-VITRO EVALUATION

Bone mineral affinity

100 μ L of purified conjugate solution containing approximately 60 μ g of sCT was mixed with 5 mg hydroxyapatite (HA) in 100 μ L 10 mM phosphate buffer (pH 7.0) in microcentrifuge tubes in duplicate. As a reference, control samples were incubated in tubes without HA (i.e., 0% of binding), and the effect of sCT modification (due to chemical conjugation) upon mineral affinity was also analyzed by HA binding assay of sCT-cysteine conjugates.

The tubes were incubated at room temperature on a shaker for 3 h, and centrifuged at 5000 g for 5 minutes to separate the HA from the supernatant. SCT concentration in the supernatant was determined using the micro BCA protein assay (Pierce, USA). HA centrifugate remaining after removal of supernatant was washed five times using 1 mL of water each time and the last washing after centrifugation at 5000 g for 5 minutes was collected. Both the washings and the HA centrifugate were then analyzed for sCT as described above. The amount of sCT in the supernatant, washings and HA centrifugate was then inferred by measuring the absorbance at 562 nm, with a value of 100% for control samples without HA.

Bone mineral specificity

100 μL of purified conjugate or control sCT solution containing approximately 60 μg of sCT was mixed with 5 mg each of calcium carbonate, calcium pyrophosphate, tricalcium phosphate and calcium citrate in 100 μL 10 mM phosphate buffer (pH 7.0), incubated at room temperature on a shaker for 3 h, centrifuged at 5000 g for 5 minutes, and centrifugates were washed with water and analyzed for sCT as above.

sCT secondary structure

For a more detailed analysis of the influence of BP or PEG-BP on structural alteration of sCT, the secondary structure of sCT analogues was studied using circular dichroism (CD). The CD spectrum of sCT, sCT-PEG and sCT-PEG-BP was measured in 20 mM acetate buffer pH 5.0. CD spectra were obtained with a ConvCD spectrophotometer instrument. Spectra were acquired over a wavelength range of 190 to 260 nm. The nitrogen flow rate was set at 5 L/min. The sample cuvette (100 μL) was cleaned with blank samples e. g. 20 mM sodium acetate buffer pH 5 (used for its stabilizing effect on calcitonin). The spectra of test samples, which comprised ~ 400 $\mu\text{g}/\text{mL}$ of sCT, sCT-PEG or sCT-PEG-BP in the above buffer, were recorded with the corresponding buffer serving as blanks.

***In vitro* cell viability assay**

RAW 264.7 cells (ATCC VA, USA) were seeded on 96 well plates at an initial density of 2×10^4 cells/well and incubated in 200 μ L GIBCO High Glucose 1X Dulbecco's Modified Eagle Medium (DMEM) (Invitrogen CA, USA) supplemented with 4.5 g/L D-glucose, L-glutamine, 110 mg/L sodium pyruvate, 10% heat inactivated fetal bovine serum (FBS) and 1% penicillin-streptomycin (10000 U/ mL; Invitrogen) in a Thermo Fisher Scientific Water Jacketed CO₂ incubator (37°C, 5% CO₂) until the cells were 80 % confluent.

After 72 hrs, media was replaced by 200 μ L basic DMEM media without FBS and incubated for 30 minutes. Then the media was replaced by 100 μ L basic DMEM media containing sCT, sCT-PEG and sCT-PEG-BP equivalent to 100, 500 and 1000 nM final sCT concentration and the cells were incubated for 4 hrs at 37 °C.

sCT containing media was then replaced by 100 μ L of basic media containing (3-[4,5-dimethylthiazol-2-yl]-2,5-diphenyl tetrazolium bromide) (MTT) at a concentration of 100 μ g/well and incubated for another 4 hrs at 37°C. After removing the supernatant and washing twice with phosphate buffer saline, purple formazan crystals formed were dissolved in 200 μ L solubilization solution (*in vitro* toxicology assay kit, # TOX-1, Sigma Aldrich, St. Louis, USA) and the absorbance was measured at 570 nm using a microplate reader. The experiment was performed for n=8 and the absorbance of wells containing cells without sCT treatment was

considered as 100% viable and used to calculate the relative viability of sCT treated cells.

Anti-calcitonin antibody binding ability

sCT or sCT analogues equivalent to 1µg/well were added to calcium phosphate coated osteoclast activity assay substrate plate (OCT USA, Inc.) in duplicate and the binding of BP to the calcium phosphate was allowed for 1 hour in the presence of 100 µL of 100 mM sodium phosphate buffer pH 7. Plates were then washed three times with the same buffer containing Tween 80 (PBST).

To avoid nonspecific binding, the wells were incubated with 3% Bovine Serum Albumin for 1 h at room temperature. After washing, the wells were incubated with 100µL of 1:5000 diluted mouse anti-salmon calcitonin primary monoclonal antibodies for 1 h at room temperature. The wells were washed three times with PBST and the bound antibodies were detected using secondary antibody, goat anti-mouse IgG conjugated with horseradish peroxidase (GAM-HRPO) at 1:5000 dilution for one hour at room temperature. After final washing, 100 µL of 3, 3', 5, 5'-tetramethylbenzidine (TMB substrate) was added to each well and incubated for 15 min at room temperature. The optical density (OD) was measured at 650 nm using an ELISA Vmax kinetic microplate reader (Molecular Devices Corp., California, USA).

sCT receptor binding ability and *in vitro* bioactivity

T47D cells (ATCC VA, USA) were cultured in RPMI-1640 culture medium containing 1% penicillin–streptomycin, 10% fetal bovine serum, and insulin (0.2 IU/mL). Cells were seeded on 48 well plates at an initial density of 5×10^4 cells/well and incubated in 95% air and 5% CO₂ at 37°C for 2 days. Cells were then washed with Hank's balanced salt solution (HBSS) and pre-incubated in RPMI-1640 culture medium devoid of FBS, insulin and antibiotics. Cells were then dosed with phosphodiesterase inhibitor, 3-isobutyl-1-methyl-xanthine (IBMX, 0.2 mM) and incubated at 37 °C for 30 min. 100 nM of sCT, BP-conjugated sCT, or cysteine-conjugated sCT (conjugation control) was then added to the cells and incubated for 20 min at 37 °C.

After removing the supernatant, cells were rinsed three times in cold PBS and resuspended in 500 µL of Cell Lysis Buffer. Cells were frozen at -20°C and thawed with gentle mixing. The freeze/thaw cycle was repeated three times and the mixture was centrifuged at 600 g for 10 minutes at 2-8° C to remove cellular debris. The supernatant was collected and stored at -20°C. Cyclic adenosine monophosphate (cAMP) concentrations were then measured using the cAMP Enzyme Immuno-Assay (EIA) kit (KGE002B, R & D systems, USA). Increased cAMP production in response to the different forms of sCT was calculated using a calibration curve as per the manufacturer's protocol.

2. 9. *IN VIVO* BIOACTIVITY

Normal rats

Pharmacodynamic response of sCT analogue was evaluated *in vivo* by analyzing plasma calcium concentration in the rat. Sprague Dawley female rats weighing 230-260 g (about 6 weeks old) were purchased from our University Biosciences facility and housed in our animal care facility. All experimental protocols were approved by the Animals Care and Use Committee at the University of Alberta. Rats were divided randomly into six groups of 3 animals each and the pharmacodynamic response was assessed following subcutaneous administration of sCT or analogue equivalent to 20 IU sCT/kg body weight. The control group received 160.71 ng/kg (0.547 nMol/kg) of thiol-BP in 20 mM acetate buffer pH 5. This concentration corresponded to the “three” moles of thiol-BP per sCT as if all the three amines in sCT reacted with thiol-BP. Rats were anesthetized using isoflurane inhalation anesthesia and 200 μ L blood samples were obtained from jugular vein in heparinized Eppendorf microtubes before drug injection. Then 100 μ L of sCT or equivalent analogues in 20 mM sodium acetate buffer pH 5.0 was injected and blood samples were collected at 1, 2, 3 and 4 hours post injection. Blood plasma was obtained by centrifuging samples at 5000 rpm for 10 min and collecting the supernatant. Plasma calcium level was assayed using the QuantiChrom™ calcium assay kit (BioAssay Systems, CA USA).

Osteoporotic rats

Six-week-old (~275 gm) ovariectomized (OVX) female Sprague-Dawley rats were randomly allocated into the following 4 groups (n = 4): bisphosphonate in buffer (OVX), calcimar (marketed product), sCT-BP and sCT-PEG-BP groups. All rats were confirmed to be osteoporotic using micro-CT at time 0. All treatments lasted for 12 weeks. OVX control group received 160.71 ng/kg (0.547 nMol/kg) of thiol-BP in 20 mM acetate buffer pH 5. Other groups received corresponding compounds equivalent to 2.5 IU/kg body mass of sCT for three months. All rats received daily subcutaneous injection of compounds in 20 mM acetate buffer pH 5. Samples were diluted so that the injection volume was 120 µL/kg.

According to the calcimar monograph 1 IU is approximately equivalent to 0.2-0.25 µg of sCT. IU represents the biological activity. This could be different for the same weight of sCT from the same or different manufacturers. IU is determined by s. c. administering the test sCT to normal rats. Percentage fall in plasma sCT level from the baseline is determined and compared with the decrease in plasma calcium level reduction induced by previously standardized reference sCT.

Plasma calcium can be increased by conditions other than bone resorption e. g. high calcium in diet. Hence, the development OP was confirmed by measuring the actual reduction in BMD using micro-CT as described previously. However, the effect of sCT-BP or sCT-PEG-BP on

serum calcium was measured and compared with unmodified sCT (calcimar) to see any change in bioactivity of sCT due to conjugation.

All rats were also given strontium ranelate (PROTOS[®], Servier Laboratories, Australia) 308 mg/Kg/day orally for the last 10 days prior the euthanasia as a source of Sr⁺² tracer for the dynamic labelling of bone turnover to study the mechanism of sCT, sCT-BP or sCT-PEG-BP induced bone microstructure alteration. Strontium ranelate administration was performed using an 18 gauge curved animal feeding needle (Harvard Apparatus). At the end of study period, blood plasma was obtained by centrifuging blood samples obtained by cardiac puncture at 5000 rpm for 10 min and collecting the supernatant. Plasma calcium level was assayed using the QuantiChrom[™] calcium assay kit (BioAssay Systems, CA USA).

Osteoarthritic rats

An animal model of osteoarthritis was induced in 6-week old (~260 g) female Sprague-Dawley rats surgically by medial meniscectomy surgery (Bendele 2001). In brief, rats were anesthetized with isoflurane, and the right knee joint was shaved and disinfected prior to joint exposure. The joint was exposed through the parapatellar approach. The medial collateral ligament was snipped with a scalpel, followed by medial meniscus resection. The joint surface was flushed with sterile saline after

surgery and both the joint capsule and skin were sutured using size 5-0 absorbable Vicryl suture (Ethicon Inc., CA). An analgesic dose (0.1 mg/Kg) of Meloxicam (Metacam[®], Boehringer Ingelheim Ltd, CA) was administered subcutaneously to rats immediately after the surgery. Animals were allowed to freely exercise in cages during the course of the study. Animals were euthanized at 8 weeks post surgery.

Experimental design: After the surgery animals were randomly divided into two groups: sCT-PEG-BP treatment group and untreated group (n=3). Rats were euthanized at 8 weeks. Rats in the normal group were uninjured i.e. they were not osteoarthritic.

Drug dosage: All treatments started the day after surgery and lasted until the euthanasia. Normal and OA control group received 160.71 ng/kg of thiol-BP in 20 mM acetate buffer pH 5 subcutaneously twice weekly. sCT-PEG-BP treatment OA group received sCT-PEG-BP equivalent to 2.5 IU/kg body mass of sCT subcutaneously twice weekly. Samples were diluted so that the injection volume was 120 μ L/kg.

All rats were also given strontium ranelate (PROTOS[®], Servier Laboratories, Australia) 308 mg/Kg/day orally for last 10 days prior euthanasia as described in the previously. At the end of study period, blood plasma was obtained by centrifuging blood samples obtained by cardiac puncture at 5000 rpm for 10 min and collecting the supernatant.

Plasma calcium level was assayed using the QuantiChrom™ calcium assay kit (BioAssay Systems, CA USA).

2. 10. *IN VIVO* EFFICACY IN BONE DISEASES

Osteoporotic rats

Animals: Six-week-old (~275 gm) ovariectomized (OVX) female Sprague-Dawley rats were obtained from Charles River Laboratories. They were randomly allocated into the following 4 groups (n = 4): buffer and bisphosphonate, calcimar (marketed product), sCT-BP and sCT-PEG-BP groups. All rats were confirmed to be osteoporotic using micro-CT at time 0.

Drug administration: All treatments lasted for 12 weeks. OVX and sham control group received 160.71 ng/kg of thiol-BP in 20 mM acetate buffer pH 5. Other groups received corresponding compounds equivalent to 2.5 IU/kg body mass of sCT as daily subcutaneous injection in 20 mM acetate buffer pH 5. Samples were diluted so that the injection volume was 120 µL/kg.

In vivo micro-CT: *In vivo* micro-CT was performed at 0, 1, 2 and 3 months. Isoflurane was used as the anesthetic for the duration of the procedure (~35 minutes). Rats were placed supine in the bed of a Skyscan 1076 *in vivo* X-ray microtomograph. The right hind limb was extended and secured to the gantry bed using masking tape to limit

movement. Radiographs encompassed the entire stifle joint in a single field of view. Two-dimensional (2-D) projections were obtained using an x-ray source setting of 70 kV and 139 μ A, with beam filtration through a 1.0-mm aluminum filter. Data were collected every 0.5° rotation step through 180°. The scanning width was 35 mm, and the height was 17 mm.

Reconstruction was performed employing a modified Feldkamp back projection algorithm. The resulting raw image data was Gaussian filtered and globally thresholded at the fixed range of 0.0-0.0752 cross-section to image conversion to extract the mineral phase. Using transverse image slices, trabecular bone was segmented from the cortical bone using vendor-supplied analysis software (CT-Analyser, Skyscan, BE), with semi-automated contouring. Bridging of the metaphyseal growth plate was used as the anatomical landmark for the proximal origin of trabecular bone. The selected region of interest spanned approximately 50 slices, and was analyzed using morphometric software to determine trabecular bone volume ratio (Bone Volume/Tissue Volume [BV/TV]), and volumetric cortical Bone Mineral Density (BMD, g/cm^3), after calibration with known hydroxyapatite “phantoms”.

Adjuvant arthritic rats

Animals:

Eight weeks old male Sprague Dawley rats weighing approximately 400-550g were divided into four groups (n=4/group) namely thiol-BP in 20

mM sodium acetate buffer, pH 5, calcimar, sCT-BP in in 20 mM sodium acetate buffer, pH 5, and sCT-PEG-BP in 20 mM sodium acetate buffer, pH 5. Blinding was observed to mask the identity of the compounds from the person under taking the drug administration and physical measurements.

RA induction:

Each rat received 0.3 mL of 65mg/mL *Mycobacterium butyricum* finely ground and suspended in squalene, in the tail base. Rats were then housed in standard plastic rat cages (two per cage) in a room with 12hrs day and night light cycle. They were provided with ample supply of water and standard rat chow.

Drug dosing:

Each rat was subjected to individual treatment as being decided by their specific group. Thiol-BP control group received 160.71 ng/kg of thiol-BP in 20 mM acetate buffer pH 5. Other groups received corresponding compounds equivalent to 20 IU/kg body mass of sCT. All rats received daily subcutaneous injection of compounds in 20 mM acetate buffer pH 5. Samples were diluted so that the injection volume was approximately 100 μ L/kg.

All rats were also given strontium ranelate (PROTOS[®], Servier Laboratories, Australia) 28.57 mg/Kg/day orally for the duration of study.

Rats were observed for visible signs of inflammation until 21 days. Effect of drug intervention upon pre-adjuvant arthritis development was studied by evaluating % weight loss, paw diameter, ankle joint diameter, paw swelling (i.e., volume), joint volume and bone erosion by micro-CT and compared to controls.

In vivo micro-CT: *In vivo* micro-CT was performed at base line (day 1) and at the end of study (21 days) using the method described above.

RA disease observation:

To measure the disease progression, left and right paw and ankle joint width of each animal was measured daily from day 0 to the study endpoint i. e. day 21 post adjuvant injection, using calliper. Similarly, the paw volume was measured using the water displacement method. On 21 days post injection, all animal were euthanized.

2. 11. sCT DOSE ESCALATION IN OSTEOPOROTIC RATS

Animals: Six-week-old (~275 gm) ovariectomized (OVX) female Sprague-Dawley rats were obtained from Charles River Laboratories. They were randomly allocated into the following 11 groups (n = 3): OVX buffer, OVX bisphosphonate in buffer, calcimar (marketed product) (5, 10

and 20 IU/kg), sCT-BP (5, 10 and 20 IU/kg) and sCT-PEG-BP (5, 10 and 20 IU/kg) groups. All rats were confirmed to be osteoporotic using micro-CT at time 0. μ CT scanning was performed as described in previous section and the decrease in bone mineral density (BMD) and bone volume (BV/TV %) in OVX rats was compared with sham operated rats (ovary not excised) to confirm OP development.

In human the sCT dose is 100 IU per day. This is equivalent to 1.43 IU/kg/day for an average person weighing 70 kg. As the exact dose of sCT in OP rats is not known and also the behaviour of bone targeting sCT is not previously studied, 3-13 times higher doses compared to the human doses were administered.

Drug administration: All treatments lasted for 12 weeks. OVX buffer group received 20 mM acetate buffer pH 5. OVX bisphosphonate control group received 160.61 ng/kg of thiol-BP in 20 mM acetate buffer pH 5. Calcimar (marketed product), sCT-BP and sCT-PEG-BP groups received corresponding compounds equivalent to 5, 10 and 20 IU/kg body mass of sCT. All rats received daily subcutaneous injection of compounds in 20 mM acetate buffer pH 5. Samples were diluted so that the injection volume was approximately 40 μ L rat depending on their weight.

Similarly, all rats were also given daily dose of strontium ranelate (PROTOS[®], Servier Laboratories, Australia) orally for the duration of study.

In vivo micro-CT: *In vivo* micro-CT was performed at 0, 1, 2 and 3 months as described for osteoporotic rats.

2. 12. STATISTICAL ANALYSIS

In micro-CT studies, results are presented as the mean \pm SD. Statistical analyses were conducted using the SPSS statistics software package (version 13.0; SPSS). For the quantitative measures of bone volume, unpaired t-tests were used to compare groups. P values less than 0.05 were considered significant.

In all other studies, statistical analysis was conducted using Microsoft excel 2007. Results are presented as the mean \pm standard deviation. Unpaired t-tests of two samples assuming unequal variances were used to assign significance between groups, with a P-value of less than 0.05 as the threshold for significance.

CHAPTER 3: RESULTS

3.1. SYNTHESIS OF THIOL REACTIVE sCT

sCT-SMCC

Synthetic sCT is a polypeptide of 32 amino-acids with a molecular weight of 3431.85 daltons. **Figure 7** represents MALDI-TOF spectra of sCT with a peak at 3433.7. Other peaks represent either impurities or degradation products during analysis.

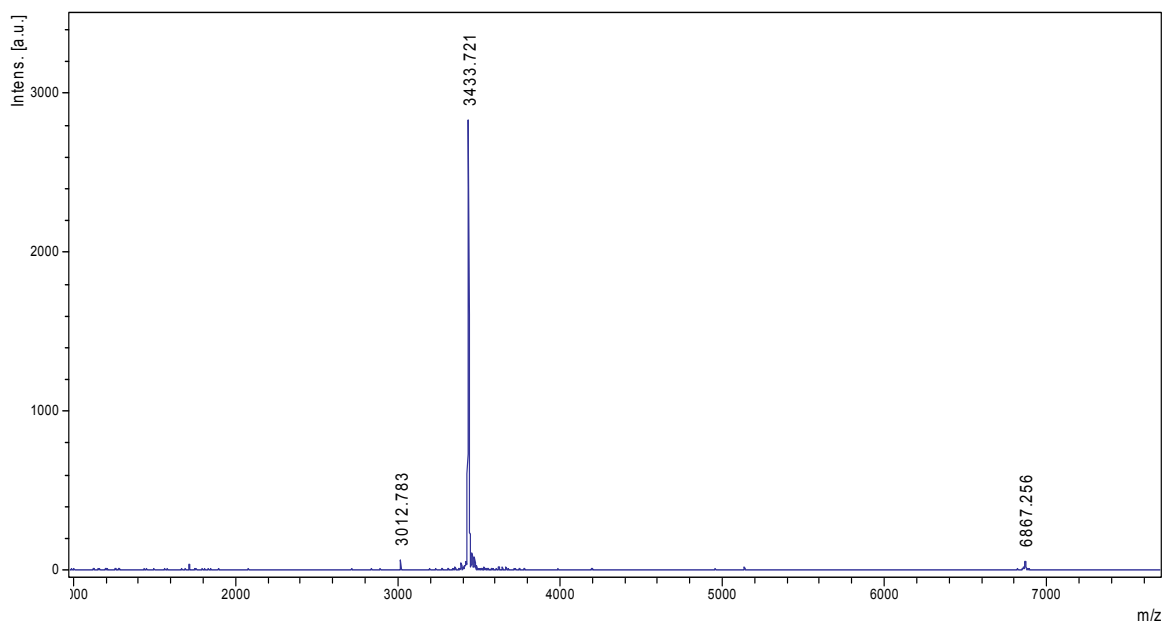


Figure 7: MALDI-TOF spectra of sCT dissolved in DMSO at a concentration of 13.72 mg/mL.

As shown in **figure 5**, when the primary amines in sCT viz Lysine 11, Lysine 18 and N-terminal are reacted with the NHS functional group of sulfo-SMCC, there exists the probability of formation of three intermediate conjugates: mono-, di- and tri-substituted products with respective molecular weights of 3651.7, 3871.9 and 4093.2.

These peaks are shown in **figure 8**. DMF was chosen as the reaction medium because of the hydrolytic instability of NHS in aqueous solution and also due to the instability of sCT in aqueous solution. TEA was added for its favourable effect in the reaction of $-NH_2$ with the NHS group in sulfo-SMCC.

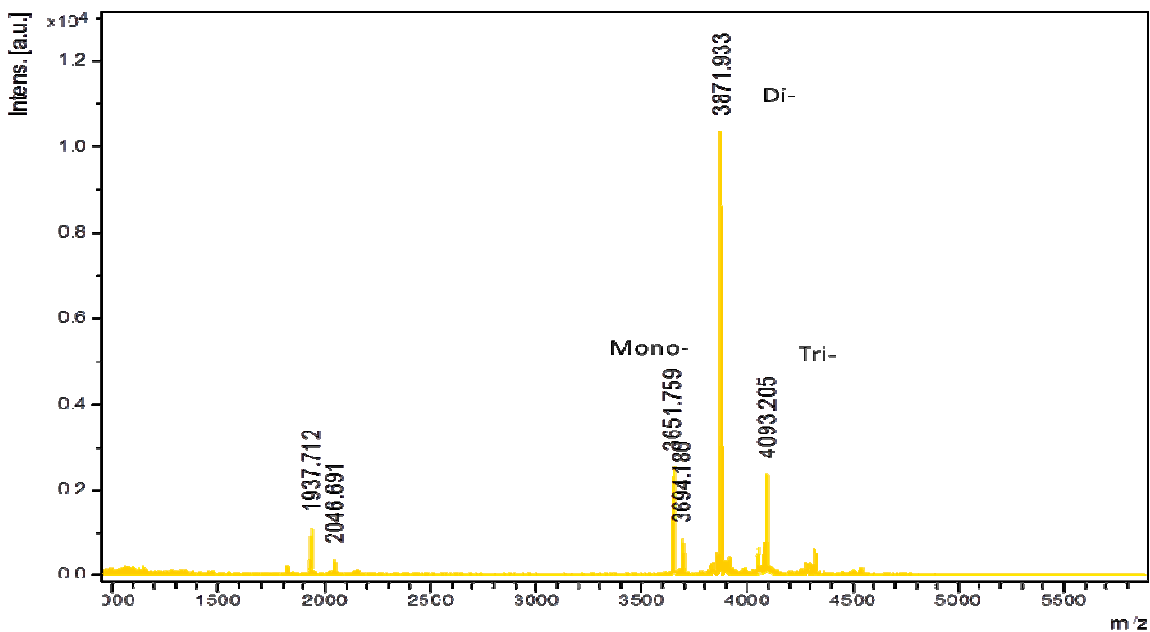


Figure 8: MALDI-TOF spectra of the products of sCT and sulfo-SMCC reaction

sCT-PEG-MAL

Possible reaction products of sCT with NHS-PEG-MAL are shown in **figure 6**. sCT has three primary amines at Lys 11, Lys 18 and N-terminal, which can react with the NHS functional group of NHS-PEG-MAL to generate three intermediate conjugates: mono-, di- and tri-substituted thiol reactive sCT analogues.

Figure 9 represents MALDI-TOF spectra of NHS-PEG-MAL with its average molecular weight. PEG is a polymer composed of ethylene glycol monomers. In case of higher molecular weight (MW) PEGs, the exact number of ethylene glycol units utilized in the reaction cannot be precisely controlled during polymerization. Hence these PEGs are polydispersed comprising of many individual polymers of different MW (the broad peak starting from ~2200-4400). The MW is expressed as average MW (~3500).

As reported in the literature, the formation of mono-PEG-sCT and di-PEG-sCT was favored over the formation of tri-PEG-sCT (**Figure 10**). However, the peak intensity and area in MALDI-TOF analysis showed that the formation of di-substituted was favored over mono-substituted. Loss of sCT peak and the appearance of major peaks representing NHS-PEG-MAL suggested that the reaction was complete. DMSO was chosen as the reaction medium because of the instability of NHS and sCT in aqueous solutions. sCT is highly soluble and highly stable in DMSO. *US Pharmacopeia (USP)* classifies DMSO as a class 3 solvent based on

historical toxicological data. Because of that low toxic potential, Class 3 solvents may be used more liberally.

3.2. PROCESS OPTIMIZATION

3.2.1. sCT-SMCC

The effect of reaction time

The effect of reaction time was studied to optimize the duration of reaction. Results are presented in **Figures 11- 16** for 10, 20, 30, 40, 50, and 60 minutes respectively. Although there was formation of mono- and di-substituted products, the reaction was incomplete at 10 minutes as a peak at 3430 representing sCT remained. However, the reaction was complete at or after 20 minutes as shown by the loss of the sCT peak. Formation of tri-substituted products increased with increased time. Formation of tri-substituted products could be favorable in terms of bone targeting potential due to the presence of more BP molecules per sCT molecule. However, in the literature, it has been reported that the increased protein substitution could substantially alter its secondary structure, receptor binding potential and hence the activity. Since sCT-BP conjugation was never reported before, we arbitrarily selected a reaction time of 30 minutes so that the reaction was complete and the tri-substitution was still minimal. Reaction time of 20 minutes could have been selected but we allowed the reaction to proceed for 10 more minutes

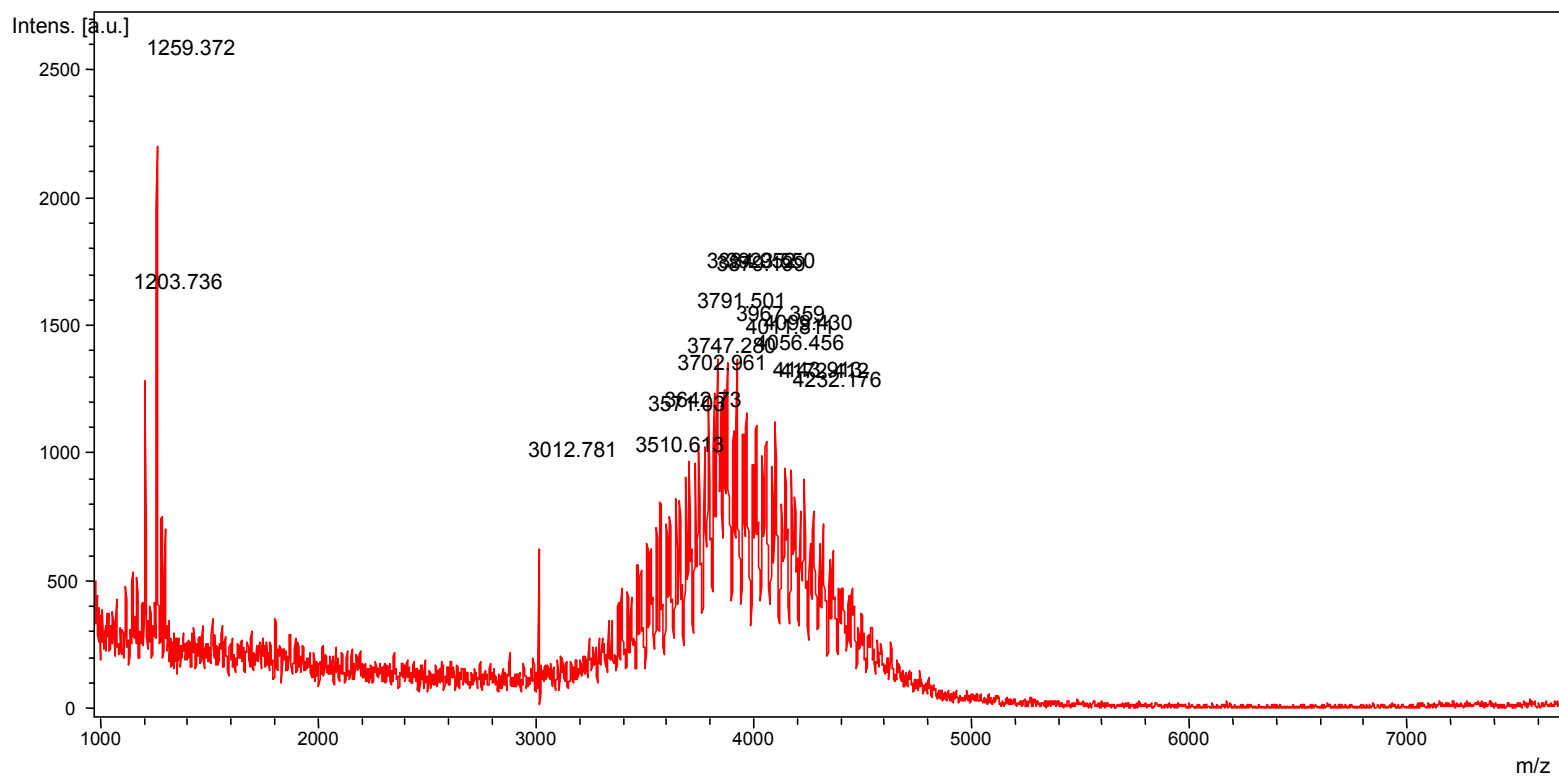


Figure 9: MALDI-TOF spectra of NHS-PEG-MAL in DMSO

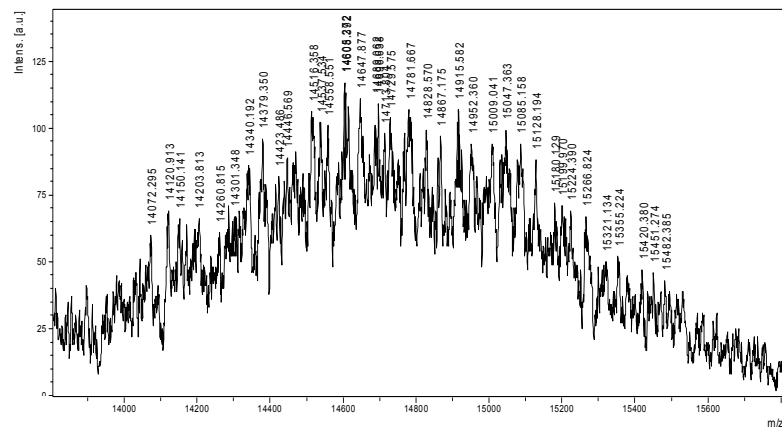
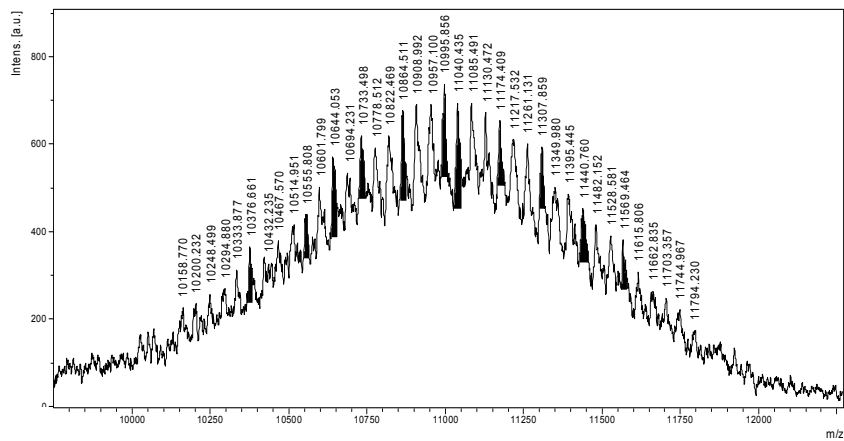
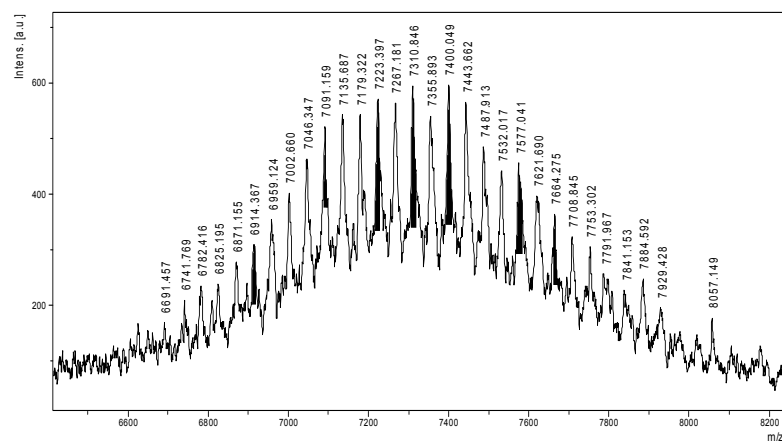
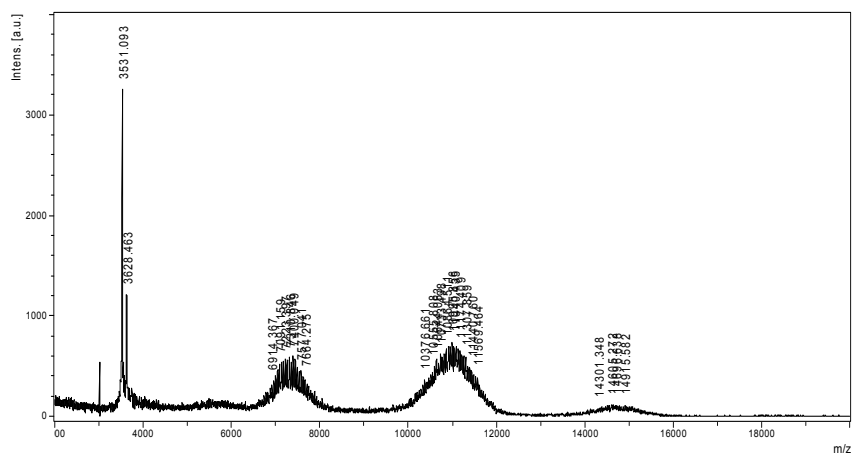


Figure 10: MALDI-TOF spectra of sCT-PEG-MAL

to further ensure the completion of reaction. This did not alter sCT receptor binding potential and bioactivity as evidenced by the cAMP generation in subsequent experiments.

Collectively, Figures 18- 23 suggested that the reaction time could have an impact on the ratio of mono-, di- and tri-substituted products. Based on those results, a reaction time of ~30 min was arbitrarily chosen, as there was no harm in prolonged reaction time, except in the alteration of the BP substitution ratio.

The effect of sulfo-SMCC concentration.

Since sCT has three available reaction sites for the NHS group in sulfo-SMCC, the effect of sulfo-SMCC concentration in the substitution was studied using sCT: sulfo-SMCC at 1: 3, 1: 5, 1: 7 and 1: 10 mol/mol ratio. Results are shown in **figures 27- 20** respectively. Although the formation of tri-substituted products was seen for all chosen ratios, the reaction was complete after a 1:5 mol/mol ratio. Since the number of SMCC substitution in sCT will be proportional with the thiol-BP substitution in later reactions and the number of thiol-BP would increase the bone targeting and localization of conjugates, a molar ratio of 1: 5 was chosen for the reactions.

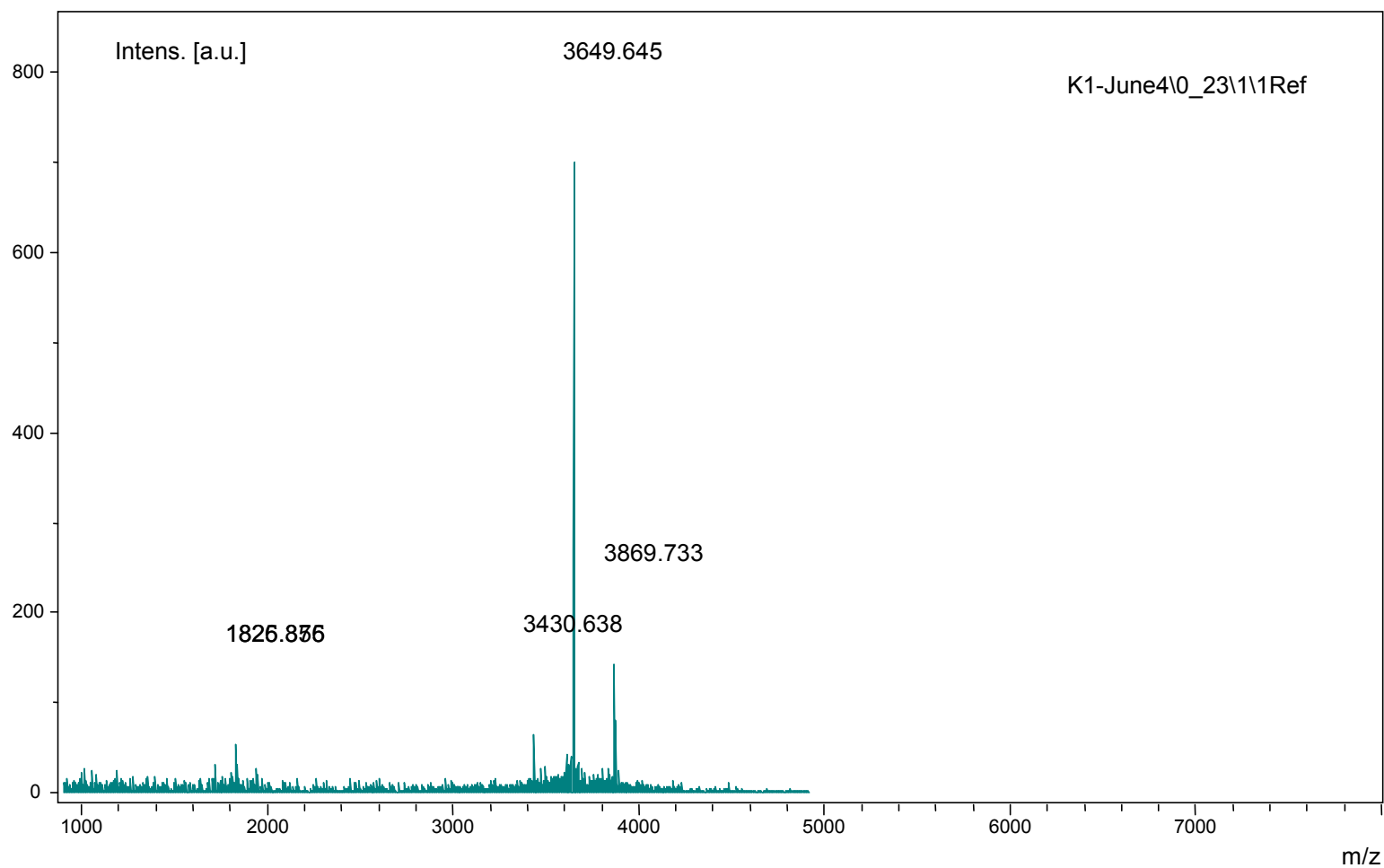


Figure 11: Optimization of reaction time when reacting sCT with sulfo-SMCC: The effect of reaction after 10 minutes.

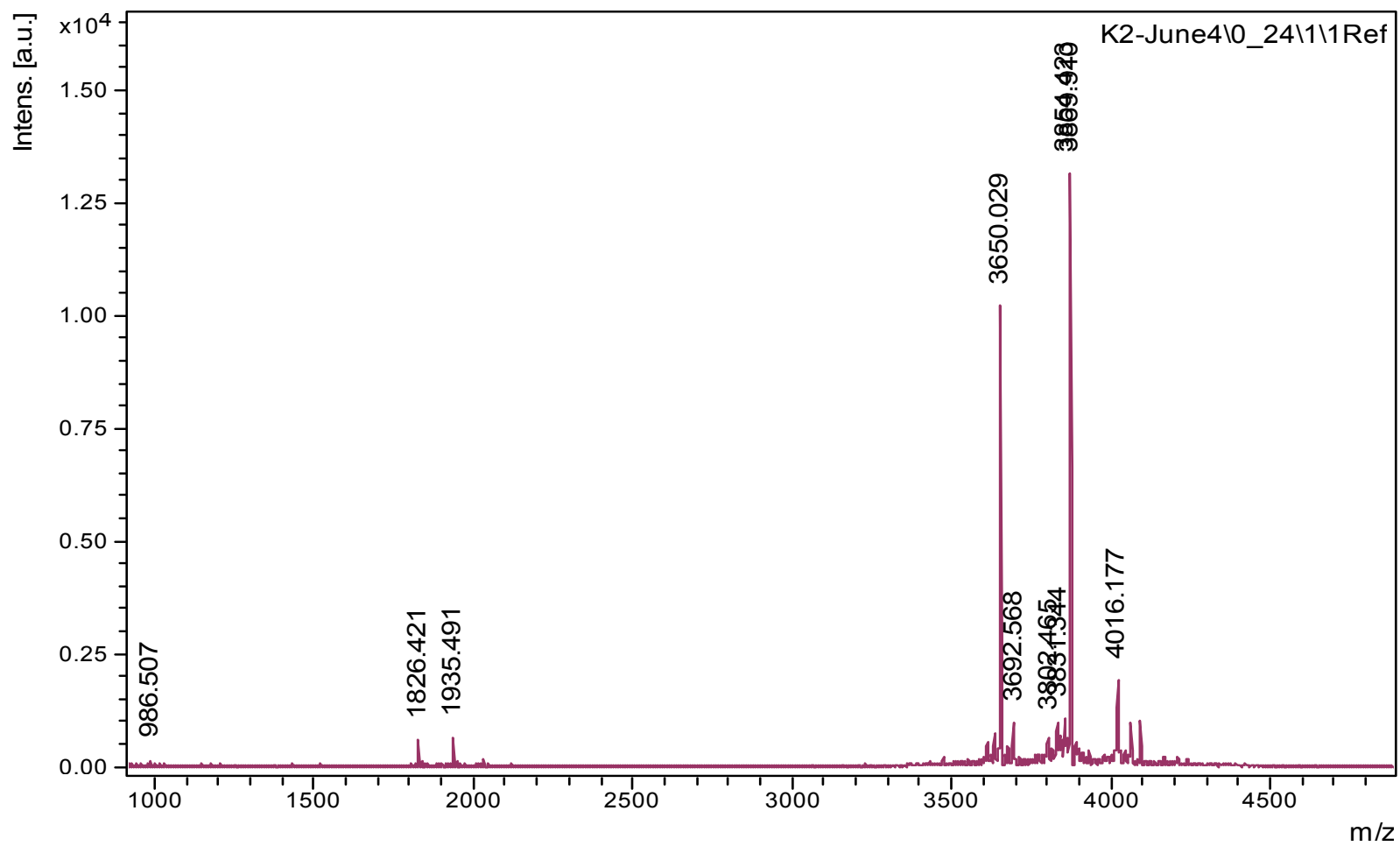


Figure 12: Optimization of reaction time when reacting sCT with sulfo-SMCC: The effect of reaction after 20 minutes.

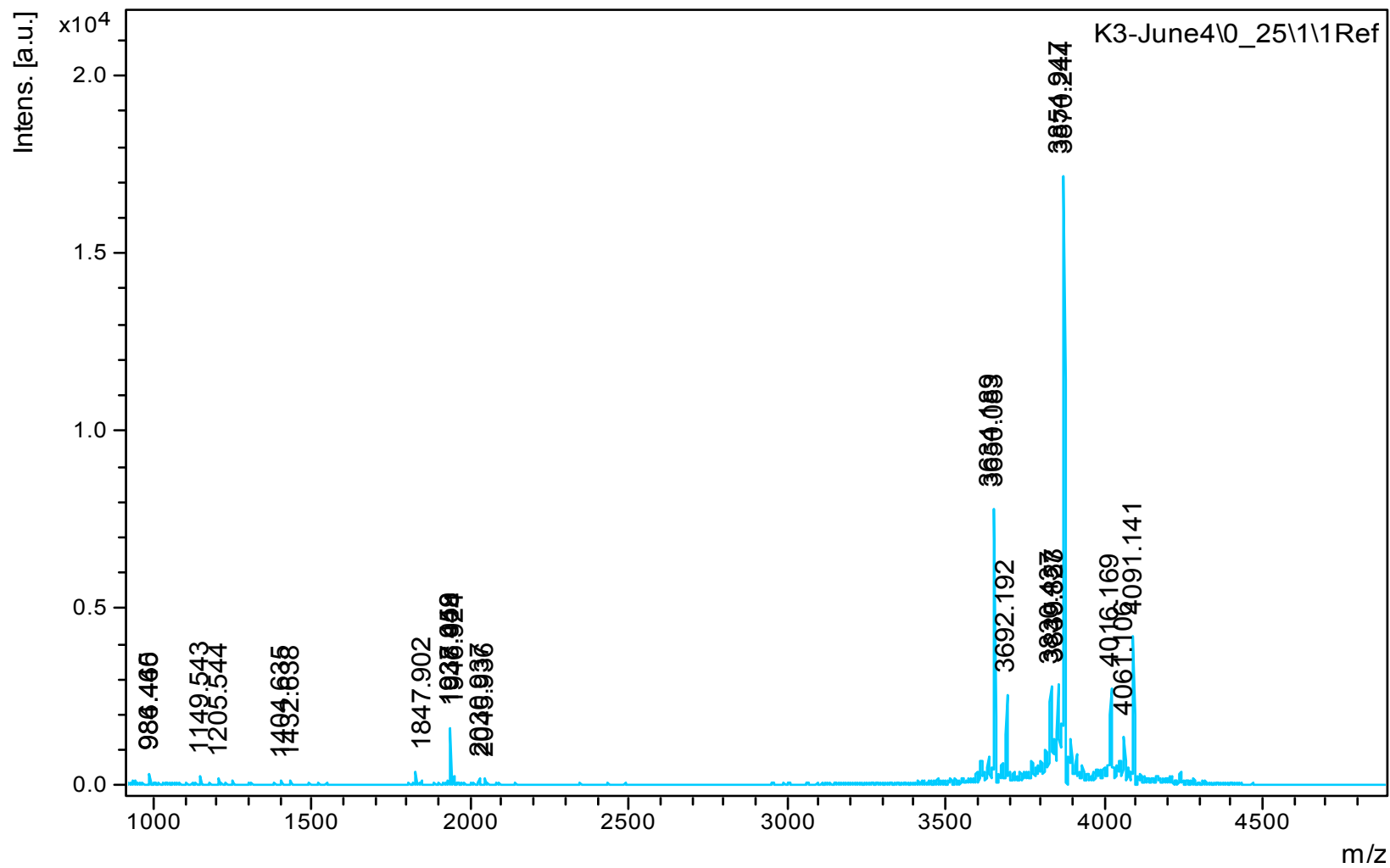


Figure 13: Optimization of reaction time when reacting sCT with sulfo-SMCC: The effect of reaction after 30 minutes.

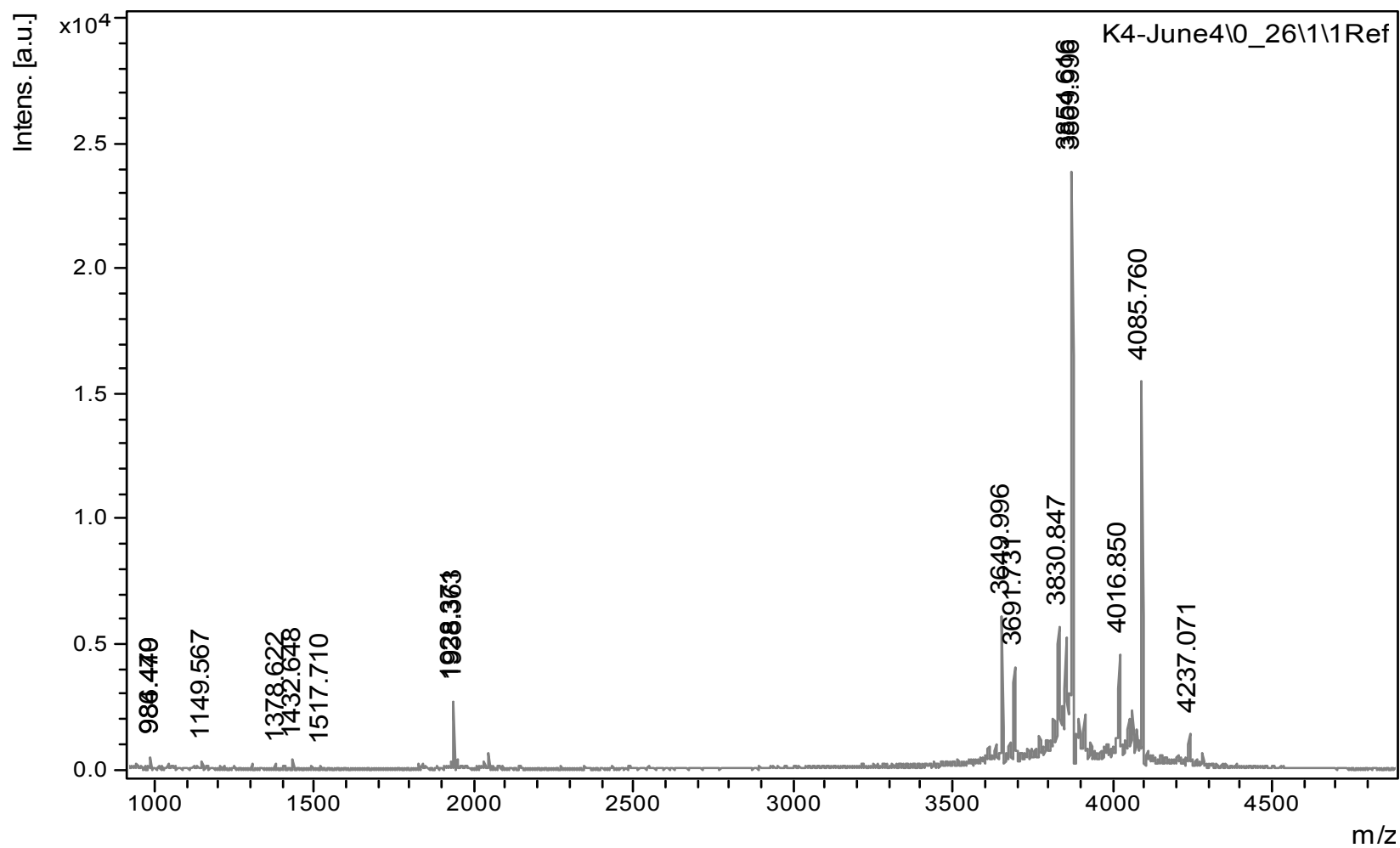


Figure 14: Optimization of reaction time when reacting sCT with sulfo-SMCC: The effect of reaction after 40 minutes.

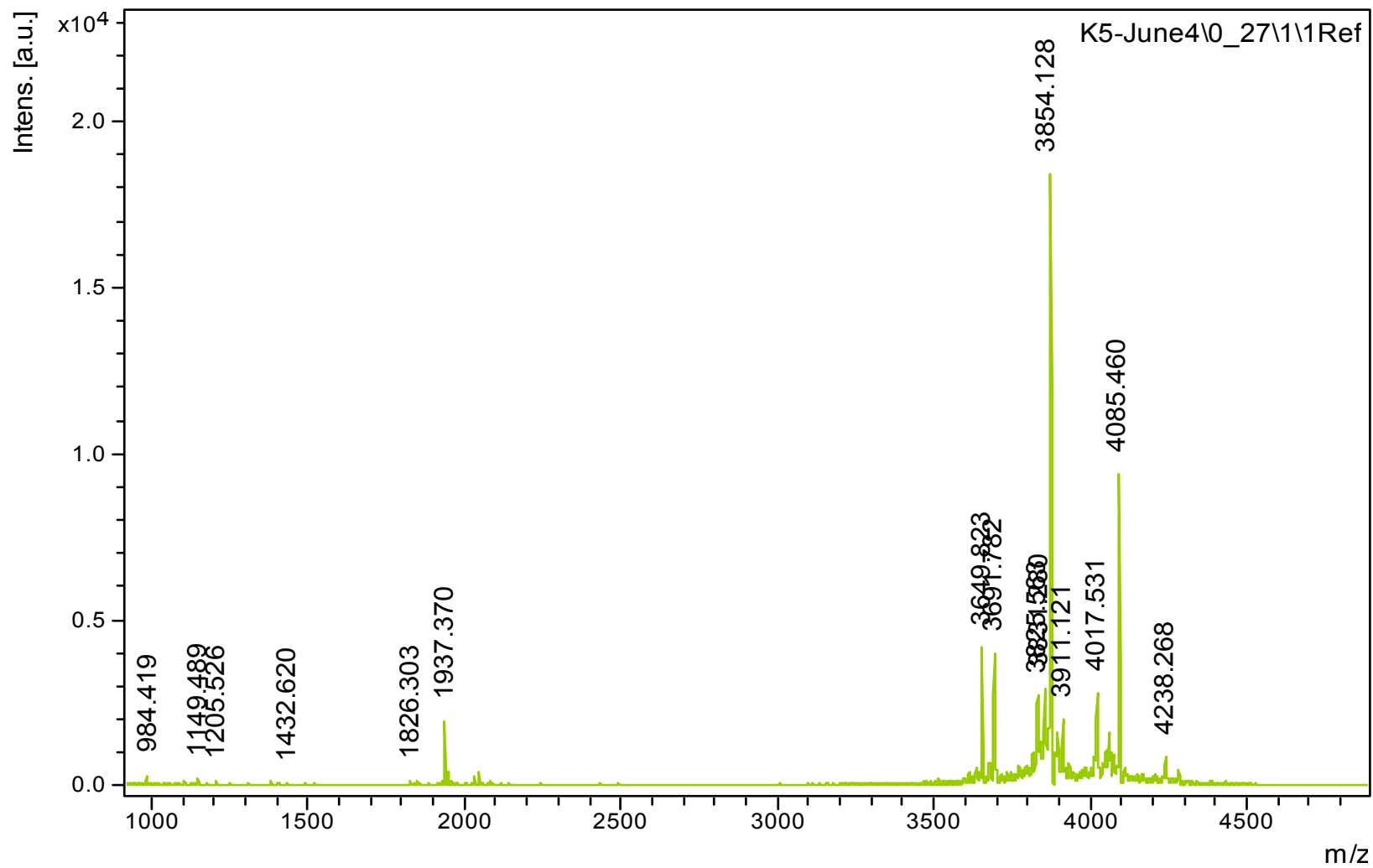


Figure 15 Optimization of reaction time when reacting sCT with sulfo-SMCC: The effect of reaction after 50 minutes.

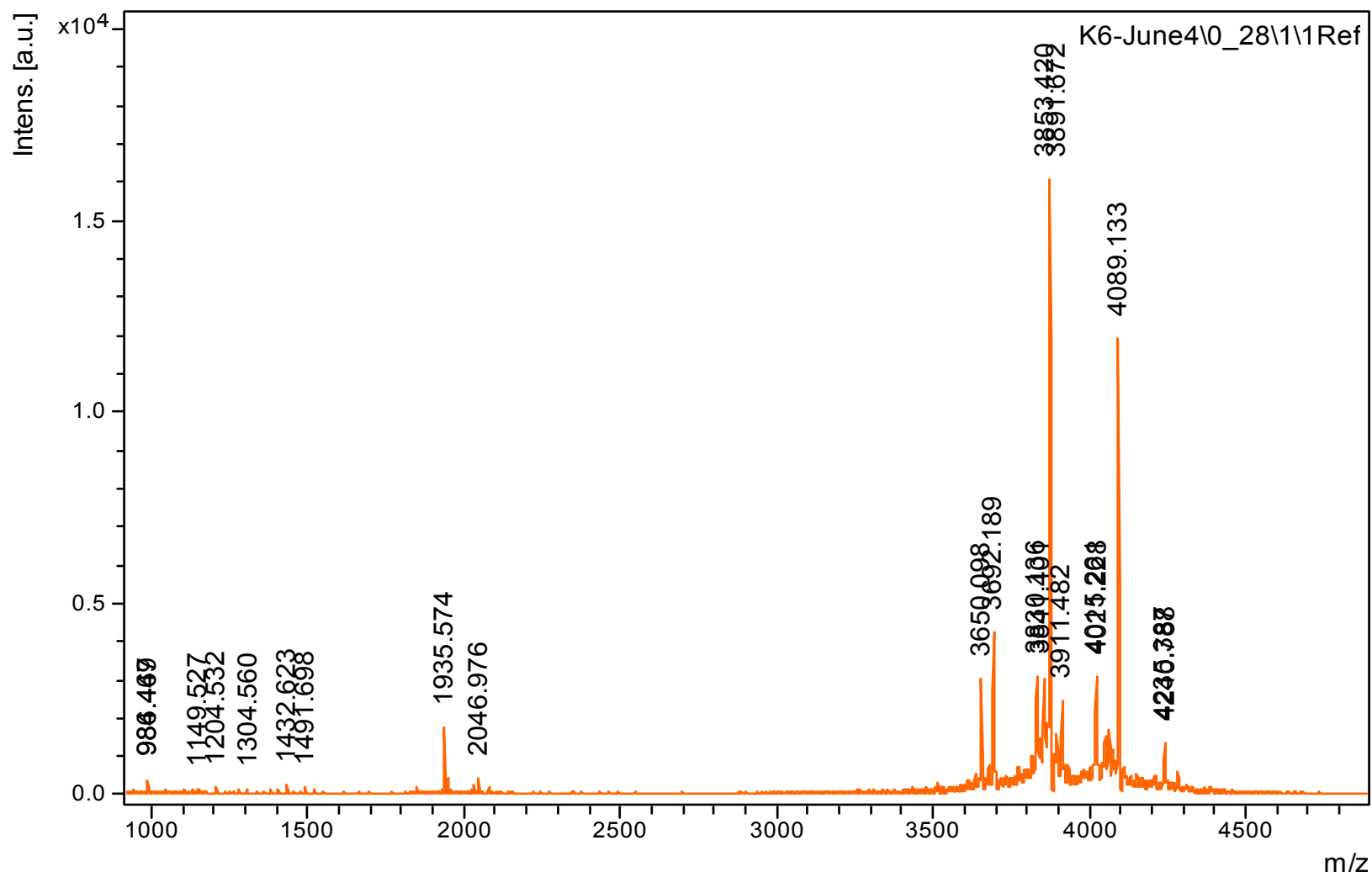


Figure 16: Optimization of reaction time when reacting sCT with sulfo-SMCC: The effect of reaction after 60 minutes.

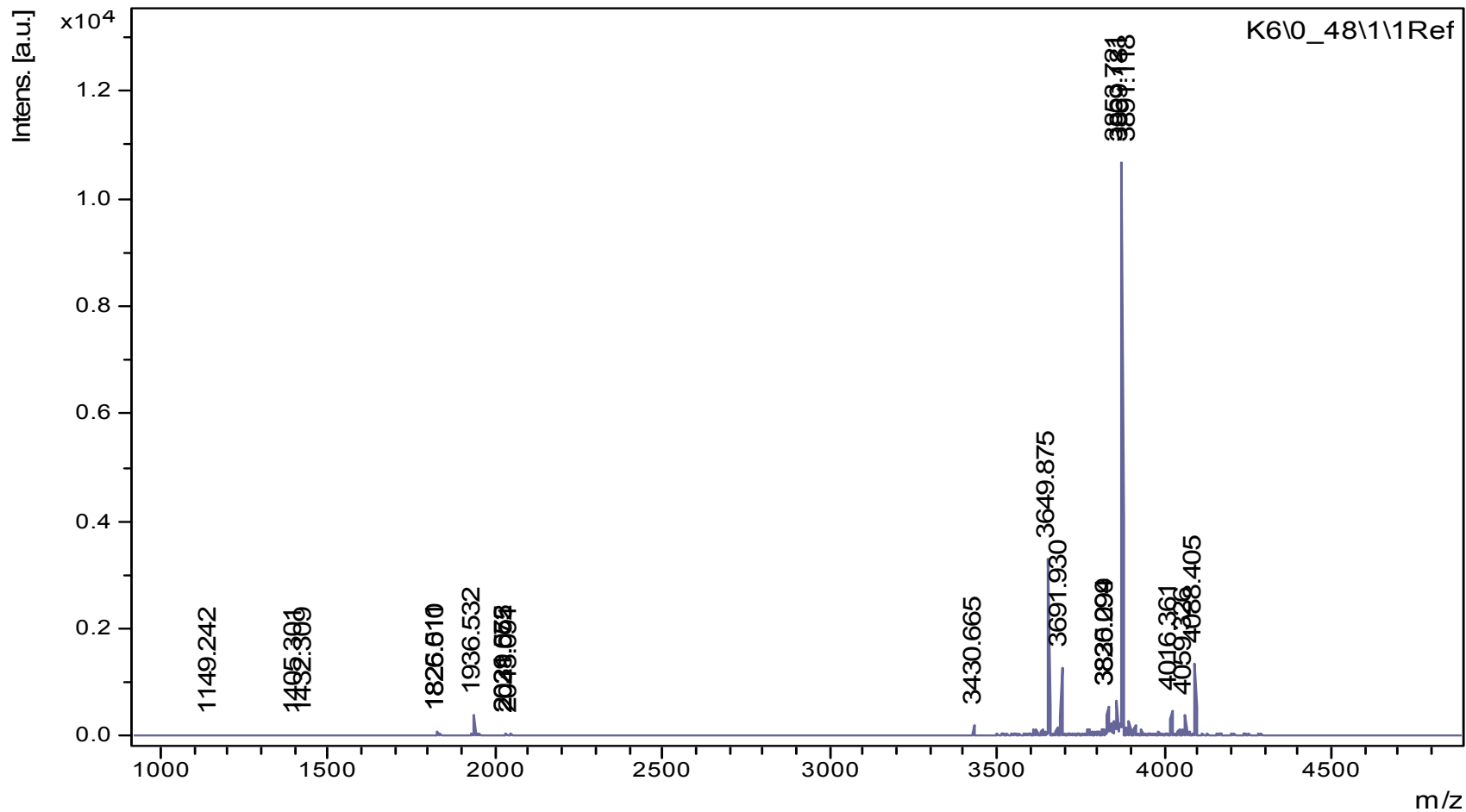


Figure 17: The effects of sulfo-SMCC concentration when reacting sulfo-SMCC with sCT: 1: 3 mol/ mol ratio of sCT to sulfo-SMCC respectively.

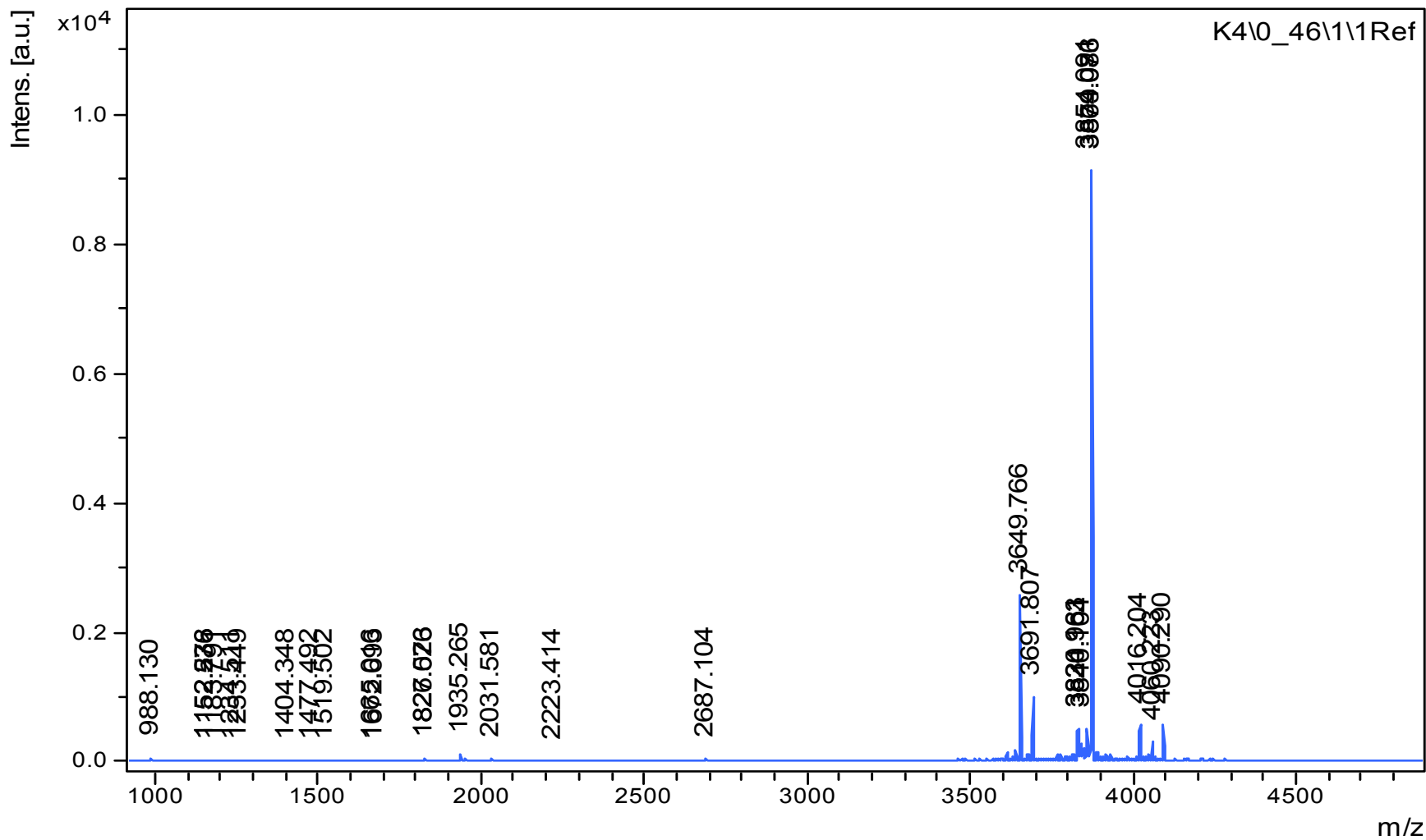


Figure 18: The effects of sulfo-SMCC concentration when reacting sulfo-SMCC with sCT: 1: 5 mol/ mol ratio of sCT to sulfo-SMCC respectively.

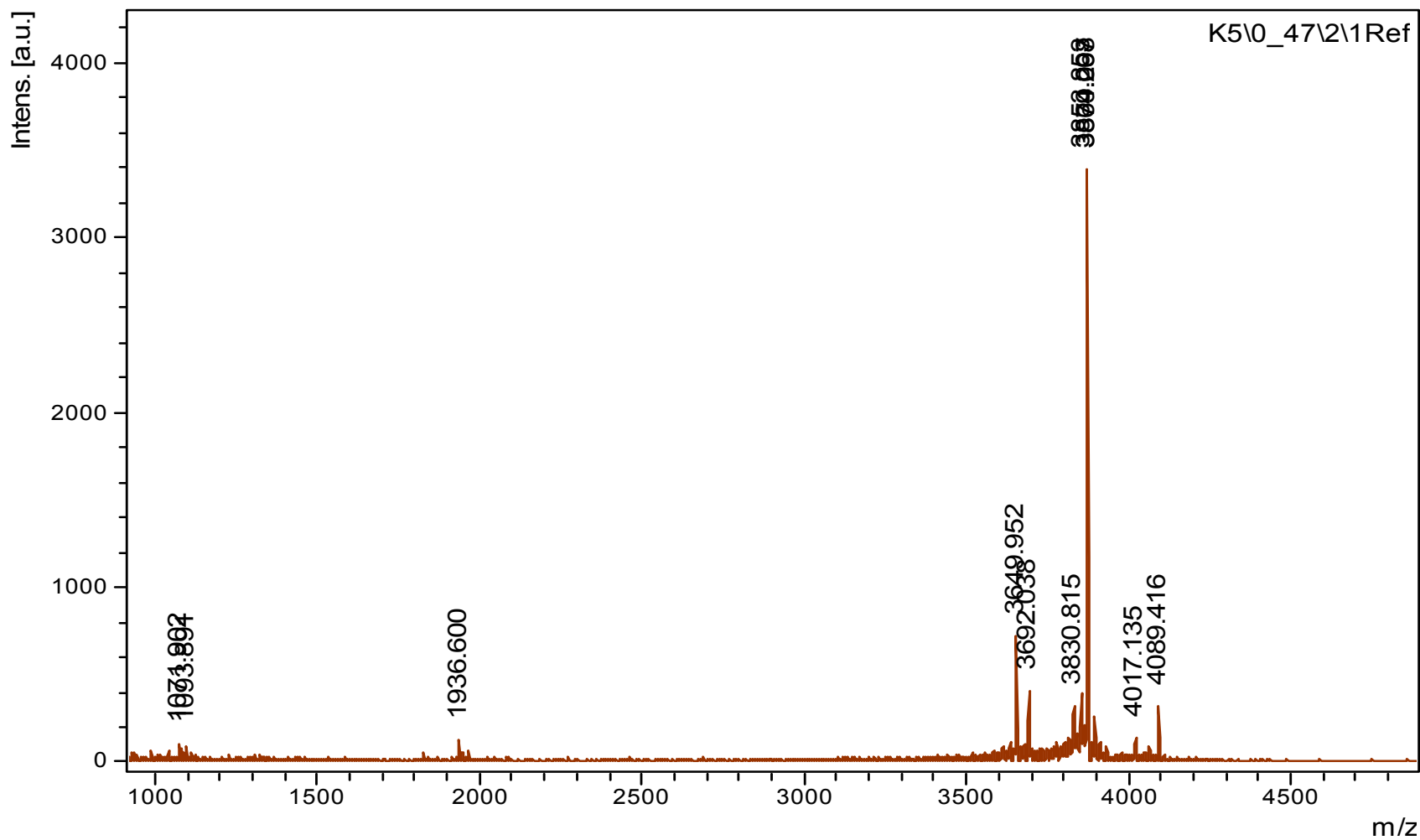


Figure 19: The effects of sulfo-SMCC concentration when reacting sulfo-SMCC with sCT: 1: 7 mol/ mol ratio of sCT to sulfo-SMCC respectively.

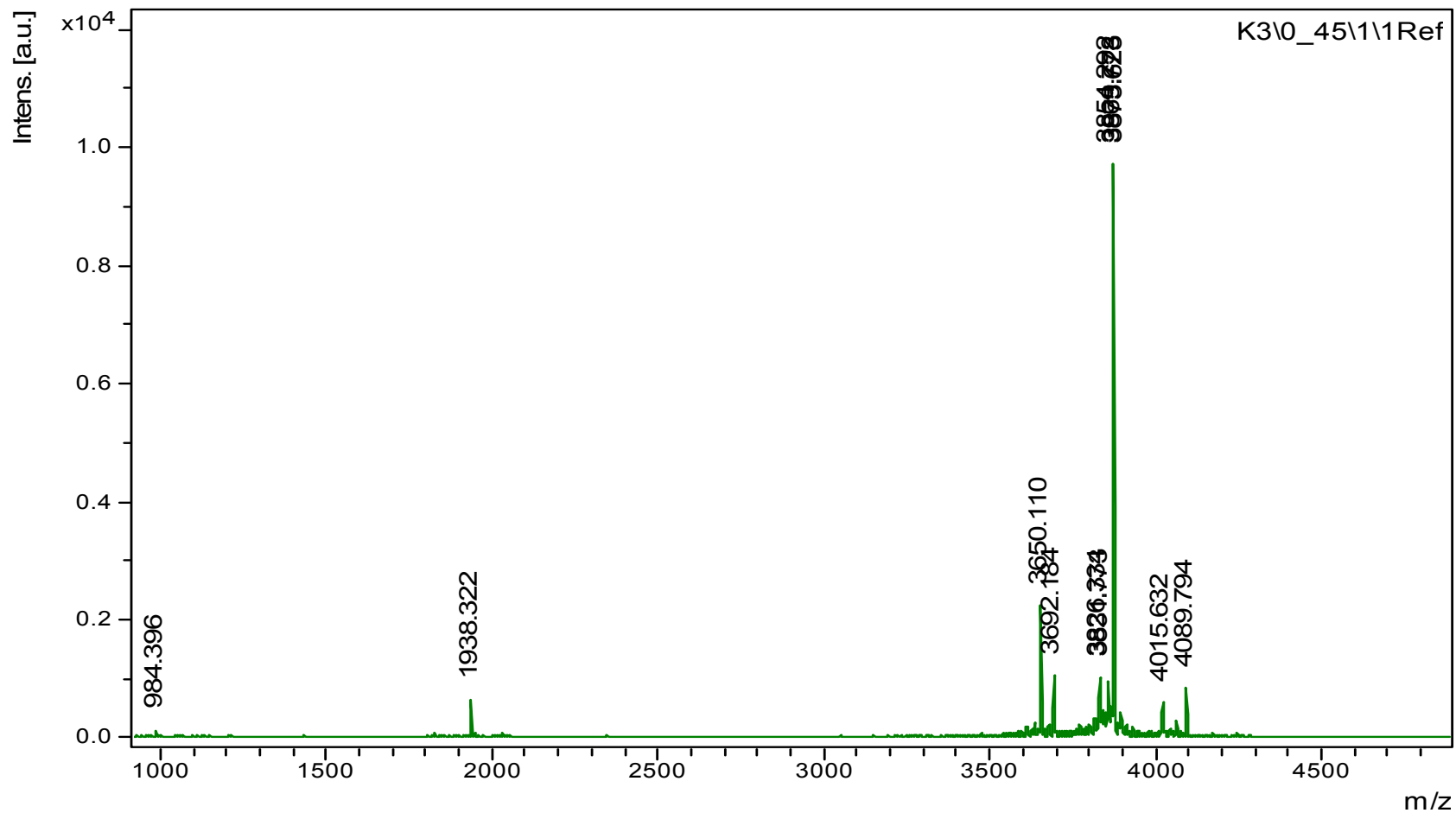


Figure 20: The effects of sulfo-SMCC concentration when reacting sulfo-SMCC with sCT: 1: 10 mol/ mol ratio of sCT to sulfo-SMCC respectively.

The effect of TEA concentration.

TEA is an organic pH modifier that increases the pH of the organic reaction media, its presence favors the reaction of -NH_2 with the NHS group in sulfo-SMCC because this reaction is more favourable at higher pH generally above 7. Hence the effect of TEA concentration was studied.

Figures 21- 25 represent the effect of TEA concentration of 0.05, 0.1, 0.2, 0.3 and 0.4% v/v. The reaction was complete for all chosen ratios and all three products were formed, and the 0.1% v/v concentration was chosen arbitrarily for further investigation.

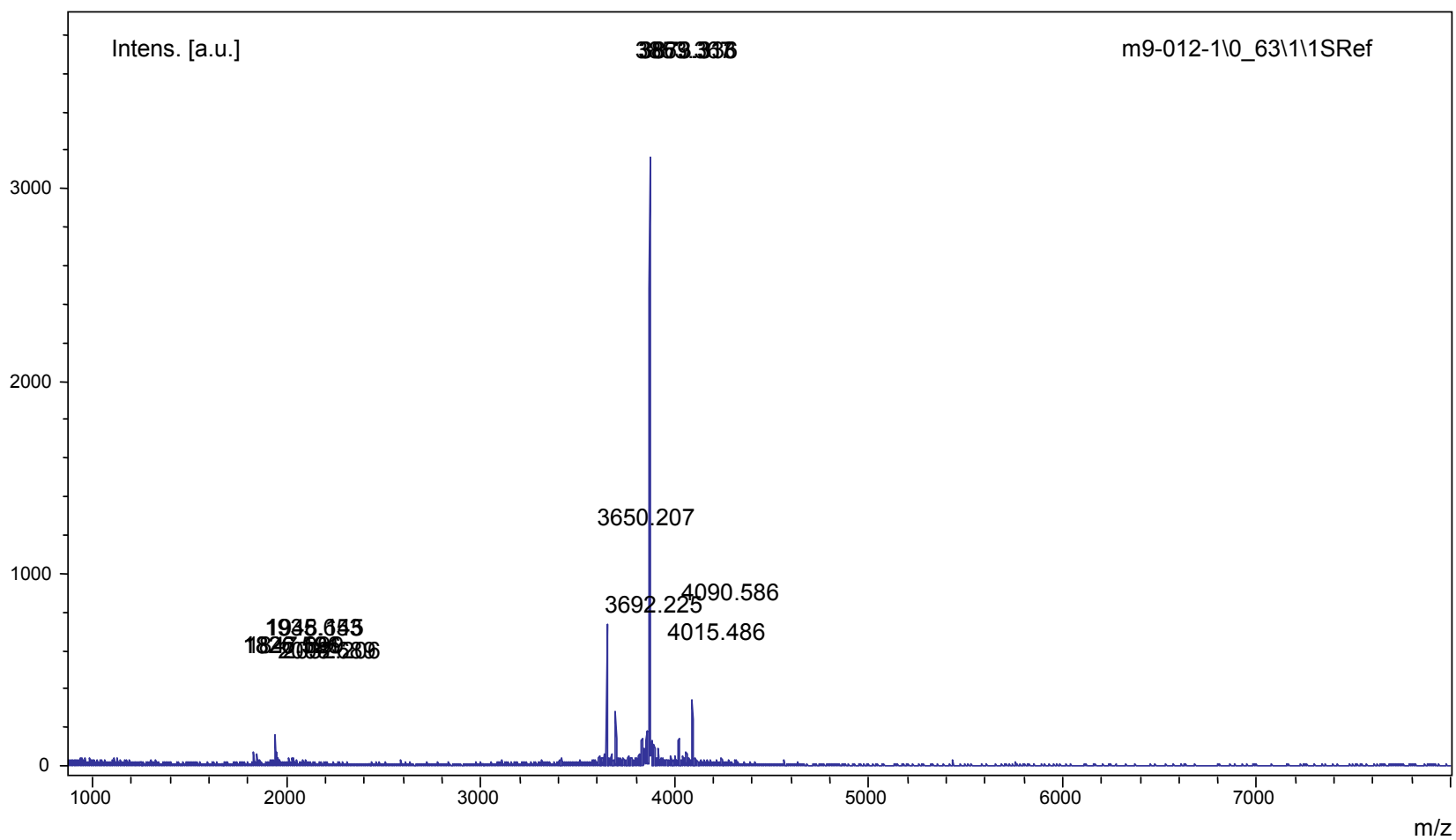


Figure 21: The effect of a TEA concentration when reacting sCT with sulfo-SMCC: 0.05% v/v TEA.

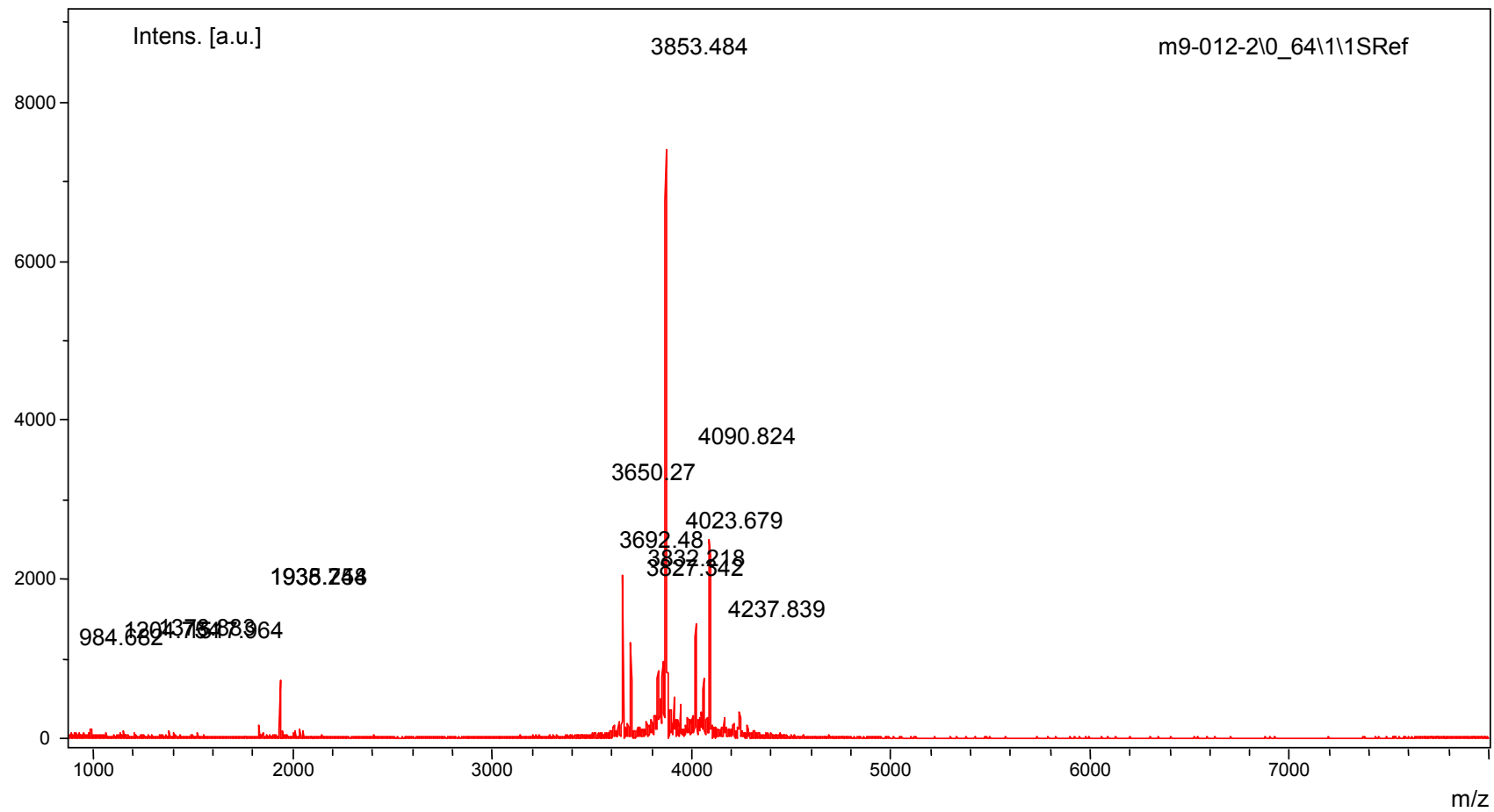


Figure 22: The effect of a TEA concentration when reacting sCT with sulfo-SMCC: 0.1% v/v TEA.

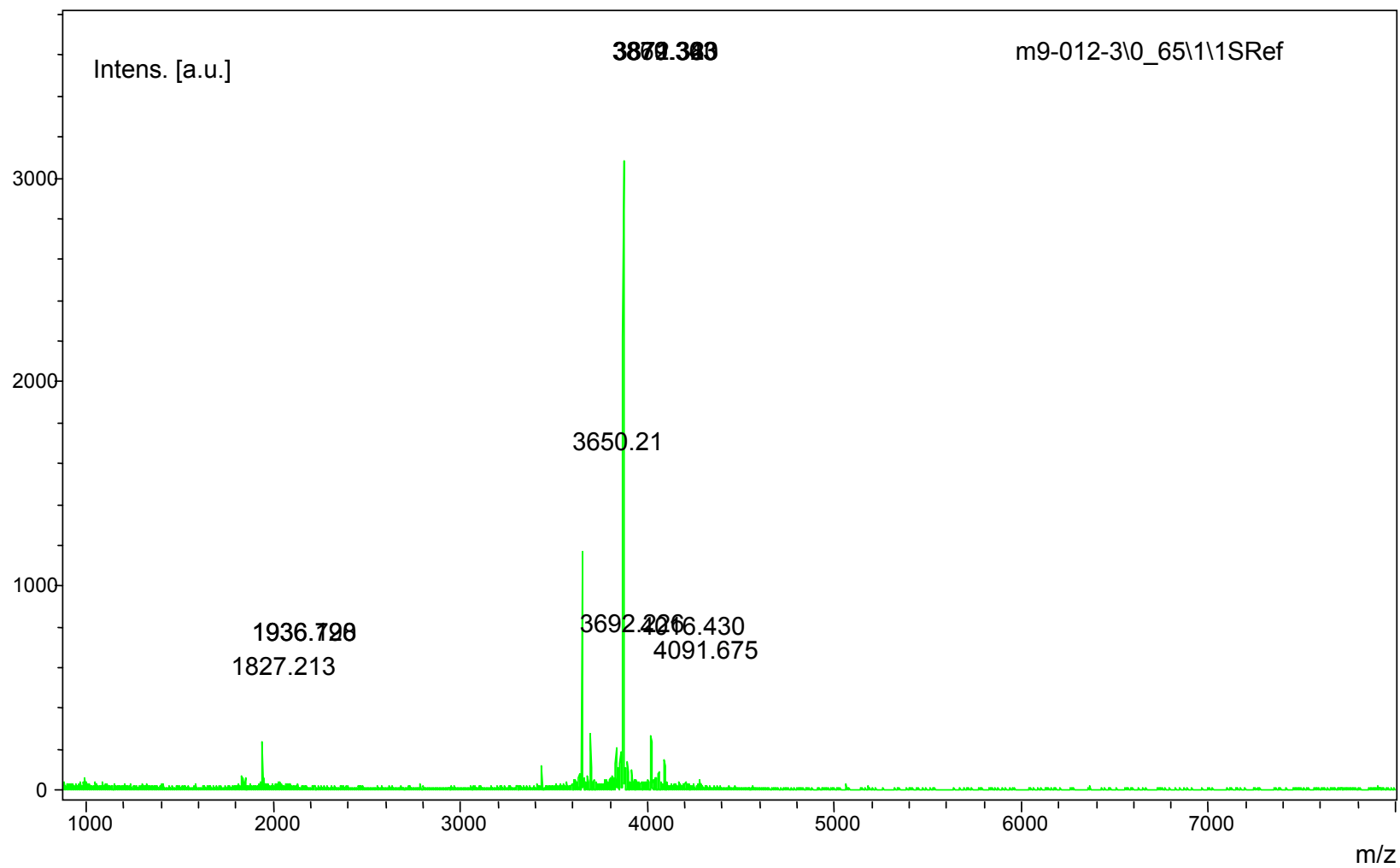


Figure 23: The effect of a TEA concentration when reacting sCT with sulfo-SMCC: 0.2% v/v TEA.

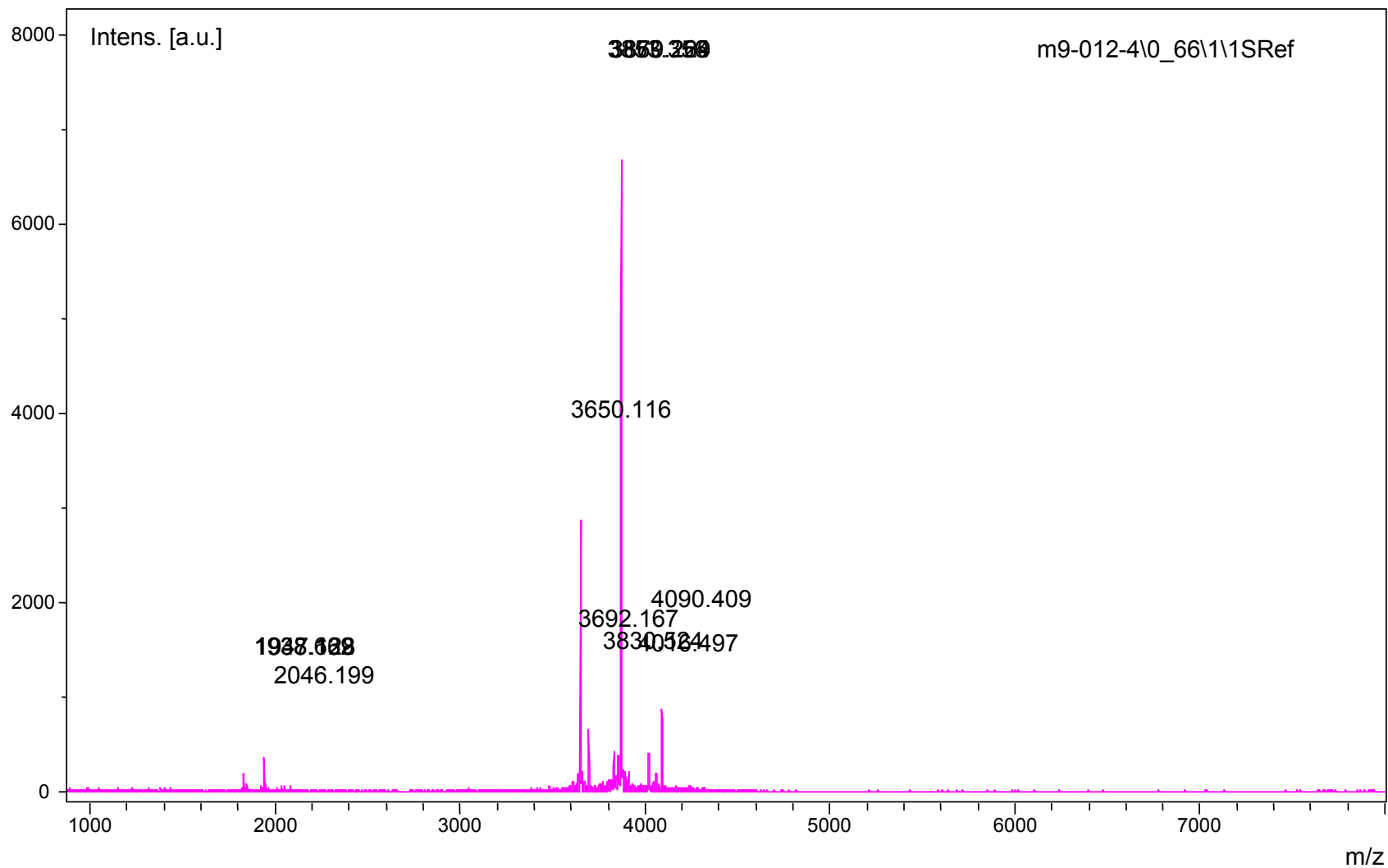


Figure 24: The effect of a TEA concentration when reacting sCT with sulfo-SMCC: 0.3% v/v TEA.

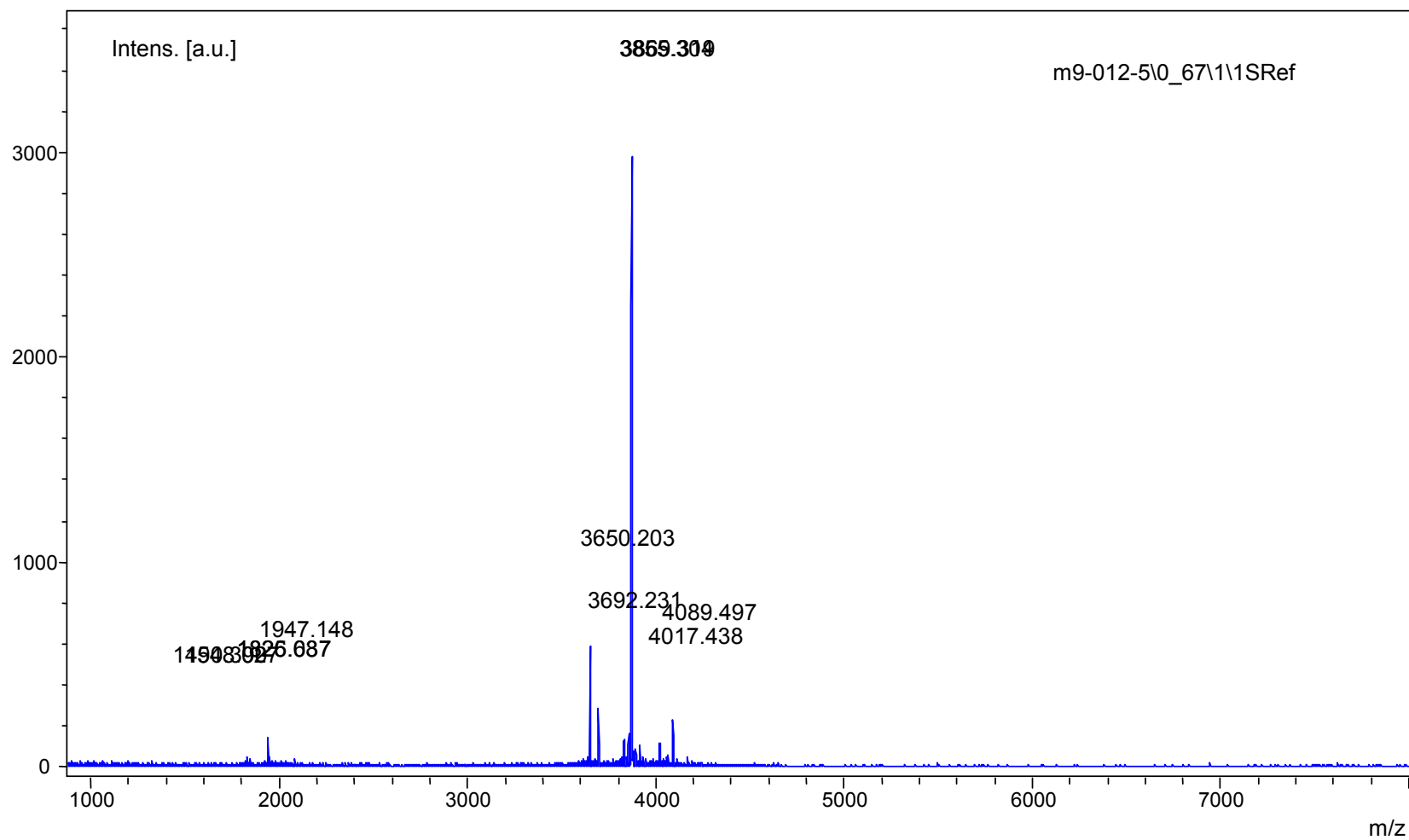


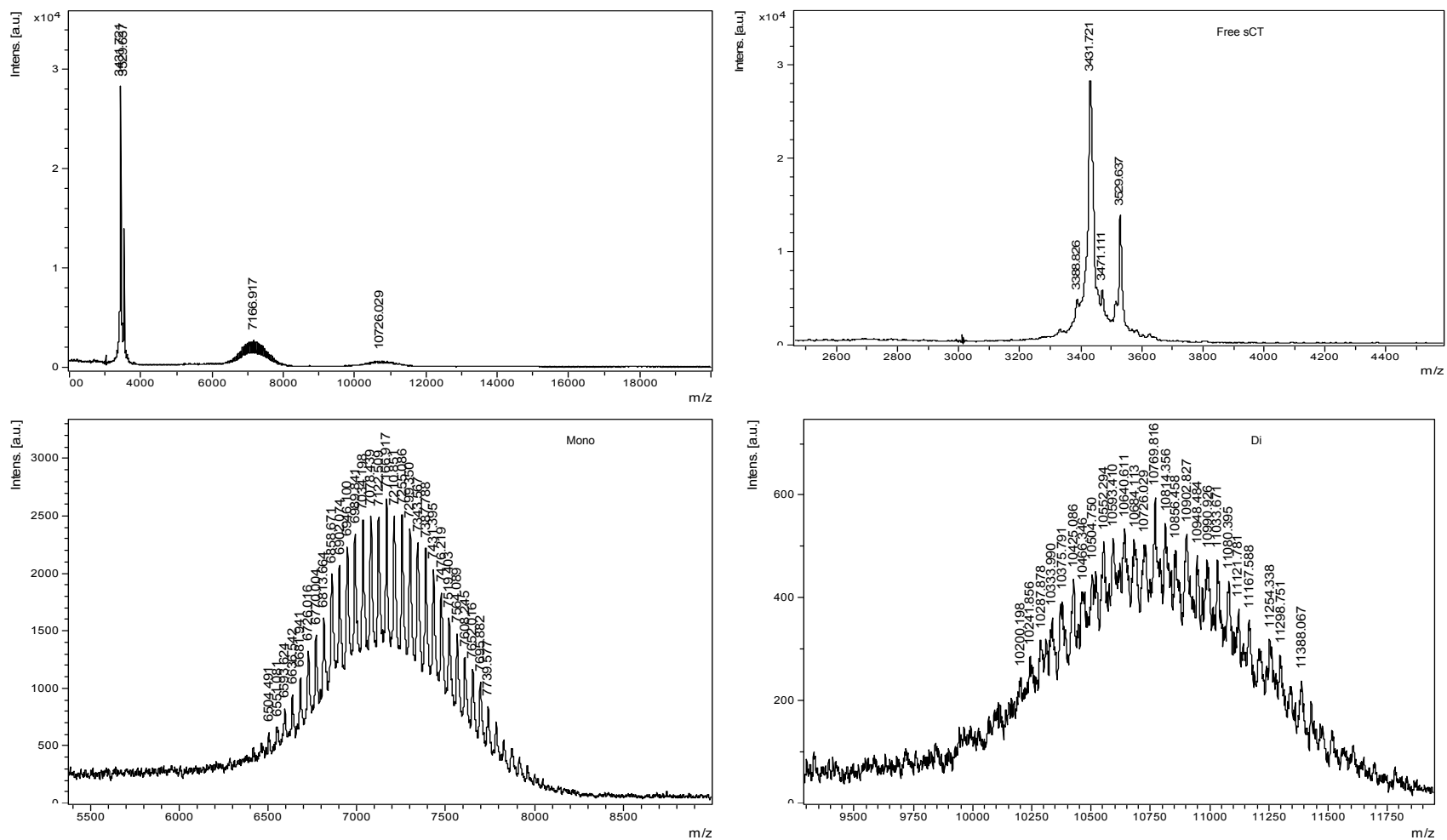
Figure 25: The effect of a TEA concentration when reacting sCT with sulfo-SMCC: 0.4% v/v TEA.

3.2.2. sCT-PEG-MAL

The effect of NHS-PEG-MAL concentration.

Since sCT has three available reaction sites for the NHS group in NHS-PEG-MAL, the effect of NHS-PEG-MAL concentration in the substitution was studied using sCT: NHS-PEG-MAL at 1:1, 1:2, 1:3, 1:5 and 1:7 mol/mol ratios. Results are shown in **figures 26- 30** respectively. The reaction was incomplete for sCT: NHS-PEG-MAL at 1:1, 1:2 molar concentration as a peak at 3430 representing sCT was seen on MALDI-TOF. The uncharacterized peak at 3528 could be of unreacted PEG (polydispersed polymer) or degradation product during MALDI analysis. However, it was complete after the ratio of 1: 3 mol/mol as shown by the loss of the sCT peak. At lower NHS-PEG-MAL concentration mono-substituted products were predominant. While di and tri-substitution favored with increasing NHS-PEG-MAL concentration. Tri-substituted products were not remarkable until 1:3 molar ratios, and were highly noticeable with further increment in NHS-PEG-MAL concentration. However, di-substituted products were major products at or after 1:3 molar ratios.

Since the formation of tri-substituted products was remarkably noticeable after 1:3 molar ratio and the reaction was incomplete before it, sCT: NHS-PEG-MAL at 1:3 mol/mol ratio was selected for further reactions. These results suggest that by monitoring NHS-PEG-MAL concentration PEG substitution on sCT can be relatively controlled.



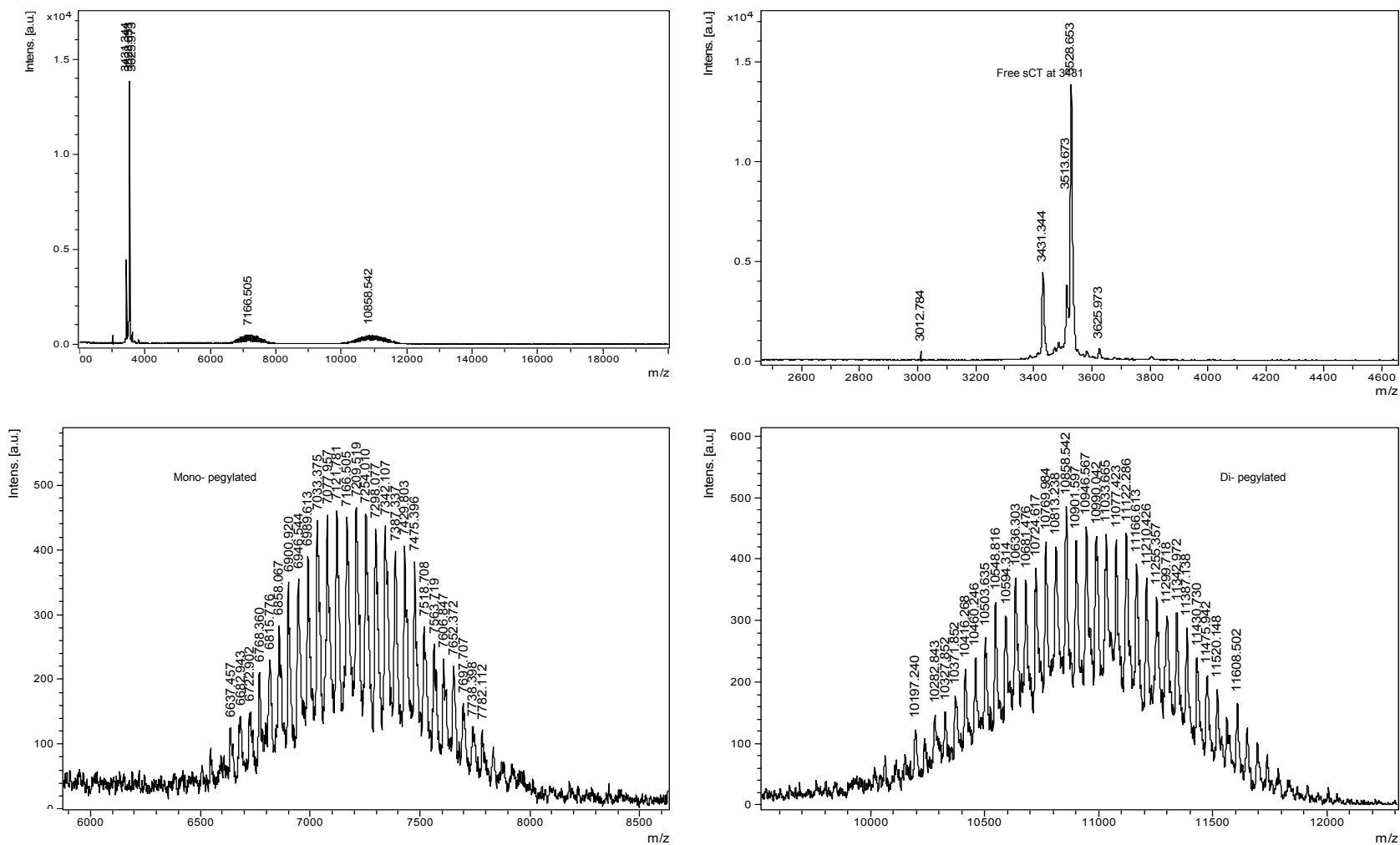
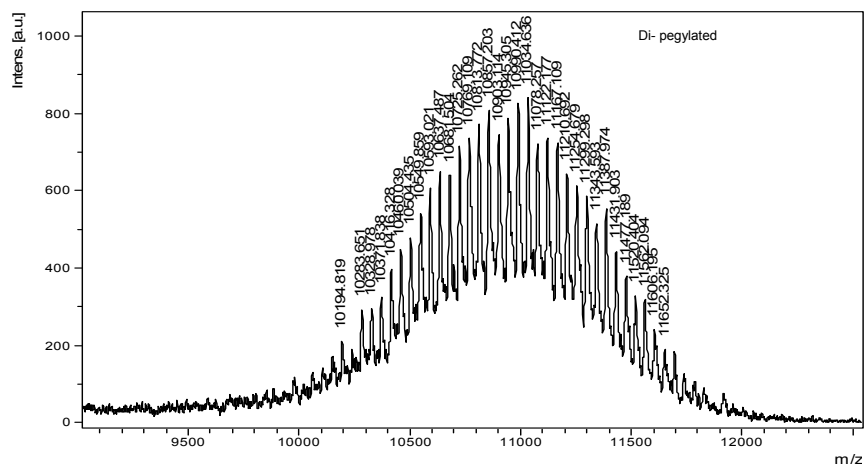
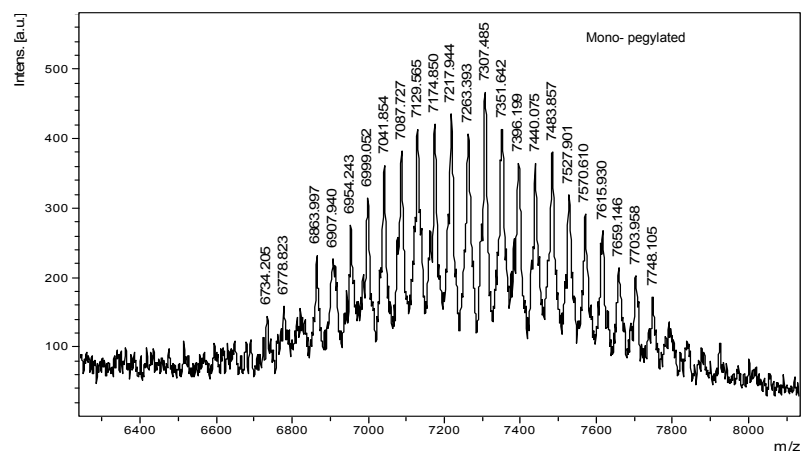
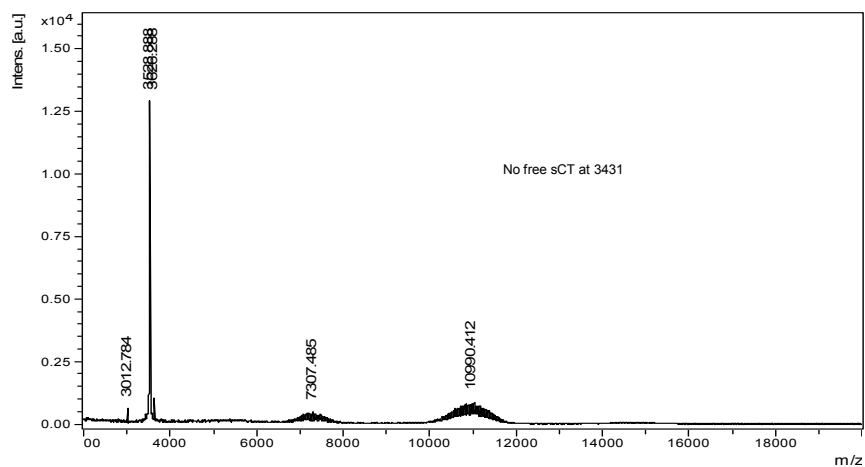


Figure 27: The effect of NHS-PEG-MAL concentration in its reaction with sCT: 1:2 mol/ mol ratio of sCT to NHS-PEG-MAL.



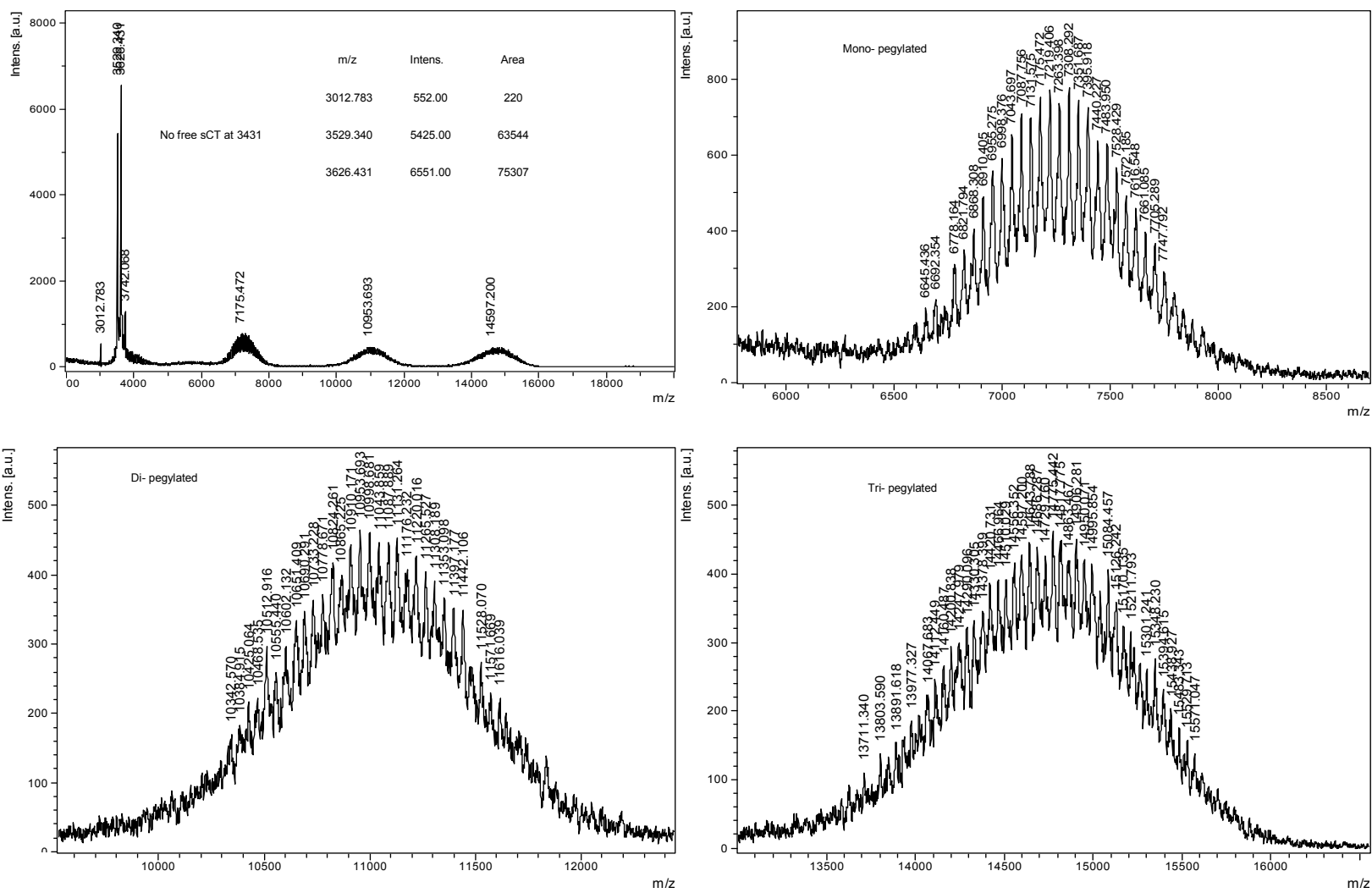


Figure 29: The effect of NHS-PEG-MAL concentration in its reaction with sCT: 1:5 mol/ mol ratio of sCT to NHS-PEG-MAL.

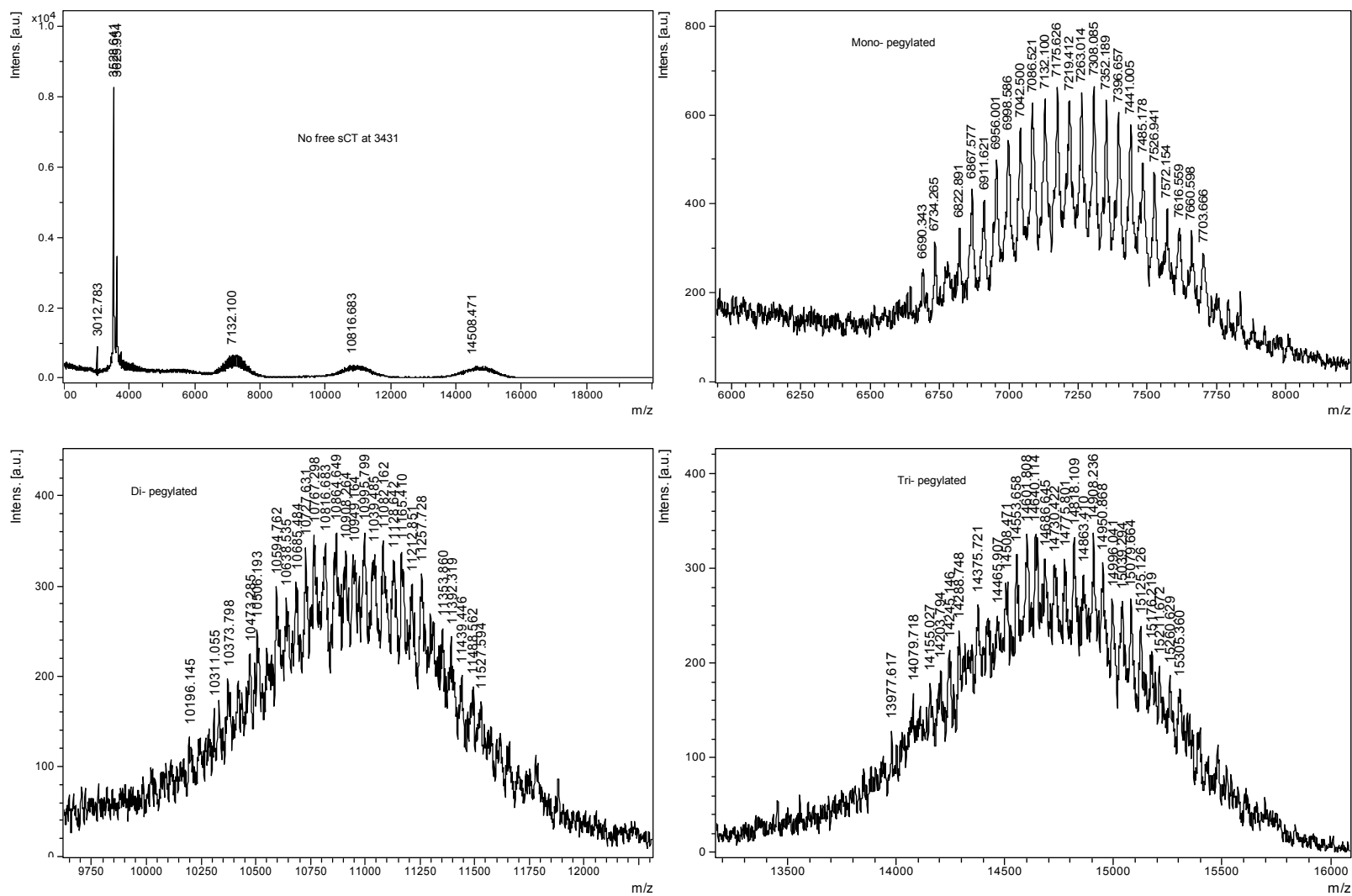


Figure 30: The effect of NHS-PEG-MAL concentration in its reaction with sCT: 1:7 mol/ mol ratio of sCT to NHS-PEG-MAL.

The effect of reaction time.

The effect of reaction time was studied to optimize the duration of reaction. Results are presented in **figures 31- 34** for 15, 30, 45, and 60 minutes respectively. Reaction was incomplete before 30 minutes as a peak at 3430 representing sCT was seen on MALDI-TOF. However, it was complete after 45 minutes as shown by the loss of the sCT peak. Formation of di and tri-substituted products were increased with time. Prolonged reaction time allowed more time for PEG molecules which were in excess to react with more primary amines in sCT to generate di-and tri-substituted compounds. Collectively, Figures 38-41 suggested that the reaction time had an impact on the ratio of mono-, di- and tri-substituted products and on the completion of reaction. Based on those results, a reaction time of ~45 min was chosen. However, there may be no harm in prolonged reaction time, except in the alteration of the BP substitution ratio.

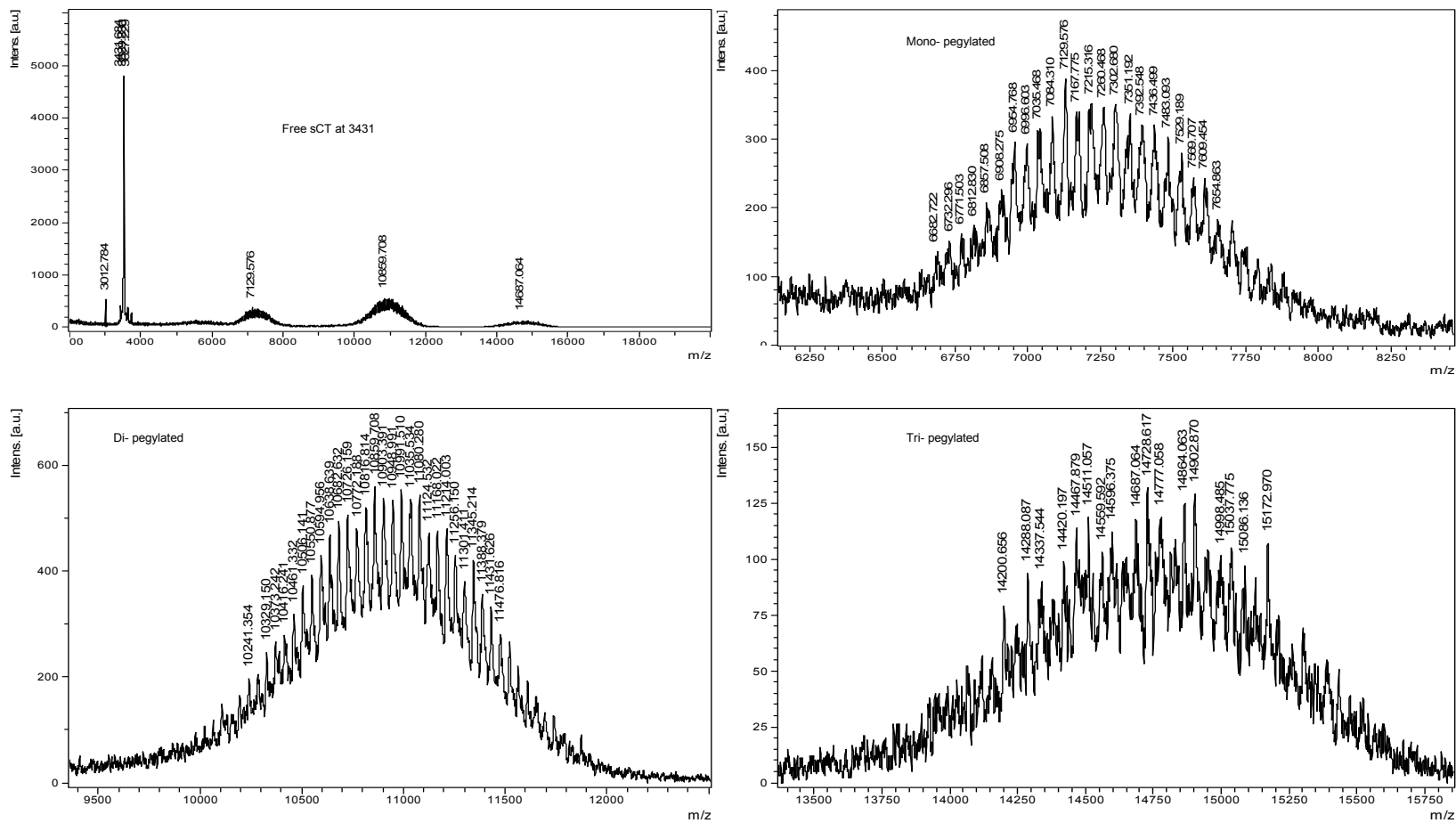


Figure 31: The effect of reaction time in the reaction of sCT with NHS-PEG-MAL: Reaction products after 15 minutes.

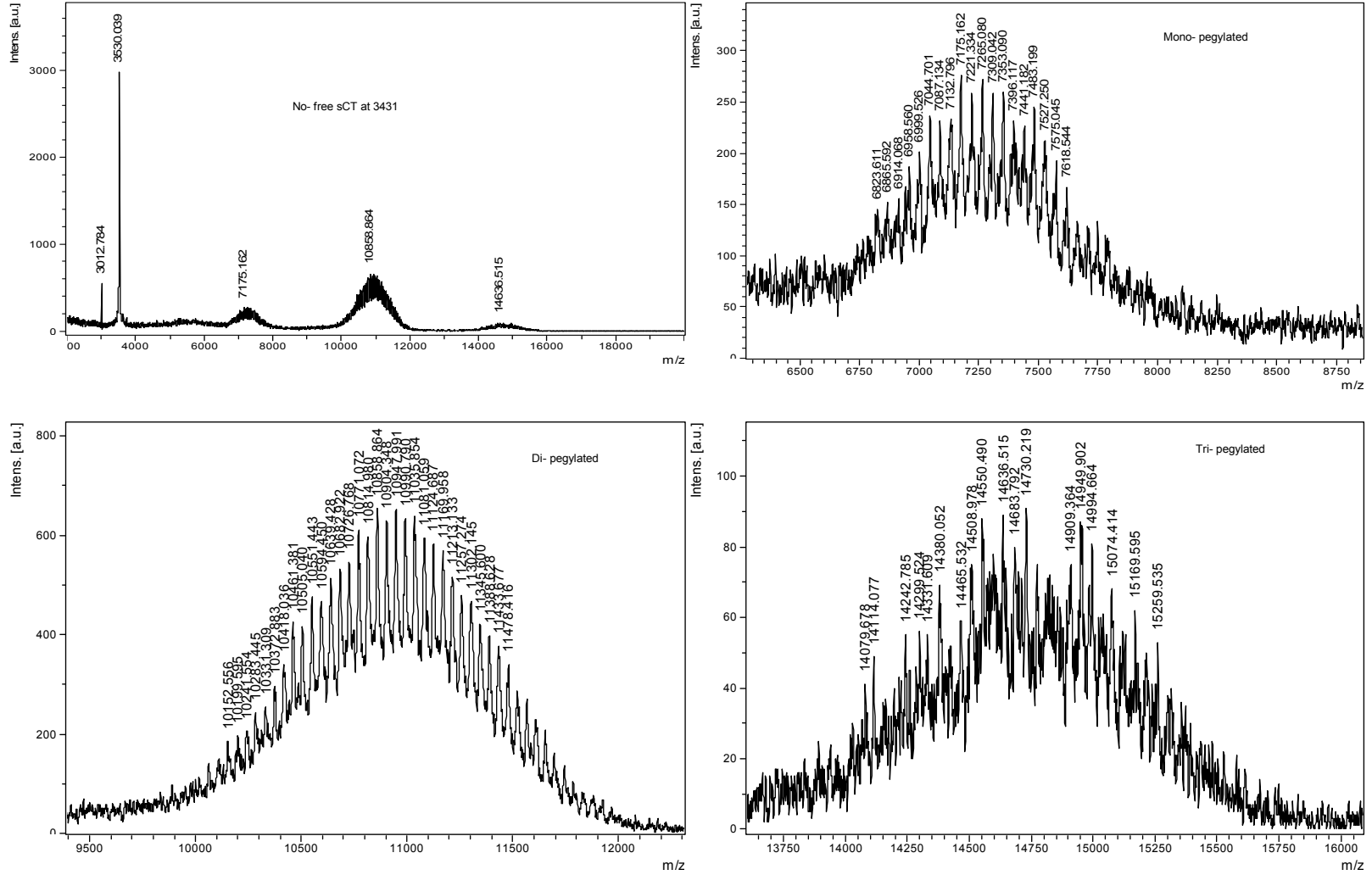
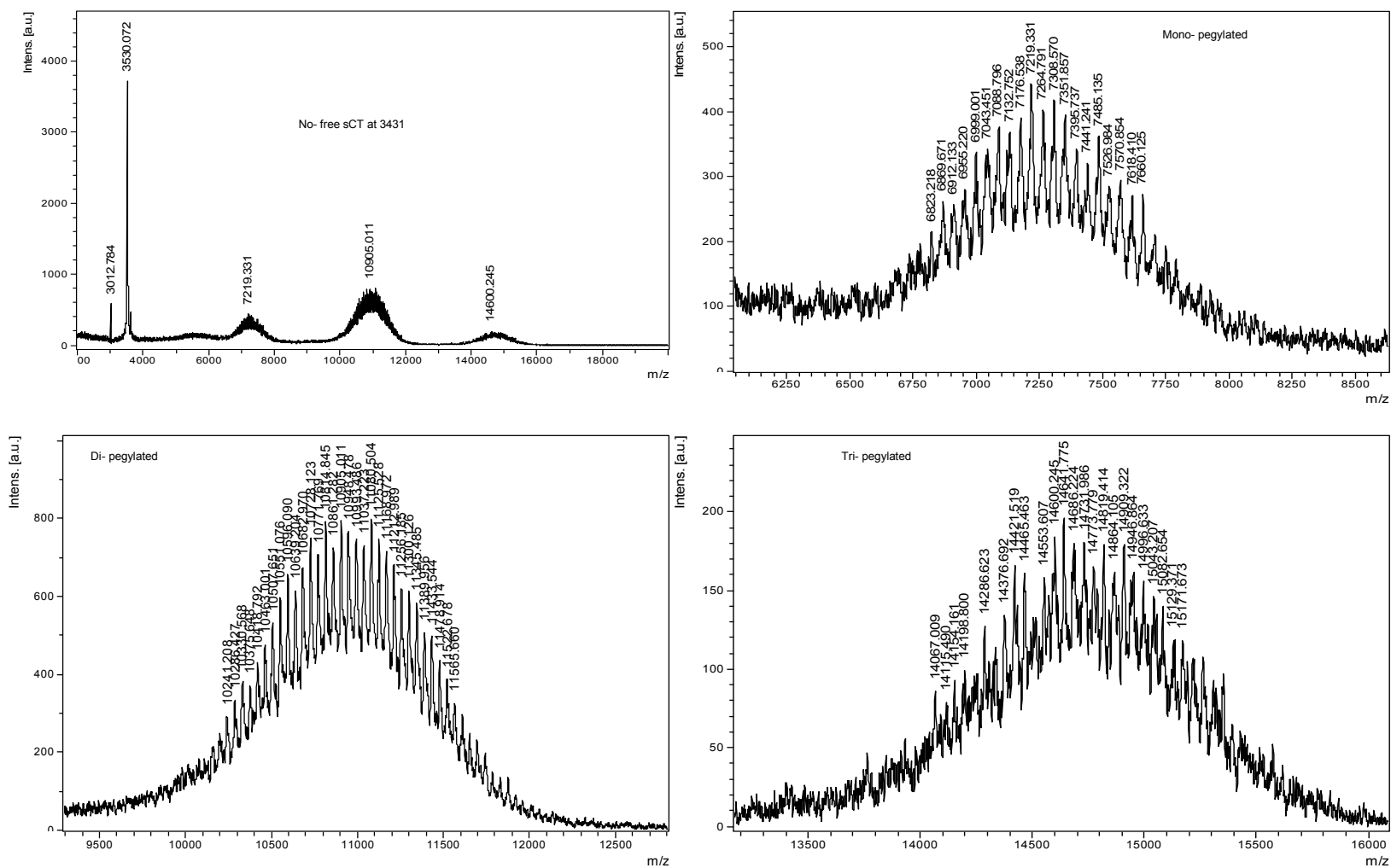


Figure 32: The effect of reaction time in the reaction of sCT with NHS-PEG-MAL: Reaction products after 30 minutes.



3. 3. THIOL-BP CHARACTERIZATION

LC-MS

As shown in **figure 36**, in negative ionization method, the mass of thiol- BP was determined to be 295 D which corresponds to its theoretical mass. The peak at 316.945 m/z was for sodium addition (295+21.989- negative mode, instead of 22.989 for sodium). However, the peak at 151 m/z could not be characterized. It could be either the degradation product or the impurity present in the thiol-BP.

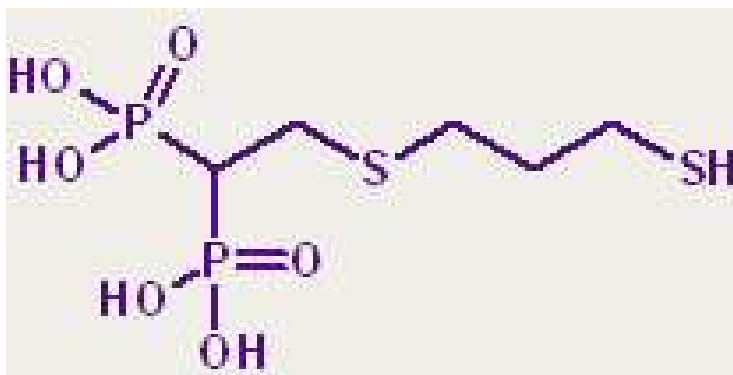


Figure 35: Structure of thiol BP. **MW = 296; C₅H₁₄O₆P₂S₂**

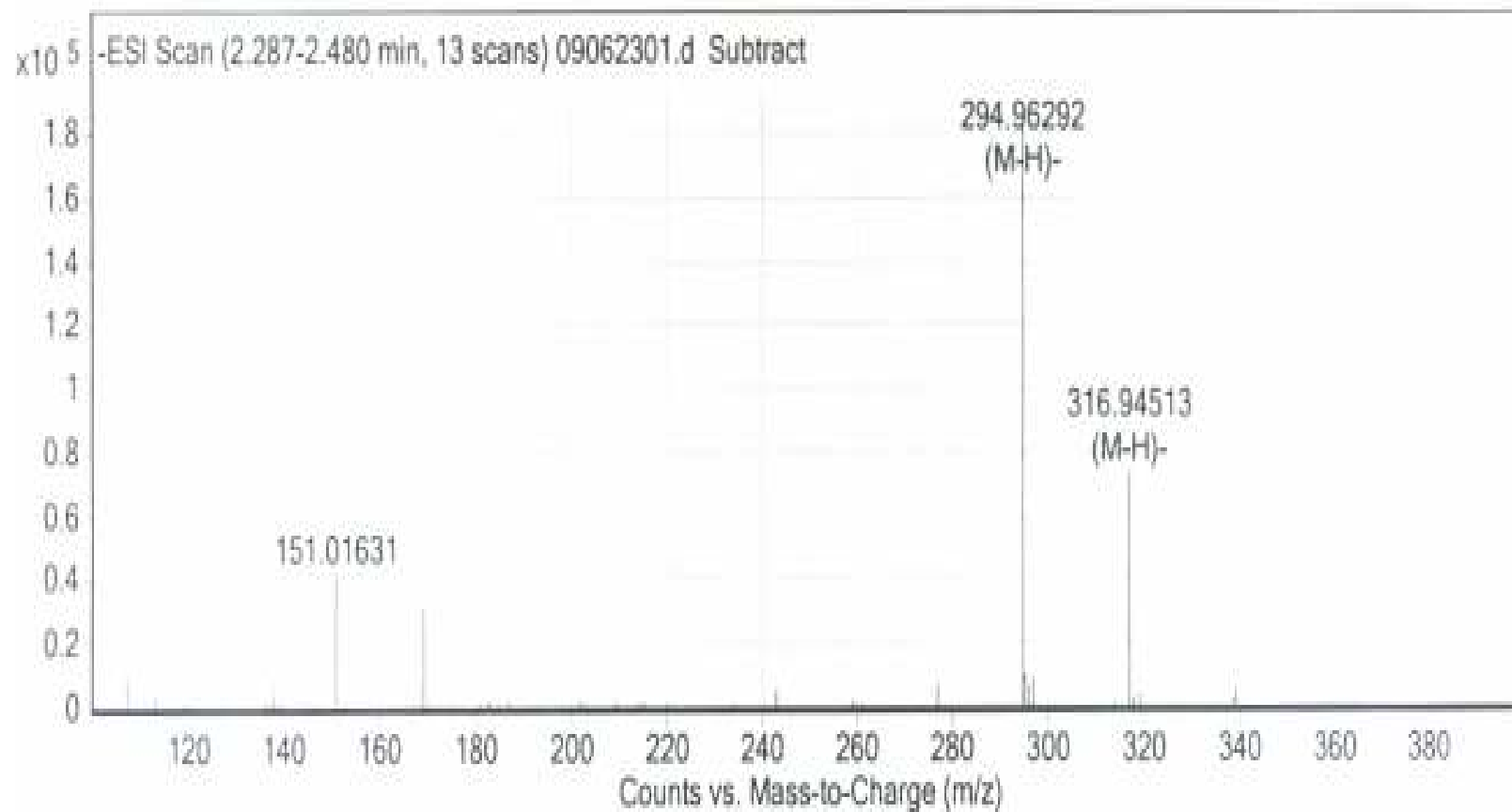


Figure 36: LC-MS spectra of thiol BP.

Reactive thiol content

Figure 37 represents the amount of reactive thiol content in thiol-BP as determined by Ellman's assay. As seen from the figure, the proportion of reactive-SH increased with increased thiol-BP concentration.

Cysteine has MW of 121.6. Similarly the MW of thiol-BP was 296. Hence the amount of thiol in the same weight of cysteine is more than double than that found in thiol-BP. However, as the both of these compounds have one thiol per molecules, the weight used in the experiment was the molar weight so that the amount of thiol was same in both of them.

When the compounds containing the same amount of reactive thiols are used in Ellman's assay the intensity of the color developed and hence the absorbance at 412 nm should be the same. We expected the same absorbance for the exactly same molar concentration of these compounds.

However, the absorbance for the same molar concentration of thiol-BP was always lower than that of the cysteine. When compared to the same molar mass of cysteine, thiol-BP had 47% of reactive thiols by weight. This decrease in thiol content is related to the unwanted peak in LC/MS of thiol-BP at 151 m/z. This impurity has an enormous effect in the concentration of reactive-SH. This factor was considered to calculate the amount of thiol-BP used in conjugation reaction.

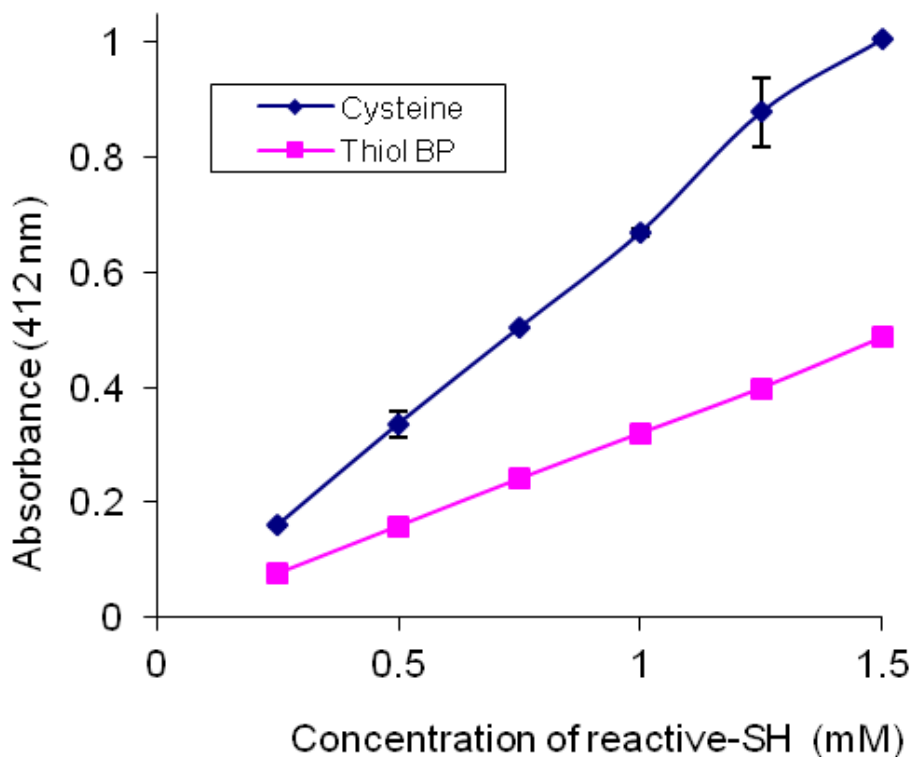


Figure 37: Reactive thiol content of thiol-BP.

Phosphate content

Figure 38 represents the amount of phosphate content in thiol-BP as determined by phosphate assay. As seen from the figure, the proportion of phosphate increased with increased thiol-BP concentration.

The MW of alendronate sodium trihydrate used was 325.12. Similarly the MW of thiol-BP was 296. Hence the amount of phosphate in the same weight of alendronate and thiol-BP are different. However, as the both of these compounds have two phosphates per molecules, the weight used in the experiment was the molar weight so that the amount of phosphate was same in both of them.

When the compounds containing the same amount of phosphate are used in phosphate assay the intensity of the color developed and hence the absorbance at 820 nm should be the same. We expected the same absorbance for the exactly same molar concentration of these compounds.

However, the absorbance for the same molar concentration of thiol-BP was always lower than that of the alendronate. When compared to the same molar mass of alendronate, thiol-BP had 70% of phosphate by weight. This decrease in the phosphate content is related to the unwanted peak in LC/MS of thiol-BP at 151 m/z. This impurity has an enormous effect in the concentration of reactive-SH. This factor was considered to calculate the amount of thiol-BP used in conjugation reaction.

3.4. COUPLING OF FUNCTIONALIZED sCT WITH THIOL-BP.

Synthesis of sCT-BP

The expected reaction products after conjugation of functionalized sCT with thiol-BP are shown in **figure 5**. Since many possible substitution sites are possible, and the thiol-BP used was a disodium salt, there exist many compounds.

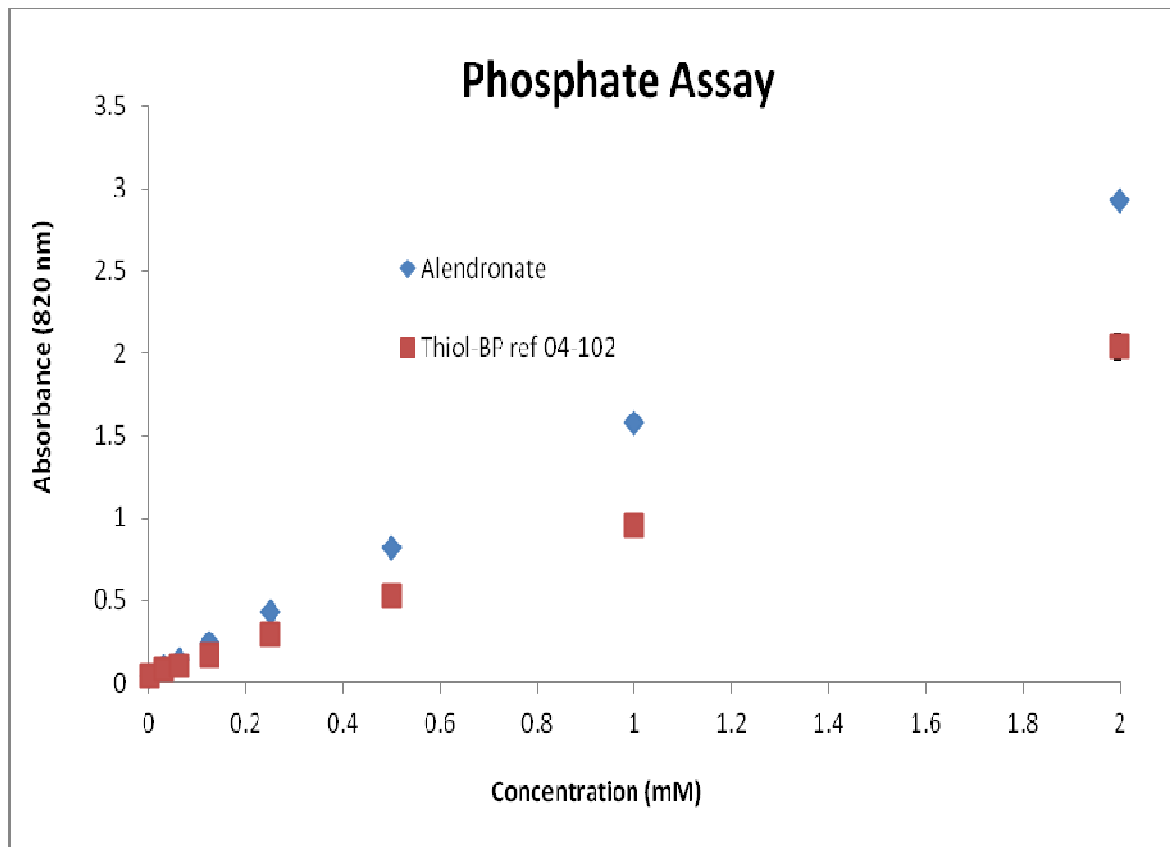


Figure 38: Phosphate content of thiol-BP.

However, they only differ in BP substitution and Na addition. MALDI-TOF results of conjugates are shown in **figure 39**. The peak at 3989.848 was of sCT-SMCC-BP +2Na and at 4167.271 for sCT-2SMCC-1BP. sCT-2SMCC-2BP on disulfide bond appeared at 4459.757 and sCT-2SMCC-2BP was found at 4463.845. Similarly, the peak at 4501.735 was of sCT-2SMCC-2BP+ 4Na (2 Na each on BP) and at 4814.287 of sCT-2SMCC-3BP+3 Na. Another tri substituted product, sCT-3SMCC-3BP, appeared at 4979.743.

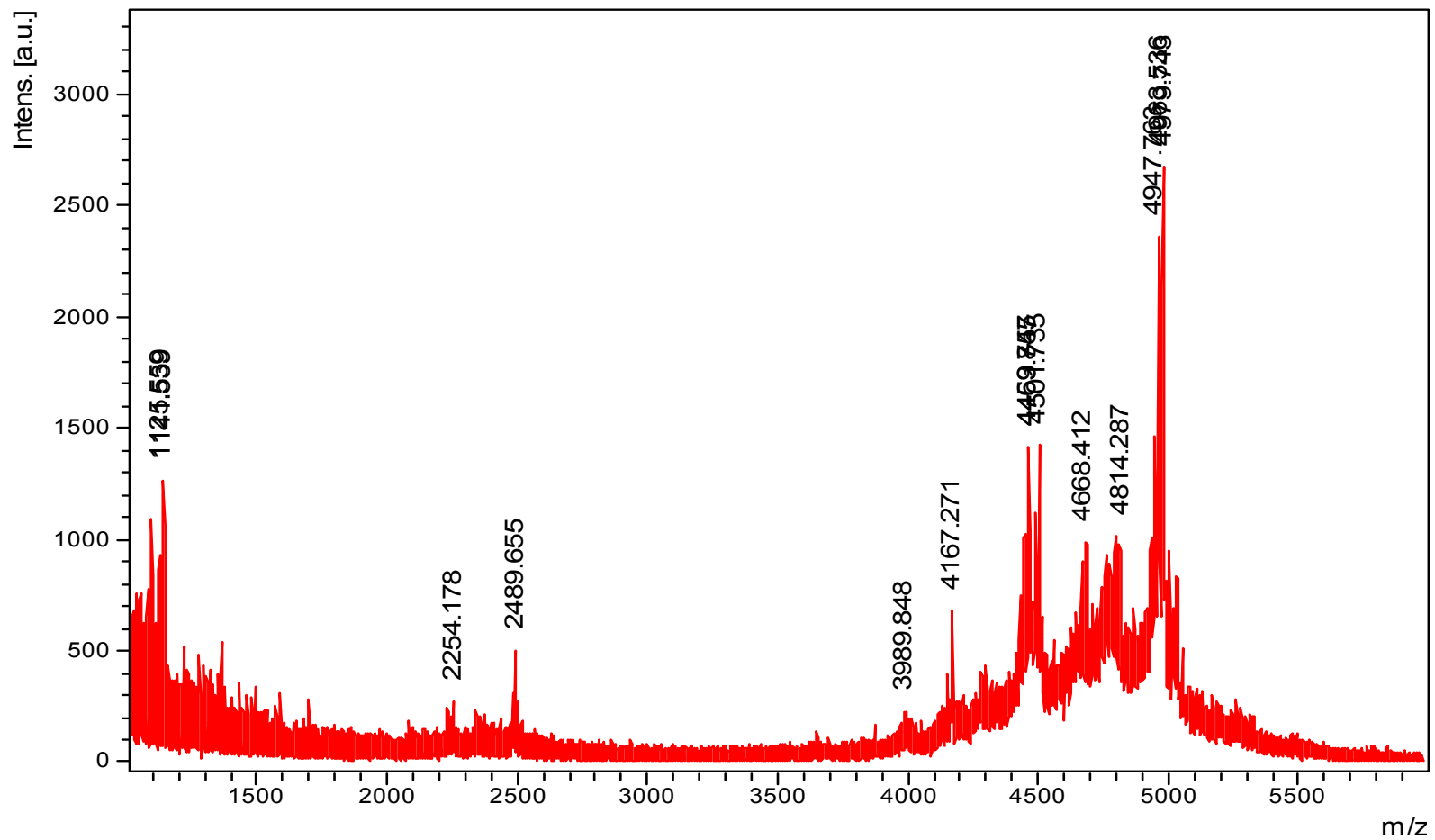


Figure 39: MALDI-TOF spectra of the products of sCT-SMCC intermediate and thiol-BP reaction.

In liquid chromatography mass spectroscopy (LC-MS/MS), thiol-BP appeared at 294.96 m/z (without sodium) and at 316.94 (with +1 Sodium). In MALDI TOF analysis, sCT-SMCC-BP peaks were seen at corresponding masses (with or without sodium). In sCT-2SMCC-1BP-1BP, two amines in Lys 11 or 18 or N-terminal in sCT were substituted by 2 SMCC, one of these SMCC reacted with 1 BP and the other did not. However 1 BP might have undergone thiol-substitution reaction with 1, 7 disulfide bond in sCT to give this product.

Synthesis of sCT-cysteine

Possible products were confirmed by MALDI-TOF and are shown in **figure 40**. Since the mono-, di- and tri-substituted sCT-SMCC had respective molecular weights of 3651.7, 3871.9 and 4093.2, coupling of L-cysteine (MW 121.16) with these functionalized sCT resulted into the formation of mono-, di- and tri-cysteine substituted sCTcysteine conjugates as represented respectively by the peaks at 3770.219, 4113.367 and 4453.437.

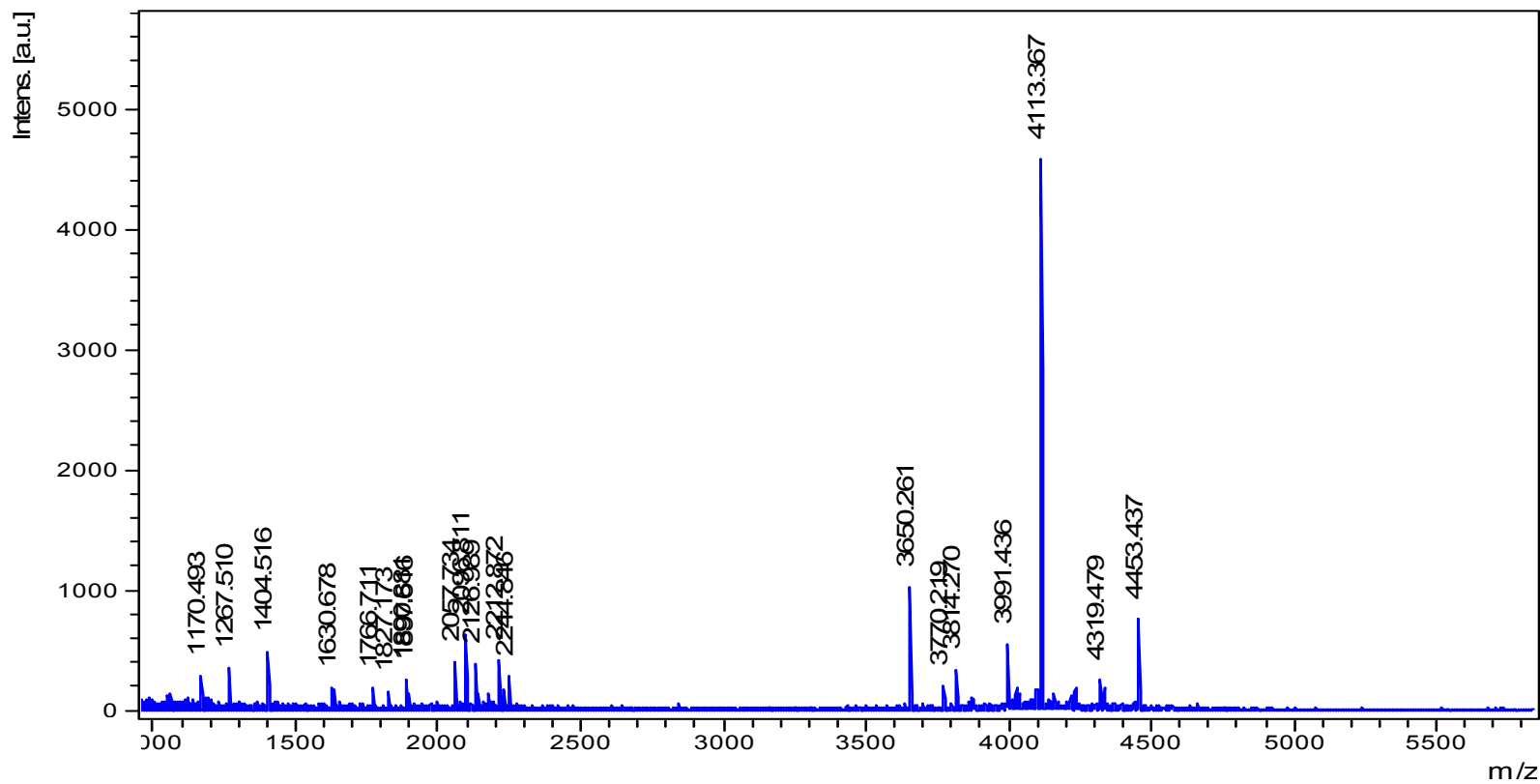


Figure 40: MALDI-TOF spectra of the products of sCT-SMCC intermediate and cysteine reaction.

Synthesis of sCT-PEG-BP

When thiol-BP (MW 294 Da) reacts with the MAL functional group of mono, di and tri substituted sCT-PEG, their molecular weights are increased by the fraction of 294 to generate mono (sCT-1PEG-1BP, MW ~7012 Da), di (sCT-2PEG-2BP, MW ~10519 Da), and tri (sCT-3PEG-3BP, MW ~14170 Da) substituted sCT analogues. Due to the polydispersed nature of NHS-PEG-MAL (**Figure 9**) spectra as shown in **figure 41** were obtained. Qualitative evaluation based on MALDI peak area suggested that the di-substituted analogues could be the major products followed by mono and tri-substituted analogues. Qualitative data from MALDI though not rigorous proved the existence of such forms.

3.5. PROCESS OPTIMIZATION FOR sCT-PEG-BP

The effect of buffer

MALDI-TOF results of conjugates using 100 mM pH 6.8 sodium acetate, ammonium acetate and sodium phosphate buffers are shown respectively in **figures 42- 44**. Sodium acetate buffer was initially chosen as the suitable reaction media because in literature, this was reported to stabilize aqueous unstable sCT better than other buffer (Capelle, Gurny et al. 2009). However, the pH was adjusted to 6.8 as it was optimum for the reaction between MAL in functionalized sCT and SH in thiol-BP.

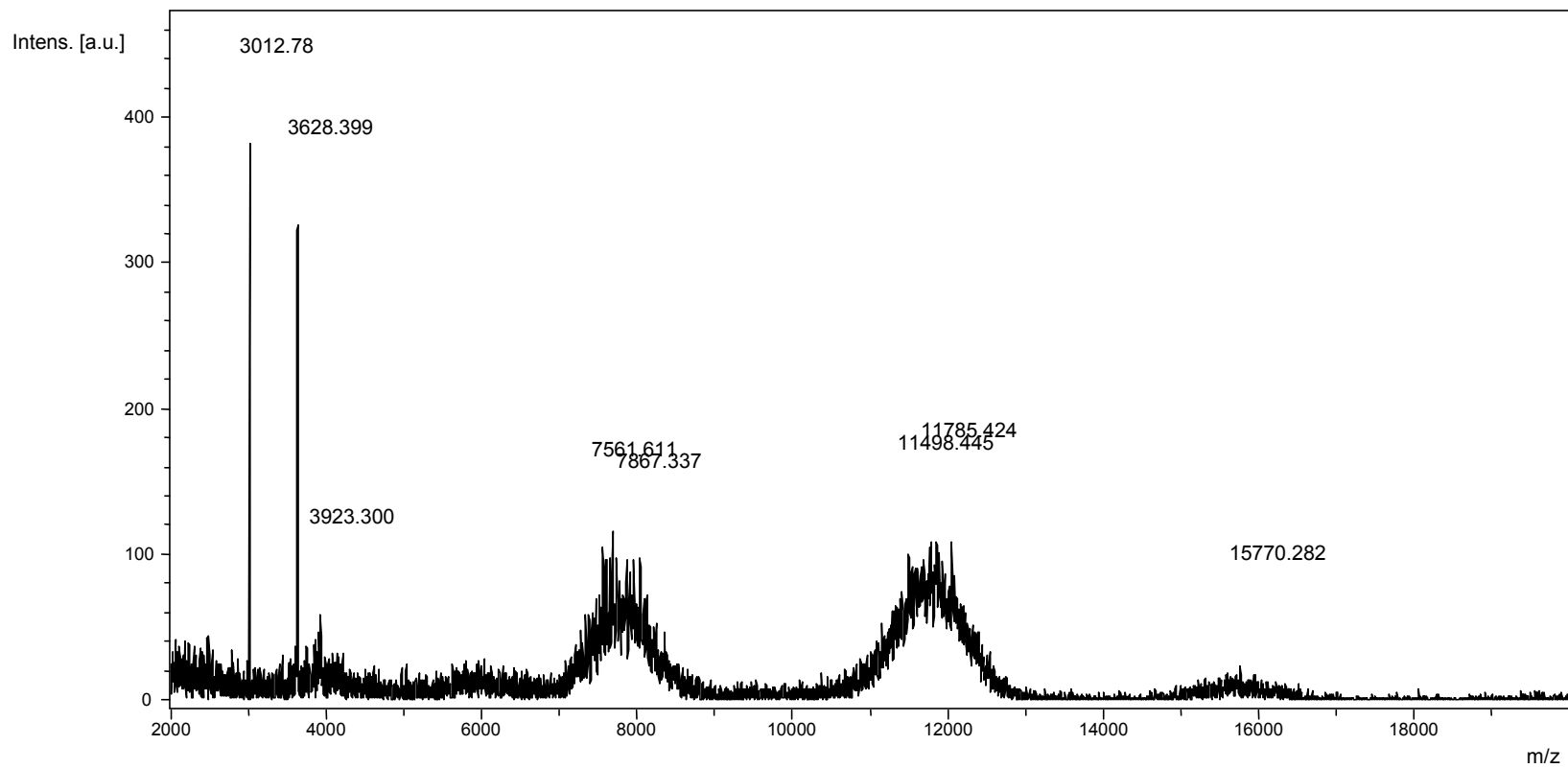


Figure 41: MALDI-TOF spectra of the products of sCT-PEG-MAL intermediate and thiol-BP reaction.

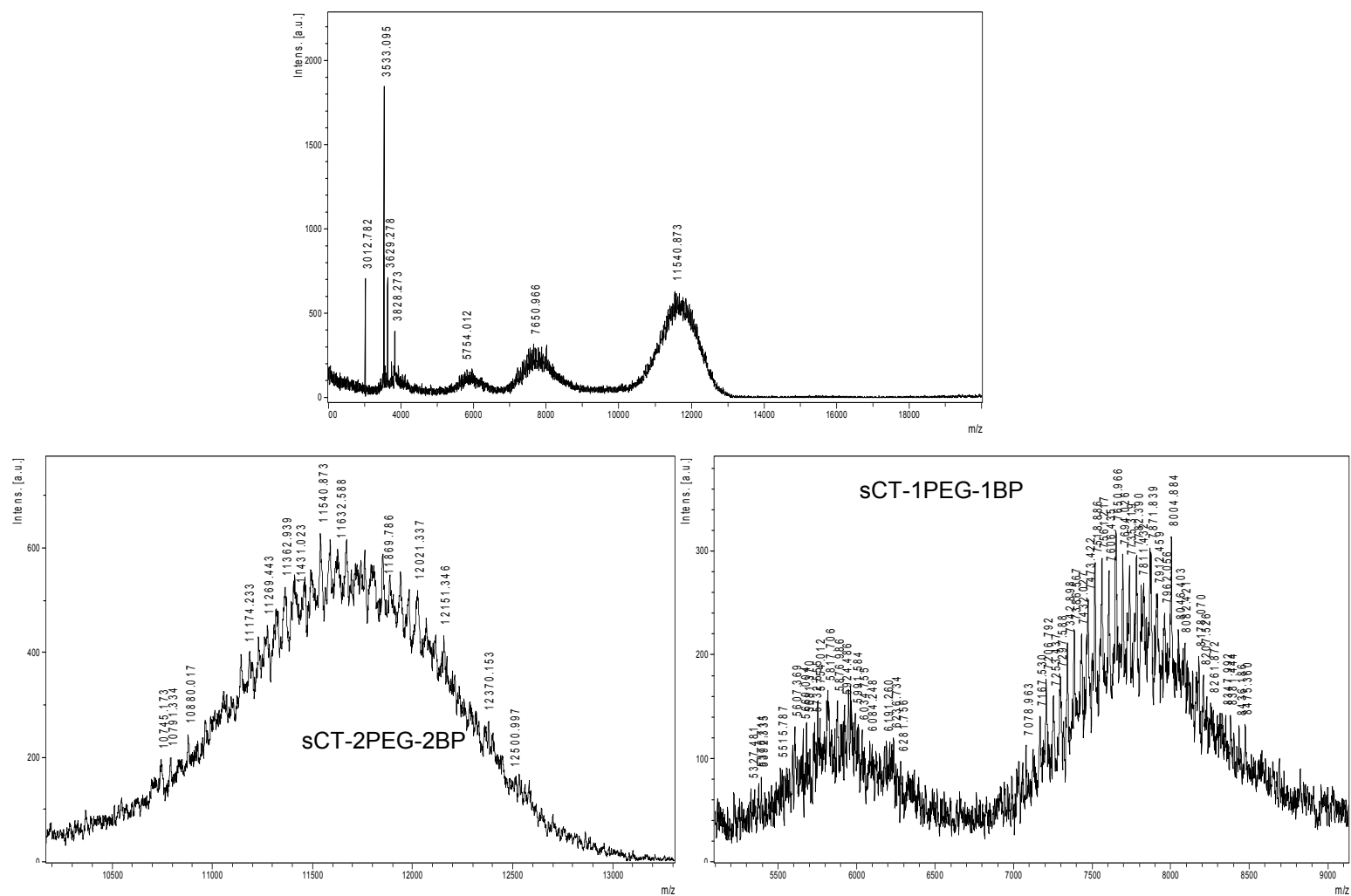


Figure 42: The effect of buffers in the reaction between sCT-PEG-MAL and thiol-BP: Effect of 100 mM sodium acetate buffer pH 6.8.

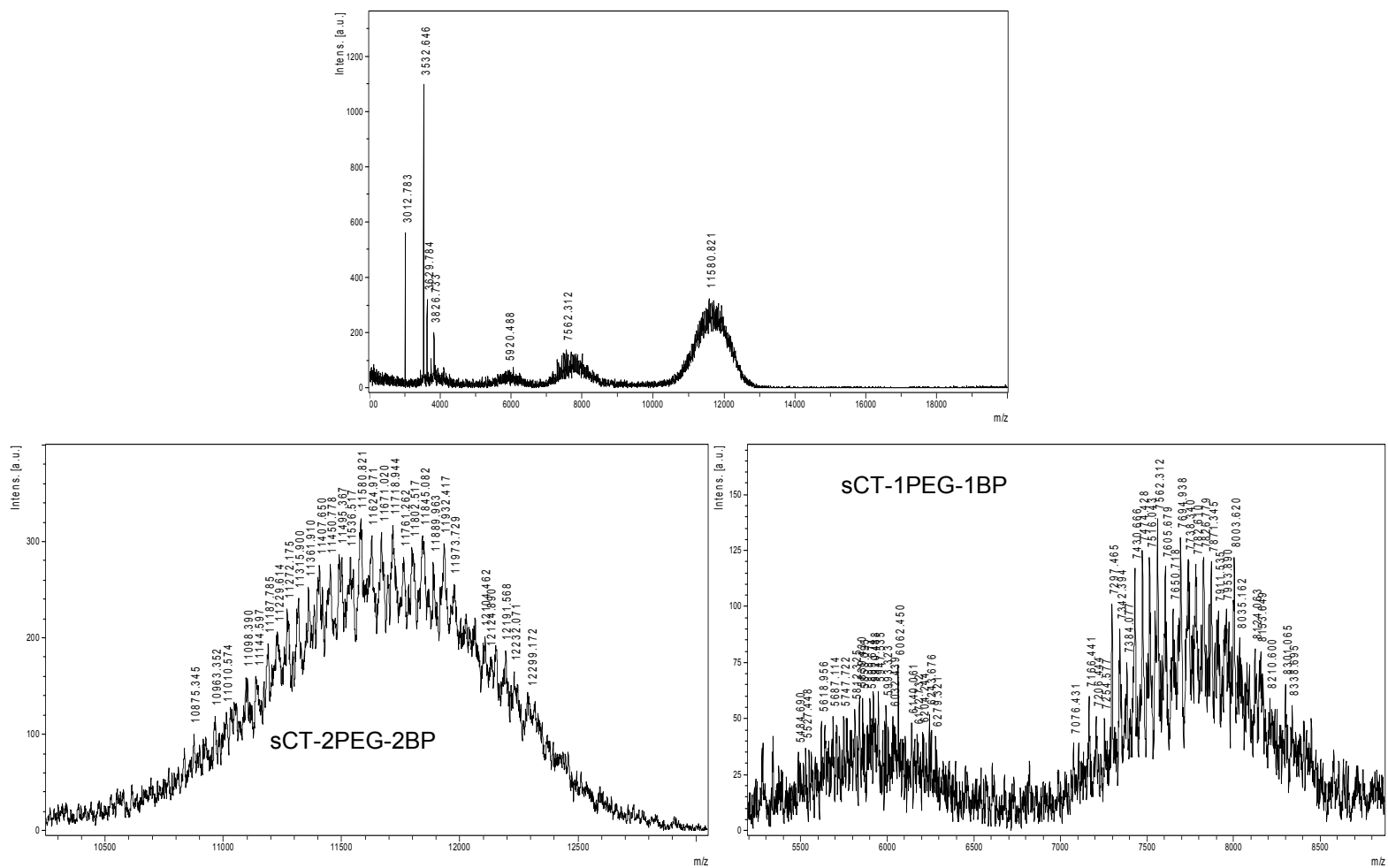


Figure 43: The effect of buffers in the reaction between sCT-PEG-MAL and thiol-BP: Effect of 100 mM ammonium acetate buffer pH 6.8.

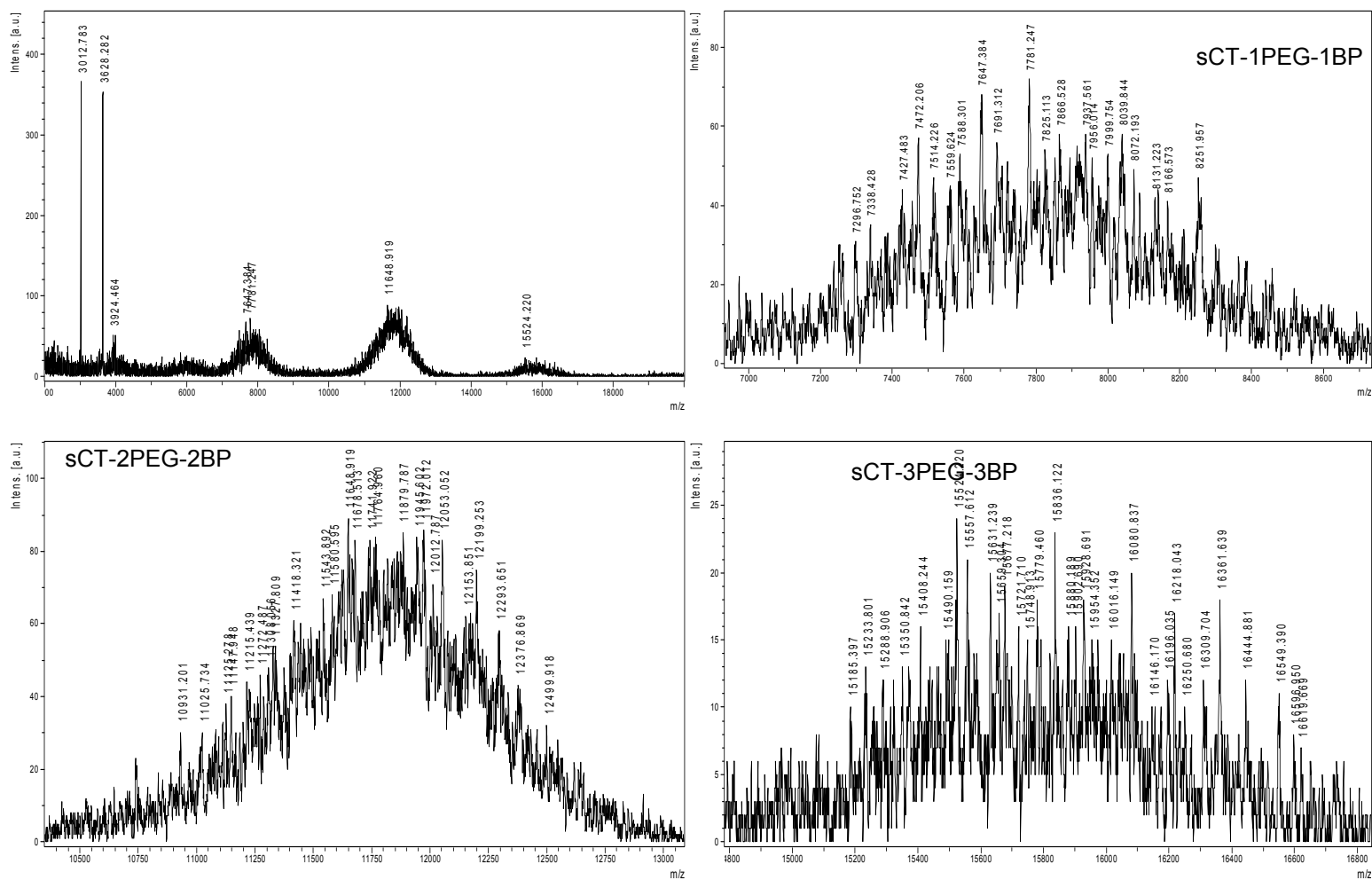


Figure 44: The effect of buffers in the reaction between sCT-PEG-MAL and thiol-BP: Effect of 100 mM sodium phosphate buffer pH 6.8.

Since the buffering capacity of any buffer is greatest at around its pKa which is 4.75 for sodium acetate buffer, at higher pH the reaction could be unfavourable as the addition of sCT and thiol-BP could alter the pH away from the optimal reaction pH that could not be efficiently resisted by the buffer.

Although ammonium acetate buffer was reported by the same authors (Capelle, Gurny et al. 2009) to have relatively better sCT stabilizing effect, the reaction was more favourable in 100 mM phosphate buffer pH 6.8. This could be due to the higher buffer capacity of phosphate buffer at that pH irrespective of sCT stability issues.

Since the reaction between sCT-PEG-Mal and thiol-BP is completed before 2 hr at room temperature, 100 mM phosphate buffer pH 6.8 was selected because of its reaction favoring effect. We assumed that the stability of sCT in phosphate buffer at the final concentration used in reaction was not a major issue as it was below 1 mg/mL and phosphate buffer was immediately exchanged by dialysis or size exclusion spin chromatography with 20 mM sodium acetate buffer pH 5 with better sCT stabilization effect (Capelle, Gurny et al. 2009). Unlike in phosphate buffer, tri-substituted products were not seen in the case of acetate buffers. This was due to more favourable reaction in phosphate buffer (**See figure 42**).

The effect of buffer concentrations

Since the coupling reaction was favoured in phosphate buffer, we evaluated the effect of phosphate buffer concentration on the reaction. 100, 50 and 10 mM phosphate buffers pH 6.8 were used in the reaction. The results are shown in **figures 44- 46**. As expected the reaction was favorable in more concentrated buffers. This was consistent with our earlier finding that the acetate buffers with low buffering capacity performed poorly compared to the phosphate buffer with better buffering capacity at pH 6.8. Mainly di-substituted products were evident in 10 mM buffer but all three products were seen in 50 and 100 mM with the formation of di-substituted products being more favorable.

From these findings the 100 mM phosphate buffer was selected for further reactions. The presence of PEG increased the solubility and stability of sCT in buffered solution.

The effect of thiol-BP concentrations

Finally, we studied the effect of thiol-BP concentration in the reaction using functionalized sCT: thiol-BP in 1:5, 1:10, 1:20 and 1:40 molar ratios per MAL in sCT-PEG-MAL. The results are shown respectively in **figures 47- 50**. Formation of di-substituted products was more favorable. The reaction was more favorable with higher thiol-BP ratio.

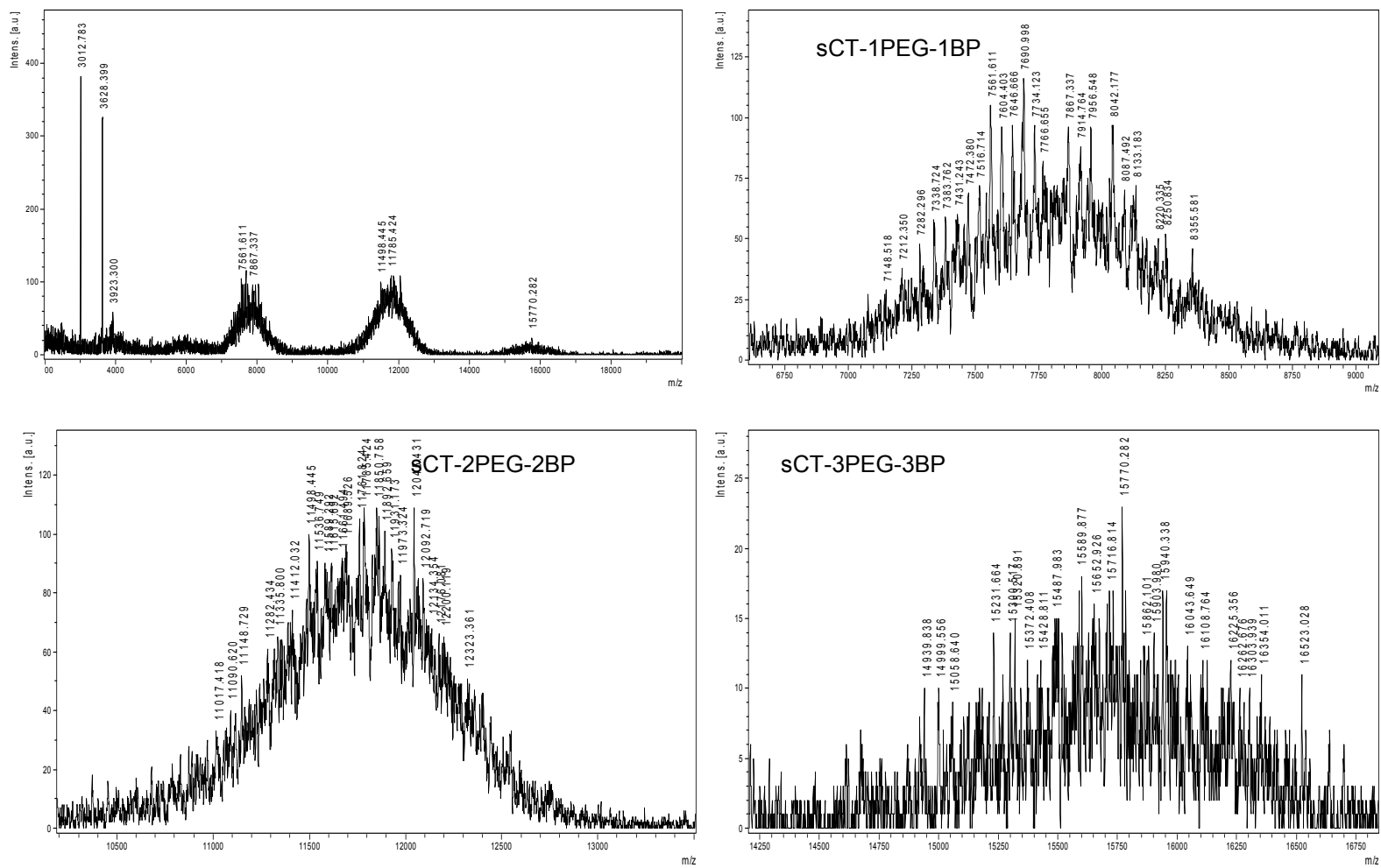


Figure 45: The effect of pH 6.8 phosphate buffers concentrations in the reaction between sCT-PEG-MAL and thiol-BP:
Effect of 50 mM sodium phosphate buffer.

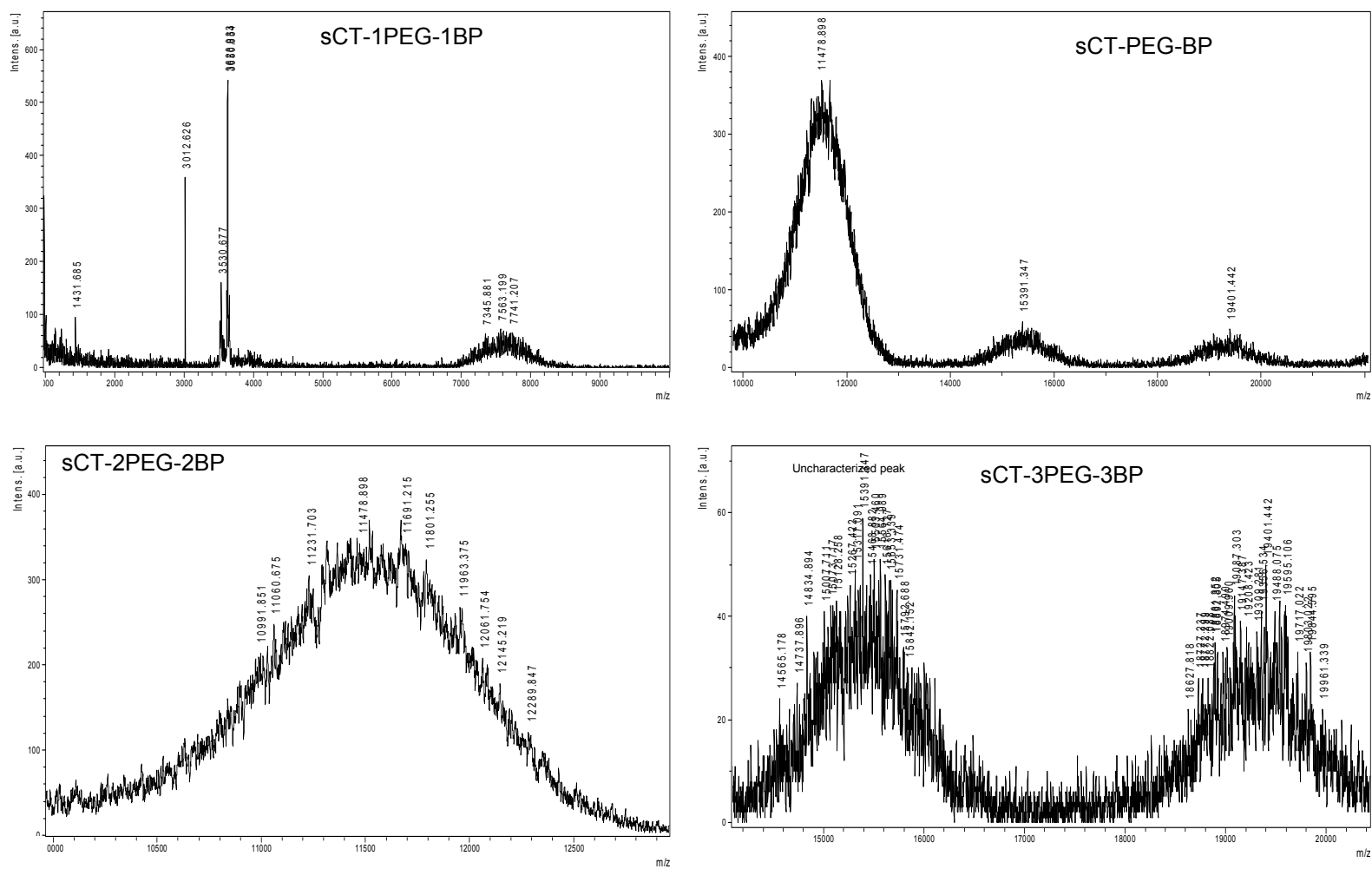


Figure 46: The effect of pH 6.8 phosphate buffers concentrations in the reaction between sCT-PEG-MAL and thiol-BP:
Effect of 10 mM sodium phosphate buffer.

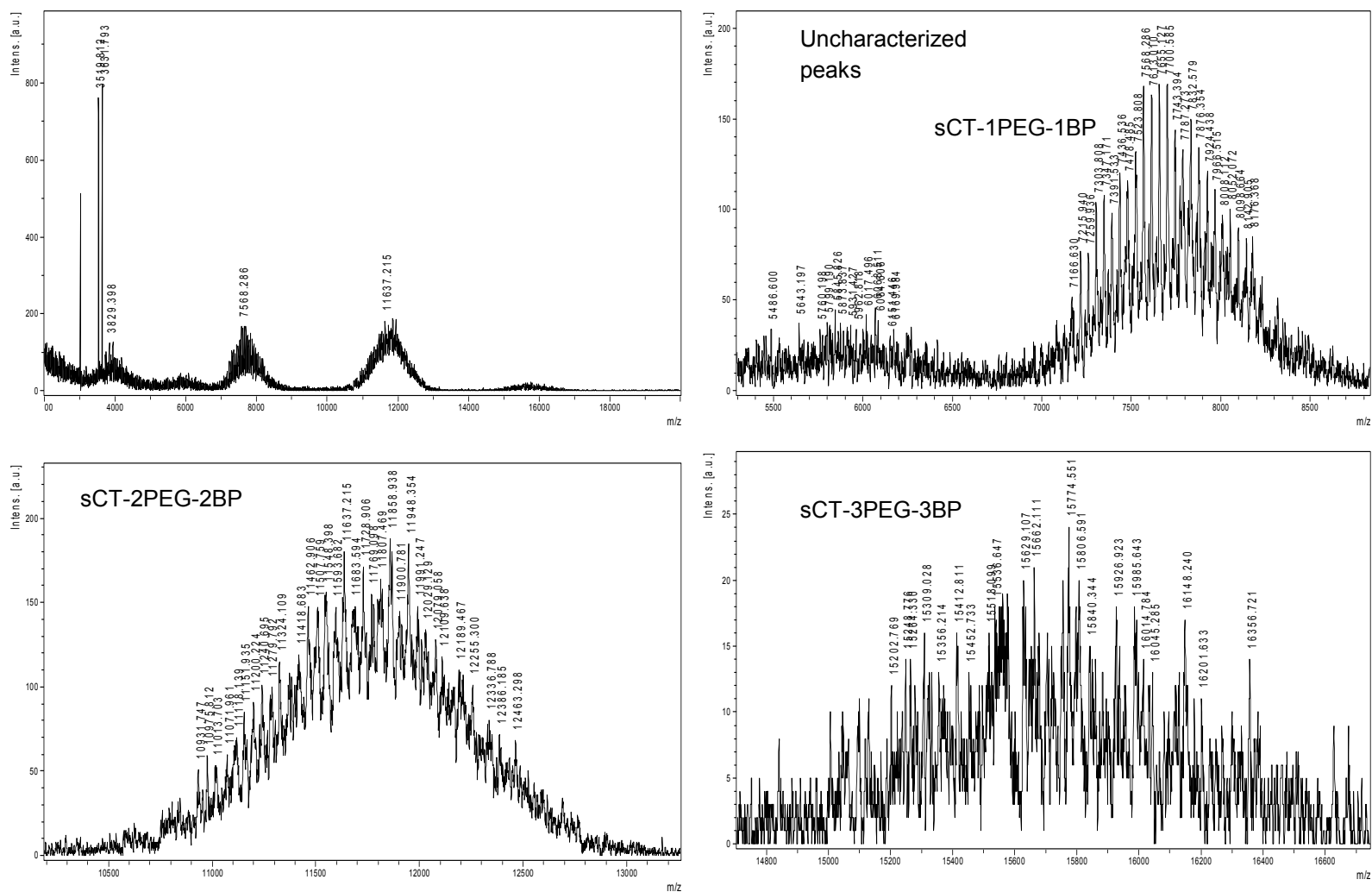


Figure 48: The effect of thiol-BP concentrations in its reaction with sCT-PEG-MAL: 1: 10 mol/ mol ratio of sCT-PEG-MAL to thiol-BP.

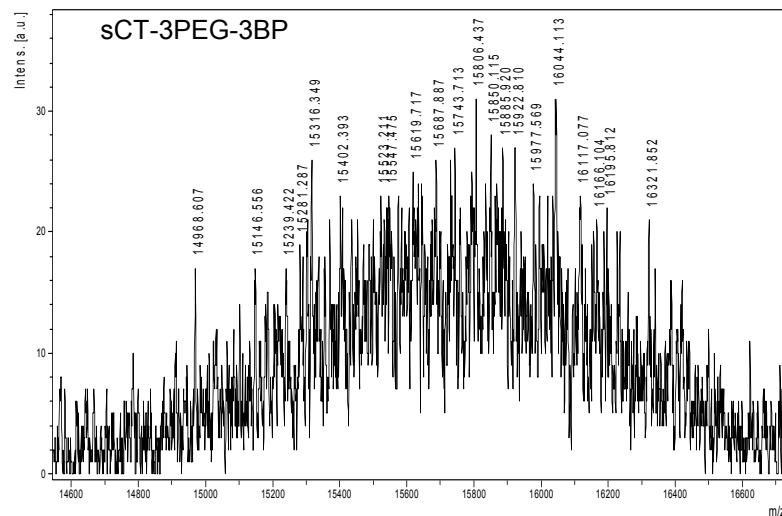
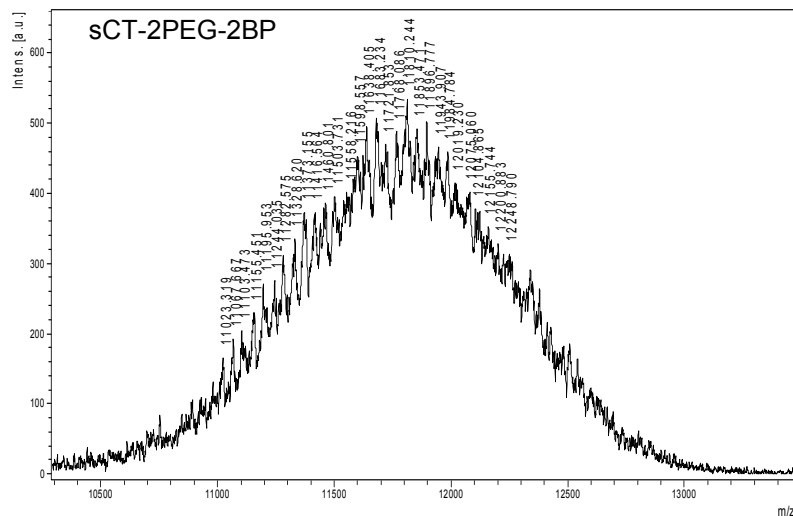
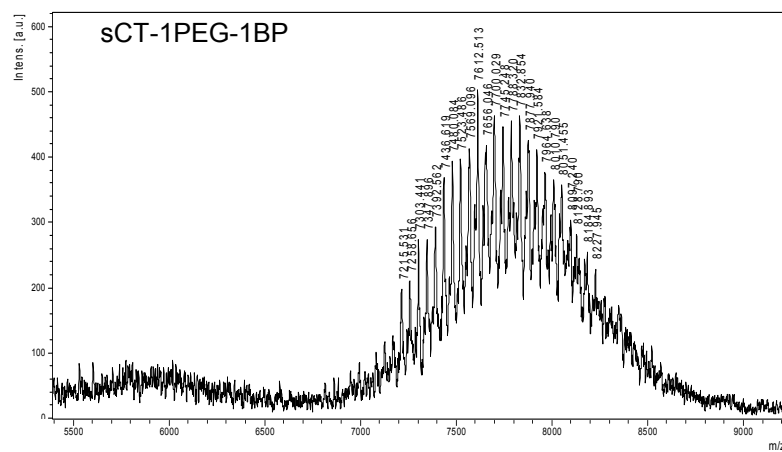
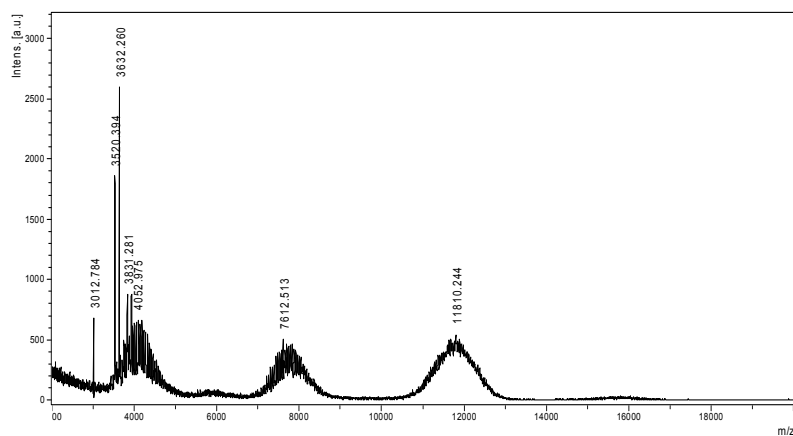


Figure 49: The effect of thiol-BP concentrations in its reaction with sCT-PEG-MAL: 1: 20 mol/ ratio of sCT-PEG-MAL to thiol-BP.

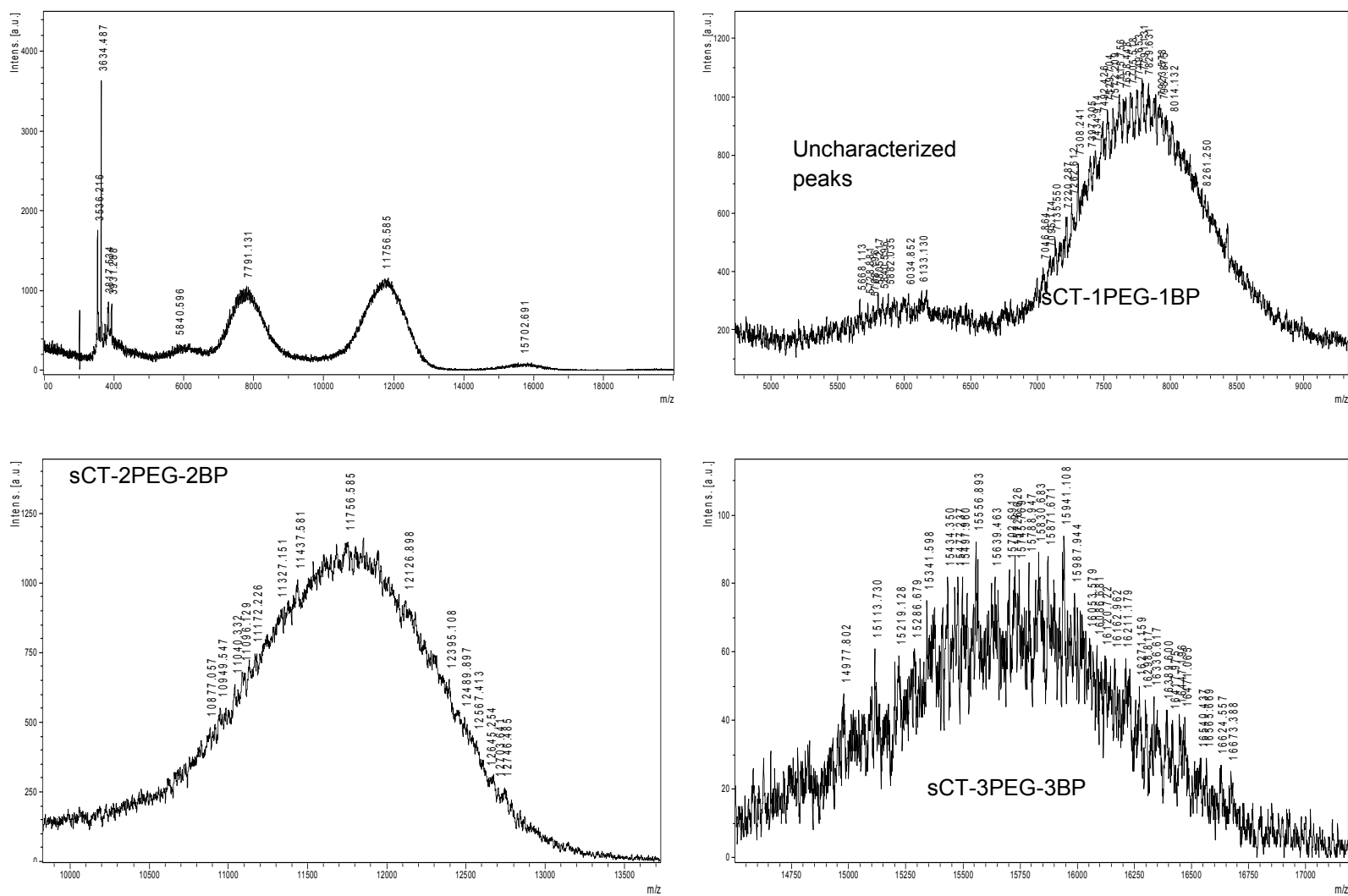


Figure 50: The effect of thiol-BP concentrations in its reaction with sCT-PEG-MAL: 1: 40 mol/ mol ratio of sCT-PEG-MAL to thiol-BP.

3. 6. CONJUGATE CHARACTERIZATION

Tris-tricine SDS-PAGE

sCT-BP:

Conjugation reaction mixtures were run in tris-tricine SDS-PAGE. However, because of the small differences in their molecular weights, they appeared as a single band and did not resolve distinctly under these conditions on SDS-PAGE gel, as shown in **figure 51**.

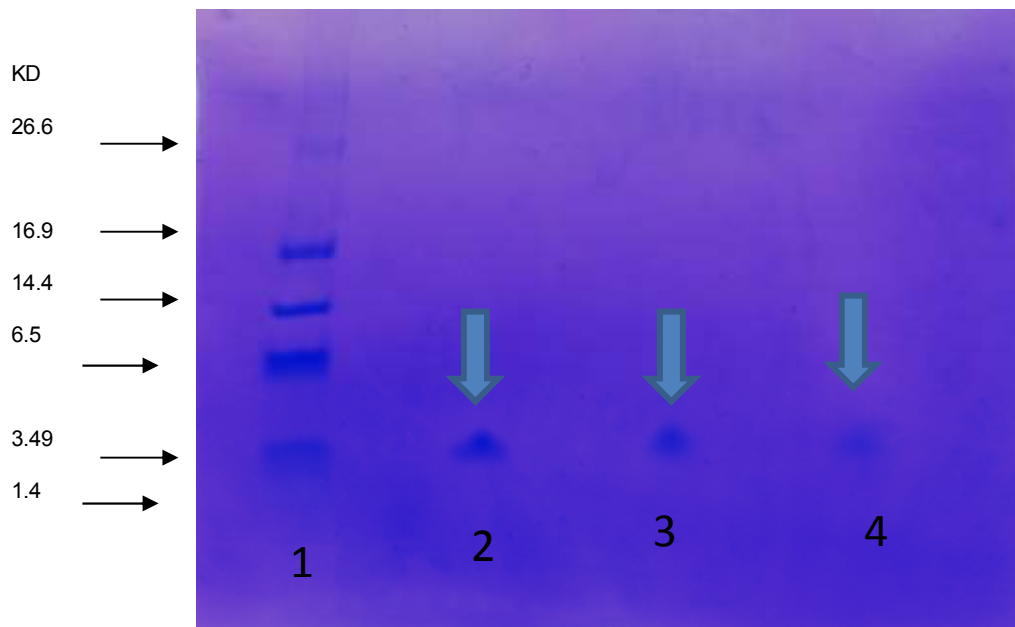


Figure 51: Tris-tricine SDS-PAGE of reaction mixtures. sCT was reacted with sulfo-SMCC in DMF in presence of TEA, followed by the reaction with thiol-BP in phosphate buffer. Lane 1. Peptide SDS-PAGE molecular weight standards. 2. Salmon calcitonin: MW (3.43 kD). 3. sCT-SMCC conjugate. 4. sCT-SMCC-BP conjugate. 5. Loading Dye.

sCT-PEG-BP:

Results of tris-tricine SDS-PAGE are shown in **figure 52**. Lane 1 represents molecular weight markers; lane 2 is for sCT, 3 for sCT-PEG-BP and 4 for sCT-PEG. Single band for sCT appeared at about 3.49 kD and two bands were seen in case of sCT-PEG above 6.5 and below 16.9 kD. Similarly sCT-PEG-BP appeared as two bands above the position of sCT-PEG. All three substitution products as shown in MALDI-TOF were not seen in SDS-PAGE.

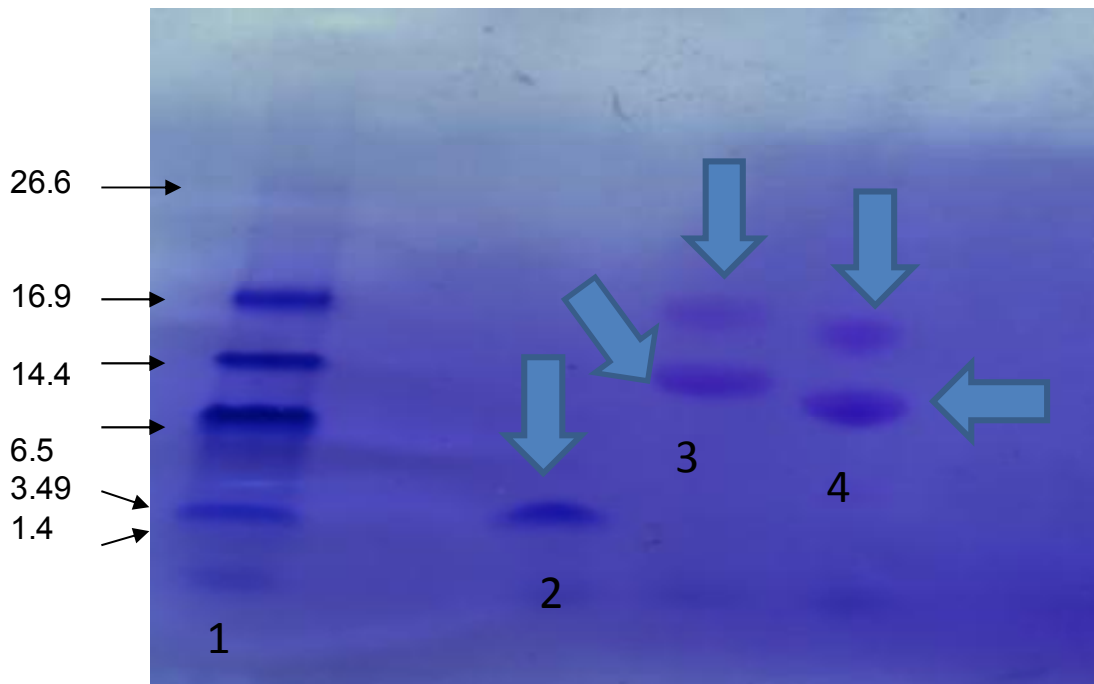


Figure 52: Tris-tricine-SDS-PAGE of reaction mixtures when sCT was reacted with NHS-PEG-MAL in DMSO, followed by the reaction with thiol-BP in phosphate buffer. (Left to right) Lane 1. Peptide SDS-PAGE molecular weight

standards. 2. Salmon calcitonin. 3. sCT-PEG-BP conjugate. 4. sCT-PEG-MAL intermediate.

From the gel scan, it appears that the mono substituted products was not present. However, in MALDI the peak ratio of mono substituted products were always noticeably higher than tri-substituted products. Thus, it can be assumed that the appeared products were major mono and di-substituted products although they were seen in an altered position than standard molecular weight markers.

Alteration of molecular shape by PEG might affect the mobility. This is possible by the fact that PEGylated peptides form micelles in aqueous solution and the electrophoretic mobility of micelles is different than pure linear peptide of same size due to their shape. This is in accordance with previous reports of such band appearance in a slightly higher molecular weight position than theoretical.

Many reports state that the exact molecular mass of the PEGylated protein/peptide could not be determined by SDS-PAGE owing to the band broadening. Also, the electrophoretic mobility of these conjugates is known not to be strictly related to the molecular weight (Kurfurst 1992; Zheng, Ma et al. 2007; Colonna, Conti et al. 2008). SDS-PAGE, although is very effective for protein analysis, may fail to give a clear image of the separation of the PEGylated product (Oda, Ishikawa et al. 2007). The presence of PEG has interference effect on the analysis.

It has also been reported that PEG and SDS may form a complex in SDS-PAGE analysis (Odom, Kudlicki et al. 1997). In some SDS-PAGE of PEG–protein, the bands were broad, not clear or even smeared, probably resulting from the complex interaction between PEG chains coupled to protein and SDS micelles, between PEG chains and protein, and between the PEGylated protein and SDS micelles (Kerwin, Chang et al. 2002). The migration property of PEGylated protein could be very different from that of protein of same molecular weight. Therefore, a simple comparison with the protein standard bands could not give the correct molecular weight information of the products (Zheng, Ma et al. 2007).

Odom *et al.* performed SDS-PAGE of standard protein markers with the addition of free PEG 8000 (Odom, Kudlicki et al. 1997). They found that under standard Laemmli SDS-PAGE conditions, the addition of PEG changed the mobilities of the proteins. By the staining method, they found that PEG, a neutral polymer without charge, also moved into the gel, and formed a long tailing band. The reason was that SDS micelles could bind PEG, forming a complex with negative charge, which can move in the electrophoresis gel (Odom, Kudlicki et al. 1997). Attachment of a big PEG molecule, could greatly enlarge the size because the hydrodynamic volume of PEG can be five to ten times greater than that of the corresponding peptides and proteins of the same molecular mass due to its ability of associating a large amount of water and its high flexibility in the solution (Yun, Yang et al. 2005; Zheng, Ma et al. 2007).

Extent of BP coupling per sCT

sCT had an average of 2 BPs per molecules. This is in accordance with the previous results of the more favorable di-substitution reaction relative to mono and tri-substitution. We did not try to find the number of BP substitution by altering NHS-PEG-MAL ratios as it was optimized in earlier reaction using MALDI and this substitution can be the maximum for the reaction condition used in this report. Moreover, as the number of BP substitution increases, so does the bone mineral binding affinity of BP conjugated protein, higher substitution would still be desirable as long as it does not significantly affect sCT secondary structure, and receptor binding affinity.

3. 7. IN-VITRO EVALUATION

Bone mineral affinity

sCT-BP:

When all compounds were assayed directly (i.e., without HA), the absorbance of protein in those samples was readily detected in the supernatant. The incubation of sCT-BP with HA substantially reduced the sCT concentration in the supernatant, due to its BP-mediated binding to the HA (**figure 61**). The alteration of primary amines in sCT alone (by the cross-linker conjugation chemistry) did not improve HA binding, as represented by the lack of sCT-cysteine control conjugate HA binding. To further confirm the HA binding of conjugates, the samples were washed

until the washings were free of sCT, then centrifuged, and the HA pellet obtained then analyzed for sCT. As shown in **figure 53**, sCT-BP was substantially bound to HA. The absorbance seen for native sCT, and for the sCT-cysteine conjugate likely represent the non-specific surface adsorption of sCT on HA.

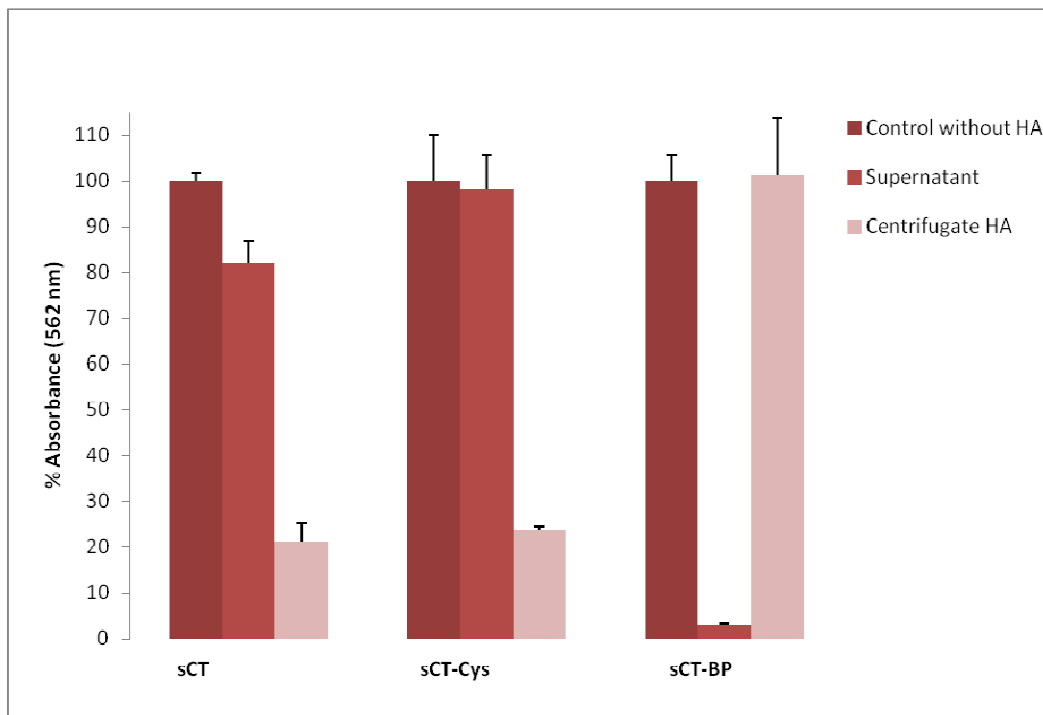


Figure 53: Determination of bone targeting potential (hydroxyapatite, HA, binding ability) of sCT-BP. sCT or equivalent concentration of sCT-Cys and sCT-BP was incubated for 1 hour with HA in 100 mM pH 7 phosphate buffer and the amount of sCT in the supernatant and centrifuged pellet was determined by micro-BCA protein assay. Hydroxyapatite (pellet): sCT versus sCT-BP: $P < 0.05$.

sCT-PEG-BP:

sCT concentration in control samples without any calcium salts or HA was taken as 100% for further calculations. Upon incubation with HA, approximately 65% sCT-PEG-BP was bound to the HA pellet (**figure 54**). Reduced sCT concentration in the supernatant was due to the BP-mediated binding to the HA. Conversely, sCT and sCT-PEG did not significantly bind to HA. As HA is the principal mineral found in bone matrix, *in vivo* administration of sCT-PEG-BP conjugates should lead to improved bone accumulation of sCT compared to free sCT or sCT conjugates that lack BP.

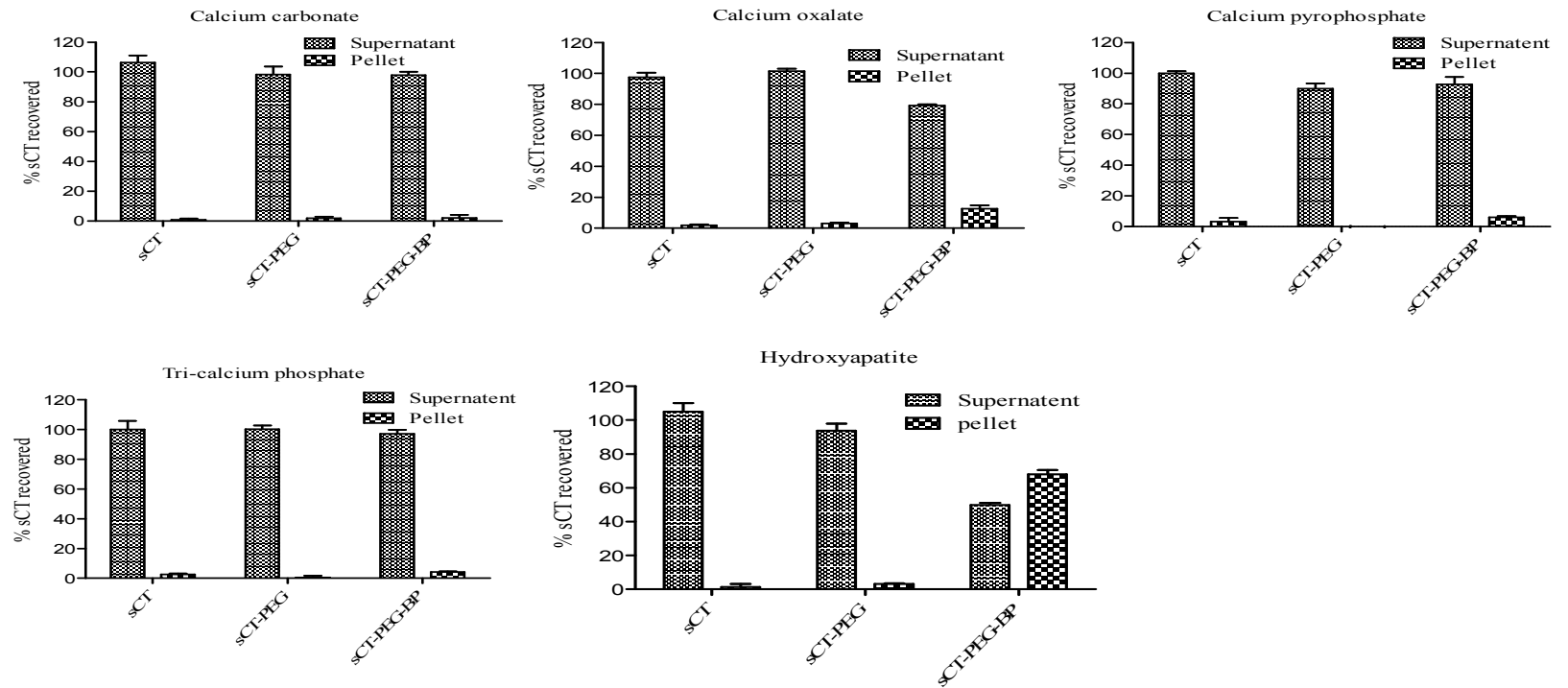


Figure 54: Determination of bone targeting potential: bone mineral affinity and specificity of sCT-PEG-BP: sCT or equivalent sCT-PEG and sCT-PEG-BP was incubated for 1 hour with HA or various calcium salts in 100 mM pH 7 phosphate buffer and the amount of sCT in the supernatant and centrifuged pellet was determined by micro-BCA protein assay. Calcium oxalate (pellet): sCT versus sCT-PEG-BP: $P < 0.05$; Hydroxyapatite (pellet): sCT versus sCT-PEG-BP: $P < 0.05$.

Bone mineral specificity

sCT-BP:

sCT, sCT-cys and sCT-BP were also assayed for their specificity to bone mineral using different calcium salts binding assay. As shown in **figure 55**, sCT was significantly bound by HA over that of other calcium salts.

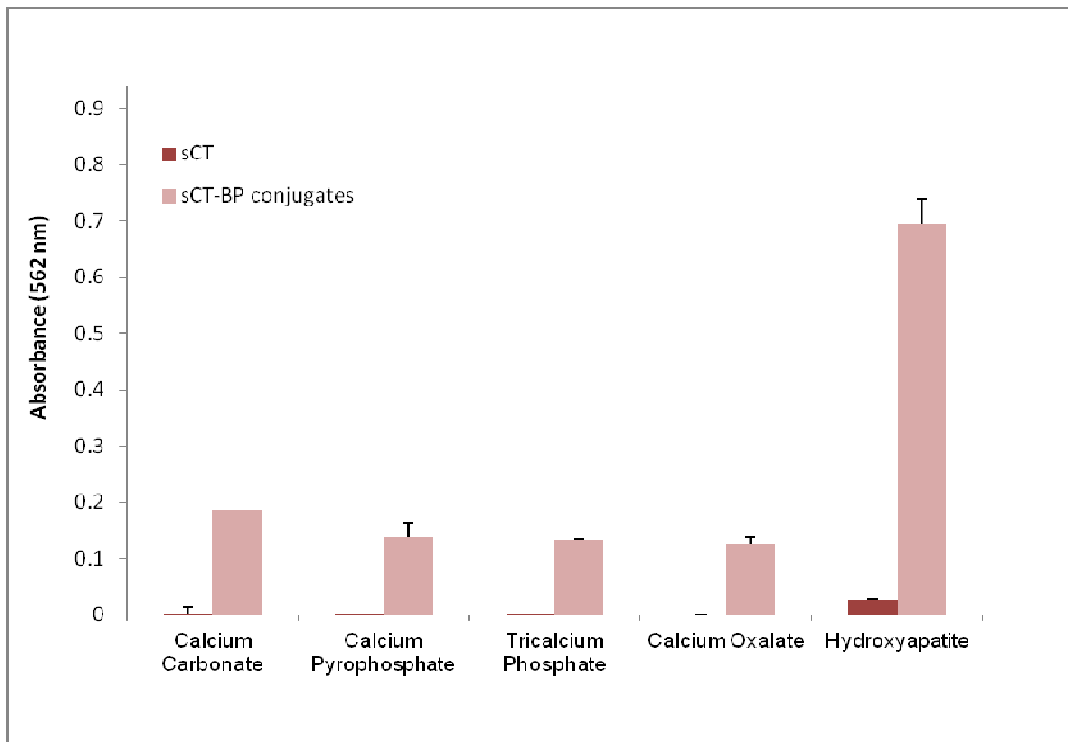


Figure 55: Determination of bone targeting potential: bone mineral specificity of sCT-BP. sCT-BP was incubated for 1 hour with various calcium salts in 100 mM pH 7 phosphate buffer and the amount of sCT in the supernatant and centrifuged pellet was determined by micro-BCA protein assay. Amount of sCT in HA pellet versus other calcium salt pellet: $P < 0.05$.

sCT-PEG-BP:

Incubation of sCT or sCT analogues with calcium carbonate did not significantly reduce sCT concentration in the supernatant (**figure 54**) suggesting that there was no significant adsorption to the calcium carbonate as confirmed by the absence of sCT in the washings from the calcium carbonate pellet. Similarly, no significant adsorption was noted in case calcium pyrophosphate and tri-calcium phosphate. However, in case of HA binding, the amount of sCT in supernatant was significantly lower for sCT-PEG-BP than for sCT. Similarly, the amount of sCT in centrifuged pellet was significantly higher for sCT-PEG-BP than for sCT ($P < 0.05$).

sCT secondary structure

As can be seen in the circular dichroism (CD) spectra in **figure 56**, sCT had very little helical content as demonstrated by the low magnitude of ellipticity at 222 nm (Erand, Erand et al. 1983; Erand, Erand et al. 1986; Siligardi, Samori et al. 1994). CD curve of sCT-PEG and sCT-PEG-BP retained the peak at 222 nm and the peak at 200 shifted slightly towards longer wavelength. In addition a positive peak appeared at below 200 nm in sCT-PEG or sCT-PEG-BP indicating the tendency of PEG to shift sCT secondary structure toward a relatively more stable and less aggregation prone helical structure (D'Santos, Nicholson et al. 1988). Shape of the CD curve of sCT-SMCC and sCT-BP showed increased peak intensity at 222 nm. CD spectra of sCT-BP in the same solvent

displayed strong α -helical character as shown by the presence of a positive peak at 198 and intense negative peaks at 208 and 222 nm. This is the first report of such helical structure in sCT after conjugation with BP. Although a perfect helical structure was not seen in the case of PEGylated sCT analogues, this may still have a significant impact towards sCT solution stability. As shown in later experiments, PEGylation and/or BP coupling had no adverse effect sCT bioactivity. Thus, in that context of unaltered activity, the shifting of sCT structure towards helical shape remains a desirable outcome.

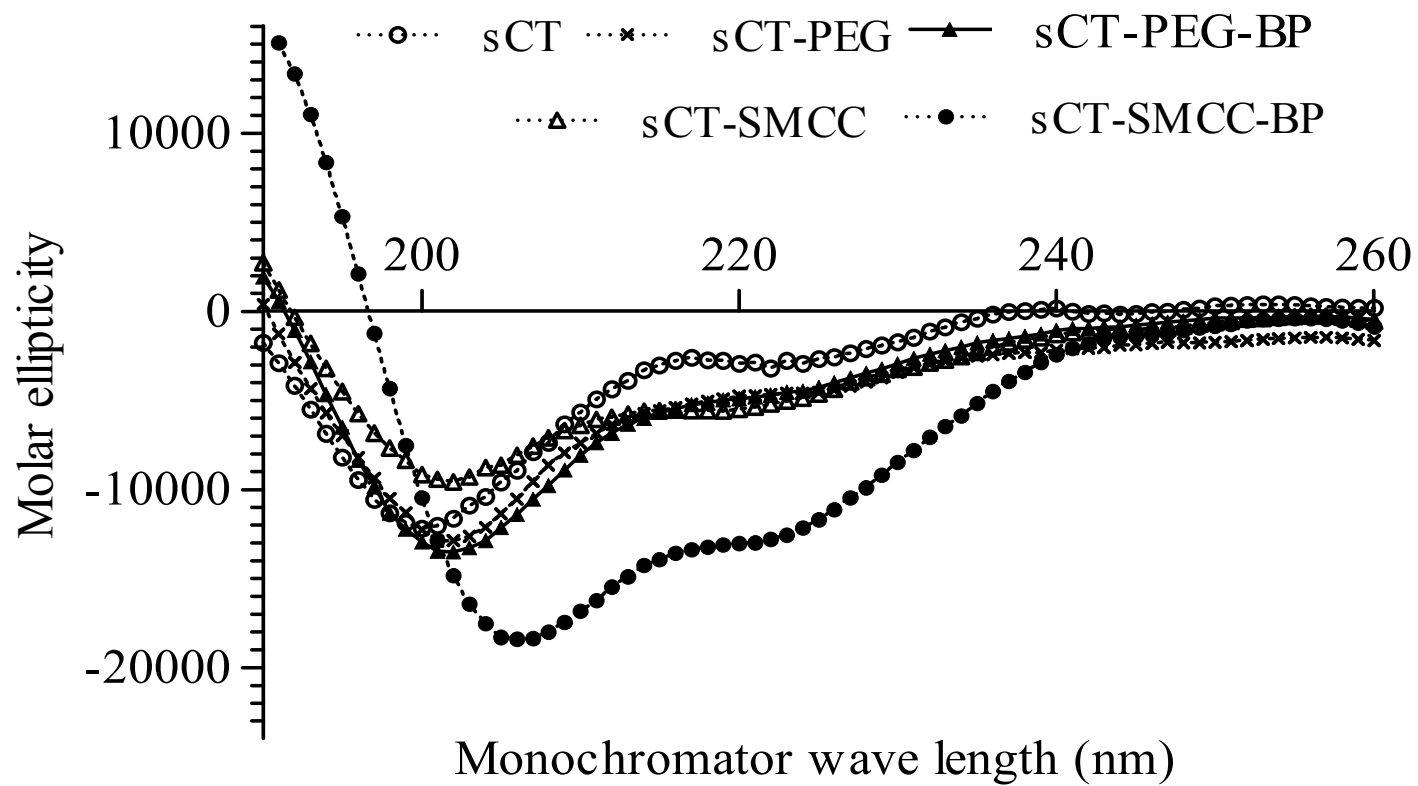


Figure 56: Circular dichroism (CD) spectra of sCT, sCT-SMCC, sCT-PEG, sCT-BP and sCT-PEG-BP to determine the effect of SMCC, SMCC-BP, and PEG or PEG-BP conjugation on sCT secondary structure.

In-vitro cell viability assay

We compared sCT and sCT analogues for any potential cytotoxicity using the MTT assay (**figure 57**).

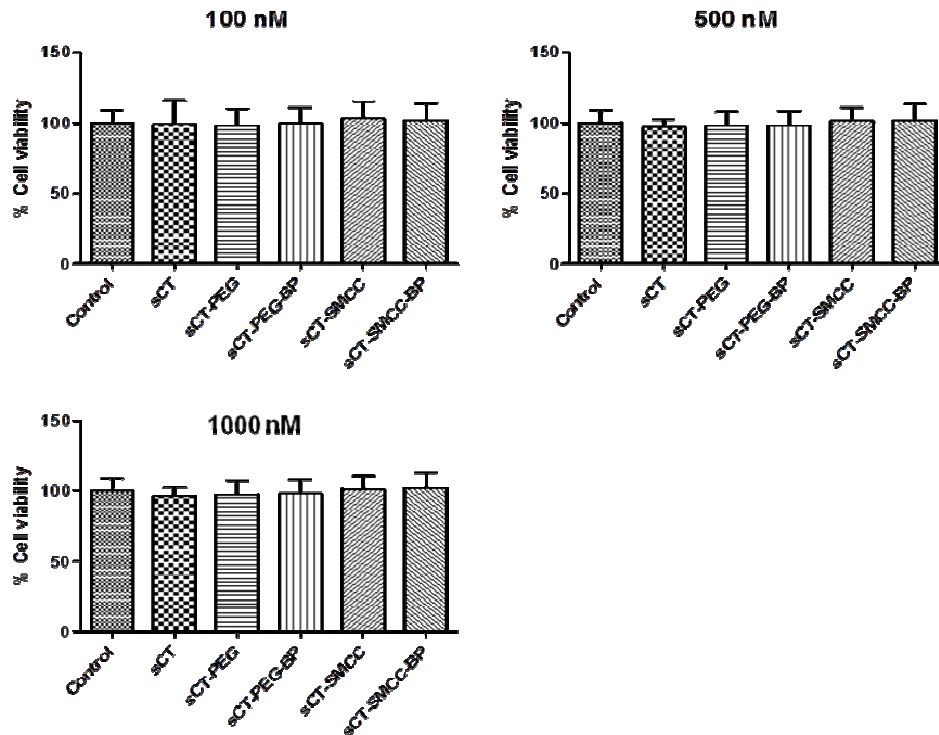


Figure 57: *In vitro* cell viability assay for sCT analogues on RAW 264.7 cells determined by MTT assay. 20000 RAW 264.7 cells/well in 96 well plate (n=8), cultured for 3 days and treated with sCT or equivalent followed by incubation at 37°C for 4 hours in basic DMEM media. Cells were treated with 100 µg/well of MTT in basic DMEM media and the absorbance of formazan crystal solution was measured using spectrophotometer at 570 nm.

For 100, 500 and 1000 nM sCT or equivalent, average % cell viability for sCT was 98.99 ± 8.99 , 96.72 ± 8.89 and 100.42 ± 8.8 respectively. For sCT-BP these values were 101.72 ± 5.6 , 101.75 ± 13.67 and $99.27 \pm 9.18\%$ respectively. Similarly, for sCT-PEG-BP these values were 99.57 ± 11.13 , 98.18 ± 10.08 and $96.75 \pm 6.41\%$ respectively. No significant difference in cell viability was observed between sCT versus sCT analogues including sCT-SMCC or sCT-PEG. Similarly, cell viability values of sCT or sCT analogues were not significantly different when compared to control samples without sC. It should be noted that concentration of sCT and sCT analogues used in our *in vitro* bioactivity and *in vivo* efficacy evaluations was equivalent to or less than 100 nM sCT, corresponding to orders of magnitude less compound than used in this study.

Anti-sCT antibody binding ability

Presence of BP resulted into the binding of these conjugates on the bone mineral surface of these plates. sCT on such bound conjugates was then reacted with anti-sCT antibody. Finally, the intensity of the developed colour was measured and the results are shown in **Figure 58**. The absorbance of sCT-PEG-BP was 6 times and sCT-BP 4 times higher than that of native sCT. When compared to sCT-PEG and sCT-SMCC, the absorbance of sCT-PEG-BP was 4 times and sCT-BP 3.5 times higher respectively. These measurements indicated significantly greater affinity of

BP conjugated sCT analogue for the bone surface than non-BP containing analogues (or unmodified sCT itself). In addition the conjugation chemistry had no effect on the antibody binding ability of sCT present in conjugates.

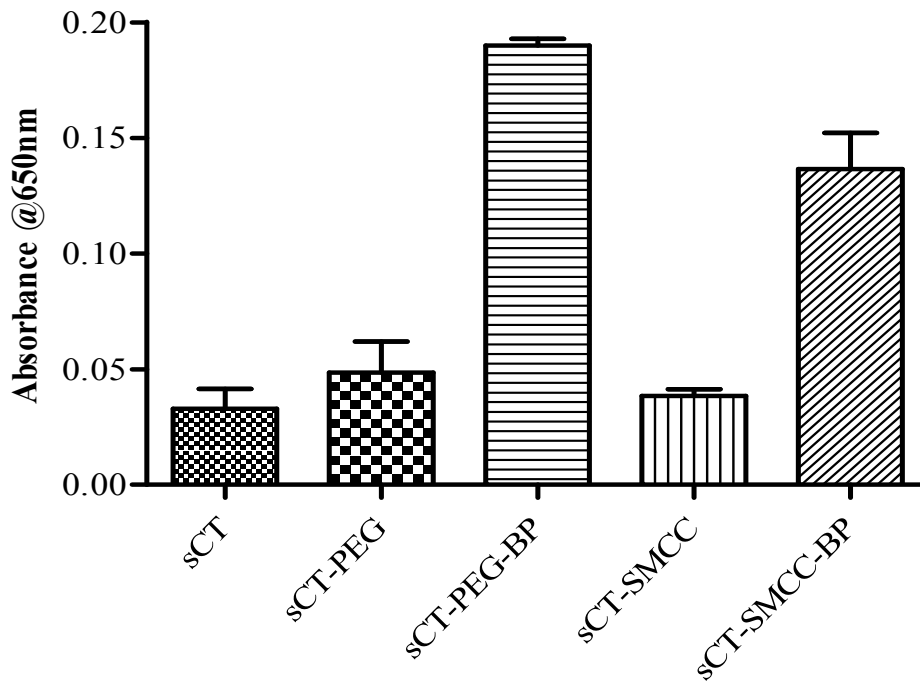


Figure 58: Determination of anti-calcitonin antibody binding ability of sCT analogue by ELISA. Plates coated with calcium phosphate were incubated with sCT or equivalent (1 μ g) in 100 μ L 100 mM phosphate buffer pH 7.0 for 1 hour, washed, and blocked with BSA. Plates were then incubated with rabbit anti-sCT antibody followed by goat anti-rabbit IgG. TMB substrate was added and the absorbance of the developed color was measured at 650 nm. sCT or sCT-PEG versus sCT-PEG-BP and sCT or sCT-SMCC versus sCT-SMCC-BP, $P < 0.05$.

In contrast, the relatively lower calcium phosphate surface binding for sCT, sCT-PEG and sCT-SMCC indicated that the absence of BP-mediated binding did not permit them to be retained on the bone mineral surface of these plates.

sCT receptor binding ability and in-vitro Bioactivity

The ability for sCT, sCT-PEG, sCT-SMCC, sCT-BP and sCT-PEG-BP to generate intracellular cAMP in presence of a phosphodiesterase inhibitor is shown in **figure 59**. The intracellular cAMP generating activities of sCT analogues was compared to sCT. There was no significant difference in the cAMP generating abilities between sCT and sCT-PEG for all doses used.

However, such activity was reduced by 20% in the case of sCT-PEG-BP compared to native sCT. In comparison to native sCT, at 10 mM concentration, sCT-SMCC and sCT-BP retained $94.3 \pm 3.48\%$ and $92.8 \pm 4.94\%$ sCT activity. Similarly, $98.05 \pm 5.67\%$ and $101.98 \pm 3.12\%$ activity was seen at 50 nM concentration, and $114.89 \pm 8.35\%$ and $99.78 \pm 14.799\%$ at 100 nM. As the antiresorptive effects of calcitonin are mediated by calcitonin receptor found primarily in bone-resorbing OC cells, the retention of sCT activity by sCT-BP and sCT-PEG-BP is of vital significance for continued antiresorptive activity after being selectively deposited in bone after systemic administration.

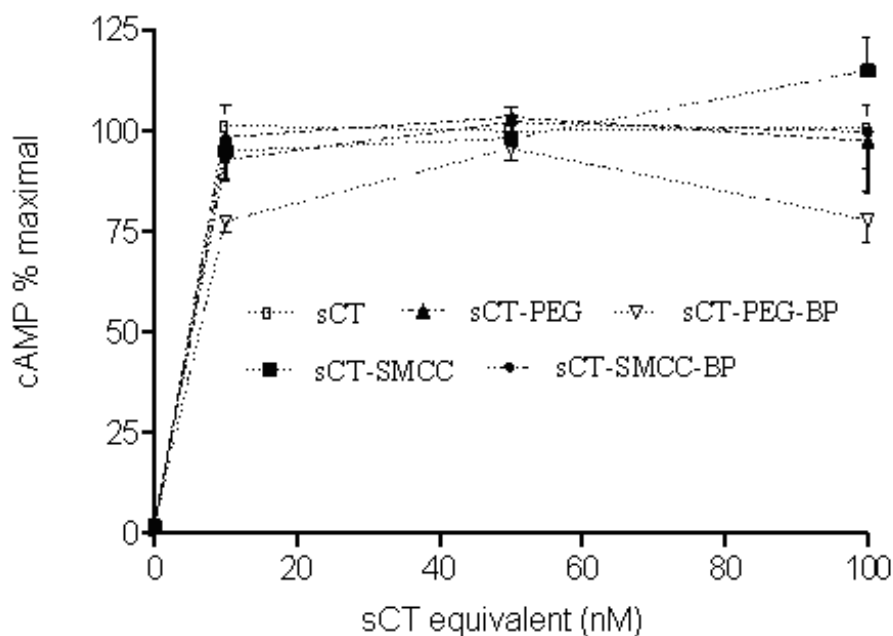


Figure 59: *In vitro* bioactivity of sCT-analogue determined using intracellular cAMP stimulation in human T47D cells. 50000 cells/well were cultured for 2 days in 48 well plates in RPMI 1640 containing insulin and phosphodiesterase activity was blocked using 3-IBMX. Cells were then treated with 0, 10, 50 and 100 nM sCT or equivalent and the generated cAMP was assayed by cAMP ELISA. cAMP % maximal, determined by considering the amount of cAMP generated by sCT for a particular concentration as 100%.

3. 8. *IN VIVO* BIOACTIVITY

Normal rats.

Biological effects of a control dose of thiol-BP and sCT, sCT-PEG, sCT-SMCC, sCT-BP and sCT-PEG-BP on plasma calcium level in normal rats are shown in **figure 60**. At equivalent doses, percentage of plasma calcium reduction induced by sCT, sCT-PEG-BP and sCT-BP were $20.4 \pm 5.5\%$, $19.7 \pm 1.9\%$, and $13.45 \pm 1.64\%$ respectively at first hour post dosing. At the end of the experiment, the total percentage calcium reduction induced by sCT, sCT-PEG-BP, and sCT-BP was $33.1 \pm 2.1\%$, $25.5 \pm 6.1\%$, and $27.36 \pm 2.28\%$ respectively. Thiol-BP in 20 mM acetate buffer pH 5.0 was used as control in OVX rats to confirm the calcium lowering effect of sCT or equivalent. Plasma calcium levels in thiol-BP dosed animals were $98.67 \pm 3.05\%$ at first hour post dosing and $98.08 \pm 4.16\%$ at the end of the experiment. Hypocalcemic effects induced by sCT or equivalents were significantly greater than that by thiol-BP ($P < 0.05$). However, there were no significant differences in hypocalcemic effects among the test group of sCT, sCT-SMCC, sCT-BP or sCT-PEG or sCT-PEG-BP ($P > 0.05$).

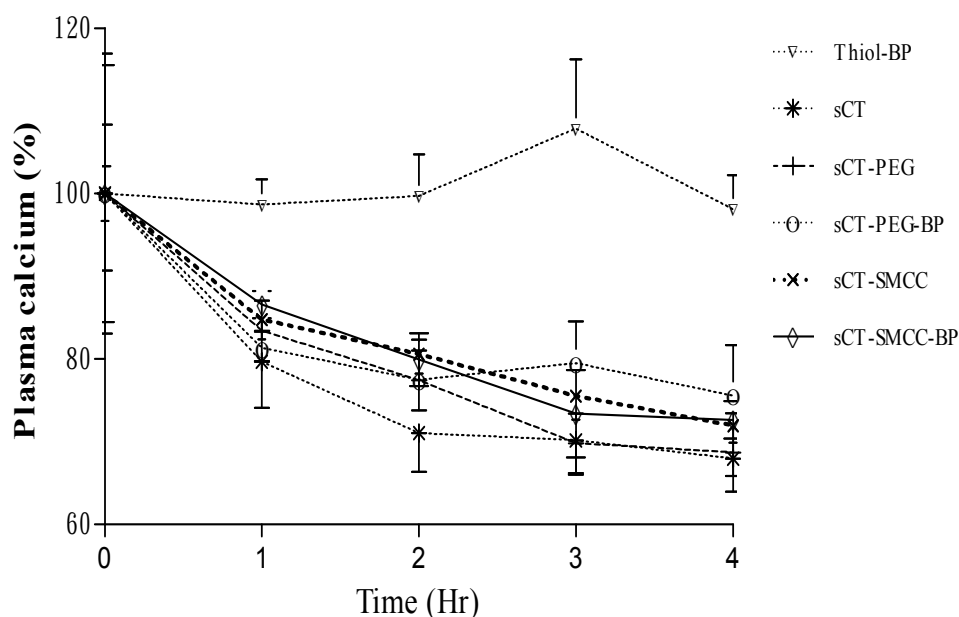


Figure 60: *In vivo* activity: effect of sCT analogues on plasma calcium level in normal rats. Rats were s. c. injected with 20 IU/kg sCT or equivalent. Blood was collected at 0, 1, 2, 3 and 4 hour intervals and the plasma was obtained by centrifuging samples at 5000 rpm for 10 min and collecting the supernatant. The amount of calcium in plasma was analyzed using the QuantiChrom™ calcium assay kit (BioAssay Systems, CA USA).

Osteoporotic rats

Plasma calcium lowering effects of a control dose of thiol-BP and the calcimar, sCT-BP and sCT-PEG-BP in OVX rats are shown in **figure 61**. Plasma calcium level after three months of daily s. c. administration of thiol-BP, calcimar, sCT-BP and sCT-PEG-BP plus daily oral administration, for the last 10 days, of 308 mg/kg of strontium ranelate in

OVX rats were approximately 11.3 (\pm 0.84) mg/dL, 10.7 (\pm 1.24) mg/dL, 10.4 (\pm 1.23) mg/dL and 10.8 (\pm 0.63) mg/dL respectively. Thiol-BP in 20 mM acetate buffer pH 5.0 was used as control in OVX rats to confirm the calcium lowering effect of sCT or equivalent. Although the plasma calcium level in calcimar, sCT-BP and sCT-PEG-BP treated group was lower than that in thiol-BP treated OVX rats, hypocalcemic effects induced by sCT or equivalents were not significantly lower than that by thiol-BP ($P > 0.05$). In addition, there were no significant differences in hypocalcemic effects of calcimar, sCT-BP or sCT-PEG-BP ($P > 0.05$).

Osteoarthritic rats

Effects of a control dose of thiol-BP and sCT-PEG-BP in OA rats are shown in **figure 62**. Plasma calcium level of normal rats which received twice weekly s. c. dose of 160.71 ng/kg (0.547 nMol/kg) of thiol-BP in 20 mM acetate buffer pH 5 were considered as 100% for the purpose of comparison. Plasma calcium level of similarly treated OA rats was higher than normal rats by approximately 6%. This increase in calcium level might be due to the increase rate of bone resorption in OA rats due to more active osteoclasts. However, the treatment with sCT-PEG-BP decreased the calcium level up to the values similar to the normal rats. Although the treatment with sCT-PEG-BP decreased the calcium level, the values were not significantly different when compared with normal rats ($P > 0.05$).

Osteoclasts are involved in early stage of OA pathogenesis and the increased activity and the number of osteoclast leads to bone resorption. This could raise plasma calcium level in OA rats. Hence, we decided to see the effect of OA in plasma calcium. Normal rats were used as control. They had no OA disease. Administration BP had no effect on plasma calcium as demonstrated in *in vivo* activity result.

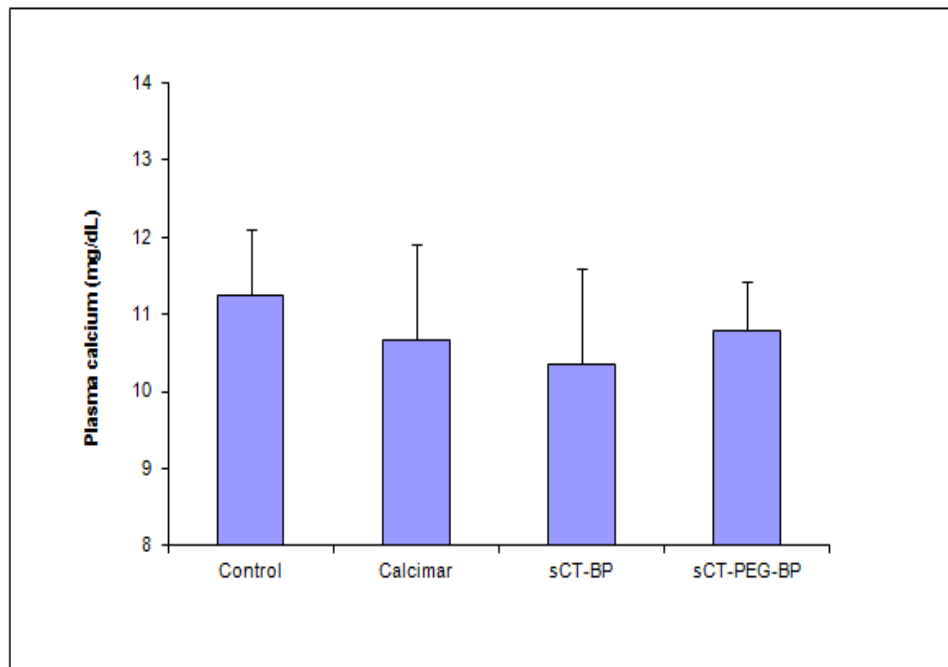


Figure 61: *In vivo* activity: effect of sCT analogues on plasma calcium level in osteoporotic (OP) rats. OP rats received daily subcutaneous injection of sCT analogues in 20 mM acetate buffer pH 5 for 12 weeks. Samples were diluted so that the injection volume was 120 μ L/kg. OVX control group received 160.71 ng/kg of thiol-BP in 20 mM acetate buffer pH 5. During the last 10 days of study rats were also given a daily oral strontium ranelate 308 mg/kg. At the end of study period, blood plasma was obtained by centrifuging blood samples at 5000 rpm for 10 min and collecting the supernatant. Plasma calcium was determined using QuantiChrom™ calcium assay kit (BioAssay Systems, CA USA).

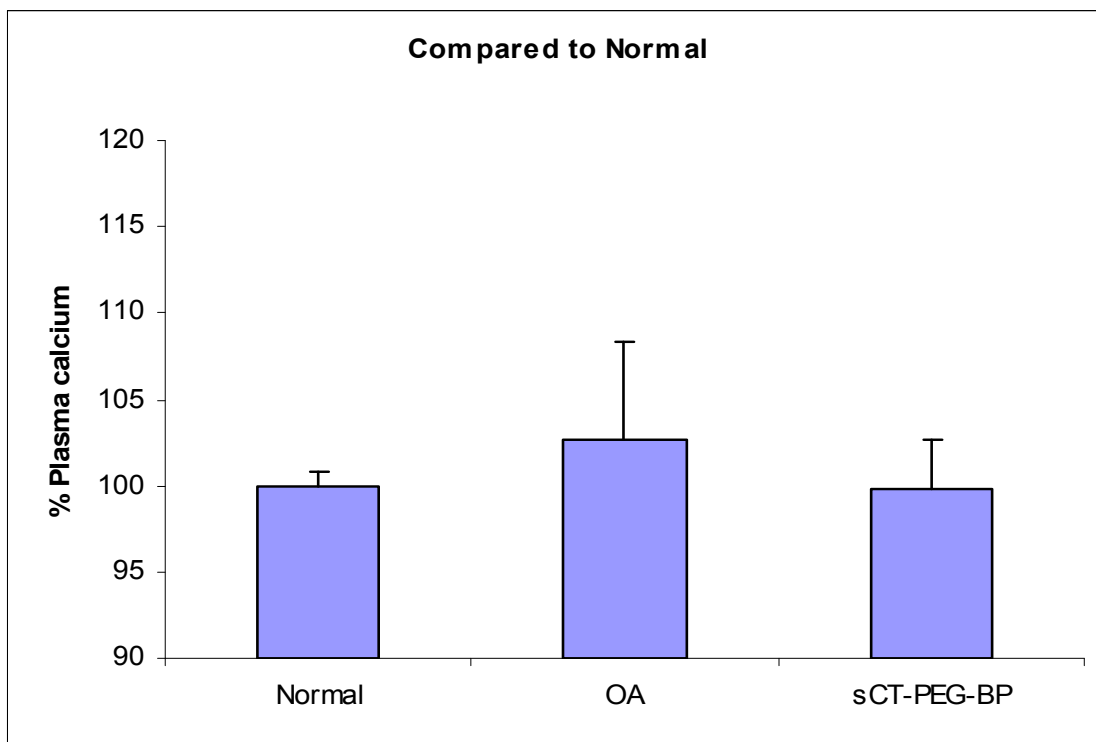


Figure 62: *In vivo* activity: effect of sCT analogues on plasma calcium level in osteoarthritic (OA) rats. OA was induced by knee surgery. Drug administration started on the next day after surgery and lasted for 8 weeks. sCT-PEG-BP treatment group received sCT-PEG-BP equivalent to 2.5 IU/kg body mass of sCT subcutaneously twice weekly. Samples were diluted so that the injection volume was 120 μ L/kg. Normal and OA group received 160.71 ng/kg of thiol-BP in 20 mM acetate buffer pH 5 subcutaneously twice weekly. All rats were given strontium ranelate (PROTOS[®], Servier Laboratories, Australia) orally as source of Sr⁺² tracer for the last 10 days prior euthanasia. At the end of study period, blood plasma was obtained by centrifuging samples at 5000 rpm for 10 min and collecting the supernatant. Plasma calcium level was assayed using the QuantiChrom[™] calcium assay kit (BioAssay Systems, CA USA).

3. 9. *IN VIVO* EFFICACY IN BONE DISEASES

Osteoporotic rats.

The effects of calcimar and sCT analogues upon bone volume and bone mineral density (BMD) were assessed in a rat model of osteoporosis (secondary to OVX) by measuring the trabecular bone volume percentage and BMD at the proximal tibial metaphysis, using micro-CT. The *in vivo* micro-CT analysis confirmed the development of significant osteopenia in OVX rats (**figures 63- 65**) using trabecular bone morphometric analysis (**figure 65**). The sham group represents rats (n=4) in which laparoscopic surgical incision was performed, however the ovaries were not removed.

Thiol-BP treated rats were call OVX control as they did not receive sCT or conjugate. These rats received 160.71 ng/kg (0.547 nMol/kg) of thiol-BP in 20 mM acetate buffer pH 5. This concentration corresponded to the “three” moles of thiol-BP per sCT as if all the three amines in sCT reacted with thiol-BP. The reason for this was to remove the effect of BP (if any) in conjugates. The thiol-BP used was first generation BP which is not considered therapeutically effective. 160.71 ng/kg dose is 1000s times lower than the human dose of aledronate.

Baseline values represent the data at time zero (week 0). The visibly lower baseline values measured for bone volume and BMD in OVX control and other OVX treatment groups (compared to the sham group) was an indication of the OP-like osteopenia that had developed during recovery housing after OVX surgery at the Charles River facility and prior

to the shipping and receiving of the OVX and sham-operated rats at our university animal care facility, at 2 weeks post-surgery. Nonetheless, bone volume and BMD values were not significantly different at baseline (week 0) across all treatment groups.

Using micro-CT based bone volume and BMD measurements, we measured the significant reduction in BMD (**figure 63**) and bone mass (**figure 64**) in both the untreated OVX and sCT treated OVX rats compared to the sham-operated controls out to the 12 weeks study endpoint. In contrast, temporal micro-CT measurements revealed that only bone targeted sCT-BP and sCT-PEG-BP dosed groups showed a trend towards reduced loss of trabecular bone volume and BMD at the sCT dosage used (2.5 IU/kg body mass) compared to the untreated OVX controls, out to 8 weeks. In particular, only the sCT-PEG-BP treated group resulted in the significant preservation of bone volume and BMD at the end of 3 month study endpoint compared to thiol-BP treated OVX control or commercial sCT group.

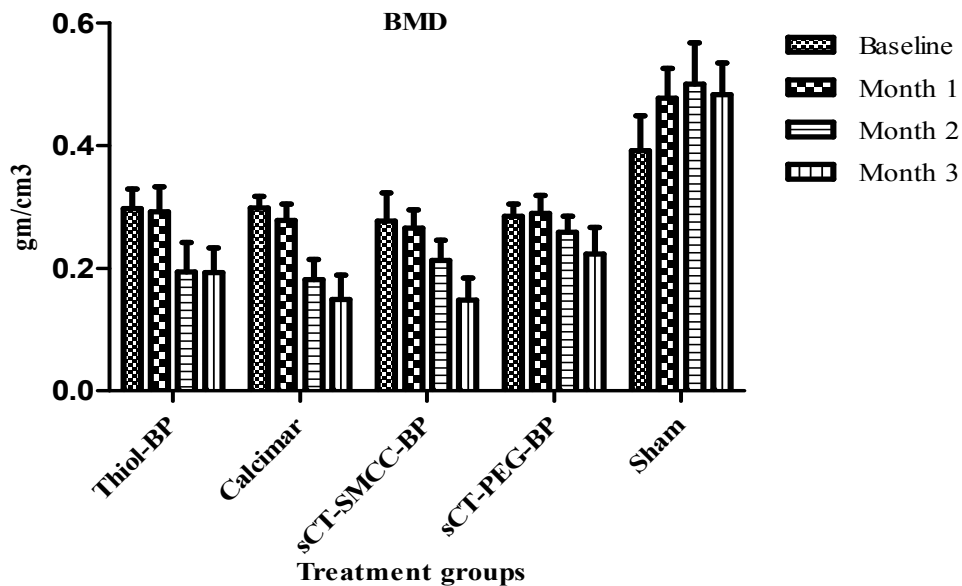


Figure 63: *In vivo* efficacy: effect of sCT analogues on bone mineral density (BMD) in osteoporotic (OVX) rats using *in vivo* micro-computed tomography (micro-CT). Six week old female OVX rats were daily s. c. injected with 2.5 IU/kg/day sCT or equivalent analogues. Rats were analyzed for disease progression with Skyscan *in-vivo* micro-CT for BMD at 0, 1, 2 and 3 months. For 2nd and 3rd months BMD of sCT-PEG-BP treat group versus thiol-BP or commercial sCT (calcimar) treatment group $P < 0.05$.

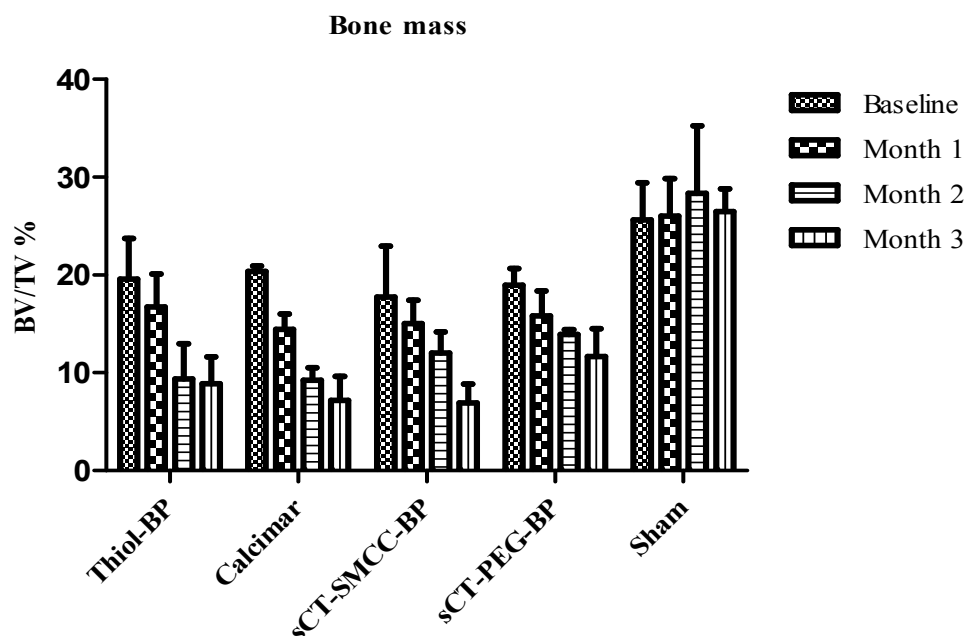


Figure 64: *In vivo* efficacy: effect of sCT analogues on bone volume in osteoporotic (OVX) rats using *in vivo* micro-computed tomography (micro-CT). Six week old female OVX rats were daily s. c. injected with 2.5 IU/kg/day sCT or equivalent analogues. Rats were analyzed for loss of trabecular bone volume using the Skyscan 1076 *in-vivo* micro-CT for bone volume at 0, 1, 2 and 3 months. For 2nd and 3rd months, bone volume of sCT-PEG-BP treated group versus thiol-BP or calcimar treated group $P < 0.05$.

Adjuvant arthritic rats

% change in body weight:

Figure 66 shows the effect of arthritis induction and co-treatment using various sCT analogues in % body weight change from base line values. After taking the base line weight before arthritis induction, rats were

reweighed on days 2, 12 and 21 post induction/drug dosing. Change in their body weight was expressed as % change from baseline values. As seen from the figure, weight of

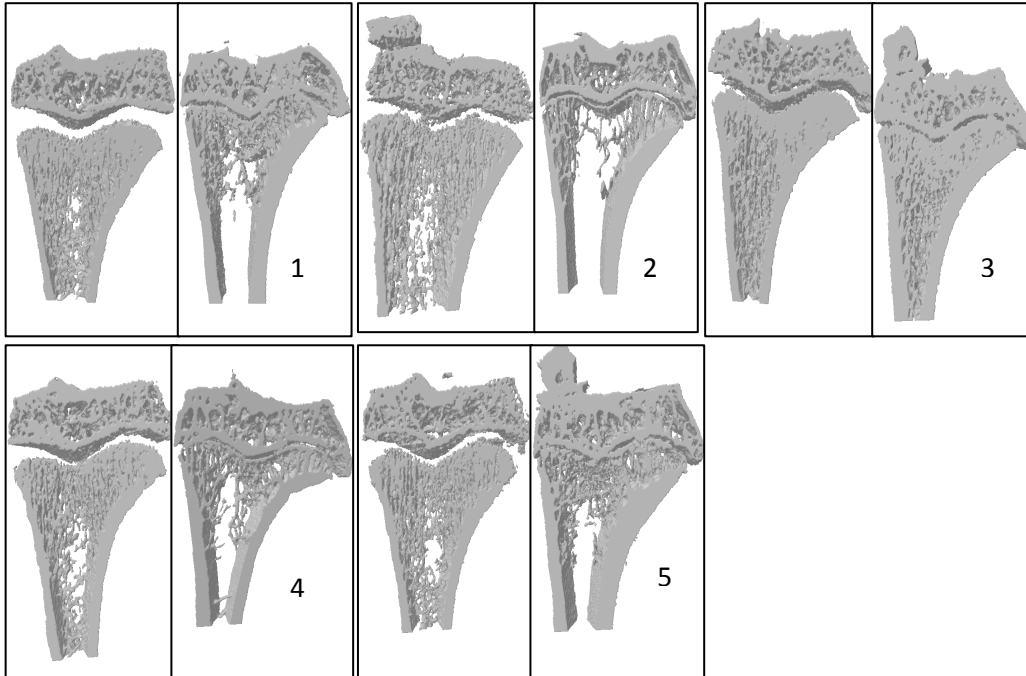


Figure 65: Three-dimensional micro-CT rendering of trabecular bone volume at baseline (week 0, left panel) and at 12 weeks (study end point, right panel). 1, thiol-BP treated OVX control. 2, calcimar treated OVX. 3, Buffer treated sham. 4, sCT-BP treated OVX and 5, sCT-PEG-BP treated OVX group.

The weight of AA rats decreased significantly compared to normal rats whose weight increased. On day 12, the decrease in the body weight for thiol-BP, calcimar, sCT-BP and sCT-PEG-BP group was -7.4%, -6.9%, -7.5% and -8.4% respectively.

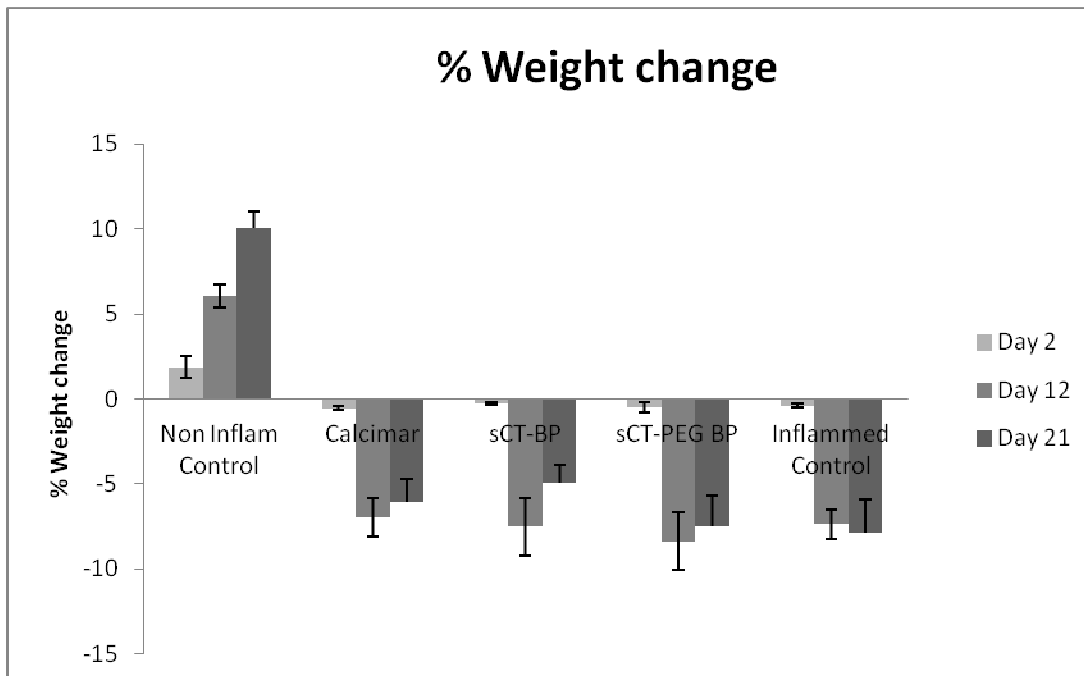


Figure 66: Efficacy in adjuvant arthritis: % change in body weight: After taking the base line weight, rats were injected 0.3 mL suspension of 65 mg/mL *Mycobacterium butyricum* in squalene into the tail base. Following this, thiol-BP control group received 160.71 ng/kg of thiol-BP and other groups received corresponding compounds equivalent to 20 IU/kg/day of sCT in 20 mM acetate buffer pH 5 by s. c. injection. Rats were also given strontium ranelate (PROTOS®) 28.57 mg/Kg/day orally for the duration of study as source of Sr⁺² tracer for the dynamic labelling of bone turnover, for subsequent post-mortem analysis. Rats were reweighed on days 12 and 21. Change in their body weight was expressed as % change from baseline values. There was a significant decrease ($p < 0.05$) in body weight for AA groups compared to day 2 versus 12 or 21 days weights.

Similarly, these values for 21 days were -7.8%, -6.0%, -4.9% and -7.5% respectively. There was a significant decrease ($p < 0.05$) in body weight for AA groups compared to day 2 versus 12 or 21 days weights. However, no significant difference was observed from days 12 versus days 21.

% change in paw diameter:

As shown in **Figure 67**, paw diameter in AA groups was significantly increased ($p < 0.05$) from day 2 versus 12 or 21 days. However, sCT-BP and sCT-PEG-BP treatment groups had significantly lower ($P < 0.05$) paw diameter compared to the control or calcimar group at 21 days. Days 2 value for thiol-BP, calcimar, sCT-BP and sCT-PEG-BP group was 1.0%, 0.35%, 0.7% and 0.68% respectively. However, at 21 days the paw diameter was increased to 15.7%, 16.1%, 8.8% and 8.9% respectively. Increase in diameter from 12 to 21 days indicated the arthritis development and inflammation. While the lower values in sCT analogues treated groups indicate their disease protecting effect relative to control.

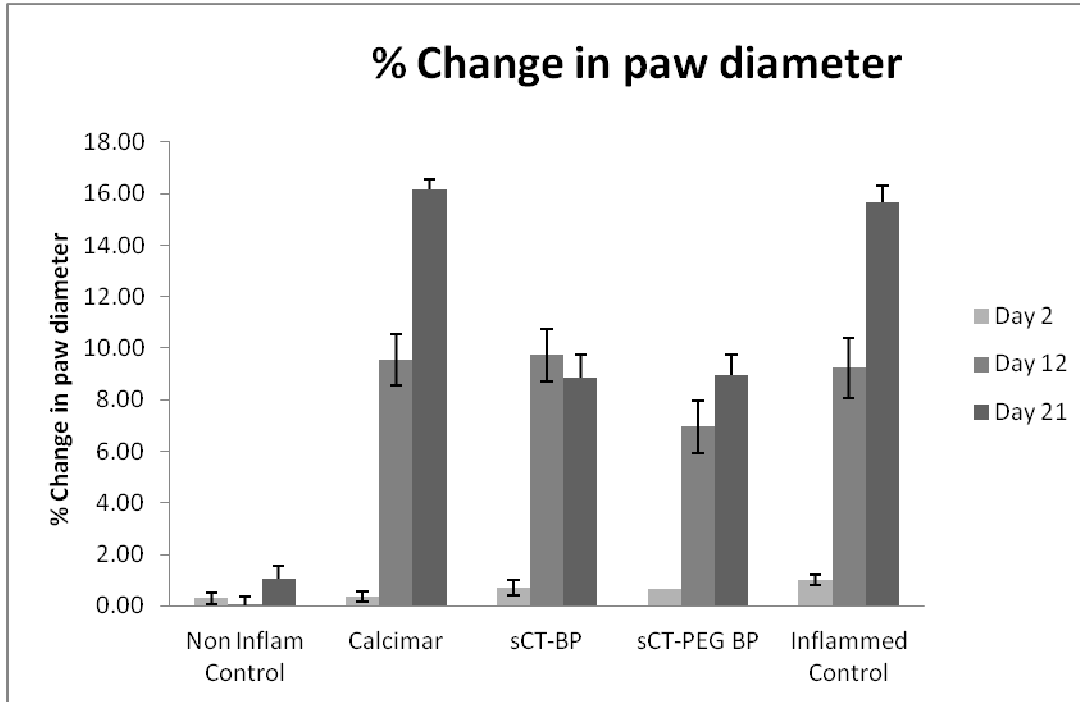


Figure 67: Efficacy in adjuvant arthritis: % change in paw diameter: After taking the base line paw diameter, rats were injected 0.3 mL suspension of 65 mg/mL *Mycobacterium butyricum* in squalene into the tail base. Following this, drug treatment was started along with the oral administration of strontium ranelate (PROTOS[®]). Paw diameters were measured again on days 12 and 21. Change in diameter was expressed as % change from baseline values. Paw diameter in AA groups was significantly increased ($p < 0.05$) from day 2 versus 12 or 21 days. However, sCT-BP and sCT-PEG-BP groups had significantly lower ($P < 0.05$) paw diameter compared to calcimar or AA control group at 21 days.

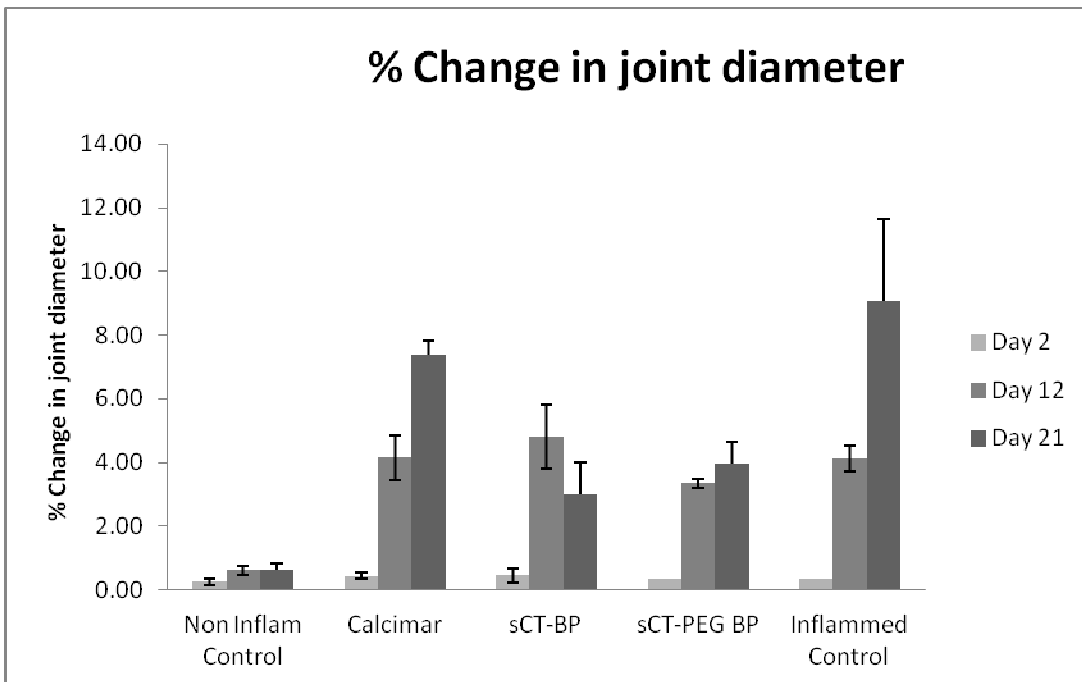


Figure 68: Efficacy in adjuvant arthritis: % change in ankle joint diameter: After taking the base line joint diameter, rats were injected 0.3 mL suspension of 65 mg/mL *Mycobacterium butyricum* in squalene into the tail base. Following this, drug treatment was started along with the oral administration of strontium ranelate (PROTOS®). Diameters were measured again on days 12 and 21. Change in diameter was expressed as % change from baseline values. For AA groups, there was significant increase in joint diameter from day 2 versus days 12 or 21 ($P < 0.05$). However, for sCT-BP and sCT-PEG-BP groups, % change in joint diameter was not significant ($p > 0.05$) from days 12 versus 21 days. However, the diameter was significantly increased in AA control group at 12 days versus 21 days.

% change in ankle joint diameter:

Figure 68, represents the % change in the ankle diameter. For AA groups, there was significant increase in joint diameter from day 2 versus days 12 or 21 ($P < 0.05$). However, for sCT-BP and sCT-PEG-BP groups, % change in joint diameter was not significant ($p > 0.05$) from days 12 versus 21 days. The diameter was significantly increased in the AA control group at 12 days versus 21 days.

The day 2 value for thiol-BP, calcimar, sCT-BP and sCT-PEG-BP group was 0.35%, 0.45%, 0.45% and 0.36% respectively. However, at 21 days the change in their diameter was 9.1%, 7.4%, 3% and 3.9% respectively. An increase in diameter from 12 to 21 days in the control group indicated the arthritis development and inflammation, while the significantly decreased values in calcimar or analogues treated groups indicate their disease protecting effect relative to control.

% change in paw volume:

Figure 69 represents the % change in the paw volume. For AA groups there was a significant increase in paw volume from day 2 versus days 12 or 21 ($P < 0.05$). For sCT-BP, joint volume was significantly decreased ($p < 0.05$) from days 12 versus 21 days. However, the volume was significantly increased in AA control group at 12 days versus 21 days.

Day 2 values for thiol-BP, calcimar, sCT-BP and sCT-PEG-BP group was 0.5%, 3.5%, 2.3% and 0.1% respectively.

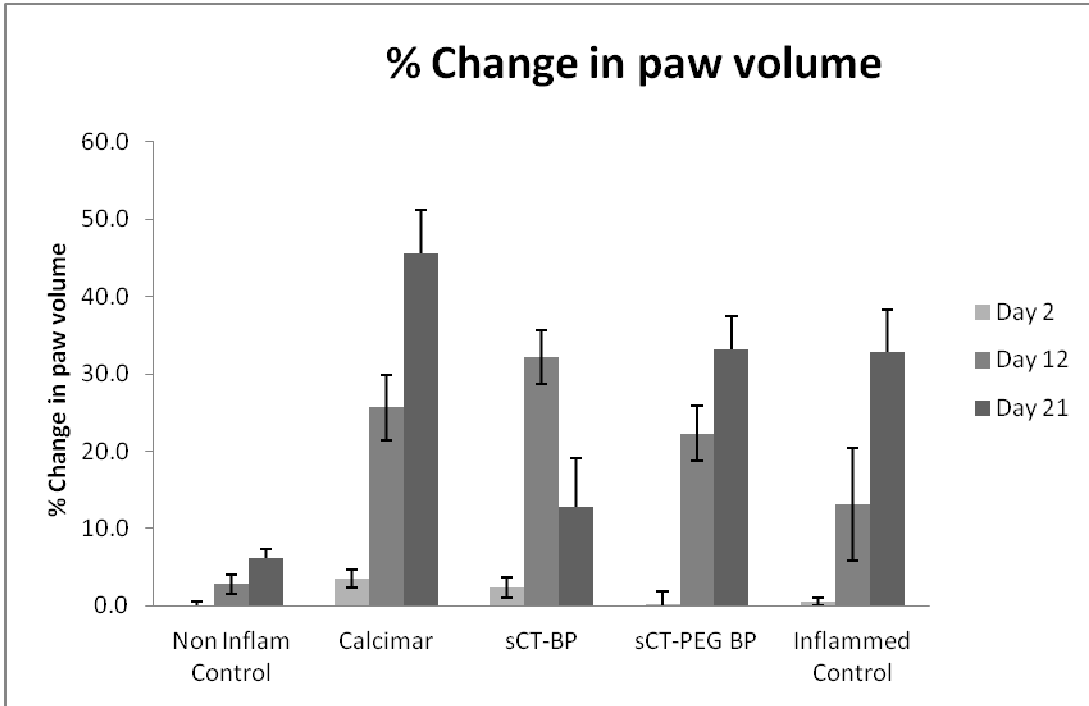


Figure 69: Efficacy in adjuvant arthritis: % change in paw volume: After taking the base line volume, rats were injected 0.3 mL suspension of 65 mg/mL *Mycobacterium butyricum* in squalene into the tail base. Following this, drug treatment was started along with the oral administration of strontium ranelate (PROTOS®). Volumes were measured again on days 12 and 21. Changes in volume were expressed as % change from baseline values. For AA groups there was a significant increase in paw volume from day 2 versus days 12 or 21 ($P < 0.05$). For sCT-BP, volume was significantly decreased ($p < 0.05$) from days 12 versus 21 days. However, the volume was significantly increased in AA control group at 12 days versus 21 days.

However, at 21 days the change was 32.8%, 45.6%, 12.8% and 33.1% respectively. Increase in volume from base line to 12 and from 12 to 21 days in control group indicated the arthritis development and inflammation. While the lower values in sCT-BP treated group indicate its disease protecting effect relative to control.

Bone mineral density (BMD) and bone volume (BV/TV %):

The effects of calcimar and sCT analogues upon bone volume and bone mineral density (BMD) were assessed in a rat model of adjuvant arthritis (secondary to adjuvant injection) by measuring the trabecular bone volume percentage and BMD, using micro-CT (**figures 70- 72**). Bone volume and BMD values were not significantly different ($P>0.05$) at baseline (day 0) across all treatment groups. However, there were visible changes in 3D image (**figure 72**).

Treatment with calcimar and sCT-BP insignificantly increased BMD from baseline to 21 days post treatment. However, there was no significant change in BMD in control and sCT-PEG-BP group.

Bone volume of control and calcimar treated group was decreased substantially from their base line values. However, there was a significant increase ($P<0.05$) in bone volume in sCT-BP and sCT-PEG-BP treated group at 21 days compared to the baseline values. Baseline bone volume for control, calcimar, sCT-BP and sCT-PEG-BP treated group was 11.97,

13.66, 5.42 and 7.84% respectively. At 21 days these values were changed to 9.5, 11.1, 9.7 and 12.9% respectively. Increase bone volume at the end of 21 days could indicate the disease protective effect of bone targeting sCT analogues. Insignificant changes in BMD could be due to the fact that, unlike in osteoarthritis the rheumatoid arthritis typically affects the lining of the bone more than the bone density.

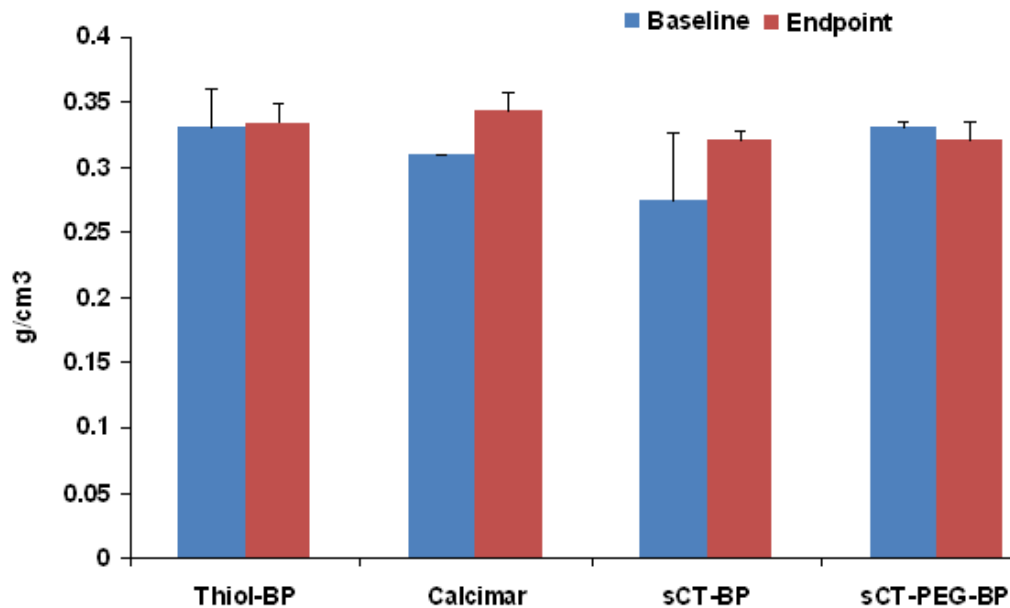


Figure 70: *In vivo* efficacy: effect of sCT analogues on bone mineral density (BMD) in adjuvant arthritic (AA) rats using *in vivo* micro-computed tomography (micro-CT). Male AA rats were daily s. c. injected with 20 IU/kg/day calcimar or equivalent analogues. Rats were analyzed for disease progression with Skyscan *in vivo* micro-CT for BMD at 1 and 21 days. Treatment with calcimar and sCT-BP insignificantly increased BMD from baseline to 21 days post treatment. However, there was no significant change in BMD in control and sCT-PEG-BP group.

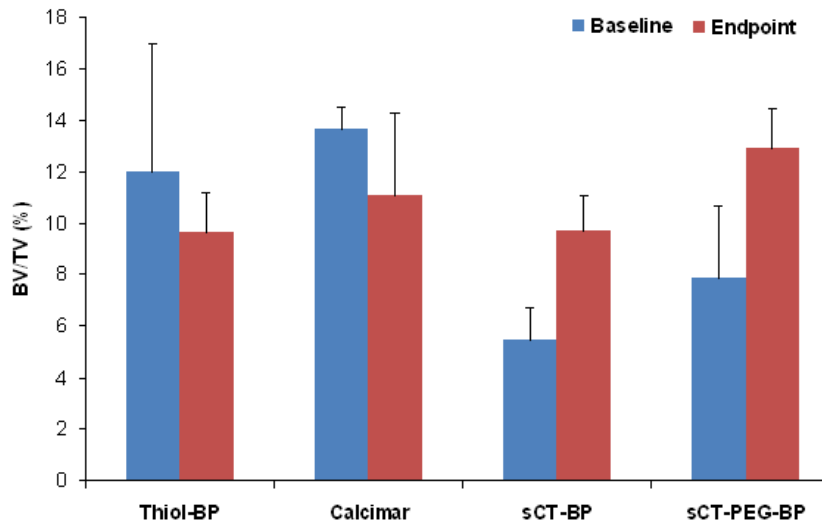


Figure 71: *In vivo* efficacy: effect of sCT analogues on bone volume in adjuvant arthritic (AA) rats using *in vivo* micro-computed tomography (micro-CT). Male AA rats were daily s. c. injected with 20 IU/kg/day calcimar or equivalent analogues. Rats were analyzed for disease progression with Skyscan *in-vivo* micro-CT for BV/TV% at 1 and 21 days. Bone volume of control and calcimar treated group was decreased substantially from their base line values. However, there was a significant increase ($P < 0.05$) in bone volume in sCT-BP and sCT-PEG-BP treated group at 21 days compared to the baseline values.

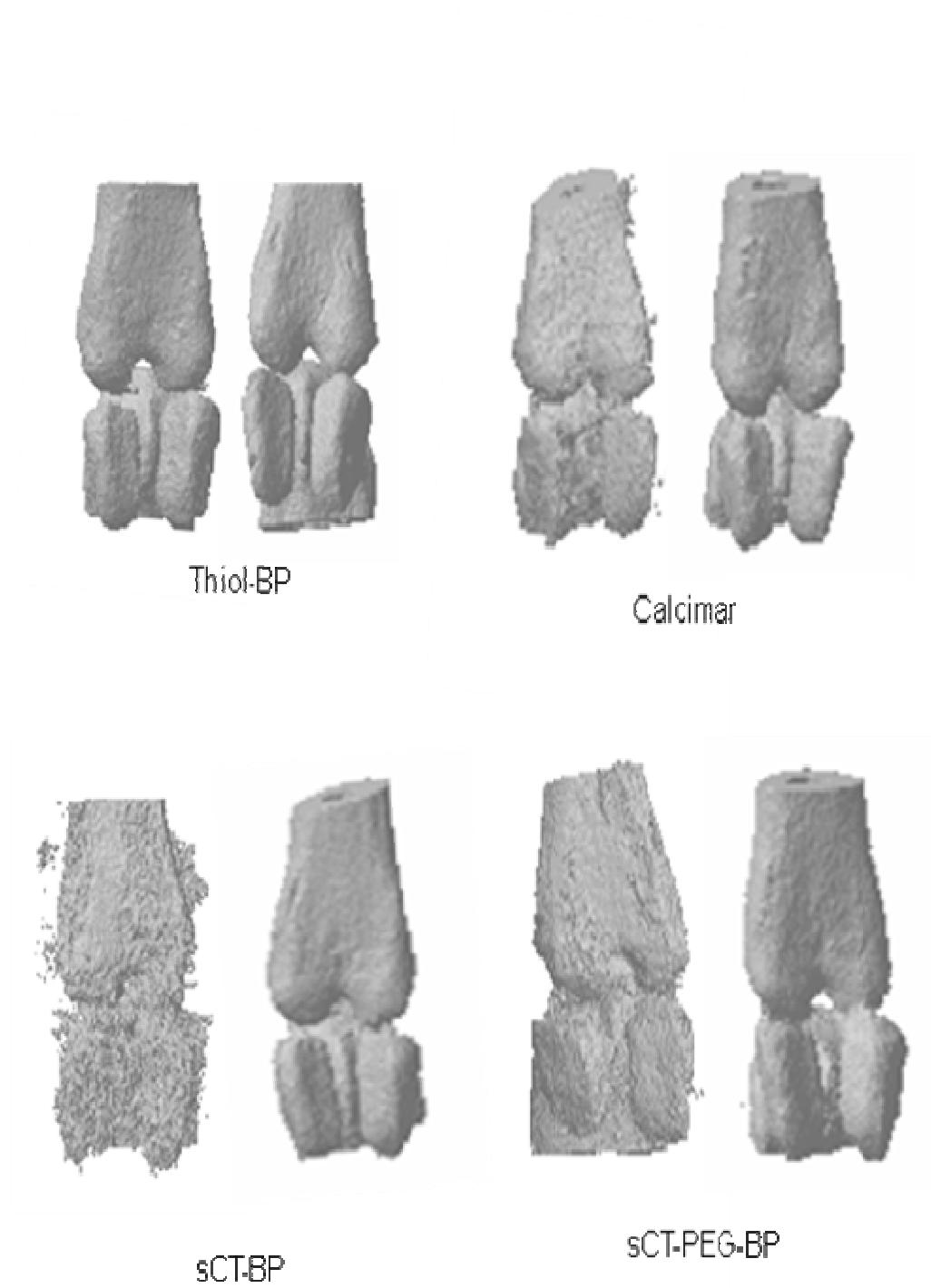


Figure 72: Three-dimensional micro-CT renderings of trabecular bone volume at baseline (day 1, left panel) and at 21 days (study end point, right panel).

3. 10. sCT DOSE ESCALATION IN OSTEOPOROTIC RATS

The effects of 5, 10 and 20 IU/kg daily s. c. dose of calcimar and sCT analogues upon bone volume and bone mineral density (BMD) were assessed in a rat model of osteoporosis (secondary to OVX) by measuring the trabecular bone volume percentage and BMD at the proximal tibial metaphysis, using micro-CT. The *in vivo* micro-CT analysis confirmed the development of significant osteopenia in OVX rats (**figure 73- 80**) using trabecular bone morphometric analysis (**figure 81- 83**).

Baseline values represent the data at time zero (week 0). Nonetheless, bone volume and BMD values were not significantly different at baseline (week 0) across all treatment groups. Using micro-CT based bone volume and BMD measurements, we measured the significant reduction ($P < 0.05$) in BMD (**figure 73- 75**) and bone mass (**figure 77- 79**) from base line values in OVX rats treated with 5 IU/kg calcimar or equivalent sCT-BP and sCT-PEG-BP, compared to the BMD and BV/TV % at 12 weeks study endpoint.

Temporal micro-CT measurements revealed that only calcimar, buffer and thiol-BP dosed groups showed a trend towards reduced loss of trabecular bone volume and BMD at all doses compared to the base line values. In contrast, only bone targeted sCT-BP and sCT-PEG-BP dosed groups showed a trend towards increased BMD and bone volume at 4, 8 and 12 weeks compared to base line values. Significant preservation of bone volume and BMD as evidenced by insignificant ($P > 0.05$) loss of bone

volume and BMD at the end of 3 month study endpoint was seen in animals dosed with 20 IU/kg of compounds compared to thiol-BP treated OVX control or commercial sCT group.

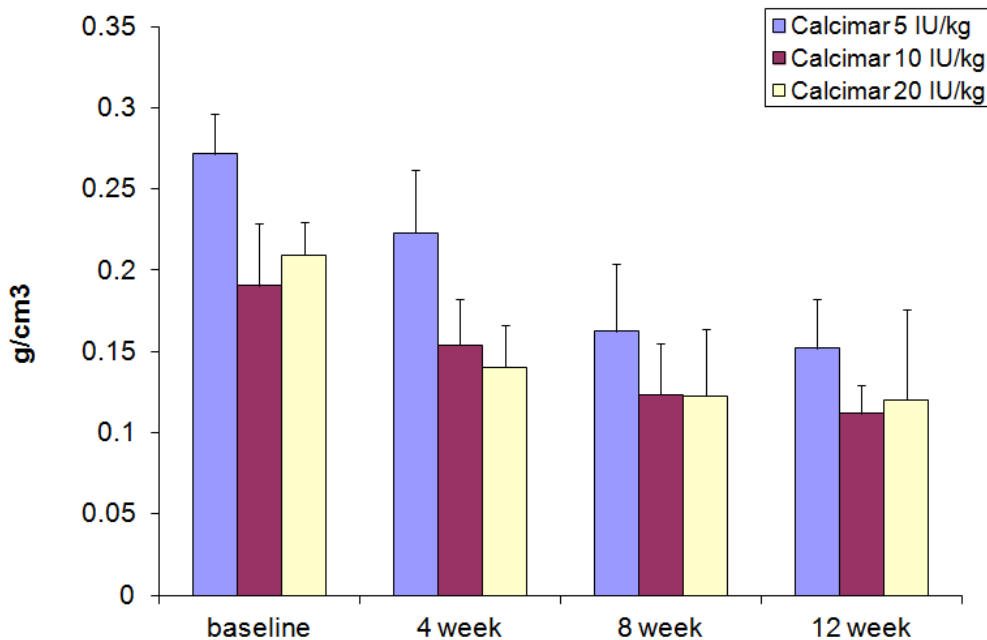


Figure 73: Dose escalation: effect of different doses of calcimar on bone mineral density (BMD) in osteoporotic (OVX) rats using *in vivo* micro-computed tomography (micro-CT). Six week old female OVX rats were daily s. c. injected with 5, 10 and 20 IU/kg/day calcimar. All rats were also given daily oral dose of 28.5 mg/kg strontium ranelate (PROTOS[®], Servier Laboratories, Australia) as a source of Sr⁺² tracer. Rats were analyzed for disease progression with Skyscan *in-vivo* micro-CT for BMD at 0, 1, 2 and 3 months. There was significant decrease in BMD from baseline (week 0) versus week 12 (3 months) for all doses (P<0.05).

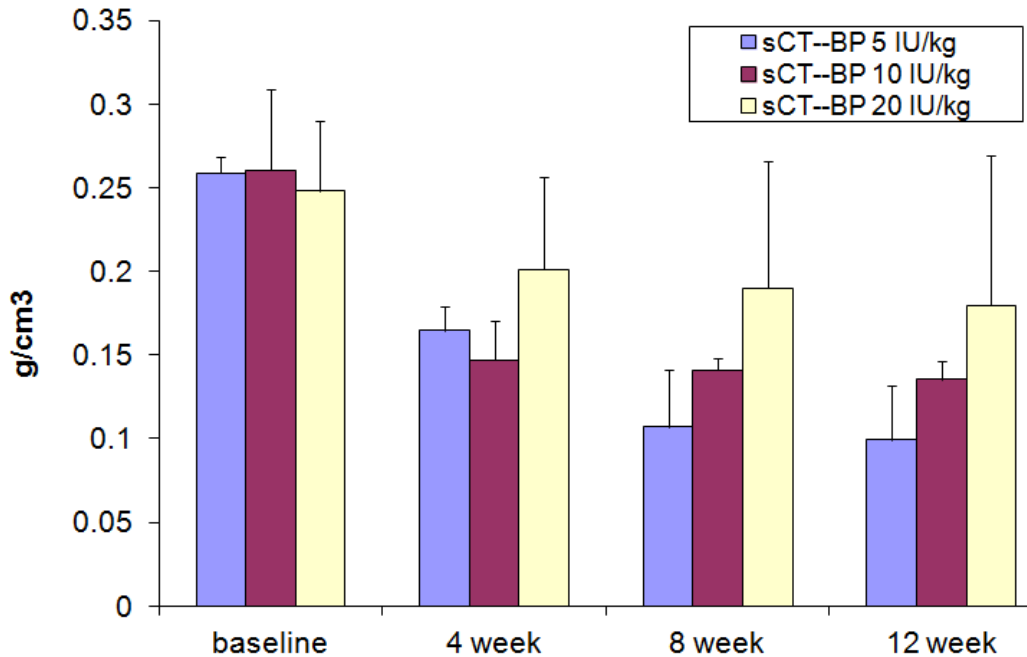


Figure 74: Dose escalation: effect of different doses of sCT-BP on bone mineral density (BMD) in osteoporotic (OVX) rats using *in vivo* micro-computed tomography (micro-CT). Six week old female OVX rats were daily s. c. injected with sCT-BP equivalent to 5, 10 and 20 IU/kg/day sCT. All rats were also given daily oral dose of 28.5 mg/kg strontium ranelate (PROTOS[®], Servier Laboratories, Australia) as a source of Sr⁺² tracer. Rats were analyzed for disease progression with Skyscan *in-vivo* micro-CT for BMD at 0, 1, 2 and 3 months. There was significant decrease in BMD from baseline (week 0) versus week 12 (3 months) for 5 and 10 IU/kg doses ($P < 0.05$). However, at 20 IU/kg, the decrease in BMD from week 0 versus week 12 was not significant ($P > 0.05$), indication preserved BMD at 20 IU/kg.

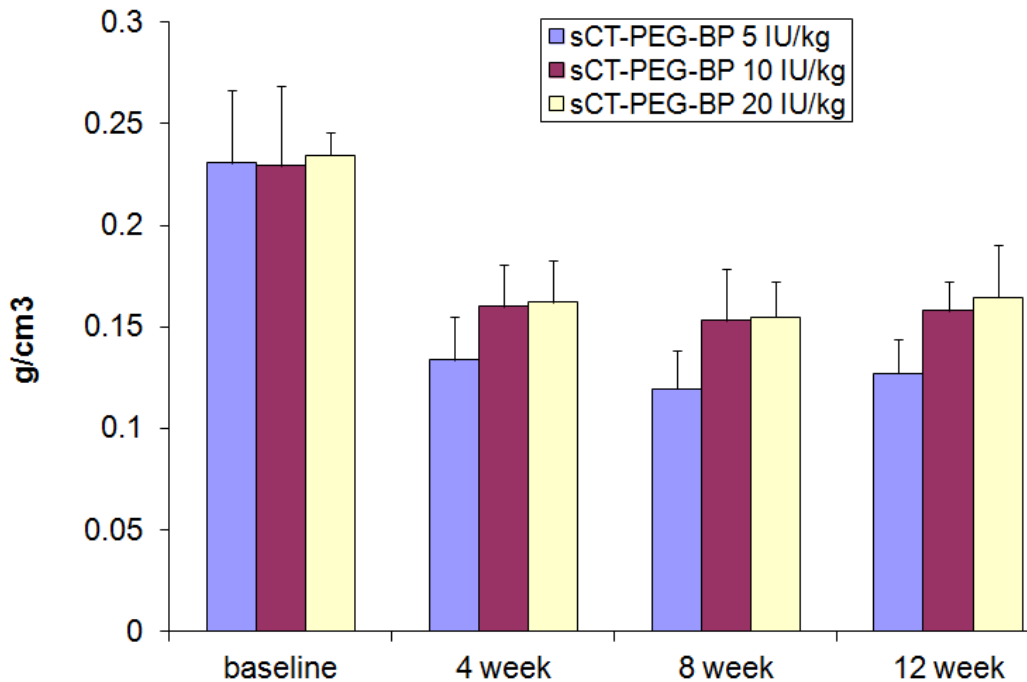


Figure 75: Dose escalation: effect of different doses of sCT-PEG-BP on bone mineral density (BMD) in osteoporotic (OVX) rats using *in vivo* micro-computed tomography (micro-CT). Six week old female OVX rats were daily s. c. injected with sCT-PEG-BP equivalent to 5, 10 and 20 IU/kg/day sCT. All rats were also given daily oral dose of 28.5 mg/kg strontium ranelate (PROTOS[®], Servier Laboratories, Australia) as a source of Sr⁺² tracer. Rats were analyzed for disease progression with Skyscan *in-vivo* micro-CT for BMD at 0, 1, 2 and 3 months. There was significant decrease in BMD from baseline (week 0) versus week 12 (3 months) for 5 and 20 IU/kg doses (P<0.05).

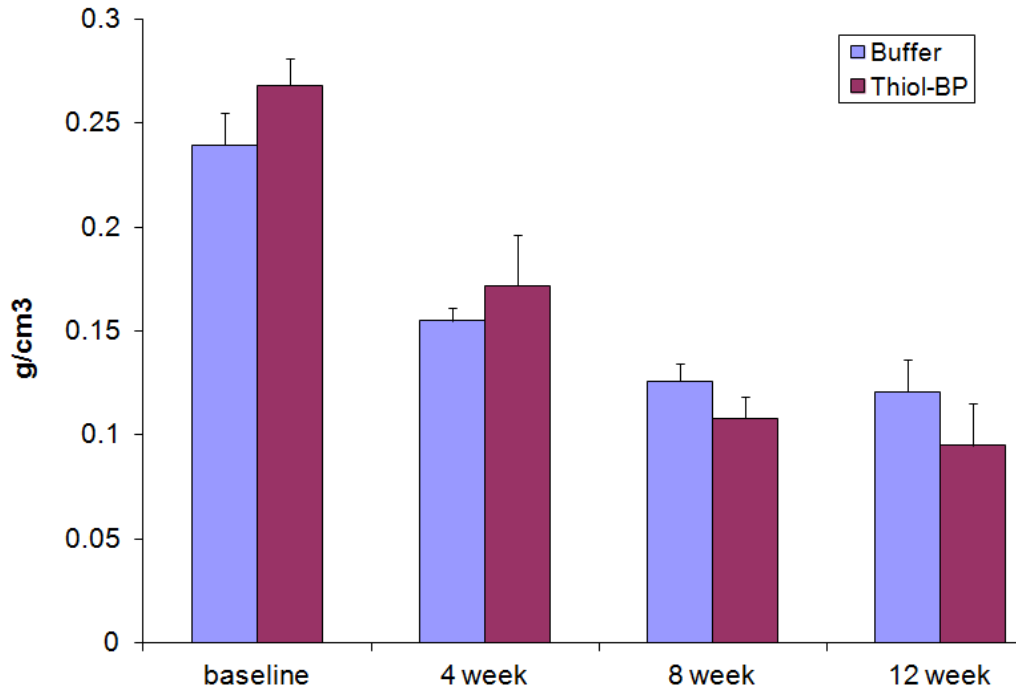


Figure 76: Dose escalation: effect of buffer and thiol-BP on bone mineral density (BMD) in osteoporotic (OVX) rats using *in vivo* micro-computed tomography (micro-CT). Six week old female OVX rats were daily s. c. injected with buffer and thiol-BP in the same buffer. All rats were also given daily oral dose of 28.5 mg/kg strontium ranelate (PROTOS[®], Servier Laboratories, Australia) as a source of Sr⁺² tracer. Rats were analyzed for disease progression with Skyscan *in-vivo* micro-CT for BMD at 0, 1, 2 and 3 months. There was significant decrease in BMD from baseline (week 0) versus week 12 (3 months) for buffer and thiol-BP (P<0.05).

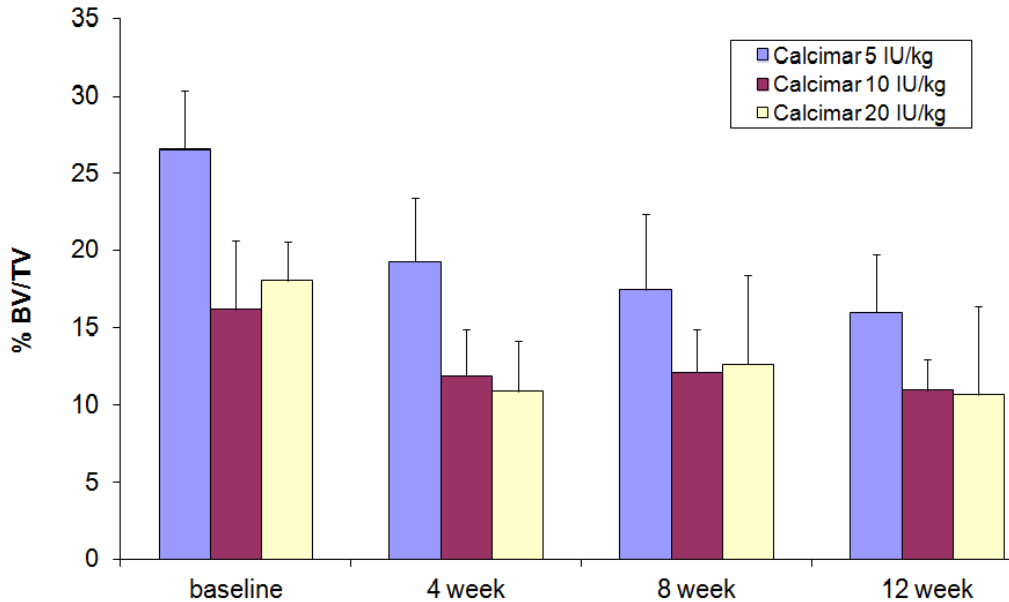


Figure 77: C. Dose escalation: effect of different doses of calcimar on bone volume (BV/TV%) in osteoporotic (OVX) rats using *in vivo* micro-computed tomography (micro-CT). Six week old female OVX rats were daily s. c. injected with 5, 10 and 20 IU/kg/day calcimar. All rats were also given daily oral dose of 28.5 mg/kg strontium ranelate (PROTOS[®], Servier Laboratories, Australia) as a source of Sr⁺² tracer. Rats were analyzed for disease progression with Skyscan *in-vivo* micro-CT for BMD at 0, 1, 2 and 3 months. There was significant decrease in bone volume (BV/TV %) from baseline (week 0) versus week 12 (3 months) for 5 IU (P<0.05). However, this was not significant for 10 and 20 IU/kg.

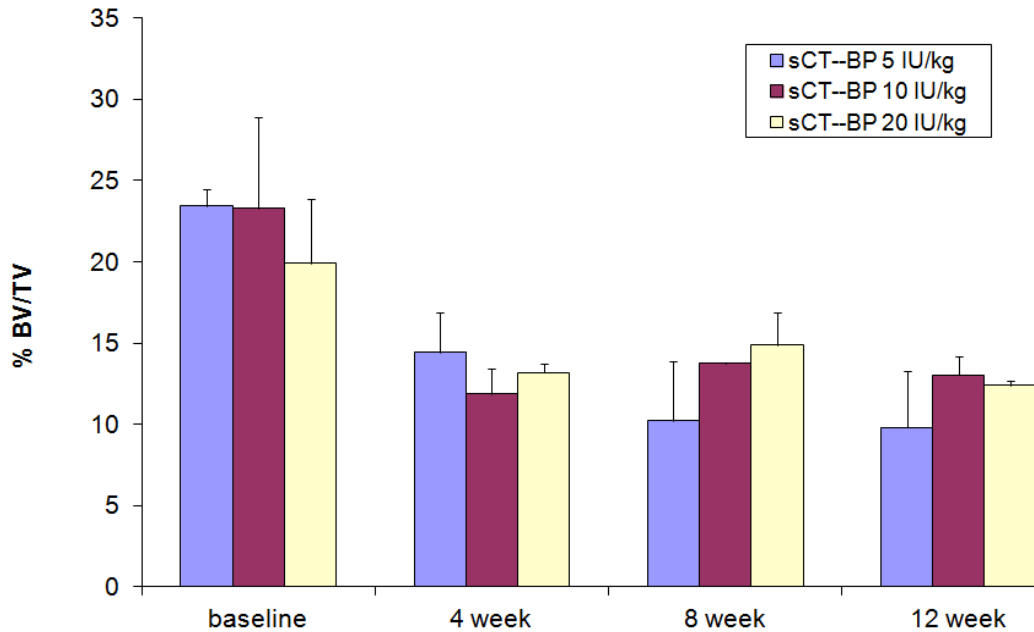


Figure 78: Dose escalation: effect of different doses of sCT-BP on bone volume in osteoporotic (OVX) rats using *in vivo* micro-computed tomography (micro-CT). Six week old female OVX rats were daily s. c. injected with sCT-BP equivalent to 5, 10 and 20 IU/kg/day sCT. All rats were also given daily oral dose of 28.5 mg/kg strontium ranelate (PROTOS[®], Servier Laboratories, Australia) as a source of Sr⁺² tracer. Rats were analyzed for disease progression with Skyscan *in-vivo* micro-CT for bone volume at 0, 1, 2 and 3 months. There was significant decrease in bone volume from baseline (week 0) versus week 12 (3 months) for 5 IU/kg doses ($P < 0.05$). However, at 10 and 20 IU/kg, the decrease in bone volume from week 0 versus week 12 was not significant ($P > 0.05$).

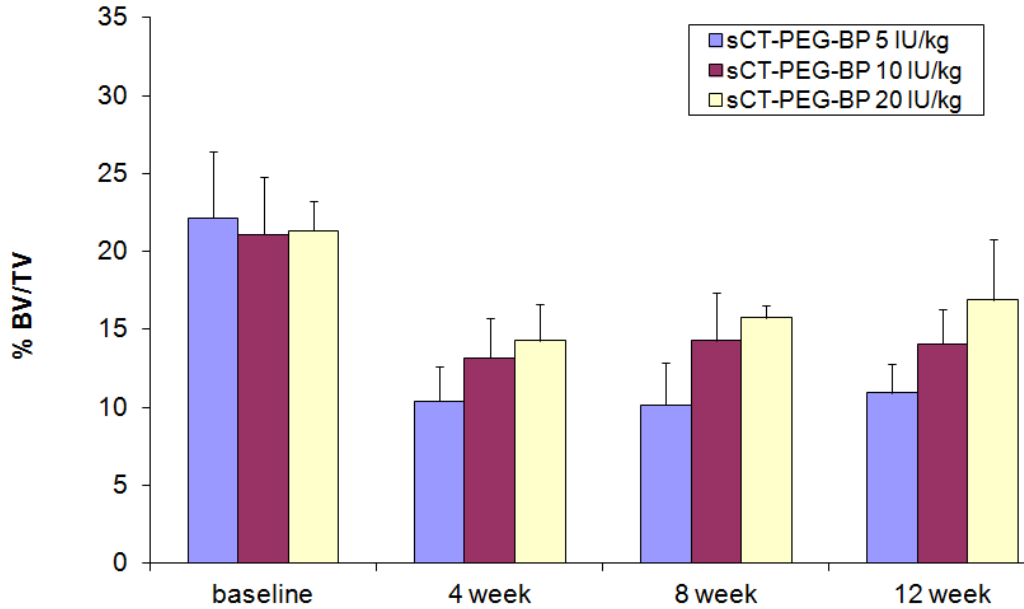


Figure 79: Dose escalation: effect of different doses of sCT-PEG-BP on bone volume in osteoporotic (OVX) rats using *in vivo* micro-computed tomography (micro-CT). Six week old female OVX rats were daily s. c. injected with sCT-PEG-BP equivalent to 5, 10 and 20 IU/kg/day sCT. All rats were also given daily oral dose of 28.5 mg/kg strontium ranelate (PROTOS[®], Servier Laboratories, Australia) as a source of Sr⁺² tracer. Rats were analyzed for disease progression with Skyscan *in-vivo* micro-CT for bone volume at 0, 1, 2 and 3 months. There was significant decrease in bone volume from baseline (week 0) versus week 12 (3 months) for 5 and 10 IU/kg doses ($P < 0.05$). However, at 20 IU/kg, the decrease in bone volume from week 0 versus week 12 was not significant ($P > 0.05$).

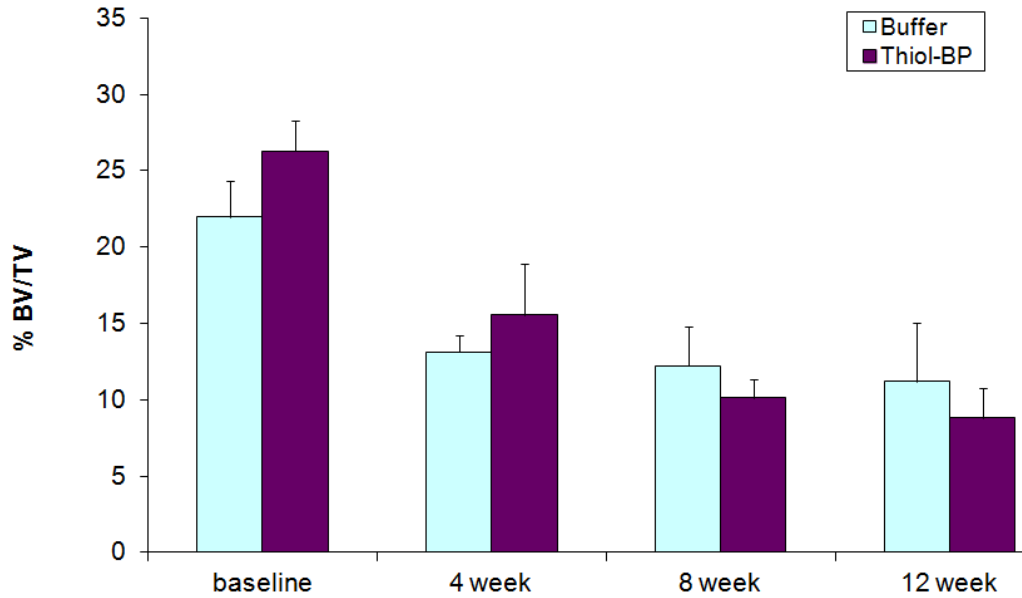


Figure 80: Dose escalation: effect of buffer and thiol-BP on bone volume in osteoporotic (OVX) rats using *in vivo* micro-computed tomography (micro-CT). Six week old female OVX rats were daily s. c. injected with buffer and thiol-BP in the same buffer. All rats were also given daily oral dose of 28.5 mg/kg strontium ranelate (PROTOS[®], Servier Laboratories, Australia) as a source of Sr⁺² tracer. Rats were analyzed for disease progression with Skyscan *in-vivo* micro-CT for bone volume at 0, 1, 2 and 3 months. There was significant decrease in volume from baseline (week 0) versus week 12 (3 months) for buffer and thiol-BP (P<0.05).

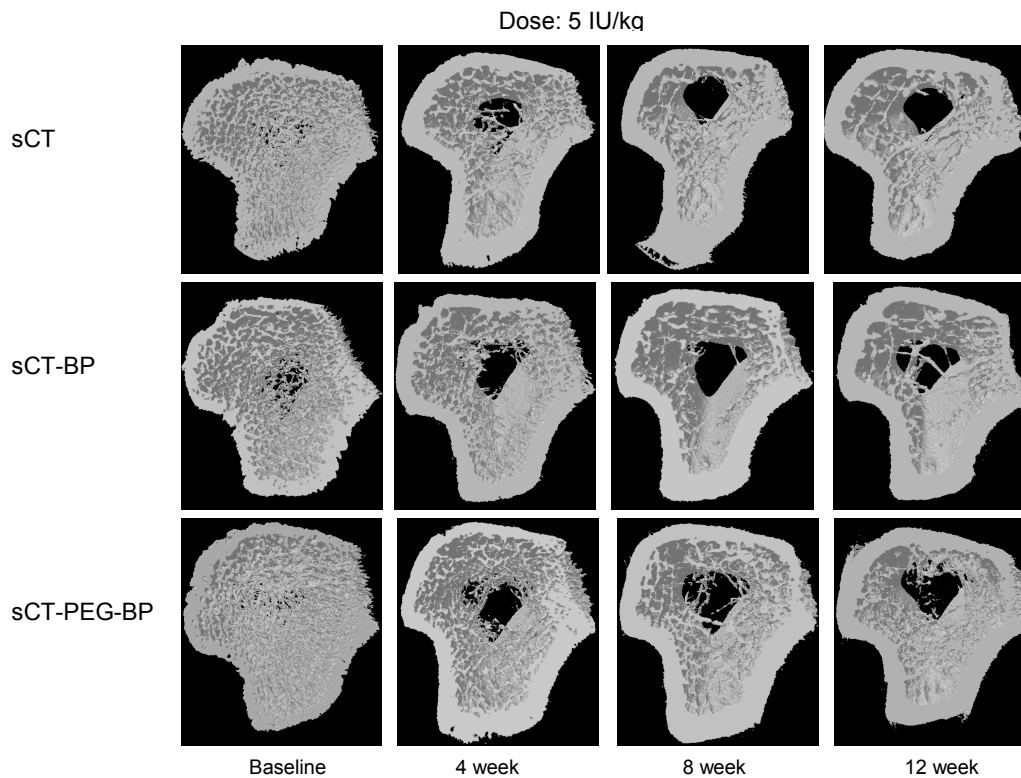


Figure 81: Dose escalation: three-dimensional micro-CT renderings of trabecular bone volume at baseline (week 0, left panel), 4, 8 and 12 weeks. Six week old female OVX rats were administered 5 IU/kg daily s. c. dose of calcimar or equivalent sCT-BP or sCT-PEG-BP. All rats were also given daily oral dose of 28.5 mg/kg strontium ranelate (PROTOS[®], Servier Laboratories, Australia) as a source of Sr⁺² tracer. Rats were analyzed for disease progression with Skyscan *in-vivo* micro-CT for bone volume at 0, 1, 2 and 3 months.

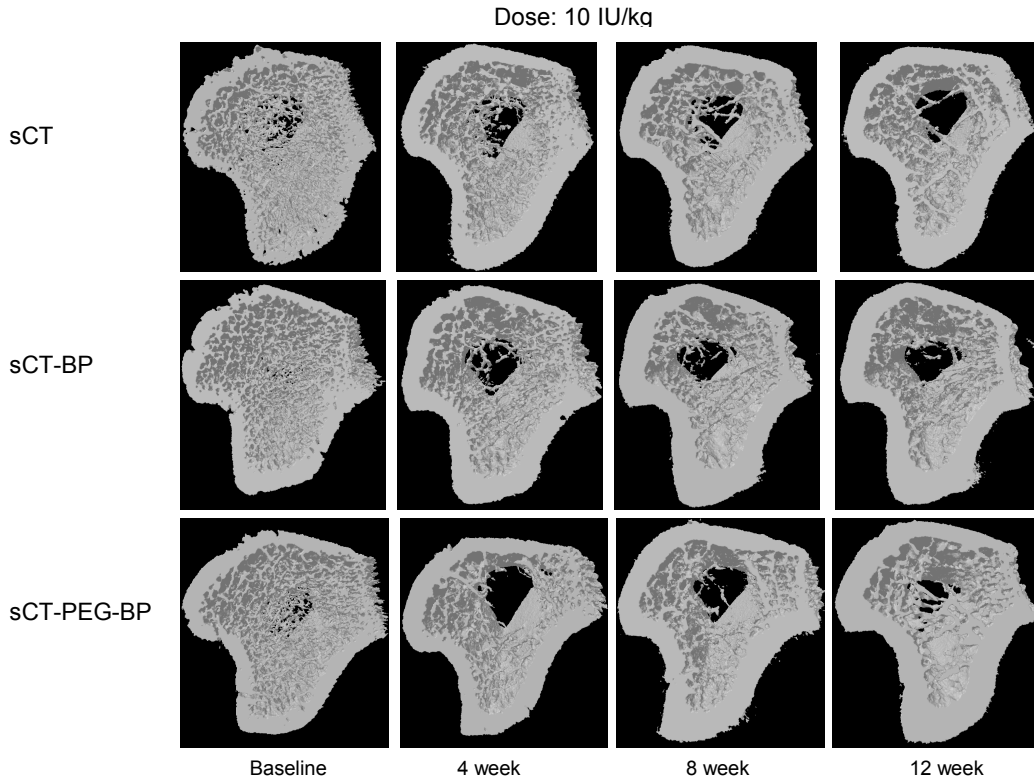


Figure 82: Dose escalation: three-dimensional micro-CT renderings of trabecular bone volume at baseline (week 0, left panel), 4, 8 and 12 weeks. Six week old female OVX rats were administered 10 IU/kg daily s. c. dose of calcimar or equivalent sCT-BP or sCT-PEG-BP. All rats were also given daily oral dose of 28.5 mg/kg strontium ranelate (PROTOS[®], Servier Laboratories, Australia) as a source of Sr⁺² tracer. Rats were analyzed for disease progression with Skyscan *in-vivo* micro-CT for bone volume at 0, 1, 2 and 3 months.

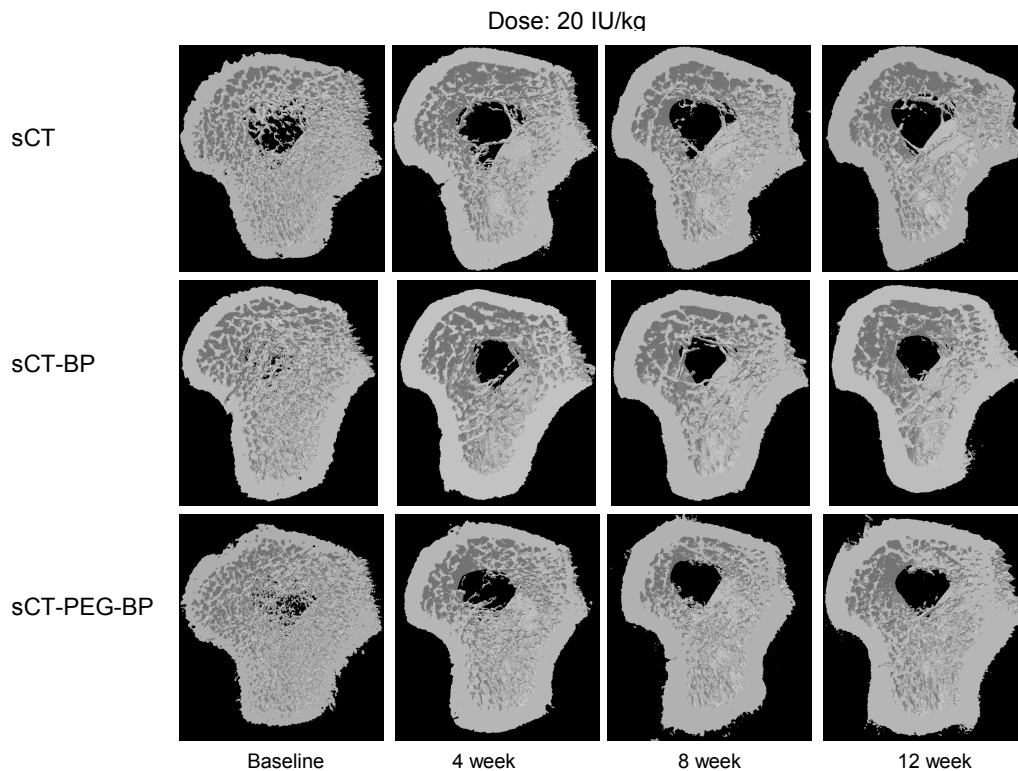


Figure 83: Dose escalation: three-dimensional micro-CT rendering of trabecular bone volume at baseline (week 0, left panel), 4, 8 and 12 weeks. Six week old female OVX rats were administered 20 IU/kg daily s. c. dose of calcimar or equivalent sCT-BP or sCT-PEG-BP. All rats were also given daily oral dose of 28.5 mg/kg strontium ranelate (PROTOS[®], Servier Laboratories, Australia) as a source of Sr⁺² tracer. Rats were analyzed for disease progression with Skyscan *in-vivo* micro-CT for bone volume at 0, 1, 2 and 3 months.

CHAPTER 4: DISCUSSION AND CONCLUSION

Antiresorptive therapy of bone disease utilizing conventional sCT is hampered by the poor systemic uptake of sCT and its short half-life, contributing to its poor and variable bioavailability and reported antiresorptive efficacy. In response, investigators have attempted to increase the duration of sCT circulation by conjugation to linear polyethylene glycol (PEG). Compared to native sCT, the PEGylated conjugates showed reduced systemic clearance due to altered tissue distribution. They also showed enhanced *in vivo* hypocalcaemic efficacy versus native sCT for both the intra-intestinal and pulmonary delivery routes (Fujisaki, Tokunaga et al. 1997; Lee, Park et al. 2003; Shin, Jung et al. 2004; Youn, Jung et al. 2006; Cheng, Satyanarayanajois et al. 2007; Cenni, Granchi et al. 2008; Chae, Jin et al. 2008). However, increasing the circulation time of non bone targeting formulations of sCT would not necessarily translate into optimal bone-based therapeutic effects, as the competitive uptake of sCT by non-bone tissue resident CTRs would still remain despite PEGylation. Thus, a delivery system increasing sCT targeting, localization and retention to bone is justified and it has the potential to positively impact sCT therapy, whilst reducing the drug concentration in non-bone loci containing the CTR.

Previous studies also demonstrated that the replacement of lysine₁₁ and lysine₁₈ amino acid residues by other amino acids or N-terminus acetylation or antibody conjugation did not affect sCT bioactivity. Thus, we

hypothesized that chemical coupling of a bone targeting moiety with sCT or sCT-PEG generated utilizing these sites would be a feasible approach in order to develop novel bone targeting sCT analogues.

PEGylation could also confer additional advantages such as enhanced resistance toward systemic enzymatic metabolism, increased circulation time and reduced immunogenicity (Veronese and Pasut 2005; Hamidi, Azadi et al. 2006; Fee 2007; Doschak, Kucharski et al. 2009; Kang, Deluca et al. 2009; Jevsevar, Kunstelj et al. 2010; Ryan, Frias et al. 2011).

A simple, first generation (i.e., non-nitrogen containing) BP was selected as a model bone targeting moiety for its proven ability to impart HA (the mineral phase of bone which is not present in other tissues) (Rogers, Frith et al. 1999), binding ability to candidate drugs (Doschak, Kucharski et al. 2009). Nonetheless, our experience with BP conjugative strategies has demonstrated that each protein or peptide will behave differently during the conjugation process because of their unique solubility, stability, and bioactivity issues (Uludag, Gao et al. 2000; Uludag, Kousinioris et al. 2000; Gittens, Matyas et al. 2003; Doschak, Kucharski et al. 2009). Accordingly, one “generalized” conjugation procedure will not work as a universal reaction scheme for all therapeutic peptides and proteins and individualized strategies will need to be considered and employed on a “case-by-case” basis for individual peptide or protein candidates, as previously hypothesized (Hirabayashi and Fujisaki 2003).

The conjugation of BP to sCT proved challenging due to their contradictory chemical and physical properties. CT is highly unstable in aqueous buffered reaction conditions that are generally suitable for protein or peptide coupling. In aqueous solutions, CT has a pronounced tendency to aggregate into long, thin fibrillar aggregates, yielding a viscous and turbid dispersion (Bauer, Aebi et al. 1995; Cholewinski, Luckel et al. 1996). Thus, the reaction methods utilized for larger model proteins that are soluble and stable in buffered solution could not be applied to sCT.

sCT-BP conjugation was further hampered by the physical and chemical properties of the BP. Although CT is highly stable in organic solvents, the insolubility of BP in organic solvents and the low reactivity of the functional group in thiol-BP further complicated the conjugation. Thus, we avoided aqueous reaction conditions in the initial reaction step to minimize the instability of CT and used mild aqueous conditions in subsequent reaction steps to minimize BP solubility issues. A lower concentration buffer than those generally used was also employed to minimize the aggregation and precipitation of sCT in buffer, in order to proceed with the second step of the reaction. Incorporation of PEG in sCT to generate sCT-PEG before coupling with thiol BP imparted a positive effect in the overall chemistry. PEG imparted a stabilizing and solubilizing effect upon sCT and allowed for more efficient thiol coupling.

We also confirmed the conjugate's chemical identity in detail using MALDI-TOF, and optimized the reaction conditions for various key parameters so that they were reproducible and consistent.

The bone mineral affinity and specificity of this sCT delivery system were subsequently investigated using an HA binding test, followed by different calcium salt binding affinity assays. If the sCT was targeted to HA as a result of BP conjugation, then after centrifugation and complete removal of unbound sCT, the majority of remaining sCT should be detected in the pelleted HA centrifugate compared to other calcium salts. As a control, native sCT was reacted with HA under identical conditions. To ensure that there was no direct binding of the cross-linking chemistry employed with HA, we also tested a non-BP containing conjugate (sCT-cysteine) that was reacted with HA under identical conditions. In the aggregate, those *in vitro* assays confirmed that the sCT-BP conjugates were specifically bound to HA. As HA is the principal mineral found in bone matrix, the *in vivo* administration of sCT-BP conjugates should lead to improved bone accumulation of sCT compared to free sCT or sCT conjugates without BP.

Our bone targeting sCT analogues retained sCT bioactivity and effectively targeted bone HA mineral after BP conjugation. CD spectral studies suggested a change in the secondary structure of sCT, which initially was of low helical content that increased in the case of sCT-SMCC, sCT-BP, sCT-PEG or sCT-PEG-BP. Helical structure plays an

important role in the retention of sCT biological activity and reducing aggregation and fibril formation (Green, Lynch et al. 1987) due to its stronger dipole moment (Querol, Perez-Pons et al. 1996). As even small increases in the fraction of non-polar monomers in the protein chain leads to a substantial decrease in solubility (Gupta, Hall et al. 1998) and increase in aggregation (Gupta, Hall et al. 1998), structural alteration induced by amphiphilic PEG and hydrophilic BP likely imparts a positive impact after conjugation to aggregation prone sCT. That phenomenon might explain why sCT-PEG or sCT-SMCC did not precipitate during its reaction with BP in high concentration phosphate buffer – conditions not generally recommended as an initial solubilizing solution for sCT (Bhandari, Newa et al. 2010).

As the secondary structure of sCT was altered by conjugation, we evaluated its effect upon antibody binding abilities of sCT. The results confirmed that strong binding recognition was retained after conjugation. OC activity assay substrate plates contain calcium phosphate mineral for culturing OC-like cells, in order to evaluate bone resorption activity by pit formation. In this study, we used these plates (as the first report of its kind) to confirm the strong binding ability of the bone-targeting BP moiety for mineralized bone surfaces, and subsequent recognition of sCT by anti-sCT antibody after the peptide's structural alteration by conjugation. The BP in sCT-PEG-BP or sCT-BP strongly bound the artificial bone surface of the plates, and when unbound molecules were removed by washings, the

mineralized plate surface mimicked the bound antigen phase in subsequent ELISA-based detection.

We further evaluated the effect of conjugation towards retained sCT bioactivity *in vitro*. Human breast carcinoma T47D cells were used, as CTRs containing just a single CT binding site are highly expressed in this cell line (Martin, Findlay et al. 1980). Binding of CT with its receptor on OC in bone inhibits osteoclast-mediated resorptive activity by activating adenylyl cyclase, an enzyme responsible for generation of cyclic adenosine monophosphate (cAMP). Our cAMP assay results confirmed that the modification of sCT did not adversely affect the ability for sCT to trigger its biological activity, wherein cAMP levels are increased. The cAMP increasing effect did not demonstrate a dose-dependent increase from 50 to 100 nM. That implied the cAMP increasing effect reached a plateau. That finding was similar to the maximal calcium lowering effect reported previously for sCT (Deftos, Nolan et al. 1997).

Marginal loss of *in vitro* bioactivity of sCT was measured after conjugation to PEG-BP; however it was not statistically significant and did not inhibit function, as evidenced in the bone volume and BMD measurements in OP rats. For this investigation, we measured the hypocalcemic effect of sCT or sCT analogue administration (rather than assaying sCT plasma concentrations), as the hypocalcemic effect reflects the sensitivity of the response to sCT, and was thus of greater clinical relevance than simple quantification of systemic sCT levels. It is also

important to recognize that our bone targeting variant of sCT would attach to the surface of bone faster than native sCT, sCT-SMCC or sCT-PEG, so that their plasma concentration would likely be less than that of non-BP conjugated controls – despite imparting greater antiresorptive efficacy.

Early effects of OP pathogenesis on bone volume and BMD was assessed by measuring bone volume and BMD in OVX rats. Micro-CT measurements revealed the reduction in loss of BMD and bone volume, and the significant preservation of bone volume and BMD in sCT-PEG-BP dosed groups (compared with untreated OVX controls, non-PEGylated bone targeting counterpart or non-bone targeting marketed compound at the 3 month study endpoint). Those observations indicate a clear therapeutic advantage of bone targeting PEGylated sCT, even at the preliminary dosage attempted (2.5 IU/kg body mass).

Although BPs are known to reduce the rate of bone loss (BMD and bone mass), in our experiments, thiol-BP was used for its potential as a bone targeting agent (not for its clinical effect) to deliver sCT to the bone mineral surface. Thiol-BP in acetate buffer was used as a control to know if the improved effect of BP conjugated sCT was due to bone targeting and PEGylation of sCT or simply due to the presence of BP. It should be noted that the concentration of thiol-BP used was less than accepted therapeutic dose. For example, the clinical dose of Alendronate in osteoporosis treatment is 10 mg daily (~143µg/kg). However, the thiol-BP dose used in these experiments was 160.71 ng/kg. This concentration was the highest

possible concentration that corresponded to the “three” moles of thiol-BP per sCT as if all the three amines in sCT reacted with thiol-BP.

In rat model of adjuvant arthritis (AA), effects of AA pathogenesis on body weight, paw diameter, paw volume, joint diameter, joint volume, bone volume and BMD was assessed. Micro-CT measurements revealed the reduction in loss of BMD and bone volume in controlled rats, and the significant preservation of bone volume and BMD in sCT-BP or sCT-PEG-BP dosed groups. Similarly, in the measurements of paw diameter, paw volume, joint diameter and joint volume, bone targeting sCT analogues showed disease progress reducing effect compared to control or the non-bone targeting sCT. Those observations indicate a clear therapeutic advantage of bone targeting sCT.

Since the dose could impact the therapeutic outcome, we measured the impact of different doses of these analogues in OP pathogenesis in terms of bone volume and BMD in OVX rats. Micro-CT measurements revealed the reduction in loss of BMD and bone volume by non-bone targeting sCT. However, a significant preservation of bone volume and BMD in bone targeting sCT analogues dosed groups (compared with untreated OVX controls, or non-bone targeting marketed compound) were observed at the 3 month study endpoint. Those observations indicate a clear therapeutic advantage of bone targeting sCT.

Problems, limitations and future study considerations:

Although the bone targeting sCT analogues were successfully synthesized, characterized and evaluated in appropriate rat disease models, there are many factors to be considered for successful scale up and first time in human clinical trials of these analogues. The following discussion is not the comprehensive lists of problems and limitations of current study nor does it try to encompass all corrective measures. However, it includes many issues that are to be addressed in future studies.

In the case of starting raw materials, the problem starts from sCT itself. Since it was an expensive peptide manufactured by a limited number of manufacturers, vendor qualification and a thorough evaluation study is needed. sCT prices for some manufacturers are ten times higher than the product used in this study. If the price is considered to be the vendor selection factor then it might not assure the quality of sCT to be used in later studies. Good manufacturing practice (GMP) grade starting material is needed to reduce lot to lot variability and also for efficient reaction optimization for bone targeting sCT analogues synthesis. Purity of the sCT is of foremost importance.

However, the sCT used in this study was only 87% pure in terms of peptide content as determined by HPLC analysis by the supplier. In addition, the impurities or storage vehicles were not disclosed by the

manufacturer irrespective of our request to reveal such information. Enhanced weight due to the presence of 13% impurities could play a negative role in reaction efficiency particularly in context of sCT instability and insolubility. A corrective calculation was carried out in this study by adding more samples to make 100%. This allowed to use the required quantity of sCT but also increased the presence of unwanted impurities in the reaction mixture. An efficient USP sCT assay and identification tests must be employed in scale-up procedures in order to reduce the variability induced by sCT lot to lot differences. The vendor should be selected based on quality and in house product evaluation report.

When we consider NHS-PEG-MAL, unlike sCT, there exist numerous suppliers and manufacturers. This makes it very difficult to evaluate a vendor without proper techniques to assay and quantify PEG in-house. One of the most common problems in PEGylation is lot to lot variability in the product from the same manufacturer or the quality variability between different manufacturers. As the reported molecular weight of this polymer is based on its average molecular weight, the lowest and highest molecular weight range in the polydispersed samples plays an important role for average molecular weight determination. This factor eventually leads to the generation of many derivatives in later reactions. If the average molecular weight is variable by a huge range then the pharmacokinetic parameters of the compounds synthesized using

such PEG will also vary accordingly. This might eventually lead to variable and unpredictable pharmacodynamic parameters.

Hence in order to obtain the full advantages of PEGylation the monodispersed PEG starting material is desirable from a reaction efficiency point of view and also from a regulatory point of view. However monodispersed products are not commercially available for the entire PEG molecular weight ranges. At the moment they are available for MW up to 2400. Use of monodispersed PEGs will also reduce the burden of purification steps to generated desired products.

The major problem that was faced in this study was the low reactivity or reaction efficiency of thiol-BP. Amino-BPs were reported to have low reactivity and earlier studies supported the use of thiolated BPs, however there still exists the problem of low reactivity. This was due to the presence of unwanted impurities comprising up to 50% of the sample. As shown in this study, when compared to cysteine the reactive thiol in the freshly synthesized and received compounds was reduced to almost 50%. The problem observed with the phosphate assay using Alendronate as standard. This was further substantiated by carrying the LC-MS analysis of thiol-BP which showed the presence of a prominent unwanted peak at 150m/z.

Beside the impurity, there is one more problem associated with BP. There are not many suppliers of BP and the BP used in this study was

custom synthesized by Surfactis inc., France. Although the ^{13}C , ^{32}P , ^1H NMR supplied by the manufacturer showed the presence of desired product in optimum ratios, our in house studies to determine the reactive thiol and phosphate was unexpected. This was either due to the degradation of the product when delivered from France or due to an inefficient reaction or synthesis protocol at their end.

However, no dimer formation due to the disulfide bond formation was observed in LC-MS analysis as the peak at this molecular weight range was absent. In methods of bisphosphonate synthesis utilizing strongly basic conditions and elevated temperature, the reaction is complicated by rearrangement. This rearrangement generates isomeric compounds containing two chemically different phosphorus-carbon bonds, including a tetra-alkyl phosphonophosphate; this might be another reason for the presence of an impurity. Hence, a further study or back-up supplier is needed to provide highly pure thiol-BP. If this can be done then the reaction will be highly efficient eventually resulting into improved yields.

This fact was proved using cysteine in this study as a substitute for thiolated bisphosphonate and also to determine the effect of reaction chemistry of sCT modification in later studies. Although this did not affect the sCT properties, activity and efficacy, it had a great effect on the reaction efficiency. Use of cysteine led to a better and more efficient reaction as evidenced by clean MALDI-TOF spectra.

When we consider the reaction itself, there are multiple issues. Although calcitonin is a simple peptide in terms of amino acid sequence and secondary structure folding, it behaves very differently in solution and is highly unstable in general aqueous buffered reaction conditions (Arvinte and Drake 1993). In aqueous solutions, CT has a pronounced tendency to aggregate into long, thin fibrillar aggregates, yielding a viscous and turbid dispersion.

Hence, unlike other model proteins reported in earlier studies to impart bone mineral affinity using BP conjugation, sCT is highly unstable in general reaction conditions suitable to those proteins. Unfortunately those reaction conditions are the best conditions for the linker chemistry used in such derivatization including the synthesis of bone targeting sCT analogues. In contrast to those proteins, sCT is soluble in organic solvents, indicating that the aqueous reaction conditions should be minimized in the specific case of CT.

Although CT is highly stable in organic solvents, the insolubility and low reactivity of bisphosphonate in organic solvents is another major obstacle that prevents the conjugation strategies employed in all previously published BP-conjugation strategies.

We avoided aqueous reaction conditions in the initial reaction step to minimize the instability of CT and used mild aqueous conditions in subsequent reaction steps to minimize BP solubility issues. A lower

concentration buffer than those generally used was also employed to minimize the aggregation and precipitation of sCT in the buffer, in order to proceed with the second step reaction. Similarly, incorporation of PEG in sCT to generate sCT-PEG before coupling with thiol BP imparted a positive effect in the overall chemistry. PEG imparted a stabilizing and solubilizing effect upon sCT and allowed for more efficient thiol coupling.

Similarly, new reactions techniques should be devised and optimized, for example blocking the specific amine group in sCT could lead the reaction into the generation of the desired products not just mixtures of all possible amine substitution. This strategy, along with use of monodispersed PEG or the PEG in a very narrow range of polydispersibility could generate lesser number of closely related compounds making the purification easier and the biological effects more predictable.

With regards to conjugate characterization, we used two techniques. One was the characterization by determining the number of bisphosphonates molecules per calcitonin molecule. The other was by determining the precise molecular weight of these analogues using MALDI-TOF analysis. However, the former was not as scientifically precise as MALDI-TOF analysis.

MALDI-TOF analysis is not free from disadvantages. The most common and important one is the fact that the characterization was

qualitative not quantitative. The costs, time and technical limitations associated with MALDI-TOF are to be resolved to appropriately quantify the product. In addition, there are issues related to machine and personnel. We had done MALDI in the department of Biochemistry, core facility. However, the same analyst was not guaranteed. This might lead to operator variability if their method of analysis was not appropriately validated.

Although the HPLC can be used for characterization, purification and quantification purposes, it has its own limitation to be used in these kinds of studies. There were no reference standards for PEGylated or bone targeted sCT. Use of USP sCT reference is not a very good idea as it may not work in case of these polydispersed PEGylated compounds. Their molecular weight and lipophilicity varied by a narrow range.

A pilot HPLC project to separate and characterize individual compounds was unsuccessful. The peaks were overlapped for example in case of mono-substituted products, all peaks related to polydispersed PEGylated compounds eluted at the same time as a single, large and broad peak. We were not able to devise an appropriate HPLC method for their separation. Had there been such a method, the manufacturers of PEG would have used it to provide a monomeric PEG product. Similarly, the lipophilicity of the mono or di or tri substituted products was not significantly different unlike their molecular weight. This made it difficult to

isolate a single substituted product in manageable scale-up condition.

Further studies are hence needed to resolve these issues.

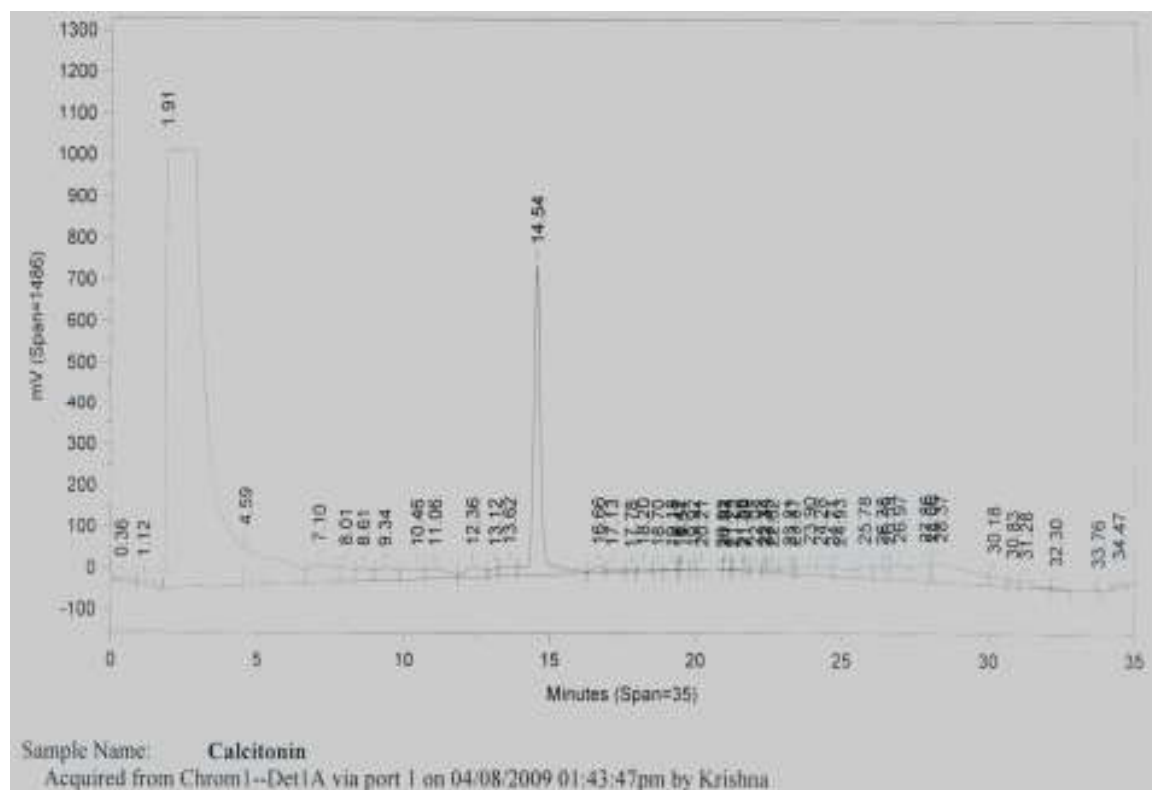


Figure 84: Sample HPLC spectra of sCT. Gradient elution from 0 minute (A-100, B-0%) to 35 minutes (A-0%, B-100%). A-0.1 %v/v Trifluoroacetic acid in water, B: 0.1% v/v Trifluoroacetic acid in 95% v/v acetonitrile in water.

For purification, one of the methods applied was dialysis using appropriate molecular weight cut off dialysis tubes. This process was acceptable in an academic setting but not for industrial scale-up and manufacturing in a GMP environment. There exists a wide range of closely related pore size in the dialysis membrane, leading both to the loss of desired product and retention of unwanted ones. In addition, this technique is time consuming needing many hours. This could lead to stability problems for this peptide drug. As the BP exists as a charged ion in buffer solution, adsorption of these ions could be another problem. Process loss was very high in dialysis and we were unable to separate mono, di and tri substituted products.

Commercial spin column technology using size exclusion principle was very fast and efficient. However, it could not separate mono, di and tri substituted compounds. Moreover, these columns are not available for industrial scale and lower sample loading volume capacities for separation requires the use of many columns in a serial manner when large quantities of products are required for a large animal study.

In our case the BP contained 50% impurities and additional sample was added to correct the percentage purity. Plus, the reaction between functionalized sCT and BP was carried out at 1:20-30 mol/mol ratios respectively. Hence, there was a large amount of small molecular weight impurity to be separated by the columns. This was addressed by passing

the sample through multiple columns. This would lead to increased process loss and cost in an industrial setting.

Finally, the evaluation of individual products in disease models to determine the most effective product should be considered. This will allow the determination of most active compound of these bone targeting sCT analogues. If such a compound with highest activity could be isolated and purified, it could show further improved efficacy in bone diseases. *In-vivo* experiments need to be carried out in a sufficient number of animals for suitable analytical power of analysis. Since this project was a proof of principle, the number of animals used was n=3 to 4. A further efficacy evaluation utilizing higher numbers of animals should be considered. Moreover, inter species variability should be evaluated and necessary precautions should be implemented at an early stage of product development process. Hence an efficacy study in animals other than rats such as swine is worth consideration.

Conclusion

In conclusion, it is generally accepted that the clinical utility of sCT in the treatment of bone diseases such as osteoporosis, Paget's disease, and hypercalcemia of malignancy relies upon its ability to reduce osteoclast activity. Our novel BP-conjugated sCT analogues exhibited potential for preferential bone accumulation (as demonstrated by HA

binding), desirable structural properties, unaltered antibody binding ability and retention of bioactivity. Preclinical evaluation in a rat model of osteoporosis and adjuvant arthritis indicated significantly preserved bone volume and bone mineral density after administration of bone-targeting salmon calcitonin analogue. In the aggregate, our results indicate that bisphosphonate mediated bone targeting of sCT showed significantly improved efficacy over current commercial formulations of sCT and has potential of improving clinical outcomes for sCT therapy in conditions characterized by excessive bone turnover.

REFERENCES

- Aerts, N. E., E. J. Dombrecht, et al. (2008). "Activated T cells complicate the identification of regulatory T cells in rheumatoid arthritis." Cell Immunol **251**(2): 109-115.
- Aida, S., M. Okawa-Takatsuji, et al. (1994). "Calcitonin inhibits production of immunoglobulins, rheumatoid factor and interleukin-1 by mononuclear cells from patients with rheumatoid arthritis." Ann Rheum Dis **53**(4): 247-249.
- Alvarez, H. M., O. Y. So, et al. (2011). "Effects of Pegylation and Immune Complex Formation on the Pharmacokinetics and Biodistribution of Recombinant Interleukin 10." Drug Metab Dispos.

Andersson, M. K., P. Lundberg, et al. (2007). "Effects on osteoclast and osteoblast activities in cultured mouse calvarial bones by synovial fluids from patients with a loose joint prosthesis and from osteoarthritis patients." Arthritis Res Ther **9**(1): R18.

Ang, E. S., N. J. Pavlos, et al. (2011). "Paclitaxel inhibits osteoclast formation and bone resorption via influencing mitotic cell cycle arrest and RANKL-induced activation of NF-kappaB and ERK." J Cell Biochem.

Arai, F., T. Miyamoto, et al. (1999). "Commitment and differentiation of osteoclast precursor cells by the sequential expression of c-Fms and receptor activator of nuclear factor kappaB (RANK) receptors." J Exp Med **190**(12): 1741-1754.

Arvinte, T., A. Cudd, et al. (1993). "The structure and mechanism of formation of human calcitonin fibrils." J Biol Chem **268**(9): 6415-6422.

Arvinte, T. and A. F. Drake (1993). "Comparative study of human and salmon calcitonin secondary structure in solutions with low dielectric constants." J Biol Chem **268**(9): 6408-6414.

Aubin, C. E., J. Dansereau, et al. (1998). "Three-dimensional measurement of wedged scoliotic vertebrae and intervertebral disks." Eur Spine J **7**(1): 59-65.

Ballica, R., K. Valentijn, et al. (1999). "Targeted expression of calcitonin gene-related peptide to osteoblasts increases bone density in mice." J Bone Miner Res **14**(7): 1067-1074.

Bauer, H. H., U. Aebi, et al. (1995). "Architecture and polymorphism of fibrillar supramolecular assemblies produced by in vitro aggregation of human calcitonin." J Struct Biol **115**(1): 1-15.

Beglinger, C., W. Born, et al. (1992). "Intracolonic bioavailability of human calcitonin in man." Eur J Clin Pharmacol **43**(5): 527-531.

Bendele, A. M. (2001). "Animal models of osteoarthritis." J Musculoskeletal Neuronal Interact **1**(4): 363-376.

Benslay, D. N. and A. M. Bendele (1991). "Development of a rapid screen for detecting and differentiating immunomodulatory vs. anti-inflammatory compounds in rats." Agents Actions **34**(1-2): 254-256.

Berry, P. A., R. A. Maciewicz, et al. (2010). "Markers of bone formation and resorption identify subgroups of patients with clinical knee osteoarthritis who have reduced rates of cartilage loss." J Rheumatol **37**(6): 1252-1259.

Bettica, P., G. Cline, et al. (2002). "Evidence for increased bone resorption in patients with progressive knee osteoarthritis: longitudinal results from the Chingford study." Arthritis Rheum **46**(12): 3178-3184.

Bhandari, K. H., M. Newa, et al. (2010). "Synthesis, characterization and in vitro evaluation of a bone targeting delivery system for salmon calcitonin." Int J Pharm **394**(1-2): 26-34.

Black, D. M., P. D. Delmas, et al. (2007). "Once-yearly zoledronic acid for treatment of postmenopausal osteoporosis." N Engl J Med **356**(18): 1809-1822.

Blair, H. C., S. L. Teitelbaum, et al. (1989). "Osteoclastic bone resorption by a polarized vacuolar proton pump." Science **245**(4920): 855-857.

Blavier, L. and J. M. Delaisse (1995). "Matrix metalloproteinases are obligatory for the migration of preosteoclasts to the developing marrow cavity of primitive long bones." J Cell Sci **108 (Pt 12)**: 3649-3659.

Boissy, P., T. R. Lenhard, et al. (2003). "An assessment of ADAMs in bone cells: absence of TACE activity prevents osteoclast recruitment and the formation of the marrow cavity in developing long bones." FEBS Lett **553**(3): 257-261.

Bonni, A., A. Brunet, et al. (1999). "Cell survival promoted by the Ras-MAPK signaling pathway by transcription-dependent and -independent mechanisms." Science **286**(5443): 1358-1362.

Boron, W. F. (2004). "Regulation of intracellular pH." Adv Physiol Educ **28**(1-4): 160-179.

Bouyer, P., S. R. Bradley, et al. (2004). "Effect of extracellular acid-base disturbances on the intracellular pH of neurones cultured from rat medullary raphe or hippocampus." J Physiol **559**(Pt 1): 85-101.

Boyle, W. J., W. S. Simonet, et al. (2003). "Osteoclast differentiation and activation." Nature **423**(6937): 337-342.

Brantus, J. F. and P. D. Delmas (1997). "[Osteoporosis. Epidemiology, etiology, diagnosis, prevention]." Rev Prat **47**(8): 917-922.

Breimer, L. H., I. MacIntyre, et al. (1988). "Peptides from the calcitonin genes: molecular genetics, structure and function." Biochem J **255**(2): 377-390.

Brennan, F. M., A. L. Hayes, et al. (2002). "Evidence that rheumatoid arthritis synovial T cells are similar to cytokine-activated T cells: involvement of phosphatidylinositol 3-kinase and nuclear factor kappaB pathways in tumor necrosis factor alpha production in rheumatoid arthritis." Arthritis Rheum **46**(1): 31-41.

Buclin, T., M. Cosma Rochat, et al. (2002). "Bioavailability and biological efficacy of a new oral formulation of salmon calcitonin in healthy volunteers." J Bone Miner Res **17**(8): 1478-1485.

Burckhardt, P. (1989). "[The various forms of osteoporosis and their treatment]." Schweiz Med Wochenschr **119**(50): 1797-1805.

Burge, R., B. Dawson-Hughes, et al. (2007). "Incidence and economic burden of osteoporosis-related fractures in the United States, 2005-2025." J Bone Miner Res **22**(3): 465-475.

Campion, J. M. and M. J. Maricic (2003). "Osteoporosis in men." Am Fam Physician **67**(7): 1521-1526.

Capelle, M. A., R. Gurny, et al. (2009). "A high throughput protein formulation platform: case study of salmon calcitonin." Pharm Res **26**(1): 118-128.

Care, A. D., R. F. Bates, et al. (1970). "A possible role for the adenyl cyclase system in calcitonin release." J Endocrinol **48**(1): 1-15.

Carlson, R. P., L. J. Datko, et al. (1985). "Comparison of inflammatory changes in established type II collagen- and adjuvant-induced arthritis using outbred Wistar rats." Int J Immunopharmacol **7**(6): 811-826.

Carstens, J. H., Jr. and J. D. Feinblatt (1991). "Future horizons for calcitonin: a U.S. perspective." Calcif Tissue Int **49 Suppl 2**: S2-6.

Casez, J. P., P. Tschopp, et al. (2003). "Effects of nasal calcitonin on bone mineral density following parathyroidectomy in patients with primary hyperparathyroidism." Horm Res **59**(6): 263-269.

Cenni, E., D. Granchi, et al. (2008). "Biocompatibility of poly(D,L-lactide-co-glycolide) nanoparticles conjugated with alendronate." Biomaterials **29**(10): 1400-1411.

Chabre, O., B. R. Conklin, et al. (1992). "A recombinant calcitonin receptor independently stimulates 3',5'-cyclic adenosine monophosphate and Ca²⁺/inositol phosphate signaling pathways." Mol Endocrinol **6**(4): 551-556.

Chae, S. Y., C. H. Jin, et al. (2008). "Preparation, characterization, and application of biotinylated and biotin-PEGylated glucagon-like peptide-1 analogues for enhanced oral delivery." Bioconjug Chem **19**(1): 334-341.

Chambers, T. J. (1982). "Osteoblasts release osteoclasts from calcitonin-induced quiescence." J Cell Sci **57**: 247-260.

Chambers, T. J. and N. N. Ali (1983). "Inhibition of osteoclastic motility by prostaglandins I₂, E₁, E₂ and 6-oxo-E₁." J Pathol **139**(3): 383-397.

- Chambers, T. J. and J. A. Darby (1985). "[Role of calcitonin in bone]." Presse Med **14**(40): 2061.
- Chambers, T. J. and C. J. Dunn (1983). "Pharmacological control of osteoclastic motility." Calcif Tissue Int **35**(4-5): 566-570.
- Chambers, T. J. and K. Fuller (1985). "Bone cells predispose bone surfaces to resorption by exposure of mineral to osteoclastic contact." J Cell Sci **76**: 155-165.
- Chambers, T. J. and C. J. Magnus (1982). "Calcitonin alters behaviour of isolated osteoclasts." J Pathol **136**(1): 27-39.
- Chambers, T. J. and A. Moore (1983). "The sensitivity of isolated osteoclasts to morphological transformation by calcitonin." J Clin Endocrinol Metab **57**(4): 819-824.
- Chang, Y. H., C. M. Pearson, et al. (1980). "Adjuvant polyarthritis. IV. Induction by a synthetic adjuvant: immunologic, histopathologic, and other studies." Arthritis Rheum **23**(1): 62-71.
- Chausmer, A., C. Stuart, et al. (1980). "Identification of testicular cell plasma membrane receptors for calcitonin." J Lab Clin Med **96**(5): 933-938.
- Chen, P., J. M. Lai, et al. (2000). "Relative bioavailability of salmon calcitonin given intramuscularly." Zhonghua Yi Xue Za Zhi (Taipei) **63**(8): 619-627.

Chen, X., R. Park, et al. (2004). "Pharmacokinetics and tumor retention of 125I-labeled RGD peptide are improved by PEGylation." Nucl Med Biol **31**(1): 11-19.

Cheng, S. L., F. Lecanda, et al. (1998). "Human osteoblasts express a repertoire of cadherins, which are critical for BMP-2-induced osteogenic differentiation." J Bone Miner Res **13**(4): 633-644.

Cheng, W., S. Satyanarayanajois, et al. (2007). "Aqueous-soluble, non-reversible lipid conjugate of salmon calcitonin: synthesis, characterization and in vivo activity." Pharm Res **24**(1): 99-110.

Cholewinski, M., B. Luckel, et al. (1996). "Degradation pathways, analytical characterization and formulation strategies of a peptide and a protein. Calcitonine and human growth hormone in comparison." Pharmaceutica acta Helvetiae **71**(6): 405-419.

Cholewinski, M., B. Luckel, et al. (1996). "Degradation pathways, analytical characterization and formulation strategies of a peptide and a protein. Calcitonine and human growth hormone in comparison." Pharm Acta Helv **71**(6): 405-419.

Colonna, C., B. Conti, et al. (2008). "Site-directed PEGylation as successful approach to improve the enzyme replacement in the case of prolidase." Int J Pharm **358**(1-2): 230-237.

Cudd, A., T. Arvinte, et al. (1995). "Enhanced potency of human calcitonin when fibrillation is avoided." Journal of pharmaceutical sciences **84**(6): 717-719.

- D'Santos, C. S., G. C. Nicholson, et al. (1988). "Biologically active, derivatizable salmon calcitonin analog: design, synthesis, and applications." Endocrinology **123**(3): 1483-1488.
- Datta, S. R., A. Brunet, et al. (1999). "Cellular survival: a play in three Akts." Genes Dev **13**(22): 2905-2927.
- Deftos, L. J., J. J. Nolan, et al. (1997). "Intrapulmonary drug delivery of salmon calcitonin." Calcif Tissue Int **61**(4): 345-347.
- Delaisse, J. M., T. L. Andersen, et al. (2003). "Matrix metalloproteinases (MMP) and cathepsin K contribute differently to osteoclastic activities." Microsc Res Tech **61**(6): 504-513.
- Delmas, P. D., N. H. Bjarnason, et al. (1997). "Effects of raloxifene on bone mineral density, serum cholesterol concentrations, and uterine endometrium in postmenopausal women." N Engl J Med **337**(23): 1641-1647.
- Delmas, P. D. and A. D. Woolf (1997). "Osteoporosis: outstanding issues." Baillieres Clin Rheumatol **11**(3): 645-649.
- Devogelaer, J. P., J. P. Brown, et al. (2007). "Zoledronic acid efficacy and safety over five years in postmenopausal osteoporosis." Osteoporos Int **18**(9): 1211-1218.
- Donahue, H. J., F. Guilak, et al. (1995). "Chondrocytes isolated from mature articular cartilage retain the capacity to form functional gap junctions." J Bone Miner Res **10**(9): 1359-1364.

Donahue, H. J., K. J. McLeod, et al. (1995). "Cell-to-cell communication in osteoblastic networks: cell line-dependent hormonal regulation of gap junction function." J Bone Miner Res **10**(6): 881-889.

Doschak, M. R., C. M. Kucharski, et al. (2009). "Improved bone delivery of osteoprotegerin by bisphosphonate conjugation in a rat model of osteoarthritis." Mol Pharm **6**(2): 634-640.

Eghbali-Fatourehchi, G., S. Khosla, et al. (2003). "Role of RANK ligand in mediating increased bone resorption in early postmenopausal women." J Clin Invest **111**(8): 1221-1230.

El-Mabhouh, A. and J. R. Mercer (2005). "188Re-labeled bisphosphonates as potential bifunctional agents for therapy in patients with bone metastases." Applied radiation and isotopes : including data, instrumentation and methods for use in agriculture, industry and medicine **62**(4): 541-549.

El-Mabhouh, A. A., C. A. Angelov, et al. (2006). "A 99mTc-labeled gemcitabine bisphosphonate drug conjugate as a probe to assess the potential for targeted chemotherapy of metastatic bone cancer." Nuclear medicine and biology **33**(6): 715-722.

El-Mabhouh, A. A. and J. R. Mercer (2008). "188Re-labelled gemcitabine/bisphosphonate (Gem/BP): a multi-functional, bone-specific agent as a potential treatment for bone metastases." European journal of nuclear medicine and molecular imaging **35**(7): 1240-1248.

Epand, R. M., R. F. Epand, et al. (1983). "Amphipathic helix and its relationship to the interaction of calcitonin with phospholipids." Biochemistry **22**(22): 5074-5084.

Epand, R. M., R. F. Epand, et al. (1986). "Conformational flexibility and biological activity of salmon calcitonin." Biochemistry **25**(8): 1964-1968.

Epstein, S. (2006). "Ibandronate treatment for osteoporosis: rationale, preclinical, and clinical development of extended dosing regimens." Curr Osteoporos Rep **4**(1): 14-20.

Erlacher, L., J. Kettenbach, et al. (1997). "Salmon calcitonin and calcium in the treatment of male osteoporosis: the effect on bone mineral density." Wien Klin Wochenschr **109**(8): 270-274.

Espie, M. and P. H. Cottu (2003). "[Breast cancer in young women: problem and questions]." Pathol Biol (Paris) **51**(7): 391-392.

Espie, M., J. P. Daures, et al. (2007). "Breast cancer incidence and hormone replacement therapy: results from the MISSION study, prospective phase." Gynecol Endocrinol **23**(7): 391-397.

Ettinger, B., D. M. Black, et al. (1999). "Reduction of vertebral fracture risk in postmenopausal women with osteoporosis treated with raloxifene: results from a 3-year randomized clinical trial. Multiple Outcomes of Raloxifene Evaluation (MORE) Investigators." JAMA **282**(7): 637-645.

Everts, V., J. M. Delaisse, et al. (2002). "The bone lining cell: its role in cleaning Howship's lacunae and initiating bone formation." J Bone Miner Res **17**(1): 77-90.

Ezra, A., A. Hoffman, et al. (2000). "A peptide prodrug approach for improving bisphosphonate oral absorption." J Med Chem **43**(20): 3641-3652.

Faccio, R., D. V. Novack, et al. (2003). "Dynamic changes in the osteoclast cytoskeleton in response to growth factors and cell attachment are controlled by beta3 integrin." J Cell Biol **162**(3): 499-509.

Faccio, R., S. Takeshita, et al. (2003). "c-Fms and the alphavbeta3 integrin collaborate during osteoclast differentiation." J Clin Invest **111**(5): 749-758.

Faccio, R., W. Zou, et al. (2003). "High dose M-CSF partially rescues the Dap12^{-/-} osteoclast phenotype." J Cell Biochem **90**(5): 871-883.

Farley, J., H. P. Dimai, et al. (2000). "Calcitonin increases the concentration of insulin-like growth factors in serum-free cultures of human osteoblast-line cells." Calcif Tissue Int **67**(3): 247-254.

Fee, C. J. (2007). "Size comparison between proteins PEGylated with branched and linear poly(ethylene glycol) molecules." Biotechnol Bioeng **98**(4): 725-731.

Feige, U., A. Schulmeister, et al. (1994). "A constitutive 65 kDa chondrocyte protein as a target antigen in adjuvant arthritis in Lewis rats." Autoimmunity **17**(3): 233-239.

Ferrari, S. L., K. Traianedes, et al. (2000). "A role for N-cadherin in the development of the differentiated osteoblastic phenotype." J Bone Miner Res **15**(2): 198-208.

Fouchereau-Peron, M., M. S. Moukhtar, et al. (1981). "Characterization of specific receptors for calcitonin in porcine lung." Proc Natl Acad Sci U S A **78**(6): 3973-3975.

Francis, M. D. and W. W. Briner (1973). "The effect of phosphonates on dental enamel in vitro and calculus formation in vivo." Calcif Tissue Res **11**(1): 1-9.

Francis, M. D. and A. H. Meckel (1963). "The in vitro formation and quantitative evaluation of carious lesions." Arch Oral Biol **8**: 1-2.

Francis, M. D. and D. J. Valent (2007). "Historical perspectives on the clinical development of bisphosphonates in the treatment of bone diseases." J Musculoskelet Neuronal Interact **7**(1): 2-8.

Fujisaki, J., Y. Tokunaga, et al. (1997). "Osteotropic drug delivery system (ODDS) based on bisphosphonic prodrug. V. Biological disposition and targeting characteristics of osteotropic estradiol." Biol Pharm Bull **20**(11): 1183-1187.

Gallagher, J. C. (1992). "Pathophysiology of osteoporosis." Semin Nephrol **12**(2): 109-115.

Garnero, P. and P. D. Delmas (1997). "Osteoporosis." Endocrinol Metab Clin North Am **26**(4): 913-936.

Garnero, P., M. Ferreras, et al. (2003). "The type I collagen fragments ICTP and CTX reveal distinct enzymatic pathways of bone collagen degradation." J Bone Miner Res **18**(5): 859-867.

Ghayor, C., R. M. Corroero, et al. (2011). "Inhibition of osteoclast differentiation and bone resorption by N-methylpyrrolidone." J Biol Chem **286**(27): 24458-24466.

Girotra, M., M. R. Rubin, et al. (2006). "The use of parathyroid hormone in the treatment of osteoporosis." Rev Endocr Metab Disord **7**(1-2): 113-121.

Gittens, S. A., J. R. Matyas, et al. (2003). "Imparting bone affinity to glycoproteins through the conjugation of bisphosphonates." Pharm Res **20**(7): 978-987.

Goltzman, D. and J. Mitchell (1985). "Interaction of calcitonin and calcitonin gene-related peptide at receptor sites in target tissues." Science **227**(4692): 1343-1345.

Gorn, A. H., H. Y. Lin, et al. (1992). "Cloning, characterization, and expression of a human calcitonin receptor from an ovarian carcinoma cell line." J Clin Invest **90**(5): 1726-1735.

Granholm, S., P. Lundberg, et al. (2007). "Calcitonin inhibits osteoclast formation in mouse haematopoietic cells independently of transcriptional regulation by receptor activator of NF- κ B and c-Fms." J Endocrinol **195**(3): 415-427.

Granholm, S., P. Lundberg, et al. (2008). "Expression of the calcitonin receptor, calcitonin receptor-like receptor, and receptor activity modifying proteins during osteoclast differentiation." J Cell Biochem **104**(3): 920-933.

Green, F. R., 3rd, B. Lynch, et al. (1987). "Biological and physical properties of a model calcitonin containing a glutamate residue interrupting

the hydrophobic face of the idealized amphiphilic alpha-helical region."

Proc Natl Acad Sci U S A **84**(23): 8340-8344.

Gruber, H. E. and N. Brautbar (1984). "Metabolic bone disease and the elderly: current approach to diagnosis and therapy." Nephron **38**(2): 76-86.

Gruber, H. E., D. H. Gutteridge, et al. (1984). "Osteoporosis associated with pregnancy and lactation: bone biopsy and skeletal features in three patients." Metab Bone Dis Relat Res **5**(4): 159-165.

Gruber, H. E., J. L. Ivey, et al. (1984). "Long-term calcitonin therapy in postmenopausal osteoporosis." Metabolism **33**(4): 295-303.

Gu, G., T. A. Hentunen, et al. (2005). "Estrogen protects primary osteocytes against glucocorticoid-induced apoptosis." Apoptosis **10**(3): 583-595.

Guise, T. A. and G. R. Mundy (1998). "Cancer and bone." Endocr Rev **19**(1): 18-54.

Gupta, P., C. K. Hall, et al. (1998). "Effect of denaturant and protein concentrations upon protein refolding and aggregation: a simple lattice model." Protein Sci **7**(12): 2642-2652.

Halleen, J. M., S. R. Raisanen, et al. (2003). "Potential function for the ROS-generating activity of TRACP." J Bone Miner Res **18**(10): 1908-1911.

Halleen, J. M., S. L. Tiitinen, et al. (2006). "Tartrate-resistant acid phosphatase 5b (TRACP 5b) as a marker of bone resorption." Clin Lab **52**(9-10): 499-509.

- Hamidi, M., A. Azadi, et al. (2006). "Pharmacokinetic consequences of pegylation." Drug Deliv **13**(6): 399-409.
- Han, Y., S. C. Cowin, et al. (2004). "Mechanotransduction and strain amplification in osteocyte cell processes." Proc Natl Acad Sci U S A **101**(47): 16689-16694.
- Hanley, D. A. and R. G. Josse (1996). "Prevention and management of osteoporosis: consensus statements from the Scientific Advisory Board of the Osteoporosis Society of Canada. 1. Introduction." CMAJ **155**(7): 921-923.
- Harigai, M., M. Hara, et al. (2004). "Amplification of the synovial inflammatory response through activation of mitogen-activated protein kinases and nuclear factor kappaB using ligation of CD40 on CD14+ synovial cells from patients with rheumatoid arthritis." Arthritis Rheum **50**(7): 2167-2177.
- Harris, J. M., N. E. Martin, et al. (2001). "Pegylation: a novel process for modifying pharmacokinetics." Clin Pharmacokinet **40**(7): 539-551.
- Harris, S. T., N. B. Watts, et al. (1999). "Effects of risedronate treatment on vertebral and nonvertebral fractures in women with postmenopausal osteoporosis: a randomized controlled trial. Vertebral Efficacy With Risedronate Therapy (VERT) Study Group." JAMA **282**(14): 1344-1352.
- Hejdova, M., V. Palicka, et al. (2005). "Effects of alendronate and calcitonin on bone mineral density in postmenopausal osteoporotic women. An observational study." Pharm World Sci **27**(3): 149-153.

Henriksen, K., L. B. Tanko, et al. (2007). "Assessment of osteoclast number and function: application in the development of new and improved treatment modalities for bone diseases." Osteoporos Int **18**(5): 681-685.

Hentunen, T. A., P. T. Lakkakorpi, et al. (1991). "Inhibition of bone resorption by a monoclonal antibody that reacts with a 150 kD membrane protein in chicken osteoclasts." J Bone Miner Res **6**(10): 1091-1097.

Hentunen, T. A., P. T. Lakkakorpi, et al. (1995). "Effects of recombinant human osteogenic protein-1 on the differentiation of osteoclast-like cells and bone resorption." Biochem Biophys Res Commun **209**(2): 433-443.

Hentunen, T. A., J. Tuukkanen, et al. (1990). "Osteoclasts and a small population of peripheral blood cells share common surface antigens." Calcif Tissue Int **47**(1): 8-17.

Hermine, O., P. Mayeux, et al. (1992). "Granulocyte-macrophage colony-stimulating factor and erythropoietin act competitively to induce two different programs of differentiation in the human pluripotent cell line UT-7." Blood **80**(12): 3060-3069.

Hersel, U., M. Kreuzer, et al. (2009). "Tailor made pharmacokinetics of peptides by transient PEGylation." Adv Exp Med Biol **611**: 277-278.

Heymsfield, S. B., A. Pietrobelli, et al. (2005). "The end of body composition methodology research?" Curr Opin Clin Nutr Metab Care **8**(6): 591-594.

Hirabayashi, H. and J. Fujisaki (2003). "Bone-specific drug delivery systems: approaches via chemical modification of bone-seeking agents." Clin Pharmacokinet **42**(15): 1319-1330.

Hirayama, T., L. Danks, et al. (2002). "Osteoclast formation and activity in the pathogenesis of osteoporosis in rheumatoid arthritis." Rheumatology (Oxford) **41**(11): 1232-1239.

Hizmetli, S., H. Elden, et al. (1998). "The effect of different doses of calcitonin on bone mineral density and fracture risk in postmenopausal osteoporosis." Int J Clin Pract **52**(7): 453-455.

Holtrop, M. E. and G. J. King (1977). "The ultrastructure of the osteoclast and its functional implications." Clin Orthop Relat Res(123): 177-196.

Horowitz, M. C., A. L. Bothwell, et al. (2005). "B cells and osteoblast and osteoclast development." Immunol Rev **208**: 141-153.

Horton, M. A., D. Lewis, et al. (1985). "Monoclonal antibodies to osteoclastomas (giant cell bone tumors): definition of osteoclast-specific cellular antigens." Cancer Res **45**(11 Pt 2): 5663-5669.

Ide, M. and Y. Suzuki (2001). "[Drug therapy for osteoporosis associated with rheumatoid arthritis (calcitonin)]." Clin Calcium **11**(5): 638-642.

Inoue, D., C. Shih, et al. (1999). "Calcitonin-dependent down-regulation of the mouse C1a calcitonin receptor in cells of the osteoclast lineage involves a transcriptional mechanism." Endocrinology **140**(3): 1060-1068.

Inzerillo, A. M. and M. Zaidi (2002). "Osteoporosis: trends and intervention." Mt Sinai J Med **69**(4): 220-231.

Inzerillo, A. M., M. Zaidi, et al. (2002). "Calcitonin: the other thyroid hormone." Thyroid **12**(9): 791-798.

Itzstein, C., F. P. Coxon, et al. (2011). "The regulation of osteoclast function and bone resorption by small GTPases." Small Gtpases **2**(3): 117-130.

Jansen-Olesen, I., A. Mortensen, et al. (1996). "Calcitonin gene-related peptide is released from capsaicin-sensitive nerve fibres and induces vasodilatation of human cerebral arteries concomitant with activation of adenylyl cyclase." Cephalalgia **16**(5): 310-316.

Jevsevar, S., M. Kunstelj, et al. (2010). "PEGylation of therapeutic proteins." Biotechnol J **5**(1): 113-128.

Jones, G., D. B. Hogan, et al. (1996). "Prevention and management of osteoporosis: consensus statements from the Scientific Advisory Board of the Osteoporosis Society of Canada. 8. Vitamin D metabolites and analogs in the treatment of osteoporosis." CMAJ **155**(7): 955-961.

Kang, J. S., P. P. Deluca, et al. (2009). "Emerging PEGylated drugs." Expert Opin Emerg Drugs **14**(2): 363-380.

Karsdal, M. A., K. Henriksen, et al. (2008). "Calcitonin: a drug of the past or for the future? Physiologic inhibition of bone resorption while sustaining osteoclast numbers improves bone quality." BioDrugs **22**(3): 137-144.

Karsdal, M. A., P. Qvist, et al. (2006). "Optimising antiresorptive therapies in postmenopausal women: why do we need to give due consideration to the degree of suppression?" Drugs **66**(15): 1909-1918.

Kartner, N., Y. Yao, et al. (2010). "Inhibition of osteoclast bone resorption by disrupting vacuolar H⁺-ATPase α 3-B2 subunit interaction." J Biol Chem **285**(48): 37476-37490.

Kasugai, S., R. Fujisawa, et al. (2000). "Selective drug delivery system to bone: small peptide (Asp)₆ conjugation." J Bone Miner Res **15**(5): 936-943.

Katzenellenbogen, B. S. and J. A. Katzenellenbogen (2002). "Biomedicine. Defining the "S" in SERMs." Science **295**(5564): 2380-2381.

Kelley, T. W., M. M. Graham, et al. (1999). "Macrophage colony-stimulating factor promotes cell survival through Akt/protein kinase B." J Biol Chem **274**(37): 26393-26398.

Kerwin, B. A., B. S. Chang, et al. (2002). "Interactions between PEG and type I soluble tumor necrosis factor receptor: modulation by pH and by PEGylation at the N terminus." Protein Sci **11**(7): 1825-1833.

Kim, K. P., J. D. Cha, et al. (2008). "PEGylation of bacteriophages increases blood circulation time and reduces T-helper type 1 immune response." Microb Biotechnol **1**(3): 247-257.

Kong, Y. Y., W. J. Boyle, et al. (1999). "Osteoprotegerin ligand: a common link between osteoclastogenesis, lymph node formation and lymphocyte development." Immunol Cell Biol **77**(2): 188-193.

Kong, Y. Y., U. Feige, et al. (1999). "Activated T cells regulate bone loss and joint destruction in adjuvant arthritis through osteoprotegerin ligand." Nature **402**(6759): 304-309.

Kong, Y. Y., H. Yoshida, et al. (1999). "OPGL is a key regulator of osteoclastogenesis, lymphocyte development and lymph-node organogenesis." Nature **397**(6717): 315-323.

Korpela, J., S. L. Tiitinen, et al. (2006). "Serum TRACP 5b and ICTP as markers of bone metastases in breast cancer." Anticancer Res **26**(4B): 3127-3132.

Kotake, S., N. Udagawa, et al. (2001). "Activated human T cells directly induce osteoclastogenesis from human monocytes: possible role of T cells in bone destruction in rheumatoid arthritis patients." Arthritis Rheum **44**(5): 1003-1012.

Kotaniemi, A., H. Piirainen, et al. (1996). "Is continuous intranasal salmon calcitonin effective in treating axial bone loss in patients with active rheumatoid arthritis receiving low dose glucocorticoid therapy?" J Rheumatol **23**(11): 1875-1879.

Krasnoperov, R. A. (1997). "[The bioavailability of endogenous calcitonin under selective pharmacological sympathectomy]." Patol Fiziol Eksp Ter(2): 11-13.

Kuca-Warnawin, E., T. Burakowski, et al. (2011). "Elevated number of recently activated T cells in bone marrow of patients with rheumatoid arthritis: a role for interleukin 15?" Ann Rheum Dis **70**(1): 227-233.

Kukita, T., A. Kukita, et al. (2001). "Osteoclast differentiation antigen, distinct from receptor activator of nuclear factor kappa B, is involved in

osteoclastogenesis under calcitonin-regulated conditions." J Endocrinol **170**(1): 175-183.

Kurfurst, M. M. (1992). "Detection and molecular weight determination of polyethylene glycol-modified hirudin by staining after sodium dodecyl sulfate-polyacrylamide gel electrophoresis." Anal Biochem **200**(2): 244-248.

Lacey, J. V., Jr., P. J. Mink, et al. (2002). "Menopausal hormone replacement therapy and risk of ovarian cancer." JAMA **288**(3): 334-341.

Lakkakorpi, P. T. and H. K. Vaananen (1991). "Kinetics of the osteoclast cytoskeleton during the resorption cycle in vitro." J Bone Miner Res **6**(8): 817-826.

Lam, J., S. Takeshita, et al. (2000). "TNF-alpha induces osteoclastogenesis by direct stimulation of macrophages exposed to permissive levels of RANK ligand." J Clin Invest **106**(12): 1481-1488.

Lecanda, F., D. A. Towler, et al. (1998). "Gap junctional communication modulates gene expression in osteoblastic cells." Mol Biol Cell **9**(8): 2249-2258.

Lee, H. J., S. Y. Kim, et al. (2010). "Fracture, bone mineral density, and the effects of calcitonin receptor gene in postmenopausal Koreans." Osteoporos Int **21**(8): 1351-1360.

Lee, K. C., S. C. Moon, et al. (1999). "Isolation, characterization, and stability of positional isomers of mono-PEGylated salmon calcitonins." Pharm Res **16**(6): 813-818.

Lee, K. C., M. O. Park, et al. (2003). "Intranasal delivery of PEGylated salmon calcitonins: hypocalcemic effects in rats." Calcif Tissue Int **73**(6): 545-549.

Lee, K. C., K. K. Tak, et al. (1999). "Preparation and characterization of polyethylene-glycol-modified salmon calcitonins." Pharm Dev Technol **4**(2): 269-275.

Lee, W. A., R. D. Ennis, et al. (1994). "The bioavailability of intranasal salmon calcitonin in healthy volunteers with and without a permeation enhancer." Pharm Res **11**(5): 747-750.

Leibbrandt, A. and J. M. Penninger (2008). "RANK/RANKL: regulators of immune responses and bone physiology." Ann N Y Acad Sci **1143**: 123-150.

Licata, A. A. (2005). "Discovery, clinical development, and therapeutic uses of bisphosphonates." Ann Pharmacother **39**(4): 668-677.

Lindsay, R., J. Nieves, et al. (1997). "Randomised controlled study of effect of parathyroid hormone on vertebral-bone mass and fracture incidence among postmenopausal women on oestrogen with osteoporosis." Lancet **350**(9077): 550-555.

Lipton, A. (2004). "Pathophysiology of bone metastases: how this knowledge may lead to therapeutic intervention." J Support Oncol **2**(3): 205-213; discussion 213-204, 216-207, 219-220.

- Ljusberg, J., Y. Wang, et al. (2005). "Proteolytic excision of a repressive loop domain in tartrate-resistant acid phosphatase by cathepsin K in osteoclasts." J Biol Chem **280**(31): 28370-28381.
- Logar, D. B., R. Komadina, et al. (2007). "Expression of bone resorption genes in osteoarthritis and in osteoporosis." J Bone Miner Metab **25**(4): 219-225.
- Luckman, S. P., D. E. Hughes, et al. (1998). "Nitrogen-containing bisphosphonates inhibit the mevalonate pathway and prevent post-translational prenylation of GTP-binding proteins, including Ras." J Bone Miner Res **13**(4): 581-589.
- Lyles, K. W., C. S. Colon-Emeric, et al. (2007). "Zoledronic Acid in Reducing Clinical Fracture and Mortality after Hip Fracture." N Engl J Med **357**: nihpa40967.
- Lyles, K. W., C. S. Colon-Emeric, et al. (2007). "Zoledronic acid and clinical fractures and mortality after hip fracture." N Engl J Med **357**(18): 1799-1809.
- Malden, N. (2007). "No causal link." Br Dent J **203**(4): 175-176.
- Malden, N., C. Beltes, et al. (2009). "Dental extractions and bisphosphonates: the assessment, consent and management, a proposed algorithm." Br Dent J **206**(2): 93-98.
- Malden, N. J. and A. Y. Pai (2007). "Oral bisphosphonate associated osteonecrosis of the jaws: three case reports." Br Dent J **203**(2): 93-97.

Mancini, L., N. Moradi-Bidhendi, et al. (2000). "Modulation of the effects of osteoprotegerin (OPG) ligand in a human leukemic cell line by OPG and calcitonin." Biochem Biophys Res Commun **279**(2): 391-397.

Marchisio, P. C., L. Bergui, et al. (1988). "Vinculin, talin, and integrins are localized at specific adhesion sites of malignant B lymphocytes." Blood **72**(2): 830-833.

Marsh, C. B., R. P. Pomerantz, et al. (1999). "Regulation of monocyte survival in vitro by deposited IgG: role of macrophage colony-stimulating factor." J Immunol **162**(10): 6217-6225.

Martin, T. J., D. M. Findlay, et al. (1980). "Calcitonin receptors in a cloned human breast cancer cell line (MCF 7)." Biochem Biophys Res Commun **96**(1): 150-156.

Mattsson, J. P., C. Skyman, et al. (1997). "Characterization and cellular distribution of the osteoclast ruffled membrane vacuolar H⁺-ATPase B-subunit using isoform-specific antibodies." J Bone Miner Res **12**(5): 753-760.

Matuszkiewicz-Rowinska, J., S. Niemczyk, et al. (2004). "[Effect of salmon calcitonin on bone mineral density and calcium-phosphate metabolism in chronic hemodialysis patients with secondary hyperparathyroidism]." Pol Arch Med Wewn **112**(1): 797-803.

Mauck, K. F. and B. L. Clarke (2006). "Diagnosis, screening, prevention, and treatment of osteoporosis." Mayo Clin Proc **81**(5): 662-672.

Maurer, D., T. Felzmann, et al. (1992). "Evidence for the presence of activated CD4 T cells with naive phenotype in the peripheral blood of patients with rheumatoid arthritis." Clin Exp Immunol **87**(3): 429-434.

Meyer, J. L. and G. H. Nancollas (1973). "The influence of multidentate organic phosphonates on the crystal growth of hydroxyapatite." Calcif Tissue Res **13**(4): 295-303.

Miyazaki, M., S. Nakade, et al. (2003). "Estimation of bioavailability of salmon calcitonin from the hypocalcemic effect in rats (I): pharmacokinetic-pharmacodynamic modeling based on the endogenous Ca regulatory system." Drug Metab Pharmacokinet **18**(6): 350-357.

Miyazaki, M., S. Nakade, et al. (2003). "Estimation of bioavailability of salmon calcitonin from the hypocalcemic effect in rats (II): effect of protease inhibitor on the pharmacokinetic-pharmacodynamic relationship after intranasal administration." Drug Metab Pharmacokinet **18**(6): 358-364.

Moonga, B. S., D. W. Moss, et al. (1990). "Intracellular regulation of enzyme secretion from rat osteoclasts and evidence for a functional role in bone resorption." J Physiol **429**: 29-45.

Morita, M., A. Ebihara, et al. (1994). "Progression of osteoporosis in cancellous bone depending on trabecular structure." Ann Biomed Eng **22**(5): 532-539.

Mosley, J. R. (2000). "Osteoporosis and bone functional adaptation: mechanobiological regulation of bone architecture in growing and adult bone, a review." J Rehabil Res Dev **37**(2): 189-199.

Murad, F., H. B. Brewer, Jr., et al. (1970). "Effect of thyrocalcitonin on adenosine 3':5'-cyclic phosphate formation by rat kidney and bone." Proc Natl Acad Sci U S A **65**(2): 446-453.

Na, D. H., Y. S. Youn, et al. (2004). "Stability of PEGylated salmon calcitonin in nasal mucosa." J Pharm Sci **93**(2): 256-261.

Nakagawa, N., M. Kinoshita, et al. (1998). "RANK is the essential signaling receptor for osteoclast differentiation factor in osteoclastogenesis." Biochem Biophys Res Commun **253**(2): 395-400.

Nakou, M., G. Katsikas, et al. (2009). "Rituximab therapy reduces activated B cells in both the peripheral blood and bone marrow of patients with rheumatoid arthritis: depletion of memory B cells correlates with clinical response." Arthritis Res Ther **11**(4): R131.

Neer, R. M., C. D. Arnaud, et al. (2001). "Effect of parathyroid hormone (1-34) on fractures and bone mineral density in postmenopausal women with osteoporosis." N Engl J Med **344**(19): 1434-1441.

Newa, M., K. H. Bhandari, et al. (2011). "Antibody-mediated "universal" osteoclast targeting platform using calcitonin as a model drug." Pharm Res **28**(5): 1131-1143.

Nicholson, G. C., C. S. D'Santos, et al. (1988). "Human placental calcitonin receptors." Biochem J **250**(3): 877-882.

Niemi, R., J. Vepsalainen, et al. (1999). "Bisphosphonate prodrugs: synthesis and in vitro evaluation of novel acyloxyalkyl esters of clodronic acid." J Med Chem **42**(24): 5053-5058.

Niyibizi, C., R. Chan, et al. (1994). "A 92 kDa gelatinase (MMP-9) cleavage site in native type V collagen." Biochem Biophys Res Commun **202**(1): 328-333.

Niyibizi, C. and D. R. Eyre (1994). "Structural characteristics of cross-linking sites in type V collagen of bone. Chain specificities and heterotypic links to type I collagen." Eur J Biochem **224**(3): 943-950.

Niyibizi, C. and M. Kim (2000). "Novel approaches to fracture healing." Expert Opin Investig Drugs **9**(7): 1573-1580.

Nolan, J. P., P. T. Morley, et al. (2003). "Therapeutic hypothermia after cardiac arrest: an advisory statement by the advanced life support task force of the International Liaison Committee on Resuscitation." Circulation **108**(1): 118-121.

O'Donnell, S., A. Cranney, et al. (2006). "Strontium ranelate for preventing and treating postmenopausal osteoporosis." Cochrane Database Syst Rev **3**: CD005326.

Obrant, K. J., K. K. Ivaska, et al. (2005). "Biochemical markers of bone turnover are influenced by recently sustained fracture." Bone **36**(5): 786-792.

- Oda, Y., M. H. Ishikawa, et al. (2007). "Differential role of two VDR coactivators, DRIP205 and SRC-3, in keratinocyte proliferation and differentiation." J Steroid Biochem Mol Biol **103**(3-5): 776-780.
- Odom, O. W., W. Kudlicki, et al. (1997). "An effect of polyethylene glycol 8000 on protein mobility in sodium dodecyl sulfate-polyacrylamide gel electrophoresis and a method for eliminating this effect." Anal Biochem **245**(2): 249-252.
- Odvin, C. V., J. E. Zerwekh, et al. (2005). "Severely suppressed bone turnover: a potential complication of alendronate therapy." J Clin Endocrinol Metab **90**(3): 1294-1301.
- Ogawa, K., T. Mukai, et al. (2006). "Development of a novel ^{99m}Tc-chelate-conjugated bisphosphonate with high affinity for bone as a bone scintigraphic agent." J Nucl Med **47**(12): 2042-2047.
- Ogawa, Y., M. Ohtsuki, et al. (2003). "Suppression of osteoclastogenesis in rheumatoid arthritis by induction of apoptosis in activated CD4⁺ T cells." Arthritis Rheum **48**(12): 3350-3358.
- Okubo, Y., K. Bessho, et al. (2000). "Effect of elcatonin on osteoinduction by recombinant human bone morphogenetic protein-2." Biochem Biophys Res Commun **269**(2): 317-321.
- Overgaard, K., D. Agnusdei, et al. (1991). "Dose-response bioactivity and bioavailability of salmon calcitonin in premenopausal and postmenopausal women." J Clin Endocrinol Metab **72**(2): 344-349.

Palmer, M., H. O. Adami, et al. (1988). "Increased risk of malignant diseases after surgery for primary hyperparathyroidism. A nationwide cohort study." Am J Epidemiol **127**(5): 1031-1040.

Palokangas, H., M. Mulari, et al. (1997). "Endocytic pathway from the basal plasma membrane to the ruffled border membrane in bone-resorbing osteoclasts." J Cell Sci **110 (Pt 15)**: 1767-1780.

Pappa, H. M., T. M. Saslowsky, et al. (2011). "Efficacy and harms of nasal calcitonin in improving bone density in young patients with inflammatory bowel disease: a randomized, placebo-controlled, double-blind trial." Am J Gastroenterol **106**(8): 1527-1543.

Pappalardo, A., A. G. Rizzo, et al. (1994). "[Evaluation of the use of calcitonin in rheumatoid arthritis by bone densitometry and the study of of phospho-calcium metabolism]." Clin Ter **144**(2): 99-105.

Paralkar, V. M., F. Borovecki, et al. (2003). "An EP2 receptor-selective prostaglandin E2 agonist induces bone healing." Proc Natl Acad Sci U S A **100**(11): 6736-6740.

Parfitt, A. M. (1994). "Osteonal and hemi-osteonal remodeling: the spatial and temporal framework for signal traffic in adult human bone." J Cell Biochem **55**(3): 273-286.

Parfitt, A. M. (1994). "Vitamin D receptor genotypes in osteoporosis." Lancet **344**(8936): 1580.

Parikka, V., Z. Peng, et al. (2005). "Estrogen responsiveness of bone formation in vitro and altered bone phenotype in aged estrogen receptor-alpha-deficient male and female mice." Eur J Endocrinol **152**(2): 301-314.

Pearson, C. M. (1956). "Development of arthritis, peri-arthritis and periostitis in rats given adjuvants." Proc Soc Exp Biol Med **91**(1): 95-101.

Pelletier, J. P., C. Boileau, et al. (2004). "The inhibition of subchondral bone resorption in the early phase of experimental dog osteoarthritis by licofelone is associated with a reduction in the synthesis of MMP-13 and cathepsin K." Bone **34**(3): 527-538.

Pierce, W. M., Jr. and L. C. Waite (1987). "Bone-targeted carbonic anhydrase inhibitors: effect of a proinhibitor on bone resorption in vitro." Proc Soc Exp Biol Med **186**(1): 96-102.

Price, N., A. Lipton, et al. (2004). "Prevention and management of osteonecrosis of the jaw associated with bisphosphonate therapy." Support Cancer Ther **2**(1): 14-17.

Querol, E., J. A. Perez-Pons, et al. (1996). "Analysis of protein conformational characteristics related to thermostability." Protein Eng **9**(3): 265-271.

Raisz, L. G. (2005). "Clinical practice. Screening for osteoporosis." N Engl J Med **353**(2): 164-171.

Raisz, L. G. (2005). "Pathogenesis of osteoporosis: concepts, conflicts, and prospects." J Clin Invest **115**(12): 3318-3325.

Reid, I. R., J. S. Davidson, et al. (2004). "Comparative responses of bone turnover markers to bisphosphonate therapy in Paget's disease of bone." Bone **35**(1): 224-230.

Reid, I. R., R. Eastell, et al. (2004). "A comparison of the effects of raloxifene and conjugated equine estrogen on bone and lipids in healthy postmenopausal women." Arch Intern Med **164**(8): 871-879.

Rho, J. Y., P. Zioupos, et al. (2002). "Microstructural elasticity and regional heterogeneity in human femoral bone of various ages examined by nano-indentation." J Biomech **35**(2): 189-198.

Rice, J. C., S. C. Cowin, et al. (1988). "On the dependence of the elasticity and strength of cancellous bone on apparent density." J Biomech **21**(2): 155-168.

Richer, E., M. A. Lewis, et al. (2005). "Reduction in normalized bone elasticity following long-term bisphosphonate treatment as measured by ultrasound critical angle reflectometry." Osteoporos Int **16**(11): 1384-1392.

Rickard, D. J., K. M. Waters, et al. (2002). "Estrogen receptor isoform-specific induction of progesterone receptors in human osteoblasts." J Bone Miner Res **17**(4): 580-592.

Rittel, W., R. Maier, et al. (1976). "[Structure-activity relationship of human calcitonin. III. Biological activity of synthetic analogues with shortened or terminally modified peptide chains (author's transl)]." Experientia **32**(2): 246-248.

Rogers, M. J. (2003). "New insights into the molecular mechanisms of action of bisphosphonates." Curr Pharm Des **9**(32): 2643-2658.

Rogers, M. J., J. C. Frith, et al. (1999). "Molecular mechanisms of action of bisphosphonates." Bone **24**(5 Suppl): 73S-79S.

Rogers, M. J., S. Gordon, et al. (2000). "Cellular and molecular mechanisms of action of bisphosphonates." Cancer **88**(12 Suppl): 2961-2978.

Roodman, G. D. (1996). "Advances in bone biology: the osteoclast." Endocr Rev **17**(4): 308-332.

Roodman, G. D. (1996). "Paget's disease and osteoclast biology." Bone **19**(3): 209-212.

Rossouw, J. E., G. L. Anderson, et al. (2002). "Risks and benefits of estrogen plus progestin in healthy postmenopausal women: principal results From the Women's Health Initiative randomized controlled trial." JAMA **288**(3): 321-333.

Russell, R. G., P. I. Croucher, et al. (1999). "Bisphosphonates: pharmacology, mechanisms of action and clinical uses." Osteoporos Int **9** **Suppl 2**: S66-80.

Russell, R. G., B. Espina, et al. (2006). "Bone biology and the pathogenesis of osteoporosis." Curr Opin Rheumatol **18** **Suppl 1**: S3-10.

Ryan, S. M., J. M. Frias, et al. (2011). "PK/PD modelling of comb-shaped PEGylated salmon calcitonin conjugates of differing molecular weights." J Control Release **149**(2): 126-132.

- Samura, A., S. Wada, et al. (2000). "Calcitonin receptor regulation and responsiveness to calcitonin in human osteoclast-like cells prepared in vitro using receptor activator of nuclear factor-kappaB ligand and macrophage colony-stimulating factor." Endocrinology **141**(10): 3774-3782.
- Seeman, E. and P. D. Delmas (2006). "Bone quality--the material and structural basis of bone strength and fragility." N Engl J Med **354**(21): 2250-2261.
- Sexton, P. M., D. M. Findlay, et al. (1999). "Calcitonin." Curr Med Chem **6**(11): 1067-1093.
- Shibakawa, A., K. Yudoh, et al. (2005). "The role of subchondral bone resorption pits in osteoarthritis: MMP production by cells derived from bone marrow." Osteoarthritis Cartilage **13**(8): 679-687.
- Shin, B. S., J. H. Jung, et al. (2004). "Nasal absorption and pharmacokinetic disposition of salmon calcitonin modified with low molecular weight polyethylene glycol." Chem Pharm Bull (Tokyo) **52**(8): 957-960.
- Siligardi, G., B. Samori, et al. (1994). "Correlations between biological activities and conformational properties for human, salmon, eel, porcine calcitonins and Elcatonin elucidated by CD spectroscopy." Eur J Biochem **221**(3): 1117-1125.
- Silverman, S. L. (2003). "Calcitonin." Endocrinol Metab Clin North Am **32**(1): 273-284.

- Silvestris, F., P. Cafforio, et al. (2008). "Expression and function of the calcitonin receptor by myeloma cells in their osteoclast-like activity in vitro." Leuk Res **32**(4): 611-623.
- Silvestroni, L., A. Menditto, et al. (1987). "Identification of calcitonin receptors in human spermatozoa." J Clin Endocrinol Metab **65**(4): 742-746.
- Sixt, M. L., K. Messlinger, et al. (2009). "Calcitonin gene-related peptide receptor antagonist olcegepant acts in the spinal trigeminal nucleus." Brain **132**(Pt 11): 3134-3141.
- Stevenson, C. L. and M. M. Tan (2000). "Solution stability of salmon calcitonin at high concentration for delivery in an implantable system." The journal of peptide research : official journal of the American Peptide Society **55**(2): 129-139.
- Stevenson, C. L. and M. M. Tan (2000). "Solution stability of salmon calcitonin at high concentration for delivery in an implantable system." J Pept Res **55**(2): 129-139.
- Sturtridge, W., B. Lentle, et al. (1996). "Prevention and management of osteoporosis: consensus statements from the Scientific Advisory Board of the Osteoporosis Society of Canada. 2. The use of bone density measurement in the diagnosis and management of osteoporosis." CMAJ **155**(7): 924-929.
- Suda, T., N. Takahashi, et al. (1992). "Modulation of osteoclast differentiation." Endocr Rev **13**(1): 66-80.

- Suzuki, H. and N. Takahashi (2001). "[Effects of calcitonin on osteoclast]." Clin Calcium **11**(9): 1158-1162.
- Tanaka, S., N. Takahashi, et al. (1992). "Osteoclasts express high levels of p60c-src, preferentially on ruffled border membranes." FEBS Lett **313**(1): 85-89.
- Tanko, L. B., M. A. Karsdal, et al. (2006). "Biochemical approach to the detection and monitoring of metastatic bone disease: What do we know and what questions need answers?" Cancer Metastasis Rev **25**(4): 659-668.
- Teitelbaum, S. L. (2000). "Bone resorption by osteoclasts." Science **289**(5484): 1504-1508.
- Teitelbaum, S. L. (2000). "Osteoclasts, integrins, and osteoporosis." J Bone Miner Metab **18**(6): 344-349.
- Teti, A., H. C. Blair, et al. (1989). "Extracellular protons acidify osteoclasts, reduce cytosolic calcium, and promote expression of cell-matrix attachment structures." J Clin Invest **84**(3): 773-780.
- Torres-Lugo, M. and N. A. Peppas (2000). "Transmucosal delivery systems for calcitonin: a review." Biomaterials **21**(12): 1191-1196.
- Troen, B. R. (2006). "Osteoporosis in older people: a tale of two studies (and three treatments)." J Am Geriatr Soc **54**(5): 853-855.
- Troen, B. R. (2006). "The regulation of cathepsin K gene expression." Ann N Y Acad Sci **1068**: 165-172.

Tuukkanen, J. and H. K. Vaananen (1986). "Omeprazole, a specific inhibitor of H⁺-K⁺-ATPase, inhibits bone resorption in vitro." Calcif Tissue Int **38**(2): 123-125.

Uludag, H., T. Gao, et al. (2000). "Bone affinity of a bisphosphonate-conjugated protein in vivo." Biotechnol Prog **16**(6): 1115-1118.

Uludag, H., N. Kousinioris, et al. (2000). "Bisphosphonate conjugation to proteins as a means to impart bone affinity." Biotechnol Prog **16**(2): 258-267.

Uludag, H. and J. Yang (2002). "Targeting systemically administered proteins to bone by bisphosphonate conjugation." Biotechnol Prog **18**(3): 604-611.

Vaananen, H. K. and M. Horton (1995). "The osteoclast clear zone is a specialized cell-extracellular matrix adhesion structure." J Cell Sci **108 (Pt 8)**: 2729-2732.

Vaananen, H. K., E. K. Karhukorpi, et al. (1990). "Evidence for the presence of a proton pump of the vacuolar H⁽⁺⁾-ATPase type in the ruffled borders of osteoclasts." J Cell Biol **111**(3): 1305-1311.

Vaananen, H. K. and T. Laitala-Leinonen (2008). "Osteoclast lineage and function." Arch Biochem Biophys **473**(2): 132-138.

Vaaraniemi, J., J. M. Halleen, et al. (2004). "Intracellular machinery for matrix degradation in bone-resorbing osteoclasts." J Bone Miner Res **19**(9): 1432-1440.

Valcourt, U., B. Merle, et al. (2007). "Non-enzymatic glycation of bone collagen modifies osteoclastic activity and differentiation." J Biol Chem **282**(8): 5691-5703.

van de Langerijt, A. G., P. L. van Lent, et al. (1994). "Susceptibility to adjuvant arthritis: relative importance of adrenal activity and bacterial flora." Clin Exp Immunol **97**(1): 33-38.

Van Vollenhoven, R. F., A. Soriano, et al. (1988). "The role of immunity to cartilage proteoglycan in adjuvant arthritis. Intravenous injection of bovine proteoglycan enhances adjuvant arthritis." J Immunol **141**(4): 1168-1173.

Veronese, F. M. and G. Pasut (2005). "PEGylation, successful approach to drug delivery." Drug Discov Today **10**(21): 1451-1458.

Veronese, F. M. and G. Pasut (2005). "PEGylation, successful approach to drug delivery." Drug discovery today **10**(21): 1451-1458.

Viguet-Carrin, S., P. Garnero, et al. (2006). "The role of collagen in bone strength." Osteoporos Int **17**(3): 319-336.

Waalén, K., O. Forre, et al. (1987). "Evidence of an activated T-cell system with augmented turnover of interleukin 2 in rheumatoid arthritis. Stimulation of human T lymphocytes by dendritic cells as a model for rheumatoid T-cell activation." Scand J Immunol **25**(4): 367-373.

Wada, S., S. Yasuda, et al. (2001). "Regulation of calcitonin receptor by glucocorticoid in human osteoclast-like cells prepared in vitro using receptor activator of nuclear factor-kappaB ligand and macrophage colony-stimulating factor." Endocrinology **142**(4): 1471-1478.

Wang, D., S. C. Miller, et al. (2005). "Bone-targeting macromolecular therapeutics." Adv Drug Deliv Rev **57**(7): 1049-1076.

Wang, Y. and D. W. Grainger (2011). "RNA therapeutics targeting osteoclast-mediated excessive bone resorption." Adv Drug Deliv Rev.

Warshafsky, B., J. E. Aubin, et al. (1985). "Cytoskeleton rearrangements during calcitonin-induced changes in osteoclast motility in vitro." Bone **6**(3): 179-185.

Warshawsky, H., D. Goltzman, et al. (1980). "Direct in vivo demonstration by radioautography of specific binding sites for calcitonin in skeletal and renal tissues of the rat." J Cell Biol **85**(3): 682-694.

Weir, E. C., M. C. Horowitz, et al. (1993). "Macrophage colony-stimulating factor release and receptor expression in bone cells." J Bone Miner Res **8**(12): 1507-1518.

Wermers, R. A., S. Khosla, et al. (1998). "Survival after the diagnosis of hyperparathyroidism: a population-based study." Am J Med **104**(2): 115-122.

Whitfield, J. F., P. Morley, et al. (1999). "Stimulation of femoral trabecular bone growth in ovariectomized rats by human parathyroid hormone (hPTH)-(1-30)NH(2)." Calcif Tissue Int **65**(2): 143-147.

Wright, J. E., S. A. Gittens, et al. (2006). "A comparison of mineral affinity of bisphosphonate-protein conjugates constructed with disulfide and thioether linkages." Biomaterials **27**(5): 769-784.

Yamaguchi, M., N. Aihara, et al. (2006). "RANKL increase in compressed periodontal ligament cells from root resorption." J Dent Res **85**(8): 751-756.

Yamamoto, Y., T. Noguchi, et al. (2005). "[Effects of calcitonin on osteoclast]." Clin Calcium **15**(3): 147-151.

Yamamoto, Y., Y. Yamamoto, et al. (2006). "Effects of calcitonin on the function of human osteoclast-like cells formed from CD14-positive monocytes." Cell Mol Biol (Noisy-le-grand) **52**(3): 25-31.

Yan, P., T. Li, et al. (2011). "Inhibition of bone resorption by econazole in rat osteoclast-like cells through suppressing TRPV5." Arch Pharm Res **34**(6): 1007-1013.

Yasuda, H., N. Shima, et al. (1998). "Identity of osteoclastogenesis inhibitory factor (OCIF) and osteoprotegerin (OPG): a mechanism by which OPG/OCIF inhibits osteoclastogenesis in vitro." Endocrinology **139**(3): 1329-1337.

Yasuda, H., N. Shima, et al. (1998). "Osteoclast differentiation factor is a ligand for osteoprotegerin/osteoclastogenesis-inhibitory factor and is identical to TRANCE/RANKL." Proc Natl Acad Sci U S A **95**(7): 3597-3602.

Yokogawa, K., K. Miya, et al. (2001). "Selective delivery of estradiol to bone by aspartic acid oligopeptide and its effects on ovariectomized mice." Endocrinology **142**(3): 1228-1233.

- Yoo, S. D., H. Jun, et al. (2000). "Pharmacokinetic disposition of polyethylene glycol-modified salmon calcitonins in rats." Chem Pharm Bull (Tokyo) **48**(12): 1921-1924.
- Yoshida, K., H. Oida, et al. (2002). "Stimulation of bone formation and prevention of bone loss by prostaglandin E EP4 receptor activation." Proc Natl Acad Sci U S A **99**(7): 4580-4585.
- Youn, Y. S., J. Y. Jung, et al. (2006). "Improved intestinal delivery of salmon calcitonin by Lys18-amine specific PEGylation: stability, permeability, pharmacokinetic behavior and in vivo hypocalcemic efficacy." J Control Release **114**(3): 334-342.
- Yun, Q., R. E. Yang, et al. (2005). "Reproducible preparation and effective separation of PEGylated recombinant human granulocyte colony-stimulating factor with novel "PEG-pellet" PEGylation mode and ion-exchange chromatography." J Biotechnol **118**(1): 67-74.
- Zaidi, M., A. M. Inzerillo, et al. (2002). "Forty years of calcitonin--where are we now? A tribute to the work of Iain Macintyre, FRS." Bone **30**(5): 655-663.
- Zhao, H., T. Laitala-Leinonen, et al. (2001). "Downregulation of small GTPase Rab7 impairs osteoclast polarization and bone resorption." J Biol Chem **276**(42): 39295-39302.
- Zheng, C., G. Ma, et al. (2007). "Native PAGE eliminates the problem of PEG-SDS interaction in SDS-PAGE and provides an alternative to HPLC

in characterization of protein PEGylation." Electrophoresis **28**(16): 2801-2807.

Zhou, Q., R. Nie, et al. (2002). "Localization of androgen and estrogen receptors in adult male mouse reproductive tract." J Androl **23**(6): 870-881.

Ziambaras, K., F. Lecanda, et al. (1998). "Cyclic stretch enhances gap junctional communication between osteoblastic cells." J Bone Miner Res **13**(2): 218-228.